Molecular mechanisms underlying growth hormone insensitivity and idiopathic short stature

David, Alessia

MOLECULAR MECHANISMS UNDERLYING GROWTH HORMONE INSENSITIVITY AND IDIOPATHIC SHORT STATURE

Alessia David

Centre for Endocrinology
William Harvey Research Institute
Barts & the London
Queen Mary University of London

PhD thesis

2009

DECLARATION OF ORIGINALITY

The molecular and statistical analysis presented in this thesis is original work undertaken by Dr Alessia David in the Centre for Endocrinology of the William Harvey Research Institute.

The molecular analysis of the STAT5b gene was undertaken by Dr V. Hwa in the Department of Paediatrics, Oregon Health and Science University, Portland, Oregon, US

Measurement of GH–dependent protein serum levels was performed by Dr F. Miraki-Moud in the laboratories of Dr C. Camacho-Hubner at Barts and the London and by Dr J Jones at the Diagnostic Systems Laboratories (DSL), GKT, School of Medicine King's Denmark Hill Campus, London, UK.

Alessia David

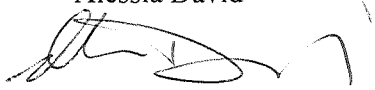

ABSTRACT

Short stature can be due to several causes, including genetically transmitted insensitivity to the action of growth hormone (GHI). In approximately 80% of referred patients, no aetiology can be identified and they are classified as having idiopathic short stature (ISS). The overall aim of this thesis was to identify and characterise the molecular mechanisms of GHI and ISS.

The genetic analysis of a large GHI population identified several novel defects in the GH receptor (*GHR)*, the signal transducer and activator of transcription (*STAT5b)* and the acid-labile subunit (*IGFALS)* genes and a genotype/phenotype relationship between *GHR* defects and GHI severity.

In approximately 20% of GHI patients a *GHR* splice mutation was present. An *in vitro* splicing assay was developed and showed to accurately identify nucleotide changes resulting in aberrant mRNA splicing. Among the splice mutations, was the one leading to the activation of a *GHR* pseudoexon. This defect was found to be a common cause of GHI and a translational approach using antisense oligonucleotides showed to effectively correct *in vitro* the aberrant GHR mRNA splicing.

During the course of the project an algorithm for the search of alternative exons and pseudoexons, was developed and allowed the identification of several potential regions, two of which were demonstrated to be expressed in human liver cDNA.

Identification and analysis of GHI patients with ALS deficiency caused by *IGFALS* defects and the observation of short stature in their heterozygote parents, led us to hypothesise the involvement of *IGFALS* in the pathogenesis of ISS. Genetic analysis of a large ISS population showed the presence of single heterozygous *IGFALS* defects in 9.6% of patients and in their short stature family members.

Identification of the genetic defects responsible for growth failure can shed new light on the physiology of longitudinal growth and guide therapy in children with short stature.

CONTENTS

LIST OF FIGURES

LIST OF TABLES

ABBREVIATIONS

ALS	Acid-labile subunit
ASO	Antisense oligonucleotides
ATP	Adenosine triphosphate
bp	Base pair
BRCA1	Breast cancer susceptible gene 1
cDNA	Complementary DNA
CHO	Chinese hamster ovary
C-terminal	Carboxyl terminal
DEPC	Diethyl pyrocarbonate
DEXA	Dual energy X-ray absorptiometry
DMEM	Dulbecco's modified eagle medium
DMSO	Dimethyl sulphoxide
DNA	Deoxyribonucleic acid
DNAse	Deoxyribonuclease
dNTP	Deoxynucleotide triphosphate
DTT	Dithiothreitol
E.coli	*Escherichia coli*
ECD	Extracellular domain
EDTA	Ethylenediamine tetraacetic acid
ESE	Exonic splicing enhancers
EST	Expressed sequence tag
FCS	Foetal calf serum
GAPDH	Glyceraldehyde-3-phosphate dehydrogenase
GAS	γ-interferon activated sequence
GH	Growth hormone
GHBP	Growth hormone binding protein
GHI	Growth hormone insensitivity
GHR	Growth hormone receptor
GHRH	Growth hormone releasing hormone
HEK	Human embryonic kidney
HeLa	Human cervical carcinoma cells (named after donor Henrietta Lacks)
hnRNP	Heterogeneous nuclear ribonucleoprotein particle
IGF	Insulin-like growth factor
IGFALS	Insulin-like growth factor binding protein, acid labile subunit
IGFBP	Insulin-like growth factor binding protein
IRSs	Insulin-receptor substrates
ISS	Idiopathic short stature
ITT	Insulin tolerance test
IVS	Intervening sequences

JAK2	Janus tyrosine kinase 2
Kb	Kilobase pairs
kDa	kilodaltons
LB	Luria Bertani
LDL	Low density lipoprotein
LHRE	Lactogenic hormone responsive element
MAPKs	Mitogen-activated protein kinase
mRNA	Messenger ribonucleic acid
N-Terminal	Amino terminal
ORF	Open reading frame
PAGE	Polyacrylamide gel electrophoresis
PCR	Polymerase chain reaction
PI-3	Phosphatidyl inositol-3 kinase
PNA	Peptide nucleic acids
PTPs	Protein tyrosine phosphatases
RNA	Ribonucleic acid
RNAsin	Ribonuclease inhibitor
rpm	Revolution per minute
RS domain	Arginine/serine domain
RT-PCR	Reverse transcription polymerase chain reaction
SC35	Splicing component 35
SDS	Standard deviation scores
SDS-PAGE	Sodium dodecyl sulphate polyacrylamide gel electrophoresis
SF2/ASF	Splicing factor 2/alternative splicing factor
SNP	Single nucleotide polymorphism
snRNPs	Small nuclear ribonucleoproteins
SOCS	Suppressor of cytokine signalling
SRp	Splicing regulatory protein
STAT5b	Signal transducer and activator of transcription 5B
TACE	Tumor necrosis factor-α converting enzyme
TAE	Tris Acetate EDTA
TBE	Tris Borate EDTA
TE	Tris EDTA
UTR	Untranslated region

ACKNOWLEDGEMENTS

I would like to thank my supervisors Professors Adrian Clark and Martin Savage for their advice and encourangement throughout my PhD. I am extremely grateful for the guidance, support and patience they have provided me with. Their expertise and optimism have been invaluable and inspirational.

A special thank to Dr Louise Metherell for her constant support, help and friendship during these years.

Finally, I would like to thank my mum and my husband for their constant and inconditional love, support and encouragement and my son Alexandros for all the joy he has brought into my life.

CHAPTER 1

INTRODUCTION

1 INTRODUCTION

In the last few years the completion of the human genome project and the advances in genetic epidemiology have shed new light in the understanding of the genetic factors involved in linear growth. Height is a classical polygenic trait influenced by the combined action of multiple, as yet undiscovered, factors. The increasing amount of data provided by genome-wide association studies has identified unexpected genes and pathways involved in height variations (Weedon et al., 2007, Gudbjartsson et al., 2008, Lettre et al., 2008, Weedon et al., 2008).

Because of the fundamental biological role of growth hormone in promoting linear growth, all participants in the growth hormone-IGF-I axis are strong candidates when searching for molecular defects causing growth failure. Nevertheless, despite this axis having received increasing attention in recent years, the biological role and effect of molecular defects occurring in its components, such as the acid-labile subunit, are still far from being elucidated.

The identification and analysis of genetic abnormalities in patients with growth failure, not only provides invaluable information on the physiology of linear growth, but can also have important therapeutic implications. In fact, better understanding of the pathogenesis of short stature is the first step towards identifying therapeutic targets and the development of new medical or gene therapies, such as the antisense-based approach for conditions due to aberrant splicing.

1.1 THE GROWTH HORMONE/ IGF-I AXIS

1.1.1 Regulation of Growth hormone secretion

Growth hormone (GH) is a key regulator of longitudinal growth and metabolism. It is secreted from the GH cells in the anterior pituitary gland under the regulation of two hypothalamic hormones: the GH releasing hormone (GHRH) and somatostatin (Fukata et al., 1985, Shimon and Melmed, 1997). Several additional neurogenic, metabolic and hormonal factors participate in the regulation of GH secretion, including ghrelin, estrogens, sleep, stress, exercise and nutrition (Schalch, 1967, Veldhuis et al., 1991) (Figure 1.1).

GH is secreted throughout life at different rates. Its secretion is low in childhood and increases with the onset of puberty, inducing the acceleration in growth rate characteristic of this developmental stage. After puberty, there is a progressive age-dependent decline in GH secretion (Ho et al., 1987). GH secretion is pulsatile and has a diurnal rhythm (Tannenbaum and Ling, 1984). Pulses of small amplitude occur approximately every 2 hours during the day (Hartman et al., 1990, Iranmanesh et al., 1994). The highest GH peaks are observed during the slow-wave phases of sleep (stages III and IV) (Van Cauter et al., 1998, Van Cauter et al., 2004). Because of this variable and pulsatile secretion, a single random blood sample cannot be used for diagnostic purposes and, although circadian blood sampling is helpful in studying spontaneous GH secretion, performance of dynamic tests with stimulatory or inhibitory agents is mandatory in the evaluation of GH secretion (Ho, 2007). Several diagnostic tests are available, among which the insulin tolerance test (ITT) is considered the gold standard. Recent consensus guidelines have indicated a GH peak < 3 μg/l after ITT as indicative of GH deficiency (Ho, 2007).

1.1.2 Growth hormone and growth hormone binding protein (GHBP)

The majority of circulating GH is bound to proteins. Approximately 50% of GH circulating in blood is bound to a high affinity protein known as the GH-binding protein (GHBP) (Baumann et al., 1987), whereas 5 to 20% is bound to low-affinity proteins such as the alpha 2 macroglobulin (Kratzsch et al., 1995). In humans and rabbits, GHBP is produced from proteolysis of the growth hormone receptor (GHR), whereas in other

species such as the rat and mouse, it is the result of alternative GHR splicing. In all species, GHBP is found in the circulation and plays an important role in modulating GH availability. Approximately one half of circulating GH is, in fact, bound to the GHBP in a 1:1 molar complex, which results in prolongation of GH half-life in the circulation (Schalch, 1967), but also inhibits GH binding to the GHR through different mechanisms, such as ligand competition with the intact GHR proteins (Mannor et al., 1991) and formation of a signalling-inactive GHR:GHBP complex (Ross et al., 1997). The GH:GHBP complex appears to be biologically inactive and protected from clearance and degradation (Baumann et al., 1987, Baumann, 1991). For this reason, production of an engineered GH:GHBP complex was recently proposed as a potential method for modulating GH action (Wilkinson et al., 2007). Moreover, since the GHBP derives from proteolysis of the growth hormone receptor, it reflects GHR tissue density and determination of its serum concentration can be a useful tool in the diagnostic assessment of patients with growth hormone resistance (Amit et al., 2000).

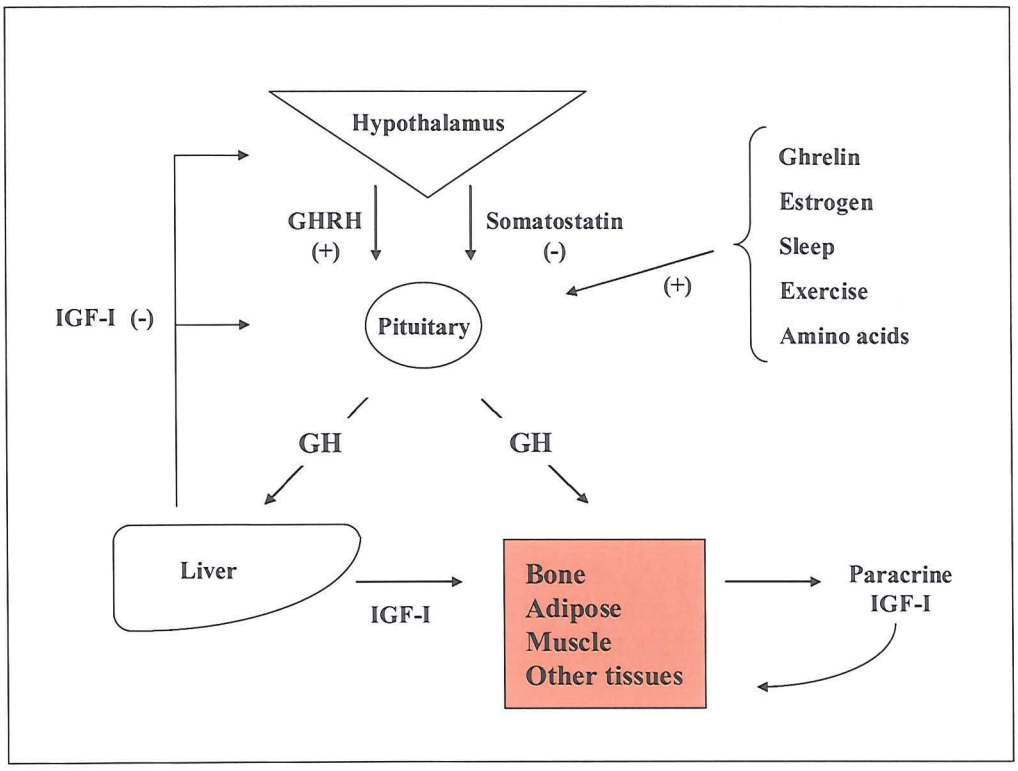

Figure 1.1 Schematic diagram of GH regulation and action. The main factors involved in pituitary GH secretion are indicated. GH exerts its function in part through direct action and in part through its main effector, IGF-I.

1.1.3 Growth hormone actions

GH exerts its effects by binding to its specific and ubiquitously expressed cell surface receptor: the growth hormone receptor. Binding of GH to its receptor activates a complex intracellular signalling cascade, leading to activation of the transcription of numerous genes, including insulin-like growth factors I (IGF-I) and II (IGF-II).

GH exerts its biological actions in part directly, but mostly through IGF-I, also known as somatomedin C, which is secreted in response to GH stimulation by the liver and other tissues targeted by GH, such as bone and muscle, in which IGF-I also acts as a paracrine/autocrine effector. IGF-I secreted by the liver circulates bound in a 150kDa ternary complex with two GH-dependent proteins: the IGF-binding proteins (IGFBP) -3 or -5 and the acid-labile subunit. IGF-I not only mediates most of the actions of the GH, but also exerts a negative feedback on GH secretion at pituitary level.

1.1.3.1 Skeletal and metabolic effects of the Growth Hormone

GH has a fundamental role in skeletal maturation. During childhood, GH promotes longitudinal growth of bone and attainment of peak bone mass. In adult life, it promotes bone remodeling and maintenance of bone mass and density (Isaksson et al., 1987, Ohlsson et al., 1998, van der Eerden et al., 2003). GH stimulates the proliferation and differentiation of chondrocytes and osteoblasts as well as collagen and non-collagen protein synthesis, both directly and through systemic and locally produced IGF-I (Isaksson et al., 1982, Ho et al., 1987, Isgaard et al., 1988). Recently the IGFBPs were also found to be involved in the modulation of bone turnover (Richman et al., 1999, Silha et al., 2003, DeMambro et al., 2008). GH deficiency in childhood is known to result in growth failure and short stature, whereas in adult life GH deficiency may result in decreased bone mass and osteoporosis (Johansson et al., 1992, Rosen et al., 1993).

GH is also an anabolic hormone involved in several metabolic processes: it stimulates protein synthesis by increasing amino acid transport in the muscle (Kostyo et al., 1959, Florini et al., 1996, Umpleby and Russell-Jones, 1996), promotes lipolysis of triglycerides and release of fatty acids from the adipose tissue and increases the number of LDL receptors in the liver. GH promotes gluconeogenesis and has an antagonistic effect to insulin. GH deficiency results in changes in body composition, characterised by

central obesity and decreased muscle mass. Moreover, it is associated with dyslipidemia, with elevated triglyceride levels, reduced high density lipoprotein cholesterol levels and increased low density lipoprotein levels. Moreover, it can affect carbohydrate metabolism, leading to insulin resistance and glucose intolerance (Rosen et al., 1995).

1.1.4 The Growth hormone receptor (GHR)

The growth hormone receptor (GHR) mediates the effects of the GH on longitudinal growth and metabolism. The GHR is present ubiquitously, but is most abundantly expressed in the liver (Ballesteros et al., 2000).

1.1.4.1 GHR gene and protein structure

The GHR protein is a member of the cytokine receptor family, which includes receptors for prolactin, erythropoietin, interferon, interleukins and numerous erythropoietic stimulating factors. The mature human GHR is a 620 amino-acid single-chain transmembrane glycoprotein, of 130 kDa. It is composed of a large extracellular domain involved in GH binding and GHR dimerisation, a single transmembrane domain which anchors the receptor to the cell surface, and an intracellular domain, involved in GH signalling.

The gene that encodes the human GHR is located on chromosome 5 p14-p12. The *GHR* coding region contains 9 exons (exons 2-10). Part of exon 2 encodes the 18 amino acids of the signal peptide. The remaining part of exon 2 and exons 3 to 7 encode the GHR extracellular domain. Exon 8 encodes the transmembrane domain and exons 9 and 10 the intracellular domain and the 3' untranslated region (Leung et al., 1987, Godowski et al., 1989).

The *GHR* is characterised by a complex 5' untranslated region that contains multiple alternative first non-coding exons (Pekhletsky et al., 1992, Edens and Talamantes, 1998). In humans, these are clustered in two main regions of approximately 2 kb in size, called module A and B.

Screening of adult and foetal libraries from different tissues have demonstrated a heterogeneity in the 5'-untranslated region of GHR mRNA transcripts. Very little is known on the mechanisms regulating the transcription of these variants, which seem to be

under the control of different promoters. The different GHR mRNA transcripts are generated by the splicing of different first non-coding exons of the 5'UTR into a common acceptor splice site, located 12 bases upstream of the UTG in exon 2, but all generate the same GHR protein. .

In humans several 5' UTR variants (V1-V9) have been detected (Goodyer et al., 2001). Three variants (V2-V9-V3) are clustered in module A. These have been shown, together with a fourth variant (V5), to be expressed in foetal, postnatal and neoplastic tissues (Zogopoulos et al., 1996, Goodyer et al., 2001). Variants V7-V1-V4-V8 are clustered in module B and are expressed in postnatal liver only (Zogopoulos et al., 1996, Goodyer et al., 2001). Alteration in the expression of tissue-specific 5'UTR GHR variants has been postulated to affect growth. Analysis of GHR transcripts in the miniature *bos indicus* cattle, a dwarf bull similar to the human Laron dwarf, has demonstrated a reduced expression of the liver specific GHR mRNA transcript (Liu et al., 1999).

Human GHR has one alternative gene variant that lacks exon 3 and results in the absence of 22 amino-acids in the extracellular domain (d3-GHR) (Pantel et al., 2000). The role and biological significance of this variant is still unclear. It has been hypothesised that the d3-GHR might have an increased affinity for GH, but studies on d3-GHR patients treated with exogenous GH therapy have, so far, provided contrasting results (Dos Santos et al., 2004, Binder et al., 2006, Blum et al., 2006, Carrascosa et al., 2006, Jorge et al., 2006, Pilotta et al., 2006).

1.1.4.2 The 1:2 GH-GHR interaction and GHR activation

The crystal structure of the extracellular domain (ECD) of the GHR (residues 1-246) was resolved in 1992 and was the basis for studying its interaction with GH. The GHR ECD is organised in two subdomains: subdomain 1 formed by residues 1-123 and subdomain 2 formed by residues 128-246. The GH protein has two binding sites, 1 and 2, which interact mainly with GHR subdomain 1, at residues 43,44,103,104,105,106,120 and 126,127 and with GHR subdomain 2, at residues 165,166 (de Vos et al., 1992, Clackson and Wells, 1995).

The GHR crystal structure also revealed a 1:2 ratio of the GH-GHR complex. Further mutational and biophysical studies demonstrated that GH binds to its receptor through a sequential chain of events. Site 1 of the GH has a high affinity for GHR (Cunningham and Wells, 1993) and is the first to bind the GHR molecule. This is followed by the binding of the GH low affinity site 2 with a second GHR molecule (Cunningham et al., 1991, Fuh et al., 1992). (Figure 1.2)

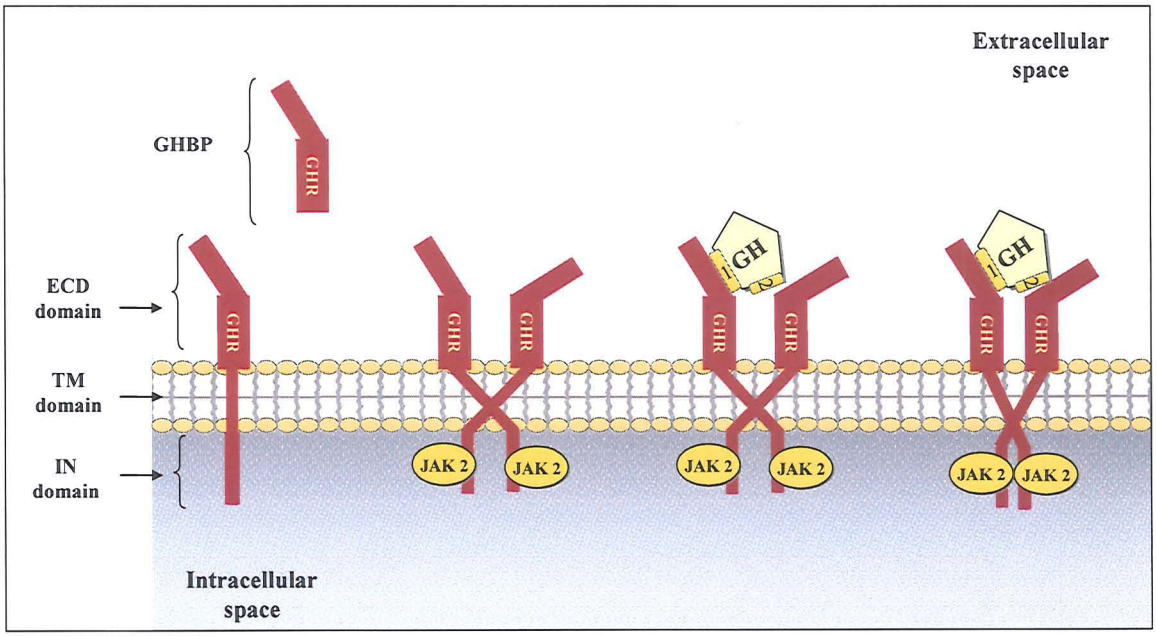

Figure 1.2 The 1:2 GH-GHR mechanism of interaction. The GHR exists at the cell surface as an inactive dimer. Binding of one GH molecule to two GHRs induces a conformational rotation of the GHR dimer and the activation of JAK2 molecules. The GHR and the GHBP are also depicted. ECD, extracellular, TM, transmembrane, IN, intracellular.

Until recently, the GHR was thought to exist as a monomer on the cell surface and its activation by GH was thought to occur through dimerisation of the GHR (Cunningham et al., 1991, Clackson and Wells, 1995). Despite previous coimmunoprecipitation studies having demonstrated the presence of GHR dimers in the absence of GH (Gent et al., 2002), the presence of inactive GHR dimers at the cell surface was only recently definitively accepted. In 2005, it was shown that GH binding activates its receptor by inducing a relative rotation of the pre-existing GHR dimer (Brown et al., 2005). This conformational change promotes the binding of Janus tyrosine kinase 2 (JAK2) to a proline-rich Box 1 region located in the proximal intracellular portion of the GHR (Argetsinger et al., 1993) and the initiation of the intracellular signalling pathway.

1.1.4.3 GHR Intracellular signalling pathway

The GHR lacks an intrinsic kinase activity and relies on recruitment of cytoplasmic tyrosine kinases for intracellular signalling. The JAK family members are constitutively associated with cytokine receptors lacking intrinsic kinase activity. The GHR mainly utilises JAK2, although JAK 1 and 3 activation following GH binding to GHR has also been reported (Carter-Su et al., 1996, Lanning and Carter-Su, 2006). JAK2 association to the GHR requires the presence of the proline-rich sequence region located in the GHR intracellular domain and known as Box 1. Formation of the GH:GHR_2 complex results in phosphorylation of JAK2, which, in turn, phosphorylates the tyrosines in the intracellular domain of the GHR. The phosphorylated JAK2 and GHR provide docking sites for numerous signalling molecules and activate a complex, incompletely elucidated, intracellular cascade with several pathways, including the signal transducers and activators of transcription (STATs), components of the mitogen-activated protein kinase (MAPKs), phosphatidyl inositol-3 kinase (PI-3), insulin-receptor substrates (IRSs) and small RAS-like GTPases. GHR activation has also been shown to increase intracellular calcium levels through JAK2-independent calcium-channel activation (Carter-Su et al., 1996).

Experimental data suggest that only four of the seven known STAT proteins, namely STAT 1, 3 and 5a and 5b, are involved in GH signalling (Meyer et al., 1994, Gronowski et al., 1995). STAT 5b appears to be the most important in the induction of GH-dependent IGF-I expression. GH-induced signalling through the STAT 5 pathway has received increasing attention since the discovery of STAT 5b-inactivating mutations in GHI patients and this is discussed separately (section 1.1.4).

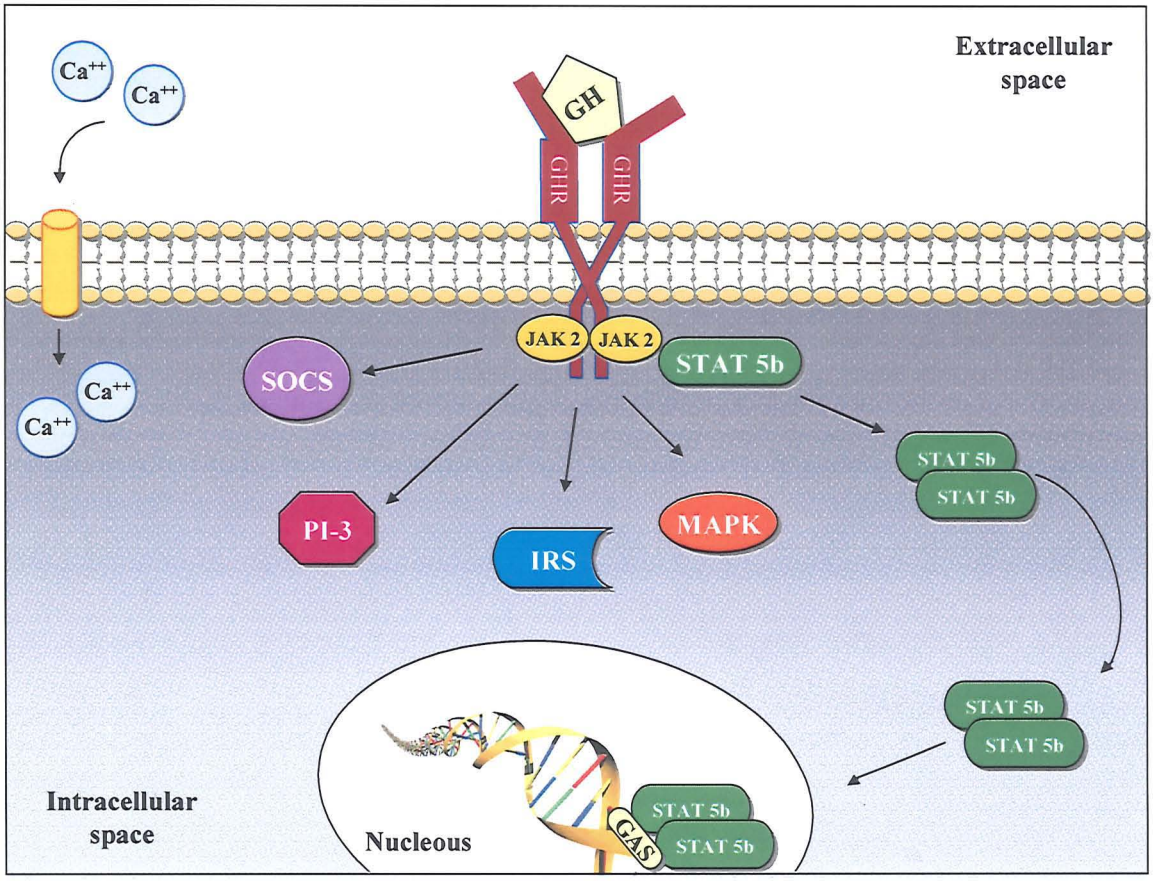

Figure 1.3 The GHR intracellular pathways. Ca++, Calcium; SOCS, suppressor of cytokine signalling; PI-3, phosphatidyl inositol-3 kinase; JAK2, Janus tyrosine kinase 2; IRS, insulin-receptor substrates; STAT5b, signal transducers and activators of transcription 5b; MAPK, mitogen-activated protein kinase; GAS, gamma-activated sites; GH, growth hormone; GHR, growth hormone receptor.

1.1.3.4. GHR negative regulation

The mechanisms responsible for the negative regulation of GHR signalling are still far from being clarified. Members of the suppressor of cytokine signalling (SOCS) family are known to be involved in this process. SOCS-1, -2, -3 and the cytokine-inducible SH2-containing protein (CIS) are thought to negatively regulate GHR signalling by binding the phosphorylated tyrosine of the JAK2/GHR complex, thus inhibiting the apposition of signalling molecules, such as STAT 5b (Hansen et al., 1999, Ram and Waxman, 1999). SOCS proteins may also be involved in the ubiquitination, internalization and degradation of the GHR/JAK2 complex (Landsman and Waxman, 2005).

Other mechanisms involved in the down-regulation of GHR signalling include recruitment of protein tyrosine phosphatases (PTPs) such as the SH2 domain-containing

protein-tyrosine phosphatase (Kim et al., 1998) and of the ubiquitin conjugation system that participates in the internalization and degradation of the GHR (Govers et al., 1999, van Kerkhof et al., 2000). Little is known on the mechanisms of GHR internalisation and degradation. In humans and rabbits the first step of this process is thought to be the cleavage of the GHR extracellular domain by metalloproteases, such as tumor necrosis factor-α converting enzyme (TACE or ADAM-17) (Zhang et al., 2000). Using a mutational approach, Comte et al. localized three ECD juxtamembranous residues important for TACE-induced GHR cleavage (residues 242-244) (Conte et al., 2002). GHR proteolysis generates a GHR remnant consisting of the transmembrane and intracellular domains and releases the ECD in the pericellular space. The GHR ECD retains its GH binding properties, is soluble and can reach the circulation, where it circulates known as GHBP.

1.1.5 The Signal transducer and activator of transcription (STAT) 5b

1.1.5.1 Gene and protein structure

The mammalian STAT family comprises of seven proteins, namely STAT 1, 2, 3, 4, 5a and 5b, 6. The two STAT 5 isoforms, 5a and 5b, share a 90% homology in their coding regions, even though encoded by two different genes located on chromosome 17 (Lin et al., 1996, Ambrosio et al., 2002). All STAT family members have a similar structure and are organised into distinct functional domains, which include an N-terminal domain, a coiled-coil domain, a DNA-binding domain, a linker domain, an SH2 domain and a transactivation domain. The SH2 domain in the STAT structure permits: 1) docking of STAT to phosphorylated tyrosines on the activated receptor, 2) STAT hetero- and homo-dimerisation, and 3) stabilisation of the STAT-DNA interaction. The NH2 terminus domain, the coiled-coil domain and the carboxyterminal domain are involved in protein-protein interaction between STATs and other regulatory elements, and in the interaction between adjacent STAT dimers (Ross et al., 2007).

1.1.5.2 Protein function

Activation of STATs depends on the activation of JAK molecules and their specific receptors. STAT proteins are activated by numerous cytokines and are involved

in the function of T and B cells (Imada et al., 1998, Welte et al., 1999, Ross et al., 2007). Unlike other STAT proteins, STAT 5a and 5b are also activated by GH, prolactin, EPO and a number of growth factors (O'Shea, 1997).

Recruitment of STAT 5b in the GHR intracellular signalling pathway follows activation by the GHR:JAK2 complex. Phosphorylated tyrosines on JAK2 and GHR form docking sites for STAT 5b proteins, which subsequently undergo phosphorylation, dimerisation, disengagement from the JAK-receptor complex and translocation to the nucleus. There, phosphorylated STAT 5b dimers are retained and can stimulate transcription of several genes, including IGF-I (Davey et al., 2001, Woelfle et al., 2003) through binding to consensus recognition motifs, known as gamma-activated sites (GAS), located in the promoters of several genes (Darnell et al., 1994, Boucheron et al., 1998, Mitchell and John, 2005).

Despite the strong similarity in their coding regions, STAT 5a and 5b have been shown to have different actions in animal models (Hennighausen and Robinson, 2008). The STAT 5b -/- mouse demonstrated growth failure and IGF-I deficiency. The male STAT 5b knockout mouse exhibited, in fact, a 30% growth reduction, wich was not present in the female STAT 5b $^{-/-}$, suggesting a role of STAT 5b in the sexually dimorphic GH-induced growth in the rodent. IGF-I levels, however, were reduced by 30% in both genders (Udy et al., 1997). The STAT 5a deficient female animal model had impaired milk production in response to prolactin, resulting from a defective lobulo-alveolar development, but no growth failure or reduced IGF-I levels (Teglund et al., 1998) Although no immune defects were present in the single gene knock out mouse model, the double knock out animal (STAT 5a/b -/-) exhibited a severely impaired immune system, particularly T cell function (Teglund et al., 1998).

In 2003 the first human case of STAT 5b deficiency was reported in a female patient with growth hormone insensitivity and decreased cell-mediated immunity (Kofoed et al., 2003). This finding shed new light on the importance of STAT 5b in GH-mediated growth and IGF-I production and demonstrated the differences in the action of STAT 5b between the animal model and humans. Further cases of STAT 5b mutations and growth failure have been reported since this first case report, confirming the above findings. The majority of patients were females and had immunological impairment

(Rosenfeld et al., 2004, Hwa et al., 2005, Vidarsdottir et al., 2006, Walenkamp et al., 2007).

1.1.6 The Acid-labile subunit

1.1.6.1 Gene and protein structure

The acid-labile subunit (ALS) is encoded by the *IGFALS*, a single copy gene located on chromosome 16-p13.3. This gene, controlled by a TATA-less promoter (Dai and Baxter, 1992, Leong et al., 1992, Boisclair et al., 1996, Rhoads et al., 2000) covers approximately 3.3 kilobases and is comprised of two exons. Exon 1 encodes the first 5 amino acids of the signal peptide and exon 2 the remaining 22 amino acid of the signal peptide and the 576 amino acid of the mature protein. The transcriptional regulation of the *IGFALS* is under GH control. A GH response element (ALSGAS1) was identified in the mouse promoter (Ooi et al., 1997, Suwanichkul et al., 2000). Its 9-base sequence (TTCCTAGAA) resembles that of the γ-interferon activated sequence (GAS) (Schindler and Darnell, 1995) and is conserved across species, including humans.. *IGFALS* transcription is activated in response to the activation of the GH signaling pathway. STAT5b dimers, resulting from GH:GHR_2 complex formation, translocate to the nucleus and activate *IGFALS* transcription, most likely through ALSGAS1 binding (Ooi et al., 1998).

IGFALS expression appears to be limited to the liver when assessed by Northern blot (Leong et al., 1992, Dai and Baxter, 1994, Delhanty and Baxter, 1996), but the use of in-situ hybridization,identified *IGFALS* expression in extrahepatic tissues such as the kidney, lungs, thymus, mammary gland, bone and ovary (Chin et al., 1994).

The ALS is a glycosylated protein of 84-86 kDa with a predicted doughnut-shape and belongs to the leucine-rich repeat family. Approximately 80% of the ALS structure is, in fact, characterised by a 18-20 leucine-rich repeat domain, which is predicted to be responsible for ALS interaction with other proteins, namely IGF-binding protein (IGFBP) -3 and -5 (Figure 1.4). ALS production increases with age until puberty, when it reaches a plateau and declines thereafter with the ageing process (Baxter, 1990). Although serum is the main source of ALS, extravascular ALS has been detected in peritoneal, synovial, ovarian and blister fluids and at very low levels in milk, amniotic and cerebrospinal fluids

(Baxter, 1990, Cwyfan Hughes et al., 1997, Khosravi et al., 1997, Labarta et al., 1997). Its role in these compartments remains to be clarified.

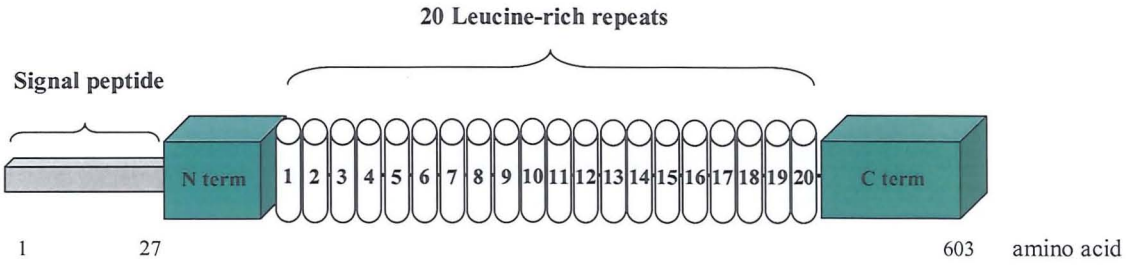

Figure 1.4 ALS protein structure.

1.1.6.2 ALS protein function

The physiological role of ALS appears to be the regulation of IGF-I and II clearance and bioavailability at a tissue level. Almost all IGF-I and II are present in the circulation bound to IGFBP-3 or -5 and to the acid-labile subunit (ALS) to form ternary complexes (IGF/IGFBP/ALS). IGFs availability at a tissue level is limited by its ability to cross the endothelial barrier and reach its receptors on the cell surface. The key limiting factor to this process is binding of the binary complex IGF-I or -II/IGFBP-3 or -5 to ALS. IGFs free or bound to IGFBPs can cross the endothelium, but formation of a large ternary complex of 150kDa with ALS, prevents IGFs and IGFS/IGFBPs from leaving the circulation (Boisclair et al., 2001) (Figure 1.5). Furthermore, binding to ALS has been demonstrated to increase the half-life of IGFs from few minutes to 12-15 hours (Guler et al., 1989). Thus, ALS can be considered the principal regulator of IGFs clearance and bioavailability at tissue level. ALS is found in excess over IGF and IGFBP in the circulation, as one half of ALS is not bound into a ternary complex.

The mechanisms by which ALS interacts with the binary complex IGFs/IGFBPs and is released from it, are still far from being elucidated. Mutagenesis studies on a conserved positively-charged aminoacid sequence present on the carboxyl-terminal domain of IGFBP-3 and -5 found it to affect ternary complex formation (Firth et al., 1998, Twigg et al., 1998). However, its counterpart on ALS has not yet been identified. The negative charges provided by sialic acids on the ALS have been suggested to influence the affinity of ALS for IGFBPs, but protein desialylation only marginally reduced the Ka of ALS for IGFBP-3 (Janosi et al., 1999).

The importance of ALS in the regulation of circulating IGF-I levels has been established by human and animal studies. Homozygous *IGFALS* knock-out mice showed a 62% and 88% reduction in plasma IGF-I and IGFBP-3 levels, respectively and significant growth failure compared to the wild type (Ueki et al., 2000). In children with homozygous *IGFALS* mutations and undetectable ALS serum levels, a dramatic reduction in serum IGF-I and IGFBP-3 levels has been documented, along with growth failure (Domene et al., 2004, Hwa et al., 2006, Domene et al., 2007). Even more interesting is the documentation of reduced IGF-I and IGFBP-3 serum levels and growth failure in *IGFALS* heterozygous knock-down mice and in parents of *IGFALS* homozygote children, obligate carriers of single heterozygous *IGFALS* mutations (Ueki et al., 2000, Hwa et al., 2006, Domene et al., 2007).

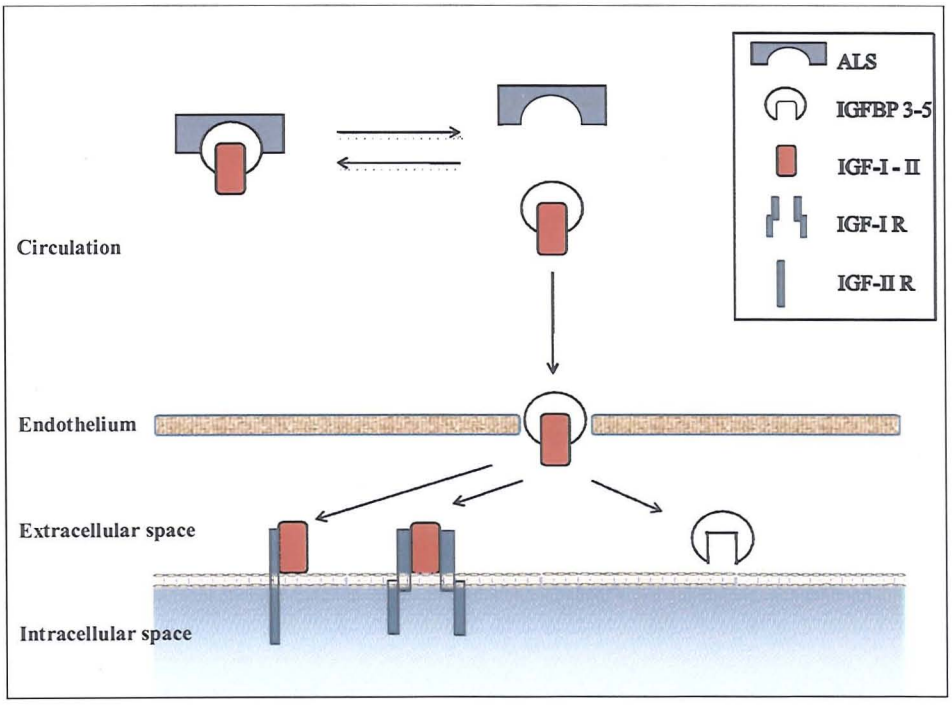

Figure 1.5 Interaction between IGFs and the acid-labile subunit. IGF-I and II exert their biological actions through interaction with receptors on the cell surface. In the circulation the majority of the IGFs is bound to IGFBP-3 and -5 and to the ALS. Free and IGFBP-bound IGFs can cross the endothelium and reach cell surface receptors. Sequestration of IGFs into a 150kDa ternary complex with ALS limits trans-endothelial passage and represents a key limiting factor to IGFs availability.

1.2 GROWTH HORMONE INSENSITIVITY

1.2.1 Definition

Growth hormone insensitivity (GHI) is characterised by elevated serum growth hormone (GH) levels and reduced IGF-I serum levels, which do not increase in response to exogenous GH administration (Laron, 1999). GHI can be acquired or congenital. Acquired GHI is common in conditions such as diabetes, infectious diseases, traumas and surgery and represents a response to catabolic stress (Carlsson, 1996). Congenital GHI is a rare condition, which is caused by genetic defects causing failure of GH to exert its biological functions. This can be due to the presence of an inactive GH or of molecular defects affecting the cellular response to GH. The latter may be the result of defects in the GH receptor, which account for the majority of cases of congenital GHI.

The first report of GHI of genetic origin came from Dr. Zvi Laron in 1966 (Laron et al., 1966). Evidence of cellular unresponsiveness to GH in primary GHI patients was, nevertheless, first reported in 1984 by Laron and colleagues, who demonstrated the lack of binding of ^{125}I GH to GHRs prepared from patients' liver membranes (Eshet et al., 1984). The advent of modern molecular biology and the cloning and characterisation of human GHR (Godowski et al., 1989) have permitted better understanding of the pathophysiology of GHI.

Since 1966, more than 250 patients with primary GHI have been identified worldwide. GHI is, in the majority of cases, an autosomal recessive disorder and in the vast majority of patients a molecular defect has been identified in the *GHR* (Burren et al., 2001). There appears to be a significant geographical clustering of patients, with most cases having been identified in Israel and Ecuador (Berg et al., 1994, Schaefer et al., 1994, Laron, 2004). At present, there is still no clear explanation for this, even though the presence of common ancestors is likely. It has, in fact, been demonstrated by family trees in reported cases that consanguinity is a major contributor to GHI propagation (Woods and Savage, 1996, Burren et al., 2001).

1.2.2 Clinical characteristics of GHI

GHI in its most severe form is known as Laron syndrome. Untreated patients have severe growth failure in childhood, resulting in short stature in adult life. GHI patients typically have low serum IGF-I, IGFBP-3 and ALS levels and are resistant to treatment with exogenous GH (Laron, 1999). Intrauterine growth is not markedly affected, although birth weight and length may be marginally subnormal. However, postnatal linear growth failure is typically seen, with a severe and rapid decline in growth velocity. If untreated, adult stature in GHI patients is 4 to 10 standard deviation scores (SDS) below the median for age and sex. Skeletal and muscular systems are also underdeveloped and osteopenia can be demonstrated by DEXA (Gluckman et al., 1992, Bachrach et al., 1998, Laron, 1999).

Laron patients display a characteristic mid-facial hypoplasia due to an underdeveloped sphenoid and mandible resulting from an impaired development of endochondral facial bones (Scharf and Laron, 1972). Patients with typical Laron facial features have a small nose with a depressed bridge and protruding foreheads. Hair is typically sparse with temporal and frontal recession (Burren et al., 2001). A pubertal growth spurt is generally absent and puberty is delayed, even though both sexes can reach full sexual development with normal sexual and reproductive function (Laron et al., 1980, Savage et al., 1993). GHI also results in metabolic abnormalities such as fasting hypoglycaemia. Despite this, a state of insulin resistance has been documented, and some patients develop diabetes in adult life (Laron et al., 1995). Dyslipidemia with hypercholesterolemia is also often present in adults.

A minority of GHI patients have normal facial features and are less severely affected with less abnormal growth and biochemical features. This milder form of GHI is known as non-classical GHI (Woods et al., 1997, Burren et al., 2001).

1.2.3 Molecular mechanisms

1.2.3.1 GHI and GHR defects

The first mutation in a patient with GHI was reported in 1989 by Godowski and colleagues who described a homozygous deletion in the coding region of the GH binding

domain (Godowski et al., 1989). So far, more than 60 mutations in the GHR gene of GHI patients have been described (Tables 1.1 and 1.2). Almost all are recessively inherited, either in homozygous or compound heterozygous forms (Savage et al., 2006). Nearly all reported defects in the *GHR* occur in the region encoding the extracellular domain of the receptor. Patients with such mutations have absent or extremely low GHBP and typical facial features of Laron syndrome (Laron and Klinger, 1994, Woods et al., 1997).

Molecular defects identified in the *GHR* range from point or gross deletions to a variety of point mutations, including missense, nonsense and splice mutations. The latter play an important role in the pathogenesis of GHI, representing approximately 20 percent of *GHR* defects identified in GHI patients. The majority of mutations causing aberrant GHR mRNA splicing disrupt major regulatory elements, such as the donor and acceptor splice sites. In two cases (defects A to G at 594 and the C to T at 723) an exonic base change has been shown to result in the activation of a cryptic splice site, causing an in-frame amino acid sequence deletion and a functionless GHR.

Among the defects causing aberrant *GHR* splicing is an intronic base change described by our group in 2001 (Metherell et al., 2001). This point mutation leads to the activation of a pseudoexon sequence and the insertion of 36 new amino acid within the receptor extracellular domain. Potential exons (pseudoexons) are frequently found within introns, but are normally not included in the mature mRNA because they fail to be recognized by the splicing machinery (Sun and Chasin, 2000). The described mutation ($A_{-1} \rightarrow G_{-1}$) is at the 5' donor splice site of one such pseudoexon (6Ψ) and leads to recognition of the pseudoexon and inclusion of an additional 108 bases between exons 6 and 7. Functional studies have shown that the mutant GHR has significantly impaired cell surface trafficking. The signaling ability of the receptor, as judged by JAK2 and STAT5 phosphorylation and LHRE reporter gene analysis, is reduced in proportion to the reduction in cell surface receptor, implying that the signaling properties of the mutant protein are unimpaired (Maamra et al., 2006).

1.2.3.1.1 GHR defects and non-classical GHI

There are few GHI cases reported in the literature in which GHBP levels are normal or elevated and this is typically the result of *GHR* defects occurring in the transmembrane or intracellular domains. In 1996, Woods et al. described a classical GHI patient with a homozygous point mutation (IVS8ds+1 G to C) in the splice donor site of

intron 8 resulting in the skipping of exon 8. This was the first description of a mutation affecting the GHR transmembrane domain. The authors suggested that the mutant GHR lacks the ability to be retained at the cell surface and is, thus, released from cells and identified in blood as GHBP (Woods et al., 1996). In 1997, Ayling et al. described the first heterozygous mutation with a dominant negative effect in the GHR intracellular domain. This was a mutation in the acceptor splice site of intron 8 (IVS8as-1 G to C) resulting in the skipping of exon 9 and the production of a truncated GHR. The mutant GHR formed heterodimers with the wild type GHR and exerted a dominant negative effect on the normal protein (Ayling et al., 1997). A second mutation (IVS9ds+1 G toA) with a similar effect was described by Iida (Iida et al., 1998). In both cases patients had positive GHBP levels and normal facial features. Other homozygous mutations in the intracellular domain resulting in an altered GHR unable to signal have been described (Kaji et al., 1997, Gastier et al., 2000, Milward et al., 2004).

The pseudoexon mutation is the only example of a defect in the GHR extracellular domain resulting in non-classical GHI. The four GHI siblings in whom it was documented had, in fact, normal facial appearance and normal GHBP levels.

1.2.3.2 GHI caused by STAT 5b defects

In 2003, Kofoed et al. (Kofoed et al., 2003) reported the first molecular defect in the GH signalling cascade in an immune-deficient child with typical signs of classical GHI. This was a homozygous mutation in exon 15 of the STAT 5b gene resulting in a protein with a mutated SH2 domain, which could not be activated by GH thus failing to induce gene transcription (Fang et al., 2006). Interestingly, the patient with severe growth retardation was female, suggesting a different pathogenetic mechanism to the mouse model, in which the STAT 5b -/- female mouse is not affected in size (Teglund et al., 1998). Since then, a few other mutations in the STAT 5b gene associated with GHI and immunological defects in male and female patients have been described (Hwa et al., 2005, Vidarsdottir et al., 2006, Walenkamp et al., 2007).

1.2.3.3 GHI and ALS defects

In 2004, Domene et al. reported the first case of an inactivating ALS mutation. The defect was a guanine deletion at position 1338, resulting in a frame-shift and the appearance of a premature stop codon. The patient had minimal postnatal growth impairment and delayed puberty. Increased GH levels were accompanied by a reduction in IGF-I and IGFBP-3, unresponsive to stimulation by GH, and by undetectable ALS levels (Domene et al., 2004). Since then, a few more cases of ALS deficiency and growth failure have been described (Hwa et al., 2006, Domene et al., 2007, Duyvenvoorde et al., 2008, Heath et al., 2008).

TABLE 1.1 NONSENSE AND MISSENSE MUTATIONS IDENTIFIED IN THE *GHR* OF GHI PATIENTS.

Mutations	Exon	Codon	Nucleotide change	Amino Acid change	Mutation	Phenotype	Ethnic origin
Nonsense	2	-15	TGG-TAG	Trp-Term	W -15X	LS	Iraqi-Jews
	3	16	TGG-TGA	Trp-Term	W16X	LS	German
	4	38	TGC-TGA	Cys-Term	C38X	LS	Mediterranean
	4	43	CGA-TGA	Arg-Term	R43X	LS	European, Ecuadorian
	4	65	CAG-TAG	Gln-Term	Q65X	LS	Indian
	5	80	TGG-TAG	Trp-Term	W80X	LS	German
	5	83	TCA-TAA	Cys-Term	C83X	LS	Not reported
	5	122	TGT-TGA	Cys-Term	C122X	ISS	Not reported
	6	141	TTA-TAA	Leu-Term	L141X	LS	Italian
	6	157	TGG-TGA	Trp-Term	W157X	LS	Turkish
	6	183	GAA-TAA	Glu-Term	E183X	LS	Ecuadorian, Jewish
	7	217	CGA-TGA	Arg-Term	R217X	LS	Jewish-Yemenite
	7	224	GAG-TAG	Glu-Term	E224X	LS	Not reported
Missense	2	-18	ATG-TTG	Met-Leu	M-18L	LS	Not reported
	4	38	TGC-AGC	Cys-Ser	C38S	LS	Algerian
	4	40	TCA-TTA	Ser-Leu	S40L	LS	Turkish
	4	42	GAG-AAG	Glu-Lys	E42K	LS	Chinese
	4	44	GAG-AAG	Glu-Lys	E44K	ISS	Not reported
	4	50	TGG-CGG	Trp-Arg	W50R	LS	German
	4	65	CCA	Ser-His	S65H	LS	Chinese
	4	71	AGG-AAG	Arg-Lys	R71K	LS	Mediterranean
	5	86	TAT-GAT	Tyr- Asp	Y86D	LS	Iranian
	5	94	TGT-TCT	Cys-Ser	C94S	LS	Austrian
	5	96	TTT-TCT	Phe-Ser	F96S	LS	Mediterranean
	5	125	GTT-GCT	Val-Ala	V125A	LS	European
	6	131	CCA-CAA	Pro-Gln	P131Q	LS	Vietnamese
	6	144	GTC-GAC	Val-Asp	V144D	LS	Mediterranean
	6	144	GTC-ATC	Val-Ile	V144I	ISS	Caucasian, Cuban
	6	150	CAT-CAG	Cys-Gln	C150Q	LS	Austrian
	6	152	GAT-CAT	Asp-His	D152H	LS	Indian, Pakistani
	6	152	GAT-GGT	Asp-Gly	D152G	LS	Taiwanese
	6	153	ATC-ACC	Ile-Thr	I153T	LS	Caucasian
	6	154	CAA-CCA	Gln-Pro	Q154P	LS	Hispanic
	6	155	GTG-GGG	Val-Gly	V155G	LS	Saudi Arabian
	6	161	CGC-TGC	Arg-Cys	R161C	LS, ISS	Middle Eastern
	6	178	TAC-TCC	Tyr-Ser	Y178S	LS	Korean
	7	208	TAT-TGT	Tyr-Cys	Y208C	LS	Swedish
	7	211	CGT-GGT	Arg-Gly	R211G	LS	Mediterranean
	7	211	CGT-CAT	Arg-His	R211H	ISS	Jewish-Iraqi
	7	222	TAT-CAT	Tyr-His	Y222H	LS	Not reported
	7	224	GAG-GAC	Glu-Asp	E224D	ISS	Not reported
	7	226	AGT-ATT	Ser-Iso	S226I	LS	Not reported
	7	244	GAT-AAT	Asp-Asn	D244N	LS	Swedish
	10	422 (*)	TGC-TTC	Cys-Phe	C422F	LS	Japanese
	10	478	GCA-ACA	Ala-Thr	A478T	LS	Not reported
	10	561 (*)	CCT-ACT	Pro-Thr	P561T	LS	Japanese

#1 SNP Iida K et al JCEM 1999; 84:4214-4219
#2 SNP Chujo S et al. Eur J Endocrinol 1996;134:560-2

TABLE 1.2 SPLICE MUTATIONS AND GENE DELETIONS IDENTIFIED IN THE *GHR* OF GHI PATIENTS.

Mutation	IVS and splice site	Exon	Nucleotide change and position in mRNA sequence	Codon	mRNA or protein change	Phenotype	Ethnic origin
Splice site	2 ds	2	G to A at 70+1		Skipping of 2	LS	Turkish
	2 ds	2	G insert at 70+1		Frameshift and premature stop codon	LS	Turkish
	4 ds	4	G to A at 266+1		Skipping of 4	LS	European, Japanese
	5 as	6	G to C at 440-1		Skipping of 6	LS	Mediterranean
	6 ds	6	G to A at 618+1		Skipping of 6	LS	Chinese
	6 as	7	G to T at 619-1		Skipping of 7	LS	Not reported
	7 ds	7	G to A at 784-1		Skipping of 7	LS	Not reported
	7 as	8	G to T at 785-1		Skipping of 8	LS	Druse
	8 ds	8	G to C at 875-1		Skipping of 8	LS	Pakistani
	8 as	9	G to C at 876-1		Skipping of 9	ISS	Caucasian
	9 ds	9	G to A at 945+1		Skipping of 9	LS	Japanese
Cryptic splice site activation	Intron 6 ds +792	Pseudo-exon	A to G at ds +792	188-189	36 amino acids inserted, in frame	ISS	Pakistani
		6	A to G at 594	180	8 amino acid missing, in frame	LS	Ecuadorian
		7	C to T at 723	223	21 amino acid missing, in frame	LS	Spanish, Bahamian
Gross deletions	4 to 6		4 Kb		Exon 5 missing, frameshift, premature stop codon	LS	Sri Lankan
	4	5	1.3 kb del		Skipping of exon 5	LS	Cambodian
	4 to 6		del 7.5Kb		Exon 5 and 6 missing	LS	Oriental Jewish (Iran-Iraq)
Small deletions		4	del of C at 162	35	Frameshift and premature stop codon	LS	Slovenian
		4	del of TT at 190	45	Frameshift and premature stop codon	LS	Not reported
		7	del of TA or AT at 742-3, or 743-4	229	Frameshift and premature stop codon	LS	Not reported
		9	13 bp del from 899-911	281	Frameshift and premature stop codon	LS	Caucasian
		10	del of C at 981	308	Frameshift and premature stop codon	LS	not reported
		10	del of 22-bp at 1323	424	Frameshift and premature stop codon	LS	Spanish
		10	del of G at 1776	560	Frameshift and premature stop codon	LS	not reported

1.3 IDIOPATHIC SHORT STATURE

1.3.1 Definition and general concepts

Idiopathic short stature (ISS) is defined as short stature of unknown aetiology and is, therefore, a diagnosis of exclusion. This category includes children with heights 2 standard deviation scores (SDS) or more below the mean for age, sex and ethnic group, in whom no endocrine or systemic diseases are present and no known genetic causes of short stature or other factors compromising growth are identifiable (Bryant et al., 2007, Wit et al., 2008a).

Short stature is one of the most common reasons for referral to paediatric endocrinologists. It has been estimated that in approximately 80% of referred children no aetiology can be identified and are, thus, classified as ISS (Wit et al., 2008b). The variability in biochemical profile and response to growth hormone (GH) treatment in ISS patients (Wit and Rekers-Mombarg, 2002, Leschek et al., 2004, Hintz, 2005) suggests that multiple, as yet unidentified, pathological mechanisms contribute to this condition.

Longitudinal growth is dependent on genetic and environmental factors (Gudbjartsson et al., 2008, Lettre et al., 2008, Weedon et al., 2008). Height is normally distributed in the general population and, thus, SDS are used to describe height in children, with 2.5% of individuals having a height below 2 SDS (Wit et al., 2008a). Because of the importance of the genetic background in determining linear growth, calculation of a child's expected height can be made by using the mean of parental centile heights (midparental height). A second important factor influencing final height is puberty onset. Estrogens, deriving from the aromatization of androgens in males, are, in fact, a potent stimulator of skeletal maturation and maintenance of bone mass. After birth, and for the first 18-24 months, linear growth shifts from a growth rate determined by maternal factors, to a growth rate determined by the infant's own genetic background. After the age of 2, however, postnatal linear growth is mainly regulated by the genetic background and follows the same percentile until puberty. During puberty, the increase in sexual steroids is a major determinant of the acceleration of growth rate, also known as growth spurt. This process is followed by a growth deceleration corresponding to the epiphyseal closure (Ho et al., 1987, Mauras et al., 1987).

The importance of a child's genetic background, reflected by his/her family height history, and of the child's pubertal onset has led clinicians to subclassify ISS according to these factors. ISS is classified as familial short stature when height is below the mean compared to the general population, but remains within the expected target range for the family (Ranke, 1996, Wit et al., 2008a). Familial short stature, in the absence of other diseases, is considered reassuring, thus limiting the need for diagnostic screening tests. However, the presence of short stature in one parent only dictates the need for more careful screening, since a genetic defect with a dominant effect, might be present. A family history of delayed puberty is also considered reassuring and does not require extensive diagnostic screening, as the same is likely to occur in the child with ISS (Wit et al., 2008a).

1.3.2 Clinical characteristics and diagnostic screening

ISS is a diagnosis of exclusion and, therefore, careful medical history taking, physical examination, biochemical and radiological tests should be performed to exclude the presence of chromosomal or genetic abnormalities, chronic illnesses or endocrine diseases responsible for the short stature (Preece et al., 1986, Wit et al., 2008a). Examples of systemic and endocrine causes of short stature are presented in Table 1.3. The presence of a normal birth size is part of the definition of ISS, and short stature children born small for gestational age (birth length/weight greater then 2 SDS) should not be diagnosed as ISS. Physical examination should exclude the presence of dysmorphic features, which may indicate syndromes such as the Russell-Silver syndrome, Noonan syndrome and Turner syndrome). Disproportionate short stature, e.g. short limbs or short limbs and back, are suggestive of skeletal dysplasia, such as achondroplasia (Hughes et al., 1986, Spranger, 1992, Wollmann et al., 1995, Wit et al., 2008a). The presence of emotional deprivation, psychological problems and malnutrition should also be excluded (Powell et al., 1967, Allen, 1994).

Since, by definition, ISS is characterised by the absence of systemic diseases, the child with ISS should be asymptomatic. However, some conditions such as renal and gastrointestinal disease, anaemia and inflammatory diseases, may affect linear growth even in initial stages, when clinical signs and symptoms have yet to manifest. For this reason, biochemical testing, such as full blood count, electrolytes, albumin, renal function

tests and inflammation markers are part of the diagnostic screening of asymptomatic short stature children. Moreover, because of the high incidence of coeliac disease in short stature children, anti-tissue transglutamase antibodies or anti-endomysium antibodies are also commonly performed to identify patients at risk (Wit et al., 2008a).

TABLE 1.3 SYSTEMIC AND ENDOCRINE CAUSES OF SHORT STATURE.

SYSTEMIC CAUSES

- Gastrointestinal
  - Coeliac disease
  - Crohn's disease
  - any cause of malabsorption
- Renal
  - Chronic renal failure
  - Renal tubular acidosis
- Respiratory
  - Cystic fibrosis
  - Asthma
  - Tubercolosis
- Cardiovascular
  - Congenital heart disease
- Psychosocial
  - Anorexia
  - Emotional deprivation

ENDOCRINE CAUSES

- Growth hormone deficiency
- Growth hormone insensitivity
- Hypothyroidism
- Cushing's syndrome
- Pseudohypoparathyroidism
- Hypopituitarism

Chromosomal analysis to exclude Turner syndrome is recommended in any short stature female, even in the absence of a characteristic phaenotype (Gravholt, 2005, Wit et al., 2008a). Thyroid function and IGF-I levels are the only endocrine tests included in the initial biochemical diagnostic screening (Wit et al., 2008a).

The fundamental role of the GH/IGF-I axis in promoting linear growth requires that growth hormone deficiency or resistance are excluded for the diagnosis of ISS to be made. A recent ISS consensus meeting (Wit et al., 2008a) recommended the study of GH secretion by means of GH stimulation test, such as the insulin tolerance test or the arginine test, in the presence of an IGF-I <2 SDS, or between -2 and 0 SDS associated with clinical signs of growth hormone deficiency. The presence of a low IGF-I and normal (> 6.7μg/l) or high (>40mUl) GH response to stimulation test suggests the presence of GH resistance, which should be investigated further by measuring IGFBP-3, ALS and GHBP and performing an IGF-I generation test and, if required, DNA screening for GHI defects.

Bone age assessment is recommended in the diagnostic assessment of paediatric short stature as it can aid in the identification of the aetiology and in the prediction of the final height. Skeletal age is calculated by comparing the maturity of the epiphyseal centres with standard radiography of the non-dominant hand and wrist (Tanner et al., 1983).

1.3.3 Molecular mechanisms

Numerous genes in the GH-IGF-I axis are known to be involved in linear growth (Walenkamp and Wit, 2006), and molecular investigations have identified functional mutations in genes coding for key proteins in patients previously labelled as having ISS (Ayling et al., 1997, Metherell et al., 2001). Defects in the Short stature HOmeoboX (SHOX) gene have been reported in up to 4% of cases of isolated or familial ISS (Rappold et al., 2002, Huber et al., 2006) and are the most frequent genetic defect identified in ISS children to date. More then 50 mutations have been reported in the SHOX gene and annotated in the SHOX gene mutation database (www.shox.uni-hd.de). *SHOX* defects are associated with a wide variability of phaenotypes, seen both in patients with different *SHOX* mutations or different *SHOX* copy number, and in patients with the same *SHOX* defect (Schiller et al., 2000). The phenotype can range from mild short stature with no additional clinical signs, to skeletal anomalies affecting long bone length and curvature. The latter includes disproportionate short stature (short lower legs and forearms, or mesomelia) and limb deformity (in Leri-Weil syndrome). A recent study on 1608 children proposed a scoring system based on clinical signs, such as arm span/height

ratio and sitting height/height ratio, for the identification of high risk short stature children in whom *SHOX* should be screened for (Rappold et al., 2007).

Altered GH responsiveness has been suggested in children with proportionate mild short stature, normal GH levels, but reduced IGF-I. Biologically inactive GH proteins unable to induce GHR activation resulting from defects in the *GH* promoter or coding region have been described (Takahashi and Chihara, 1998, Millar et al., 2003) and should be considered in such cases. Furthermore, single heterozygous defects in the *GHR* have been proposed as possible causes of ISS (Goddard et al., 1995), but data are inconclusive as cosegregation of short stature and the heterozygous state is poor (Rosenbloom et al., 1994a).

1.4 MRNA SPLICING

Approximately 20 percent of molecular defects causing a functionless GH receptor protein and thus GHI, alter the correct mRNA splicing of the *GHR*. Splicing is the mechanism by which coding exons are defined and correctly assembled to form the mature mRNA. mRNA splicing has gained increasing interest in recent years and this has led to the discovery that up to 50% of known deleterious mutations involve aberrant gene splicing. Moreover, nucleotide substitutions regarded as synonymous SNPs, have been reconsidered as mutations involving regulatory splicing elements. The growing interest in the splicing process has unveiled new potential therapeutic tools, such as the use of antisense oligonucleotides, to correct aberrant splicing processes.

The majority of *GHR* defects causing GHI, alter *GHR* mRNA splicing by disrupting the invariant 5' or 3' splice sites, while a minority activate cryptic splice sites (Savage et al., 2006). It is, however, possible that other *GHR* defects thought to cause an amino acid change or create a premature stop codon, result instead in a defective GHR protein by inducing aberrant mRNA splicing. mRNA analysis or in vitro splicing assays are, in fact, rarely performed to confirm the effect of mutations conventionally classified as nonsense or missense.

In 2001, our group discovered the first *GHR* intronic mutation resulting in the inclusion of a pseudoexon in the mature mRNA in four boys with GHI (Metherell et al., 2001). This was a major breakthrough as only a few genetic diseases are known to result from pseudoexon activation (Akker et al., 2007). Intronic mutations resulting in pseudoexon activation might be more frequent than previously thought, but can be extremely difficult to identify, especially if causing a frameshift and mRNA non-sense mediated decay. Moreover, no bioinformatics tools are available to detect intronic hot spots where a single base change may lead to pseudoexon activation. The discovery of the *GHR* pseudoexon inclusion in GHI patients is also of extreme interest because potentially curable with the application of new splicing therapeutic tools.

1.4.1 Determinants of intron-exon recognition

The coding sequence (exons) of eukaryotes is interrupted by intervening sequences (IVSs or introns). The splicing process removes introns from the pre-mRNA and joins

exons to form the mature mRNA (Lander et al., 2001). The mechanisms driving splicing are still not fully understood. The pre-mRNA of a gene can be spliced in different ways giving rise to several different proteins. This process, called alternative splicing, is abundantly used in higher eukaryotes and is thought to be responsible for their functional diversity and complexity (Modrek et al., 2001, Stetefeld and Ruegg, 2005, Blencowe, 2006). About 40-60% of human genes are in fact, subjected to alternative splicing, compared to 22 % of *C. Elegans* genes (Modrek et al., 2001). Alternative splicing is believed to play a fundamental role in producing structurally and functionally different transcripts from the same pre-mRNA in different tissues and/or developmental stages (Johnson et al., 2003).

An exon is defined by three major elements: the 5' splice site (donor) the 3' splice site (acceptor) and the branch point. These are short elements of 7-14 nucleotides that, in higher eukaryotes, can highly diverge from consensus sequences (Berget, 1995). The presence of additional regulatory elements, such as the polypyrimidine tract, and exonic or intronic enhancers and silencers is also required for the identification of an exon and its inclusion in the mature mRNA (Figure 5).

Analysis of the human genome has demonstrated that 99% of introns are flanked by GT and AG dinucleotides at the 5' and 3' splice site, respectively (Berget, 1995, Burset et al., 2000), whereas exons are flanked in over 60% of the cases by the A/CAG sequence at the donor site and a G at the acceptor site (Burset et al., 2001). Two additional splicing elements are present within 50 nucleotides upstream of the 3' splice site. These are a sequence rich in pyrimidines (the polypyrimidine tract) and a 5-nucleotide sequence (the branch point) characterised by the consensus sequence CU(A/G)A(C/U), in which A is conserved in all genes (Wu et al., 1999, Smith and Valcarcel, 2000). DNA and mRNA analysis has shown that constitutively spliced exons (exons that are always included in the mature mRNA) and alternatively spliced exons (exons expressed only in some tissues or developmental stages) differ in the characteristics of their splicing elements. Alternative exons have polypyrimidine tracts, which are less rich in pyrimidines and their splice sites deviate from the consensus sequences more than the constitutive exons (Stamm et al., 1994, Stamm et al., 2000). The implications of these differences between constitutively and alternative spliced exons are still unclear, but are thought to result in a less efficient recognition of the latter by the splicing machinery. Moreover, a difference

in exon length has been found between constitutive and alternative exons. The majority of exons in human genes have a length between 50 and 200 nucleotides (Lander et al., 2001). Alternative exons expressed in a single type of tissue have been found to be shorter (e.g. mean 78 ± 58 SD nucleotides for exons expressed in brain only). Although no explanation for this phaenomenon is yet available, the presence of a reduced number of regulatory elements, such as enhancers, in alternative exons, has been proposed.

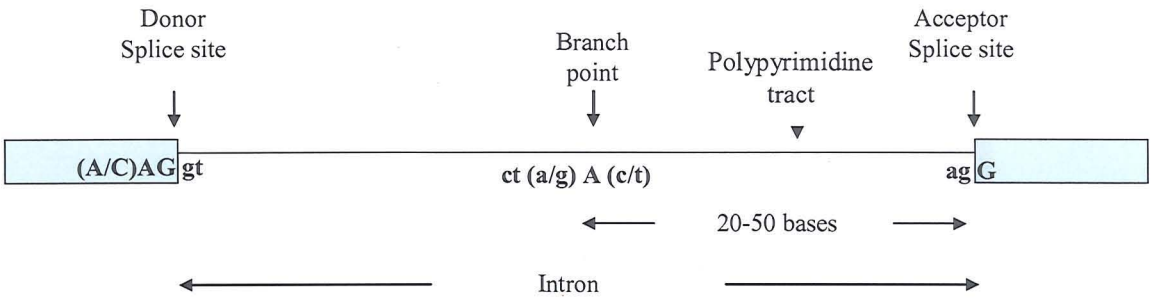

Figure 1.6 Schematic representation of splicing elements location within the intron and exon.

Exon recognition is also dependent on the environment within which the exon is located. Silencers and enhancers are additional elements playing a fundamental role in mRNA splicing (Watakabe et al., 1993, Liu et al., 1998, Blencowe, 2000, Cartegni et al., 2002). According to their function and location they are classified as exonic or intronic splicing enhancers or silencers.

Enhancer sequences are positive elements within the pre-mRNA favouring exon inclusion. The use of algorithms to identify redundant sequences that are less likely to occur by chance in a given nucleotide composition within exons have established that most enhancers are short, 4 to 9 nucleotides, purine- or AC-rich sequences. The majority of the enhancers bind to members of the serine and arginine-rich proteins (SR proteins) family (Blencowe, 2000, Zhang and Krainer, 2004). The SR proteins are pre-mRNA splicing factors belonging to a highly conserved family (Fu, 1995). They mediate the interaction between the pre-mRNA and the splicing machinery and are required for constitutive and alternative splicing (Graveley, 2000). SR proteins can recognise splicing enhancers and lead to the activation of suboptimal adjacent acceptor splice sites (Blencowe, 2000). The splicing factor 2/ alternative splicing factor (SF2/ASF), the

U2AF, SRp55, SRp38 are among the most studied SR proteins involved in enhancers recognition (Wang and Burge, 2008).

Very little is known about splicing silencers and no consensus sequence is available for these elements. Like enhancers, they can be located within or outside the exon. Silencer sequences bind to members of the heterogeneous nuclear ribonucleoprotein particle proteins (hnRNP protein) family (Krecic and Swanson, 1999, Spellman and Smith, 2006). These proteins are involved in many functions, such as gene expression and transcription, as well as mRNA splicing (Valcarcel and Green, 1996). In particular, studies have shown that hnRNP proteins are, in the majority of cases, involved in repressing gene splicing. Examples of this include the exclusion of donor splice sites following binding of the hnRNP A1 to specific mRNA binding sites and the inhibition of acceptor splice sites resulting from the competitive and antagonising role of the hnRNP I for the SF2/ASF specific mRNA binding site (Lin and Patton, 1995, Singh et al., 1995). These observations lead to two important considerations: first, that the same mRNA binding site can act as an enhancer or a silencer (Lou et al., 1999, Shin et al., 2004, Martinez-Contreras et al., 2006) and, second that, in some cases, the tissue-specific variation in the ratio between SR proteins and their antagonists, such as the case SF2/ASF and hnRNPA1, may play an important role in the regulation of alternative splicing (Zahler et al., 1993, Hanamura et al., 1998).

1.4.2 The Splicing machinery

The mechanism by which an intron is excised from the pre-mRNA is a complex and not completely understood process. In brief, it involves the recognition of splicing elements by a ribonucleoprotein complex, called the spliceosome. This consists of 4 small nuclear ribonucleoproteins (snRNPs) U1, U2, U5 and U4/U6 and 50-100 non-snRNP splicing factors (Wang and Burge, 2008).

In vitro studies using simple minigene constructs (e.g. one intron and two exons) helped elucidate the steps of the splicing reaction. This begins with the recognition of the 5'splice site by the U1 snRNP and of the branch site by the U2 snRNP. Subsequently, the U4/U5/U6 complex binds the assembled pre-mRNA, thus initiating the splicing reaction. The splicing process involves a two-step enzymatic reaction (Figure 1.7). In vitro studies have demonstrated that the first step results in the formation of two intermediates: an

exon 1 and an intron-exon 2 lariat structure. The second step involves cleavage and removal of the intron from exon 2 and the ligation of exon 1 to exon 2 (Nilsen, 1998, Burge et al., 1999, Black, 2003).

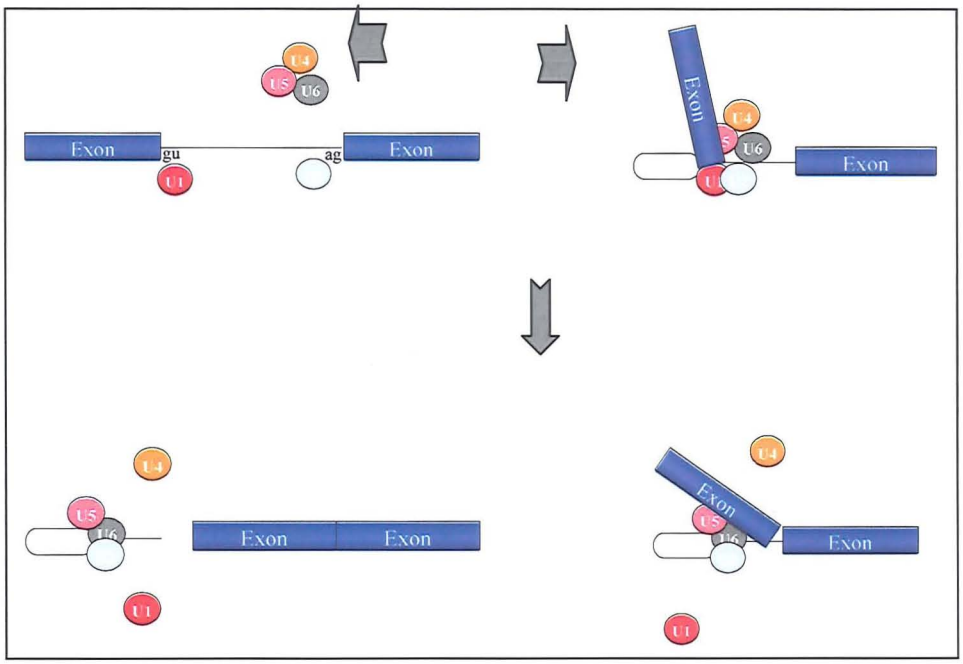

Figure 1.7 Schematic representation of the pre-mRNA-spliceosome interaction during RNA splicing.

The SR proteins are important regulators of the splicing process. Phosphorylated SR proteins such as SF2/ASF, have been shown to help binding of U1 snRNP to the 5' splice site and to constitute a bridge between donor and acceptor splice sites (Wu and Maniatis, 1993, Xiao and Manley, 1997, Xiao and Manley, 1998). Phosphorylation of SR proteins by specific kinases is thought to play a fundamental role in pre-mRNA splicing regulation. It has been suggested that the activation of genes coding for SR protein-specific kinases may be involved in coordinating gene expression during development (Sanford and Bruzik, 1999).

1.4.3 Bioinformatic tools and mRNA splicing

Analysis of human genome has led to the creation of algorithms to assess the quality of exon splice sites by calculating a score. These scoring systems estimate the degree of adherence of the splice site to the consensus sequence, with higher scores suggesting better adherence. One of the most used scoring methods was created by

Shapiro and Senepathy (Shapiro and Senapathy, 1987) and allows the calculation of scores for acceptor, donor and branch sites. Like other *in silico* programs, it reliably predicts disruption of a splice site when one of the invariant dinucleotides at the donor or acceptor sites are substituted, but becomes less reliable the further the nucleotide substitution occurs from the splice sites. Prediction programs are even less helpful in cases of nucleotide substitution occurring at the splice sites of alternative exons. These are, in fact, already characterised by a wider diversion from the consensus sequences compared to constitutively exons (Stamm et al., 2000, Thanaraj and Clark, 2001).

Although most enhancer sequences tend to be either purine- or AC-rich, studies have shown that they highly diverge from consensus sequences, making prediction by means of *in silico* enhancer prediction programs difficult. One of the most used prediction programs, the ESE finder 3.0 (http://rulai.cshl.edu/cgi-bin/tools/ESE3/esefinder.cgi?process=home) uses sequence weight matrices for scoring candidate exonic splicing enhancers (ESE) motifs corresponding to functional consensus sequences of SR proteins, such as SF2/ASF, SC35, SRp55, SRp40 (Cartegni et al., 2003, Smith et al., 2006). Despite the evidence of good correlation between changes in enhancer-predicted scores and the presence of disease (Cartegni and Krainer, 2002, Colapietro et al., 2003) , the reliability of these *in silico* prediction programs has not yet been established and all nucleotide changes modifying an enhancer score should be tested *in vitro*.

Algorithms for the detection of alternative exons have also been developed but are inaccurate due the complexity of the splicing process and the lack of understanding of the location and function of the majority of the regulatory splicing elements. The search for alternative exons relies mainly on the alignment of genomic sequences to expressed sequence tags (ESTs) and on cDNA derived from different tissues, developmental stages and diseases, available from public databases (Gelfand et al., 1999, Kan et al., 2001, Modrek et al., 2001). Different methods, such as microarray and differential hybridization techniques, have been also used, resulting in large-scale identification of cell and tissue specific alternative splicing events (Johnson et al., 2003, Pan et al., 2006).

1.4.4 Aberrant mRNA splicing

Almost 50% of DNA point mutations responsible for human genetic diseases affect the efficiency of mRNA splicing leading to mutant proteins (Lopez-Bigas et al., 2005, Wang and Burge, 2008). A mutation may interfere with the correct mRNA splicing by altering a native splice site or activating a cryptic splice site. The majority of reported splice mutations disrupt the native splice sites, through a base change within the donor or acceptor invariant dinucleotides (Krawczak et al., 1992). The result of these mutations is, in the majority of cases, exon exclusion. Rarely, this event can result in activation of a cryptic splice site (Treisman et al., 1983, Wieringa et al., 1983) or retention of an intron in the mature mRNA (Pequignot et al., 2001, Zhang et al., 2004)

Mutations within other splicing elements, such as the polypyrimidine tract and the branch point, may equally contribute to genetic diseases inducing the exclusion of a constitutive exon or inclusion of an alternative one in the mature mRNA (De Klein et al., 1998, Cartegni et al., 2002).

In recent years, the discovery of the presence of enhancers and silencers within the pre-mRNA, has led to a reconsideration of the role of nucleotide changes, conventionally considered harmless synonymous SNPs, as potential point mutations altering regulatory splicing elements and consequently gene expression (Cartegni et al., 2002, Pagani and Baralle, 2004). Moreover, genetic defects, conventionally classified as nonsense or missense mutations have been re-evaluated as possible splice defects. In this respect, the work by Liu et al. (Liu et al., 2001) has been fundamental. These authors were the first to acknowledge that nucleotide changes in the breast cancer susceptible gene (BRCA1), previously considered nonsense and missense mutations were, instead, splicing defects disrupting exonic enhancers. While splice sites mutations disrupt invariant dinucleotides and their effect can be easily predicted *in silico*, the effect of a base change within an enhancer or silencer is difficult to predict *in silico* and in vitro studies should always be performed. The complexity of splicing regulation and the importance of the exon-surrounding environment, suggests that even single intronic point mutations located distant from an exon should be taken into consideration, since they can lead to aberrant splicing through the alteration of intronic regulatory elements (Buratti et al., 2004). The impact and prevalence of splicing mutations outside the canonical splice sites is still far

from being elucidated, but has attracted increasing interest in view of the potential impact on numerous diseases, including cancer (Kalnina et al., 2005, Venables, 2006).

Another possible mechanism by which a base change can result in aberrant splicing is the creation of a new splice site, which competes with the native one. Rarely, a mutation may occur deep in the intron generating an aberrant splice site that activates a cryptic splice, resulting in the inclusion of a normally untranslated DNA sequence (pseudoexon) (Abeliovich et al., 1992, Pagani et al., 2002).

1.4.5 Pseudoexons

Introns are rich in sequences matching the consensus donor and acceptor splice sites. This suggests the presence in the IVSs of numerous potential exons, which are referred to as pseudoexons. Genome analysis has shown that pseudoexons greatly outnumber constitutive exons. The reasons behind non-inclusion of these pseudoexons in the mature mRNA are still unknown. Comparative analysis of constitutive exons versus pseudoexons has shown that the latter are rich in silencers, have less enhancers and weaker scores for splicing regulatory elements, such as donor and acceptor sites (Fairbrother and Chasin, 2000, Sun and Chasin, 2000, Sironi et al., 2004, Zhang and Chasin, 2004). Moreover, computational analysis has suggested that intronic sequences surrounding the pseudoexons may form a double stranded structure, in which the pseudoexon is included and hidden from the spliceosome (Zhang et al., 2005).

In some cases, subtle changes in the pseudoexon are sufficient to activate it. A single base change can, in fact, create or reinforce donor sites, acceptor sites or other splicing regulatory sequences and lead to recognition of the pseudoexon by the splice machinery and its inclusion in the mature mRNA. These events are generally associated with a disease and examples are the splicing mutations resulting in pseudoexon inclusion observed in patients with GHI, cystic fibrosis, Duchenne muscular dystrophy and ATM among others (Akker et al., 2007).

1.4.6 The antisense-based approach for correction of mRNA splicing

The increasing body of evidence demonstrating the relation between splicing defects and disease has led to the development of new therapeutic tools for the correction of aberrant splicing. Antisense oligonucleotides (ASO) are synthetic RNA molecules of

approximately 10-20 nucleotides, designed to be complementary to a target sequence on the pre-mRNA. The mechanism by which ASOs work is RNase H cleavage-independent and is thought to rely on the physical interference of ASOs in the apposition of spliceosome elements on the target pre-mRNA sequence (Kole and Sazani, 2001). This is in contrast with the antisense-based approach commonly utilised in the gene therapy of cancer, inflammation and viral diseases, which relies on hybridisation of an antisense oligonucleotide to a sense target sequence and the induction of the RNase H cleavage of the RNA:DNA hybrid (Crooke, 2001).

An important requirement for an ASO to be effective is resistance to RNase H degradation. This can be achieved by designing oligonucleotides modified at the 2' hydroxyl group of the ribose, through 2'-O-methylation (Manoharan, 1999). 2'-O-methyl oligonucleotides are commercially available, stable and resistant to RNase H degradation. Other possible modifications at the sugar, base or phosphodiester level have been suggested and successfully tested. Among these, is the addition of a morpholino ring or of an oligoglycine-like structure, such as the peptide nucleic acids (PNA), in the ASO backbone. These modifications have been shown to increase protection from RNase activity and confer better ASO delivery in *in vivo* studies (Stein et al., 1997, Alter et al., 2006).

Recently, the use of ASOs with a bifunctional activity has been suggested to improve the efficiency of aberrant splicing correction. Bifunctional ASOs consist of an RNA sequence complementary to the target pre-mRNA to which a non-complementary tail mimicking an ESE motif (Skordis et al., 2003) or a small peptide resembling the SR protein RS domain (e.g. the exon-specific splicing enhancement by small chimeric effectors, ESSENCE) (Cartegni and Krainer, 2003) is attached.

The use of the antisense oligonucleotide approach has been shown to be a potential therapeutic tool in correcting aberrant splicing. The use of ASOs complementary to pre-mRNA splice sites, branch point or ESEs have been shown to effectively restore aberrant splicing in *in vitro* splicing assays using minigene pre-mRNA or in cell transfection systems. Many studies have, in fact, demonstrated that ASOs can restore exon inclusion or exclusion induced by splice mutations (Dominski and Kole, 1993, Sierakowska et al., 1996, Vacek et al., 2003, van Deutekom and van Ommen, 2003, Hua et al., 2007) and can also be a useful tool in regulating the expression of alternative protein isoforms (Khoo et

al., 2007). Nevertheless, these studies have also shown a dose-dependent effect and the need for testing more than one, often several, ASOs to identify the most effective. Moreover, the use of ASOs has often resulted in unexpected and unwanted products, alongside the desired corrected mRNA. This has been explained by the activation of cryptic splice sites, which may follow the blocking of natural sites. Despite these potential difficulties, studies on animal models (Lu et al., 2005, Alter et al., 2006, Moulton et al., 2007) have been promising, and preliminary trials in humans are ongoing (Takeshima et al., 2006, van Deutekom et al., 2007).

1.5 ORIGINAL HYPOTHESIS AND AIMS OF THE THESIS

The overall aim of this thesis was to study the molecular mechanisms responsible for growth hormone insensitivity and idiopathic short stature and to combine the results with the current knowledge of mRNA splicing with the scope of developing new potential diagnostic tools and applying existing therapeutics to the endocrine field.

The first aim of this thesis was to identify the molecular defects in a large population of children with growth hormone insensitivity and analyse the genotype/phenotype relationship.

Molecular defects causing aberrant mRNA splicing are known to represent approximately 20% of *GHR* defects leading to GHI. Novel *GHR* splice defects causing a functionless GHR and GHI were, therefore, likely to be identified in this large heterogeneous GHI cohort. Nevertheless, the consequences at mRNA level of mutations located in splice elements other than the splice sites, are difficult to predict *in silico* and in these cases patient mRNA analysis becomes mandatory. Since obtaining patient samples for mRNA analysis is often difficult, another aim of this thesis was to assess the potential diagnostic application of an *in vitro* assay to study splice mutations, thus avoiding the need for patient mRNA analysis. The assay was based on a three-exon minigene system spliced in Hela nuclear extracts. A fundamental part of this project was the establishment of a rapid and reliable protocol for the creation of three-exon minigenes. The assay was tested on naturally occurring mutations identified in *GHR* splice elements of GHI patients studied in the course of this Thesis. The results of the *in vitro* assay were compared with the results obtained *in silico* and, where available, *in vivo* from patient mRNA analysis.

The third aim of this thesis was to attempt a translational approach for correcting aberrant *GHR* splicing causing GHI. An antisense-based approach was used *in vitro* and in a cell system on an intronic *GHR* mutation resulting in the activation of a pseudoexon and growth hormone insensitivity.

The last aim of this thesis was to study the effect of single heterozygote mutations in the *IGFALS* of patients with idiopathic short stature. ALS deficiency resulting from homozygous or compound heterozygous *IGFALS* defects is an established cause of GHI.

The observation that parents of ALS deficient patients, obligate carriers of single heterozygous *IGFALS* defects, have mild short stature, although in the absence of biochemical signs of GHI, led us to speculate that single heterozygous *IGFALS* defects may contribute to the pathogenesis of ISS. To test this hypothesis the *IGFALS* was sequenced in a large, ethnically homogeneous, population of ISS children.

CHAPTER 2

MATERIALS AND METHODS

2.1 DNA PREPARATION

2.1.1 DNA extraction from blood samples

Three to 10ml of blood were collected in sodium EDTA tubes. DNA was extracted using the Nucleon Extraction and Purification kit (GE healthcare), according to the manufacturer's recommendations. Briefly, cell lysis was obtained by the addition of four times the volume of blood of a lysis buffer (Reagent A: 10mM Tris-HCl, 320M sucrose, 5mM $MgCl_2$, 1% (v/v) Triton X-100, pH 8.0), followed by mixing and centrifugation at 1300g for 5 min. The pellet was resuspended by adding 2ml of resuspension buffer (Reagent B) and transferred to a 15ml centrifuge tube. Deproteinisation was achieved by adding 500µl of sodium perchlorate solution. For DNA extraction, 2ml of chloroform and 300µl of Nucleon resin were added and the sample centrifuged at 1300g for 3 min, The upper phase was transferred to a clean tube, two volumes of cold absolute ethanol were added and mixed by inversion until the precipitate appeared. Precipitated DNA was hooked out using a heat-sealed Pasteur pipette and redissolved in 100µl of sterile water.

2.1.2 DNA purification from PCR samples

PCR fragments were purified using the QIAquick PCR Purification kit, (Qiagen) according to the manufacturer's recommendations. Briefly, 5 volumes of Buffer PBI (containing guanidine hydrochloride and isopropanol) were added to one volume of the PCR sample and the sample applied to a QIAquick spin column, which contains a silica membrane able to bind the DNA, and centrifuged for 1 min. The flow-through was discarded and 0.75ml of washing buffer (Buffer PE containing ethanol) was added to the column. After 1 min of centrifugation, the flow-through was discarded and the column centrifuged for an additional 1 min. The column was placed in a new microcentrifuge tube and 30µl of sterile water was added to elute the DNA. The column was centrifuged for 1 min and the resulting sample stored at -20°C.

2.1.3 Visualization of DNA products on agarose gel

DNA samples mixed with DNA loading dye (Fermentas) in a ratio 5:1 were loaded into the wells of an agarose gel prepared as described in section 2.5.1 and run along with a DNA marker (GeneRuler DNA ladder mix 0.5µg/µl, Fermentas) at a voltage ranging

from 100 to 200 Volts. DNA products were visualised under ultraviolet light and a photograph taken using the Uvidoc gel documentation system (Uvitec).

2.1.4 DNA purification from agarose gel

The desired DNA fragment was excised from the agarose gel under UV light using a sharp razor blade and subsequently purified using the QIAquick gel extraction kit (Qiagen) according to the manufacturer's recommendations. Briefly, the gel slice was inserted in an Eppendorf tube and weighed. Three volumes of buffer QG (binding and solubilisation buffer containing guanidine thiocyanate) were added to one volume of gel and incubated at 50°C for 10 min to dissolve the gel. Then, one volume of isopropanol was added to the sample and the sample applied to the QIAquick column, which contains a silica membrane able to bind DNA, and centrifuged for 1 min at 13,000 rpm to bind the DNA. 0.75ml of washing buffer (Buffer PE) were added to the QIAquick column and centrifuged for 1 min. The flow-through was discarded and the QIAquick column centrifuged for a further 1 min. The QIAquick column was subsequently placed into a clean 1.5ml microcentrifuge tube and 50µl of sterile water were added to elute the DNA. The column was centrifuged for 1 min and the sample stored at -20°C.

2.1.5 Determination of DNA concentration and purity

DNA concentration was determined by measuring the absorbance (A) at 260 nm (A260) in a spectrophotometer. A 'blank' using 1µl of the buffer in which the DNA was diluted was employed to zero the spectrophotometer and then the absorbance of 1µl of the DNA samples was measured.

The following relationship was used to calculate the DNA concentration: absorbance at 260 nm of a 50µg/ml solution of DNA is equal to 1.

DNA purity was estimated using the ratio of the readings at 260 nm and 280 nm (A260/A280). Pure DNA is expected to have a A260/A280 ratio between 1.8 and 2.

2.2 RNA PREPARATION

2.2.1 RNA extraction from blood

RNA was isolated from human blood using the PAXgene blood RNA Kit and the PAXgene Blood RNA Tubes (PreAnalytic) according to the manufacturer's recommendations. All materials used for RNA extraction were RNase-free. RNA extraction with the PAXgene kit is based on the guanidine thiocyanate method and is schematically presented in Figure 2.1.

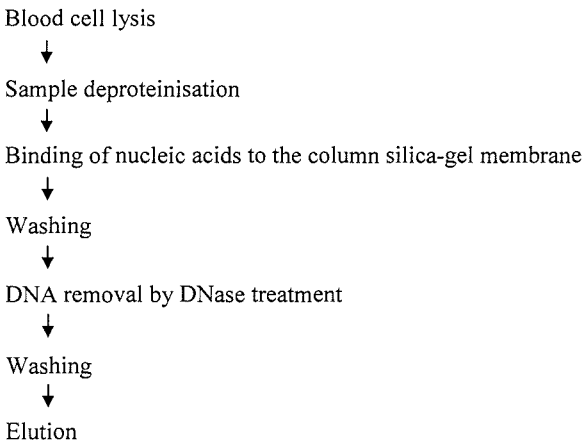

Figure 2.1 RNA purification from blood.

The PAXgene Blood RNA Tubes contain surfactants that stabilise and preserve RNA from degradation, by forming an insoluble ionic complex between the nucleic acids and the surfactant. Briefly, the blood was collected in the PAXgene tube and incubated at room temperature for 48 hours to achieve complete lysis of blood cells. Subsequently the tube was centrifuged for 10 min at 3000 g to pellet the nucleic acids and the supernantant was removed. Four ml of RNase-free water was added to the pellet. The tube was vortexed and centrifuged for 10 min and the supernatant discarded. 350µl of resuspension buffer (Buffer BR1) were added and the tube vortexed to dissolve the pellet. The sample was pipetted into a microcentrifuge tube and 300µl of binding buffer (buffer BR2 containing guanidine thiocyanate) and 40µl of proteinase K added. The tube was mixed by vortexing and incubated for 10 min at 55°C using a shaker-incubator at 400 rpm. The lysate was pipetted into a PAXgene Shredder spin column and centrifuged for 3 min at

13,000 rpm. The supernatant was transferred to a fresh microcentrifuge tube, 350µl of absolute ethanol was added and the contents were mixed by vortexing. 700µl of sample was pipetted into the PAXgene RNA spin column and centrifuged for 1 min at 13,000 rpm. This step was repeated with the remaining sample. Then, 350µl of washing buffer (Buffer BR3 containing guanidine thiocyanate and ethanol) were pipetted into the spin column and centrifuged for 1 min. To digest DNA, 1µl of DNase (5x1000U Turbo DNase, Ambion) and 79µl of buffer RDD (Invitrogen) were pipetted into the spin column. The column was left standing on the bench for 15 min at room temperature before adding 350µl of washing buffer (Buffer BR3) and centrifuging for 1 min. The flow-through was discarded and 500µl of a second washing buffer (Buffer BR4 containing ethanol) pipetted into the column and centrifuged for 1 min. This step was repeated twice. The flow-through was discarded and the spin column placed in a new microcentrifuge tube. To elute the RNA, 40µl of elution buffer (Buffer BR5) was pipetted onto the column and centrifuged for 1 min at 13,000 rpm and this step was repeated twice. (Figure 2.1) Then the eluant was incubated for 5 min at 65°C to denature the RNA and the sample was chilled on ice and immediately stored at -80°C.

2.2.2 RNA extraction from cells

Total RNA was extracted from cultured cells using the RNeasy mini kit (QIAGEN) according to the manufacturer's recommendations. Cells were harvested and disrupted using a guanidine thiocyanate method. The appropriate volume of lysis buffer (Buffer RLT: containing guanidine thiocyanate) was added to the cell culture well (350µl of buffer RLT for less then $5x10^6$ cells). Cells were homogenised by passing the lysate through a 20-gauge needle attached to a sterile syringe at least 10 times. One volume of 70% ethanol was added to homogenise the sample and 700µl of the sample was added to the RNeasy spin column and centrifuged for 15 secs at 13000 rpm. The flow-through was discarded and 350µl of washing buffer (Buffer RW1 containing ethanol) were pipetted into the spin column and centrifuged for 1 min. To digest DNA, 1µl of DNase (Turbo DNase, Ambion) and 79µl of buffer RDD (Invitrogen) were pipetted into the spin column. The column was left standing on the bench for 15 min at room temperature before adding 350µl of wash buffer and centrifuging for 1 min. To wash the column 500µl of washing buffer (Buffer RPE containing ethanol) was added to the column and

the sample centrifuged for 15 secs at 13000 rpm. This step was repeated twice. To elute the RNA, the column was placed in a new 1.5ml collection tube and 30-50µl of RNase-free water was added and the sample centrifuged for 1 min at 13000 rpm. The recovered RNA sample was immediately stored at -80°C.

2.2.3 Visualisation of RNA samples

RNA samples were mixed with RNA dye (see appendix), heated at 96°C for 5 min and then loaded in the wells of an agarose gel prepared as described in section 2.5.1 and run along with a radiolabeled DNA marker (Promega) at a voltage ranging from 100 to 200 Volts. RNA products were visualised under ultraviolet light.

2.2.4 RNA quantification

RNA concentration was determined by measuring the absorbance at 260 nm (A260) in a spectrophotometer using RNase-free cuvettes. The spectrophotometer was zeroed using 1µl of the buffer in which the RNA was diluted and then 1µl of the RNA sample were measured.

The following relationship was used to calculate the RNA concentration:

absorbance at 260 nm of a 40µg/ml solution of single stranded RNA is equal to 1.

RNA purity was estimated using the ratio of the readings at 260 nm and 280 nm (A260/A280). Pure RNA has a (A260/A280) ratio between 1.8 and 2.

2.3 CDNA SYNTHESIS

2.3.1 Reverse Transcription (RT)

Materials:

- RNasin® Ribonuclease Inhibitor (25 U/µl), Promega
- dATP, dTTP, dCTP, dGTP (100 mM) Sigma-Aldrich
- M-MLV 5x Reaction Buffer, Promega
- Moloney murine leukaemia virus reverse transcriptase (M-MLV RT) (200 U/µl) Promega
- Random Primers (0.5µg/µl hexadeoxynucleotides), Promega

All materials used for the first-strand synthesis of cDNA were RNase-free. RNA (2 - 2.5µg) was added to a sterile microcentrifuge tube, together with 0.5µg of random or a specific primer per µg of RNA, and RNase-free water to a total volume ≤ 15µl. The tube was heated at 70°C for 5 min to melt the secondary structure within the template and then immediately placed on ice to prevent secondary structure from reforming.

The following components were thereafter added to the annealed primer/template in the following order:

M-MLV 5x Reaction Buffer	5 µl
dATP 10 mM	1.25µl
dCTP 10 mM	1.25µl
dGTP 10 mM	1.25µl
dTTP 10 mM	1.25µl
RNasin® Ribonuclease Inhibitor	1 µl
M-MLV RT	1 µl
Nuclease-free water to a final volume	25 µl

The sample was mixed and incubated for 60 min at either 37°C for random primers or 42°C for other primers.

2.4 POLYMERASE CHAIN REACTION (PCR)

The polymerase chain reaction was used to amplify genomic DNA and cDNA for sample preparation for sequencing analysis, genotyping, A-tailing of blunt-ended PCR fragments and creation of minigenes for the *in vitro* splicing assay.

Materials:

- dATP, dTTP, dCTP, dGTP (100 mM), Sigma-Aldrich
- *Taq* DNA polymerase (100U, Sigma), or *Phusion* polymerase (100U, Finnzymes)
- 10x Taq polymerase Buffer (Sigma) or 10x Phusion polymerase Buffer (Finnzymes)

PCR reactions were carried out using the relevant primers pairs (sequences reported in Appendix 3). Standard PCR reactions were set up as follows:

Taq polymerase (100U)	0.1µl
10xTaq Polymerase Buffer	1.5µl
dNTP mix (10mM of each dNTP)	0.3µl
Primer 1 (10mM)	0.3µl
Primer 2 (10mM)	0.3µl
DNA (10-100ng/µl)	0.5µl
Distilled H_2O to a total volume	15 µl

PCR reactions for minigene construction were set up as follows:

Phusion polymerase	0.25µl
10x Phusion Polymerase Buffer	5.0 µl
dNTP mix (10mM of each dNTP)	0.25µl
Primer 1 (50mM)	0.25µl
Primer 2 (50mM)	0.25µl
Template DNA (50-200ng)	0.5 µl
Distilled H_2O to a total volume	25.0 µl

The final volume of the PCR mix amplified by *Taq* polymerase was typically 15µl, unless otherwise specified. The final volume of the PCR mix amplified by proof reading polymerase for minigene construction was typically 25µl. Final $MgCl_2$ concentration was typically 1.5mM.

Primer design

Oligonucleotide primers were designed from the published genomic DNA database (www.ensembl.org). Each primer was designed to have, when possible a GC content of 40-60%, and a CG rich terminal dinucleotide to improve annealing. Pairs of primers were designed to have similar melting temperatures. To avoid primer-primer annealing care was taken to avoid the presence of complementary sequences between primers pair.

Radiolabelling of PCR reaction

PCR reactions were radiolabelled by adding 0.05 μCi of α-^{32}P dCTP (9.25 MBq, Perkin-Elmer, Wellesley, MA) to the reaction.

Thermocycling conditions

Cycling conditions were as follows:

One denaturing cycle of 2 min at 95°C (if *Taq* Polymerase was used) or 98 °C (if *Phusion* Polymerase was used), followed by 25-35 cycles of steps 1 to 3:

1) denaturation for 30 sec at 95°C (*Taq* Polymerase) or 98°C (*Phusion* Polymerase),
2) annealing temperature (optimised according to primers) for 30 sec,
3) extension at 72°C for 30 sec,

and a final cycle of 5 min at 72°C.

PCR reactions were optimised by varying the annealing temperature by 2-5 °C.

2.4.1 A-tailing reaction for blunt-ended PCR fragments

PCR reactions were set up as follows and had a final volume of 25μl :

Purified PCR product (50-200 ng)	10 μl
dATP (10 mM)	1 μl
Taq DNA Polymerase	0.2μl
10x Reaction Buffer	2.5μl
deionized H_2O	11.3μl

Cycling conditions: 1 cycle at 95°C for 30 sec, 2 cycle of: 95°C for 30 sec, 55°C for 30 sec and 72°C for 30 sec, 1 cycle at 72°C for 2 min.

2.4.2 Sequencing

Direct sequencing of PCR products was performed using the ABI Prism Big Dye Sequencing kit and the ABI 3700 automated DNA/RNA Sequencer (Applied Biosystems), an automated capillary gel electrophoresis system available at the Genome Centre of the William Harvey Research Institute. Data were collected with the Data Collection Software 2.0 and results analysed with the BioEdit Sequence analysis software version 7.

2.5 ELECTROPHORESIS

2.5.1 Agarose gel for nucleic acid visualisation

Agarose gels, ranging in concentration from 1 to 2% were prepared according to the size of the DNA fragments to be visualized. To make a 1% gel, 1g of agarose (Sigma) was mixed with 100ml of 0.5xTAE (National Diagnostic) and heated in the microwave until the gel dissolved. After cooling to approximately 60°C, 1µl of ethidium bromide (5.25mg/ml in H_2O, Sigma) was added to the gel,mixed and poured into a gel electrophoresis cast and combs inserted to obtain wells. Once set, the gel was placed in a gel tank filled with 0.5xTAE buffer.

2.5.2 Preparation of denaturing polyacrylamide gels for splicing assays

Materials:

All reagents were from Sequagel Ultrapure, National Diagnostics

- Concentrate: 237.5g acrylamide, 12.5g methylene bisacrylamide and 7.5M urea in a deionized aqueous solution;
- Diluent: 7.5M urea in deionized water;
- Buffer: 0.89M Tris-Borate-20mM EDTA buffer pH 8.3 (10x TBE) and 7.5M urea.

According to the required percentage of polyacrylamide gel, the following reagents were used:

- to obtain an 8% gel: 10ml of buffer, 32ml of concentrate and 58ml of diluent to make a total of 100ml solution,

- to obtain a 4% polyacrylamide gel: 10ml of buffer, 16ml of concentrate and 74ml of diluent to make a total of 100ml solution.

Immediately before use, 4µl of TEMED (n,n,n',n'-tetramethylenediamine, Sigma) and 100µl of 10% Ammonium persulphate (Sigma) were added to 10ml of the above solutions and mixed thoroughly by inversion. The mixture was then poured into a 20cm x 20cm x 2mm supporting glass gel plate and a comb inserted. The gel was left to set at room temperature for at least 1 hour.

2.5.3 Preparation of denaturing polyacrylamide gels for genotyping

Materials

- 5% GENE-PAGE plus 6M Urea (Acrylamides 5%, Urea 6M, Tris 0.089M, Boric Acid 0.089M, EDTA 0.002M, Amresco),
- TEMED ((n,n,n′,n′-tetramethylenediamine, Sigma)
- 10% Ammonium Persulphate (Sigma)
- 10xTBE (composition in Appendix)

Polyacrylamide gels were prepared as follows: 36cm gel plates were cleaned with tap water, rinsed with copious amounts of deionised water and left to air dry. Plates were assembled with 0.2mm teflon spacers and clamped into a gel frame. To make up a 5% gel, 25ml of the 5% GENE-PAGE plus 6M Urea were used. 15µl of TEMED and 150µl of 10% ammonium persulphate (10% APS) were added immediately before pouring the gel. Gels were left to set at room temperature for at least 2 hours then pre-run at 900 Volt for 20 min. To make up a 8% polyacrylamide gel, 4ml of 30% polyacrylamide gel were mixed with 1.5ml of 1xTBE and 9.5ml of deionised water. 5.25µl of TEMED and 240µl of 10% ammonium persulphate were added, the gel mixed and immediately poured into clean glass gel plates. A comb was inserted and the gel was left to set for at least 1 hour. Gels were pre-run for 20 min at 900 Volt.

2.5.4 Preparation of non-denaturing polyacrylamide gels

Materials

- 30% (w/v) acrylamide/methylene bisacrylamide solution (37.5:1 ratio, National Diagostics)
- TEMED (n,n,n′,n′-tetramethylenediamine, Sigma)
- 10% Ammonium Persulphate (Sigma)
- 10xTBE (composition in Appendix)

To make up a 8% polyacrylamide gel, 3.99ml of 30% acrylamide solution were mixed with 1.5ml of 1xTBE and 9.51ml of deionised water. 5.25µl of TEMED and 240µl of 10% ammonium persulphate were added immediately before pouring the gel into

cleaned supporting gel glasses. A comb inserted and the gel was left to set for at least 1 hours. Gels were pre-run for 20 min at 700 Volt.

2.6 CLONING OF PCR PRODUCTS

The pGEM T-easy vector system was used for cloning in bacteria cell lines. The pcDNA 3.1 vector, characterised by a cytomegalovirus (CMV) promoter was chosen for transfection of eukaryotic mammalian cell lines.

2.6.1 Preparation of Ligation reactions

Ligations were set up using the pGEM T-easy Vector System (Promega) or pcDNA 3.1 expression vector (Invitrogen). The following reagents were added into a 0.5ml tube in the following order:

	Standard Reaction	Positive control
2x rapid ligation buffer	5µl	5µl
Vector pGEM-T easy (50 ng/µl), or pcDNA3.1 (100 ng/µl)	xµl	xµl
PCR product	x µl	-
Control insert DNA (4 ng/µl)	-	2µl
T4 DNA ligase (3 Weiss units/µl)	1µl	1µl
Deionised water to make a final volume	10 µl	10µl

The amount of PCR product (ng) to add was calculated using the formula:

(ng of vector x kb insert size) / kb vector size x insert:vector molar ratio

The ratio insert/vector was typically 2:1 for the pGEM T-easy and 1:4 for the pcDNA 3.1 vector. Reactions were mixed by pipetting and incubated for 2 hours at room temperature.

Ligation reactions were optimised by:

a) varying the insert/vector ratio (e.g. 1:1 and 3:1);
b) incubating the ligation reactions overnight at 4°C.

2.6.2 Preparation of Ampicillin culture plates

Materials:

- Agar (Sigma)
- LB broth (Sigma)
- Ampicillin (Sigma)
- IPTG (isopropyl-beta-D-thiogalactopyranoside) [Promega]
- X-gal (5-bromo-4-chloro-3-indolyl-b-D-galactopyranoside) [Promega]

7g of Agar were added to 8g of LB broth and made up to 400ml with deionised water and autoclaved. After cooling to 50°C, 4ml of 10mg/ml ampicillin was added per 400ml of LB agar and then poured in 85mm petri dishes using a sterile field created by a lit bunsen burner. Once hardened 100µl of IPTG (200 mM) and 50µl of X-gal (50 mg/ml) were added to each plate and smoothed over the surface using a sterile spreader.

2.6.3 Transformation

Materials:

- Competent cells JM109 High Efficiency (Promega)
- SOC medium (Invitrogen)

Competent cells were removed from –70°C storage and placed in an ice bath to thaw. The tube containing the ligation was centrifuged. Two µl of reaction and 50µl of competent cells were added to a sterile 1.5ml microcentrifuge tube and left on ice for 20 min. The cells were heat-shocked for 50 sec in a water bath at exactly 42°C and then immediately returned on ice for 2 min. 950µl of SOC medium was added to each tube and reactions were incubated for 1.5 hours at 37°C with shaking (150 rpm). 100µl of each transformation culture were plated onto duplicate LB/ampicillin/IPTG/X-Gal plates by smoothing over the surface with a sterile spreader. Plates were incubated overnight (16-18 hours) at 37°C.

2.6.4 Colony selection

The pGEM-T easy vector contains a multiple cloning region within the alpha-peptide coding region for the enzyme beta-galactosidase. Bacteria with a functional beta-

galactosidase enzyme convert substrates such as X-gal, to a blue product and appear as blue colonies. Insertion of the PCR product disrupts the beta galactosidase sequence and bacteria appear as white colonies. The plates were checked after overnight incubation and white colonies were picked using sterile pipette tips. Individual colonies were cultured overnight in 5ml LB Broth medium (composition in Appendix 2) containing ampicillin (final concentration 100μg/ml).

2.6.5 Isolation of Plasmid DNA

The 5ml cell cultures were pelleted by centrifugation for 10 min at 1300 g and the supernatant discarded. Minipreparation of plasmid DNA was obtained using the Qiagen plasmid mini kit (Qiagen) that uses the modified alkaline lysis method of Birnboim and Doly (Sambrook et al., 1989). Briefly, pelleted bacterial cells were resuspended in 250μl of resuspension buffer (Buffer P1: 50 mM TrisCl [pH 8.0], 10mM EDTA, 100μg/ml RNase A) and 250μl of lysis buffer (Buffer P2: 200 mM NaOH, 1% SDS) and mixed. The lysate was neutralised and adjusted to high-salt binding conditions by the addition of 350μl of neutralising buffer (Buffer N3, contains guanidine hydrochloride and acetic acid). The tube was then centrifuged for 10 min to precipitate proteins. The supernatant containing the plasmid DNA, was applied to the QIAprep silica membrane spin column and centrifuged for 30 sec at 13000rpm. The flow through was discarded, and the spin column washed by adding 0.5ml of buffer PB (wash buffer PB contains guanidine hydrochloride and isopropanol) and centrifuged for 60 sec. The flow-through was discarded and 0.75ml of buffer PE (buffer PE contains 99% ethanol) was added to the column and centrifuged for 60 sec. The flow through was discarded and the column was centrifuged for an additional 1 min to remove any remaining wash buffer. The DNA was eluted using 50μl of sterile distilled water and stored at -80C.

2.6.6 Subcloning

Parent (pGEM T-easy vector) and destination (pcDNA 3.1 vector) expression vectors were checked for the presence of common restriction sites in their multiple cloning sites (Figure 2.2). The insert product was released from the parent vector using a single digestion, purified and ligated into the destination vector and the ligation reaction transformed into competent bacterial cells. Transformed cells were screened for the presence of the insert by direct sequencing.

Restriction digestion

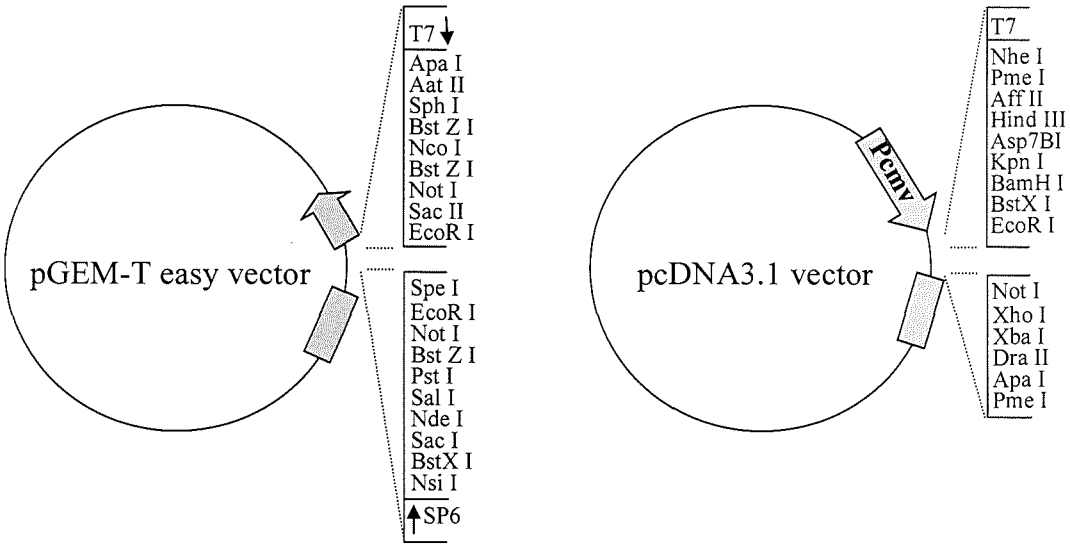

Figure 2.2 pGEM T-easy and pcDNA 3.1 vector maps.

Restriction enzymes EcoR1 (Promega) or Not1 (Promega) were selected for single digestion of parental vector and used with Buffer D (Promega). Standard digestion reactions were set up as follows:

DNA (1-2μg)	xμl
Restriction enzyme (10 U)	1μl
10x buffer	2μl
Deionised water to a final volume	20μl

Digestion reactions were incubated overnight at 37°C in order to maximise digestion of parental vector. To avoid self-recircularisation of vectors that had been cut with only one restriction enzyme, a dephosphorylation step was performed. 1μl of calf alkaline phosphatase (1U/μl, Promega) was added and the reaction was incubated at 37°C for 1 hour. Reactions were subsequently run on a 1% agarose gel. The band corresponding to the released insert product size was cut from the gel and purified by standard DNA purification from gel as described in section 2.1.4. Purified insert was ligated in pcDNA 3.1 vector by standard ligation reaction as described in section 2.6.1.

2.7 SITE-DIRECTED MUTAGENESIS

Site-directed mutagenesis was performed according to the principles of the Stratagene QuikChange ® kit.

Materials:

- *Pfu* Turbo DNA polymerase (2.5 U/µl),
- 10x reaction buffer
- *Dpn* I restriction enzyme (10 U/µl)
- dNTP mix (Promega)
- specific primers

Two mutagenic primers, complementary to opposite strands of the target sequence in the insert, were designed (see appendix). The desired base change was located in the middle of the primer with 10-15 bases of unaltered sequence on either side. The primers were designed to have a melting temperature of 78°C and a GC content of at least 40 %. The reaction was set up as follows :

dsDNA template (recommended dsDNA concentration ranging from 5 to 50 ng)	1-5 µl
10x reaction buffer	5 µl
oligonucleotide primer 1 (100 ng/µl)	1.25µl
oligonucleotide primer 2 (100 ng/µl)	1.25µl
dNTPs mix	1 µl

and distilled water to a final volume of 50µl.

1µl of *Pfu* Turbo DNA polymerase (2.5 U/µl) was then added.

Cycling parameters were:

Segment	Cycles	Temperature	Time
1	1	95°C	30 sec
2	12-18	95°C	30 sec
55°C	1 min		
68°C	1 min/Kb of plasmid length		

The number of cycles in segment 2 was dependent upon the type of mutational change required, as described below:

Type of mutation	Number of cycles
Point mutations	12
Single amino acid change	16
Multiple amino acid deletions or insertions	18

The reaction was then placed on ice for 2 min to cool. 1µl of *Dpn* I restriction enzyme (10 U/µl) was added and the reaction was centrifuged for 1 min before being incubated at 37°C for 1 hour to digest the parental supercoiled dsDNA. 1µl of *Dpn* I-treated reaction was transformed into JM109 High Efficiency Competent cells. Transformation was carried out according to the method previously described in section 2.6.3.

2.8 *IN VITRO* SPLICING ASSAY

2.8.1 DNA constructs for the *in vitro* splicing assay

No well characterised protocol was available for the creation of the three-exon minigenes and several optimisations were performed, as described below. The three-exon minigene constructs were generated by inserting the *GHR* exon of interest and its flanking introns in a well characterised splicing reporter derived from the Adenovirus Major Late first (L1) and second (L2) leader exons (Adml-par, a gift from Prof Chew, genomic sequence reported in Appendix 7). The L1 and L2 exons were amplified by PCR using specific primers (sequences reported in Appendix 3: 10.3.4). The *GHR* exon of interest was amplified by PCR using specific forward and reverse primers (sequences reported in Appendix 3: 10.3.4) of approximately 30 bases designed to have a 10 base overlap with L1 and L2 sequences, respectively. The *GHR* exon PCR fragments were inserted in between Adml-par exons L1 and L2 by two rounds of overlap-extension proof-reading PCR (Ho et al., 1989), using specific primers. The fusion of the exons relies on the annealing of the overlapping ends of the two PCR products that will then function as primers for the 3' extension of the complementary strand

Optimisation of overlap extension PCR

PCR reactions for overlap extension were optimised by:

a) varying the annealing temperature of identical PCR reactions by 5°C in the range 35°C - 55°C,
b) varying the concentrations of the PCR products for the second PCR round,
c) varying the number of exons included in the reaction; either
   including all three exons in a one-step reaction, or
   annealing the *GHR* exon to exon L1 and the resulting product to L2 in a two-step reaction,
d) varying the order of exon annealing, either
   step1: GHR exon and L1, step 2: GHRexon/L1 and L2, or
   step1: GHR exon and L2, step 2: GHRexon/L2 and L1,
e) varying primer concentrations.

The second round of overlap PCR always generated non-specific products along with the desired one. PCR products of the correct size were excised from the agarose gel, purified and sequenced. PCR products were modified using the A-tailing procedure, as described below, before being cloned into pGEM T-easy vector, as described in section 2.4.1.

2.8.2 RNA extraction from denaturing polyacrylamide gels

The desired ^{32}P-labelled RNA fragment was excised from the denaturing polyacrylamide gel (prepared as described in section 2.5.2) using a sharp razor blade. To identify the band of interest, fluorescent markers were apposed on the gel prior to autoradiography. RNA bands were excised from the gel and incubated overnight with 400µl of elution buffer (0.5M Sodium acetate pH 5.2, 1mM EDTA, 0.2% SDS). The eluate was transferred to a fresh tube. To optimise the recovery of RNA, 10 mg/ml of glycogen was added to the sample before washing with 1ml of 100% ethanol. The reaction was centrifuged for 15 min and the supernatant removed. 1ml of 70% ethanol was added to the pellet and the reaction centrifuged for 15 min. RNA was redissolved in 10µl of DEPc treated H_2O and stored at -20°C.

2.8.3 *In vitro* transcription

DNA minigene PCR products were transcribed into mRNA and labelled with a radioactive isotope by the incorporation of α-^{32}P labeled GTP (9.25 MBq, Perkin-Elmer, Wellesley, MA) using the following protocol:

DNA	1µl
10x Transcription Buffer (Ambion)	1µl
NTPs (ATP,CTP,UTP 5mM, Promega)	1µl
RNA CAP (New England Biolabs)	1µl
T7 RNA Polymerase Plus 20U/µl (Ambion)	1µl
^{32}P-GTP	xµl (corresponding to 10 µCi)

RNAse free water to a final volume of 10µl.

Reactions were incubated at 37°C for 1 hour. Ten µl of RNA loading dye (composition in Appendix 2) was added to each sample. Reactions were denatured at 98°C for 5 min and then run on a 4% polyacrylamide gel for 45 min.

2.8.4 Standard *in vitro* Splicing Reaction

Materials:

- 25xATP/CP mixture: 12.5mM ATP (Promega), 0.5M creatine phosphate (Calbiochem)
- $MgCl_2$ (80 mM)
- 13% Polyvinyl alcohol (PVA) (Sigma)
- 0.4 M Hepes-KOH, pH 7.3 (Sigma)
- Buffer D (20mM Hepes-KOH (pH 8.0), 100 mM KCl, 0.2 mM EDTA, 20% glycerol, 0.5 mM PMSF, 1 mM DTT).
- HeLa Nuclear extracts (Cilbiotech)

A splicing master mix was set on ice as follows:

25xATP/CP	0.5	µl
MgCl2 (80 mM)	0.5	µl
13% PVA	2.5	µl
Hepes (0.4 M)	0.625	µl
RNA (10 fmol)	x	µl
Buffer D	3.5	µl
Nuclear extracts	4	µl

RNAse free water to a final volume of 12.5µl

Reactions were incubated at 30°C from 20 min to 120 min and control reactions were set up and incubated on ice for the same time.

Deproteinisation, precipitation and visualisation of mRNA splicing products

At the end of the incubation time 200µl of stop solution (3M Sodium acetate pH 5.2, 10% SDS, 25µg/ml tRNA, dH_2O to a final volume of 50µl) and 200µl of Tris-saturated Phenol (Invitrogen) were added to each reaction for deproteinisation. Samples were vortexed for 2 min and then centrifuged for 10 min. The aqueous phase containing the RNA was transferred into a fresh tube with 470µl of 100% ethanol, vortexed, kept on ice for 5 min and then centrifuged for 15 min to pellet the RNA. The supernatant was carefully removed and discarded without disturbing the pellet. The pellet was then washed using 470µl of 70% ethanol. The sample was vortexed, kept on ice for 5 min and

then centrifuged for 15 min to pellet the RNA. The supernatant was carefully removed and discarded without disturbing the pellet and 3.5µl of RNA loading dye mixture added. Reactions were denatured for 5 min at 98°C and then loaded into the wells of a 4% denaturing polyacrylamide gel prepared as described in section 2.5.2. The gel was run for approximately 2 hours at 950 V in 1xTBE buffer (Sigma) before autoradiography.

2.8.5 Autoradiography

Autoradiography was used to obtain images of polyacrylamide gels resulting from *in vitro* splicing assays. Films, placed on wet polyacrylamide gels wrapped in Saran wrap were put inside a sealed cassette and exposed at -80 °C for 3-16 hours depending upon the strength of the signal. Films were then developed using an automated developing system (Compact X4, Xograph Imaging System, UK).

2.9 SIZE EXCLUSION CHROMATOGRAPHY

Materials

- IGF-I (10 μg, Invitrogen)
- Disuccinimidyl suberate (Sigma Aldrich)
- 1M Tris HCl (Sigma)
- Buffer A (composition reported in Appendix 2)

2.9.1 Iodination of IGF-I

IGF-I iodination was carried out by Dr R Edwards at the NETRIA laboratories of St Bartholomew's Hospital using a standard chloramine T iodination procedure.

2.9.2 The HiPrep 16/60 Sephacryl S-200HR column

The HiPrep 16/60 Sephacryl S-200HR column (Amersham Biosciences, GE Healthcare, USA), a prepacked gel filtration column (column volume 120ml), was used for the size exclusion chromatography assay. The column was equilibrated for first-time use with 60ml of distilled water and run at a flow rate of 0.5ml/min. 240ml of buffer A (composition in Appendix 2) was then run at a flow rate of 1ml/min. After each run the column was regenerated using 120ml of buffer A run at a flow rate of 0.8ml/min.

Protein separation and peak distribution on the HiPrep 16/60 Sephacryl S-200HR column was first assessed by running the following proteins of known molecular weight: bovine IgG (150 kDa), albumin from bovine serum (66 kDa), carbonic anhydrase from bovine erythrocytes (29 kDa) and aprotinin from bovine lung (6.5 kDa). 1.5mg of each protein was added to 500ml of buffer A and the solution run on the Sephacryl column at a flow rate of 1ml/10min. The elution of the standard proteins was measured by reading the 1ml fractions at 280nM using a spectrophotometer.

2.9.3 Size Exclusion chromatography assay

Samples were fractioned on a HiPrep 16/60 Sephacryl S-200HR column. Serum samples (100μl) were incubated overnight at 22°C with $3.5x10^6$ counts per minute of ^{125}I-labeled IGF-I and buffer A to a final volume of 500μl. Reactions were then cross-linked with 5mM disuccinimidyl suberate (Sigma Aldrich). After 30min incubation at 22°C, the

cross-linking reaction was stopped by the addition of 1M Tris HCl. The reactions were loaded into the column and run overnight at a flow rate of 1ml per 10 min. One ml fractions were collected and the amount of ^{125}I-labeled IGF-I in each fraction assessed by using a gamma counter.

Calculation of ^{125}I IGF-I incorporation in the ternary complex

Incorporation of ^{125}I-labeled IGF-I in the ternary complex was calculated according to the following formula:

(sum of iodine counts per minute in the ternary complex / total iodine count per minute) x100

2.10 SPLICING PREDICTION PROGRAMS

Splicing prediction programs that are freely available on the web were used for the *in silico* analysis of nucleotide changes occurring in the DNA of patients with GHI or ISS and to create an algorithm to search for *GHR* alternative exons.

Nucleotide changes occurring at donor or acceptor splice sites, within exons or at the branch point were studied using the Alex Dong Li's splice site finder (http://violin.genet.sickkids.on.ca/~ali/), an *in silico* prediction program that calculates the scores of donor, acceptor and branch sequences using an algorithm based on that created by Shapiro and Senapathy (Shapiro and Senapathy, 1987).

To search for the alteration/creation of exonic enhancers the ESE finder 3.0 (http://rulai.cshl.edu/cgi-bin/tools/ESE3/esefinder.cgi?process=home) was utilised. This uses sequence weight matrices for scoring candidate ESE motifs corresponding to functional consensus sequences of SR proteins, such as SF2/ASF, SC35, SRp55, SRp40 (Cartegni et al., 2003, Smith et al., 2006).

No valid prediction programs for silencers are currently available.

The scores threshold used to predict the occurrence of a splicing event by the *in silico* programs, were those set up by default by the authors, unless otherwise specified.

2.11 STATISTICAL ANALYSIS

Statistical analyses were performed using R version 2.6.2 (R Development Core Team, 2008, R Foundation for Statistical Computing, Vienna, Austria). Numerical variables were expressed as median (range), with the exception of ^{125}I IGF-I incorporation in the ternary complex which was expressed as mean ± standard deviation. Categorical variables were expressed as number (percent). Comparison between continuous variables was performed using Wilcoxon's rank sum test. Comparison between categorical variables was performed using Fisher's exact test. A two-sided p-value <0.05 was considered indicative of statistical significance.

CHAPTER 3

GENETIC CHARACTERISATION OF PRIMARY GHI

3.1 BACKGROUND

Primary or genetic growth hormone insensitivity (GHI) is a rare condition, phenotypically resembling GH deficiency, but differing from it through high levels of circulating GH. It is caused by genetic defects of the GH–IGF-1 axis and has to be differentiated from secondary or acquired GHI, in which conditions such as malnutrition, liver disease and catabolic illness result in GH resistance (Laron et al., 1993, Laron, 1999).

In its most severe form, primary GHI is known as classical GHI or Laron syndrome. Intrauterine growth is not affected, although birth weight and length may be marginally subnormal. However, postnatal linear growth failure is typically observed, with a severe and rapid decline in growth velocity. If untreated, adult stature is 4-10 standard deviation scores (SDS) below the mean for age and sex (Gluckman et al., 1992). The cardinal biochemical features of GHI are normal or increased GH levels associated with low IGF-I, IGFBP-3 and ALS levels. Patients are resistant to treatment with exogenous GH and fail to generate GH-dependent proteins during the IGF-I generation test. Patients with classical Laron syndrome display a characteristic mid-facial hypoplasia due to underdeveloped sphenoid and mandible. The nose is small, with depressed bridge and the forehead is protruding. Hair is sparse with temporal and frontal recession. GHBP levels are typically low or undetectable (Laron, 1999, Laron, 2004).

Primary GHI can present in a less severe form known as non-classical GHI. Patients present with normal facial appearance and less impaired longitudinal growth. GHBP levels are typically normal or high (Woods and Savage, 1996).

The first report of GHI of genetic origin came from Dr Zvi Laron in 1966 (Laron et al., 1966) with the demonstration of a lack of binding of GH to GHRs obtained from liver membranes of GHI patients. Since then, more than 250 patients with primary GHI have been identified worldwide. GHI is generally transmitted as an autosomal recessive disorder and is usually observed in populations with high consanguinity. Almost all GHI patients in whom a molecular defect has been identified have a mutation in the *GHR* (Woods et al., 1997).

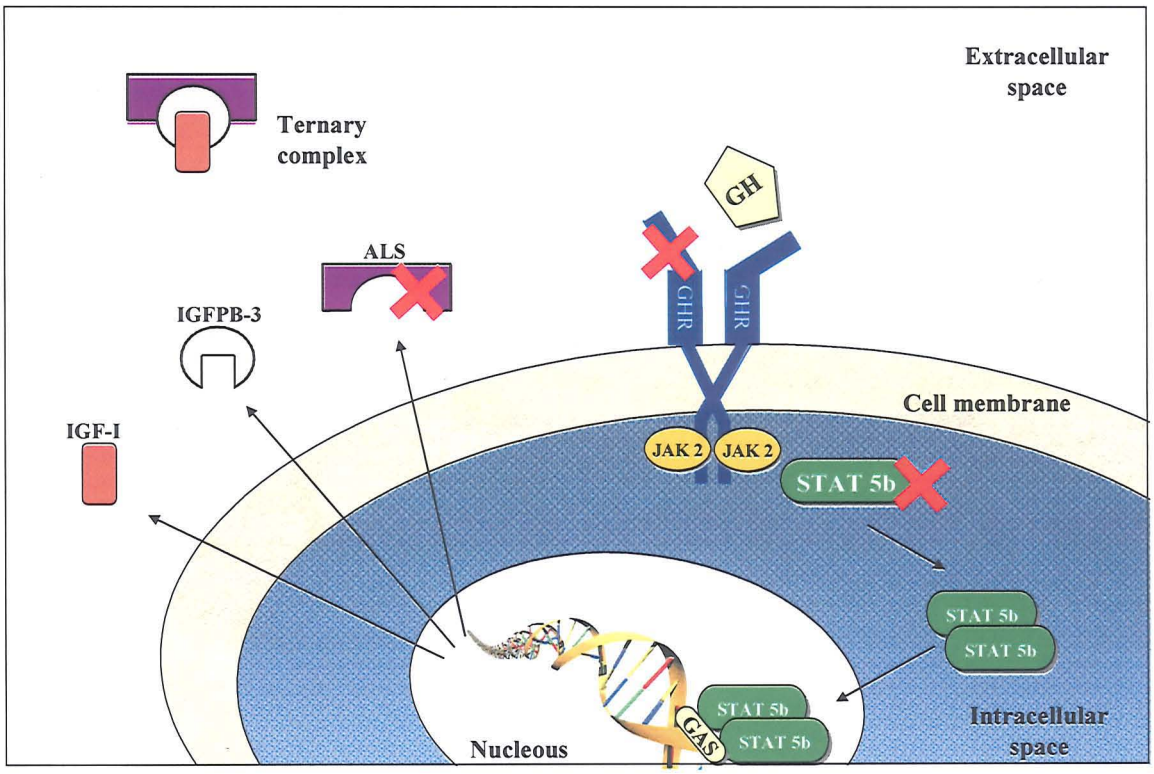

Figure 3.1 GH signalling and ternary complex formation. Proteins of the GH-IGF-I axis, in which the presence of a genetic defect results in GHI, are indicated with a red cross.

The vast majority of *GHR* defects are recessively inherited either in homozygous or compound heterozygous forms and range from exon deletions to a variety of point mutations including missense, nonsense, splice and frameshift mutations. Nearly all reported molecular defects in the *GHR* occur in the region encoding the extracellular domain of the receptor and result in classical Laron syndrome. Many of these molecular defects have a common pathogenetic mechanism, resulting in either total absence of the GHR or presence of a defective receptor, which lacks GH-binding capacity, hence the low or absent circulating GHBP levels (David et al., 2005).

Mutations in the *GHR* regions coding for the transmembrane and intracellular domain are less frequent. Patients with such defects have non-classical GHI. Their GHBP levels are normal or high, reflecting the presence of an intact extracellular GHR domain. Two such defects in the intracellular GHR domain located at the splice sites of exon 9 are of particular interest because they are the only example of *GHR* defects with a dominant negative effect (Ayling et al., 1997, Iida et al., 1998). The truncated mutant GHR

resulting from these mutations can form a heterodimer with the wild type GHR inhibiting the effect of the normal GHR protein (Iida et al., 1999).

In addition to the *GHR*, another two defective genes in the GH-IGF-I axis, namely *STAT5b* and *IGFALS,* have been involved in the pathogenesis of GHI (Figure 3.1). In 2003 Kofoed et al. reported the first *STAT5b* defect. The mutation led to a mutant protein that could not be activated by GH, thus failing to activate gene transcription (Kofoed et al., 2003). The patient had all the signs of classical GHI, with the addition of immunodeficiency, consistent with a non-functional STAT5b protein. In 2004 Domene' et al. reported the first *IGFALS* defect resulting in a frameshift and the appearance of a premature stop codon. The patient had a biochemical profile suggestive of severe GHI despite a mild short stature. Delayed puberty was also reported (Domene et al., 2004).

To date, more then 60 different mutations have been found in the *GHR.* Nevertheless, identification of novel defects and their characterisation can bring new insight into the physiology of this protein. Moreover, the relationship between different *GHR* mutations and the severity of GHI, as well as the relation between defects in different genes and the severity of GHI remains unclear.

3.2 HYPOTHESIS AND AIMS

The aim of this study was: 1) to perform a genetic analysis of a large population of patients with primary GHI from different ethnic backgrounds; 2) to define a relationship between *GHR* defects and the GHI phenotype by pooling data from the GHI cohort presented in this study, data from another large genetically heterogeneous population reported in the European Pharmacia and Upjohn Treatment Study Group published by Woods et al. in 1997 and data from the two studies on *GHR* dominant negative mutations; 3) to analyse the auxological and biochemical data from GHI patients with *IGFALS* defects identified in this study and compare their phenotype to that arising from *GHR* defects.

3.3 STUDY POPULATION

The majority of patients included in this study were recruited as part of an international collaboration led by Dr Cecilia Camacho-Hubner at St. Bartholomew Hospital London, UK, to study the effect of the recombinant IGF-I/IGFBP-3 compound (rhIGF-I/rhIGFBP-3, Insmed Incorporated, NASDAQ:INSM) on children with primary growth hormone insensitivity. Patients followed in the Paediatric Endocrine Unit at the Royal London Hospital, London, UK were also included in the study.

Patients in this study were growth hormone insensitive, defined as severe postnatal short stature associated with normal or high GH levels and low basal IGF-I levels failing to rise in response to administration of exogenous GH. Exclusion criteria were the presence of chronic illnesses or endocrine diseases possibly leading to acquired growth hormone insensitivity.

Informed consent was obtained from all patients and their parents. Ethical approval was obtained by individual centres recruiting patients. Height and weight were measured using standard anthropometric techniques (Cameron, 2002) and were converted into SDS. Pubertal status was assessed according to the criteria of Tanner (Marshall and Tanner, 1969, Marshall and Tanner, 1970). Boys were considered prepubertal if genitalia were stage 1 and testicular volume was <4 ml (Zachmann et al., 1974). Girls were prepubertal if breast development was stage 1 (Marshall and Tanner, 1969).

3.4 MATERIALS AND METHODS

3.4.1 PCR and sequencing

Genomic DNA was extracted from peripheral blood leucocytes. *GHR* coding exons, including the pseudoexon 6Ψ, and their intronic boundaries were amplified by polymerase chain reaction (PCR) using specific primers (primer sequences reported in Appendix 3: 10.3.1). Cycling conditions were 95°C for 5 min (1 cycle); 95°C for 30 secs, 55°C for 30 secs and 72°C for 30 secs (30 cycles); and 72°C for 5 min.

IGFALS coding exons and their intronic boundaries were amplified by PCR using specific primers (sequences reproted in Appendix 3: 10.3.3). Cycling conditions were 95°C for 5 min (1 cycle); 95°C for 30 secs, 63°C for 30 secs and 72°C for 30 secs (35 cycles); and 72°C for 5 min.

STAT5b genetic analysis was performed by Dr V. Hwa in the Department of Paediatrics, Oregon Health and Science University, Portland, Oregon, US.

PCR products were visualised on 1% agarose gel and sequenced using the ABI Prism Big Dye Sequencing kit and an ABI 3700 automated DNA sequencer (Applied Biosystems), in accordance with the manufacturer's instructions.

3.4.2 RNA extraction and RT-PCR

RNA was extracted from patients' leucocytes using the PAXgene blood RNA Kit as described in Materials and Methods (section 2.2.1) and used for cDNA synthesis. The standard RT-PCR technique was used to amplify cDNA using specific primer pairs (sequences reported in Appendix). To improve the specificity and sensitivity of the PCR technique, the *GHR* was amplified using a hemi-nested PCR technique. Briefly, 1µl from the first PCR reaction was used in a second 12.5µl PCR reaction and amplified with a second set of primers, one of which corresponded to the primer used in the first PCR reaction, and the second primer annealed within the first round PCR product. PCR products were visualised on 1% agarose gel and sequenced.

3.4.3 Genotyping

Genotyping was performed using two types of genetic marker: dinucleotide repeats and single nucleotide polymorphisms (SNPs).

Dinucleotide repeats

Dinucleotide repeats occur throughout the genome and can cosegregate with a nearby gene of interest. Different numbers of repeats can be identified by PCR across the region as they result in PCR fragments of different lengths whose size can be resolved by polyacrylamide gel electrophoresis. The dinucleotide markers were selected on the basis of their proximity to the *GHR* locus. Characteristics of dinucleotide repeat markers utilised in this study are according to Ensembl database (www.ensembl.org) and are reported in Table 3.1. Their position relative to the *GHR* locus is presented in Figure 3.2.

TABLE 3.1 CHARACTERISTICS OF DINUCLEOTIDE REPEAT MARKERS UTILIZED IN THIS STUDY

Marker	Heterozygosity index	No.of Alleles	Distance to GHR (Mb)	Size of PCR product (bp)
D5s2021	0.57	4	-4.6	113-119
D5s2022	0.73	9	-2.5	220-240
D5s430	0.67	8	-1.0	256-270
D5s2082	0.55	4	-0.4	186-200
D5s2087	0.76	6	+1.8	248-260
D5s474	0.63	6	+12.5	87-97

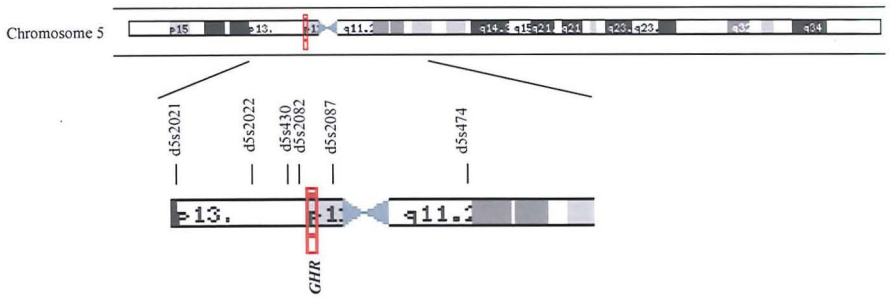

Figure 3.2 Dinucleotide repeat markers position relative to the *GHR* locus.

Dinucleotide repeat markers were amplified from genomic DNA by PCR using specific pairs of primers (sequences reported in Appendix 3: 10.3.8) one of each pair was labelled at its 5' end with a fluorescent moiety. PCR products were denatured and electrophoresed as follows:

0.5µl of each sample was mixed with 0.5µl of loading dye (Applied Biosystem) and 0.25µl of a size marker (GeneScan 500 ROX, Applied Biosystems), incubated at 95°C for 2 min to denature the DNA and immediately chilled on ice. Samples were then loaded into the wells of a 5% denaturating polyacrylamide gel (prepared as described in section 2.5.3) and electrophoresed for 2 hours at 2.5 kV. Results were analyzed using Genescan and Genotyper software (Perkin Elmer Applied Biosystems, UK). If the PCR had failed or the results were not interpretable, the PCR was repeated and the sample rerun.

Single Nucleotide Polymorphisms (SNPs)

Single Nucleotide Polymorphisms (SNPs) are single base variations that occur throughout the genome. Different patterns of SNPs in and around a gene can be used to create genotypes in a similar manner to microsatellite markers. Analysis of six SNPs in intron 9 of the *GHR* has identified 6 haplotypes (Amselem et al., 1989) and they are presented in Appendix 6. In this study we utilised these SNPs to establish the genotypes for GHI patients with identical mutations. PCR reactions were set up using specific primers (sequences reported in Appendix 3:10.3.1) to amplify the *GHR* intron 9. PCR products were checked by running on an agarose gel and analysed by direct sequencing.

3.4.4 Size exclusion chromatography

Samples were fractioned on a HiPrep 16/60 Sephacryl S-200HR column according to the protocol described in Materials and Methods (section 2.9.3). Briefly, serum sample (100µl) was incubated overnight at 22°C with $3.5x10^6$ counts per minute of ^{125}I-labeled IGF-I and was then cross-linked with 5mM disuccinimidyl suberate (Sigma Aldrich). After 30 min, the reaction was stopped by adding 1M Tris HCl. Five hundred microliters were loaded onto the column and one-milliliter fractions were collected and counted.

3.4.5 Biochemical assessment

Serum IGF-I, IGFBP-3, ALS and GHBP were measured from venous blood samples, using enzyme-linked immunosorbent assays (ELISA kit; Diagnostic System Laboratories, Inc. Webster, TX, USA), by Dr F. Miraki-Moud in the laboratories of Dr C. Camacho-Hubner at Barts and the London.

For IGF-I, assay sensitivity was 0.03ng/ml. The intra- and inter-assay coefficients of variation were 8.6% and 6.8% for mean serum concentrations of 104 and 90ng/ml, respectively. For IGFBP-3, assay sensitivity was 0.04ng/ml. Mean intra- and inter-assay coefficients of variation were 7.2% and 8.3%, respectively. For ALS, assay sensitivity was 0.7ng/ml and inter-assay coefficient of variation was 8%. For GHBP the assay sensitivity was 1.69pmol/l. The inter-assay coefficient of variation was 8.4%.

Normal values for IGF-I, IGFBP-3 and ALS were obtained from Diagnostic System Laboratories and used to calculate SDS. Since IGF-I and IGFBP-3 are not normally distributed, values were converted to their normal logarithm. For the purpose of the analysis, undetectable values were arbitrarily substituted for the values immediately below the assay sensitivity (e.g. undetectable IGF-I levels were considered = 0.02ng/ml).

3.4.6 Statistical analysis

Statistical analyses were performed using R version 2.6.2 (R Development Core Team, 2008, R Foundation for Statistical Computing, Vienna, Austria). Numerical variables were expressed as median (range). Comparison between continuous variables was performed using the Student's t-test. A two-sided p-value <0.05 was considered indicative of statistical significance. Bonferroni adjustment was performed to reduce the likelihood of type I error.

3.5 RESULTS

3.5.1 Auxological and biochemical characteristics of the GHI population

Fifty three patients (27 females, 26 males) were included in the study. Median age was 8 years (range 0.5 to 21 years) and median height SDS was –6.00 (-2.45 to -9.36). Median IGF-I SDS was -6.36 (-0.05 to -17.67) and median IGFBP-3 SDS was -8.35 (-0.49 to -24.61).

3.5.2 Genetic analysis

All GHI patients were initially screened for the presence of mutations in the *GHR*, since defects in this gene are the most common cause of congenital GHI. After exclusion of mutations in *GHR* coding exons, pseudoexon 6Ψ and their intron/exon boundaries by direct sequencing, genetic screening was performed according to the following flowchart:

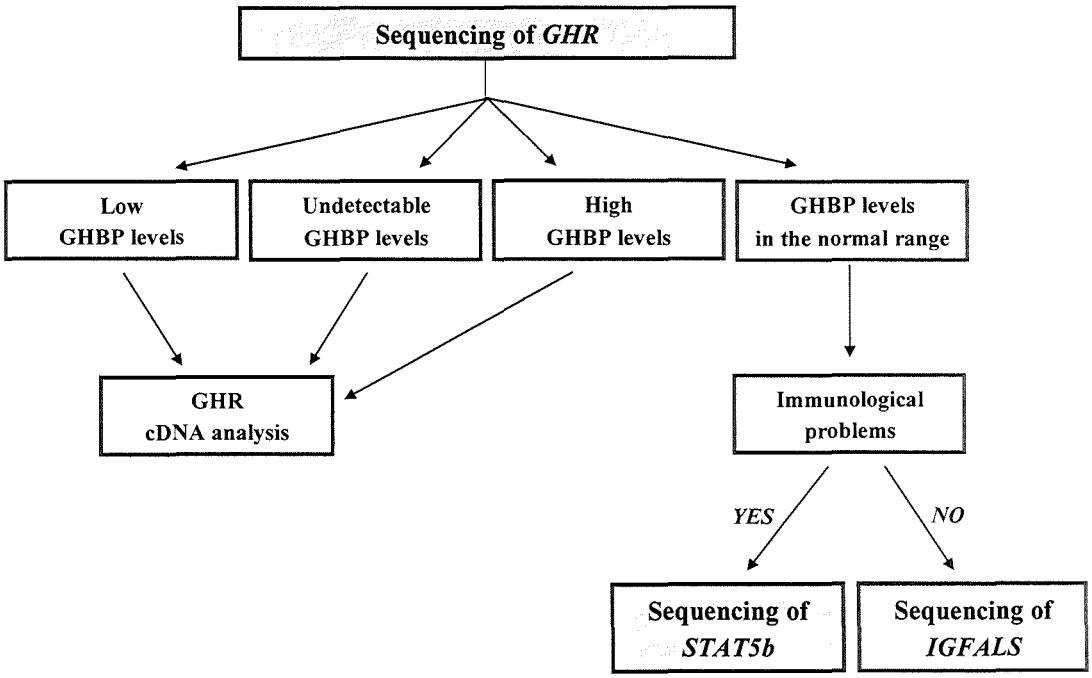

Direct sequencing of the *GHR* led to the identification of 15 different genetic defects in 38 out of 53 GHI patients (Table 3.2). Among the identified mutations, two

nonsense (C48X and Q216X), one missense (L229P) and 2 splice mutations (IVS7 as-6 T to A and IVS9 ds+2 C to T) were novel (Figure 3.3) and their characterisation is presented in this Chapter.

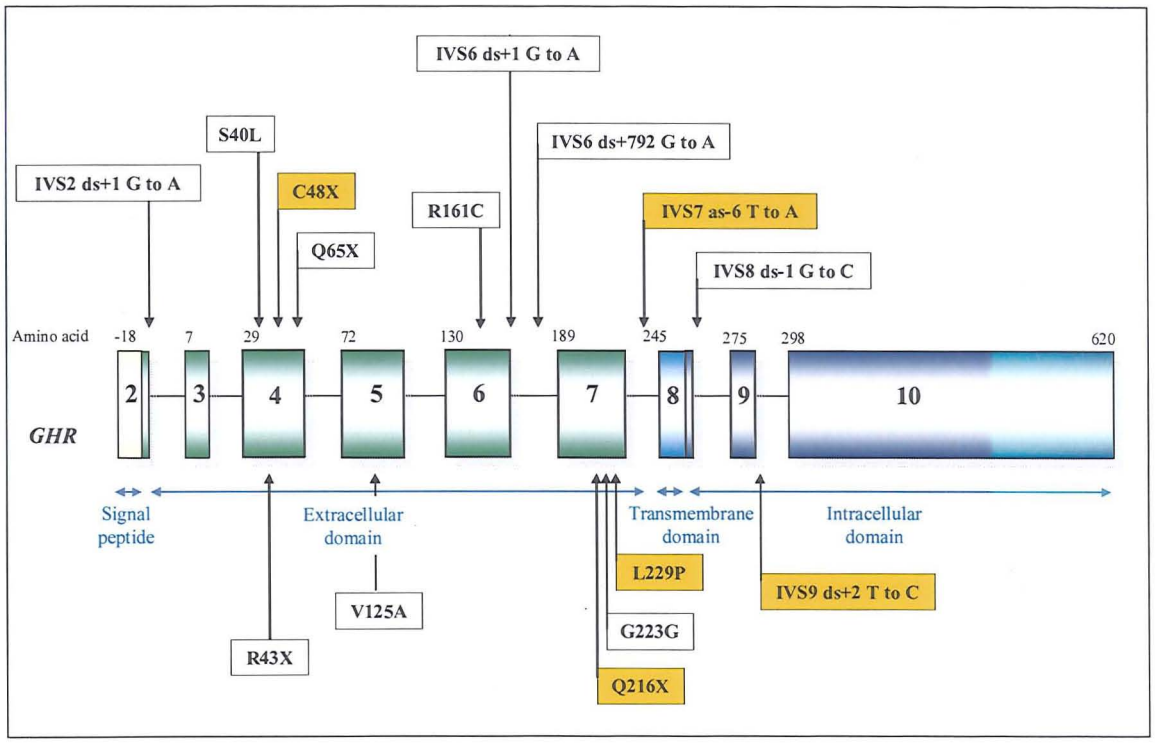

Figure 3.3 Mutations identified in the *GHR* of the GHI population. Novel defects are highlighted in orange boxes.

In 15 patients, no defects in the *GHR* were found. Six out of 15 patients (patients 39-44, Table 3.2) had normal GHBP levels. In two sisters with immunological problems (patients 39 and 40, Table 3.2), a novel *STAT5b* defect (del G at 1680) was found in collaboration with the Dept of Paediatrics, Portland, Oregon, US. Five novel *IGFALS* defects were found in 4 unrelated patients (patients 41-44, Table 3.2). The clinical details of these patients and characterisation of the *STAT5b* and *IGFALS* defects are presented later in this Chapter.

Four out of the 15 patients with no defects in the *GHR* coding region (patients 45-48, Table 3.2) had undetectable GHBP levels indicative of a deleterious defect in the *GHR*. In one of these (patient 45, Table 3.2) a single heterozygous *GHR* deleterious splice defect (C to T at mRNA position 723 leading to the activation of a cryptic splice site in exon 7, also known as G223G) was found. The same heterozygous defect was

identified in his mother who had normal stature. Even though this patient is likely to be a *GHR* compound heterozygote, DNA and cDNA analysis did not reveal a second mutation.

Five out of the 15 patients with no defects in the *GHR* coding region (patients 49-53, Table 3.2) had low GHBP levels (range 41-135 pmol/l) suggesting the presence of a deleterious *GHR* defect. All patients were of the same origin (Kuwait) and belonged to 4 families, two of which were known to be related. A novel homozygous A to C base change in IVS2 ds+4 was found in all subjects. Their parents were heterozygous for this defect. cDNA analysis revealed no GHR products. The occurrence of aberrant splicing from the IVS2 ds+4 base change was studied with the *in vitro* splicing assay, the results of which are presented in Chapter 4. No aberrant splicing was demonstrated and this base change is likely to be a novel SNP.

TABLE 3.2 CLINICAL CHARACTERISTICS AND GENETIC DEFECTS OF THE GHI POPULATION.

	Patient	Sex	Age (yrs)	Ht SDS	Pubertal stage	Gene	Mutation	Homozygosity
Patients with a genetic diagnosis	1	M	15.9	-4.86	IV	***GHR***	IVS2 ds+1 G to A	yes
	2	F	8.1	-6.78	I	***GHR***	IVS2 ds+1 G to A	yes
	3	F	9.0	-9.28	I	***GHR***	S40L	yes
	4	F	18.2	-5.55	IV	***GHR***	S40L	yes
	5	M	11.6	-8.57	I	***GHR***	S40L	yes
	6	F	7.2	-8.45	I	***GHR***	S40L	yes
	7	F	5.6	-9.00	I	***GHR***	S40L	yes
	8	M	13.5	-7.55	I	***GHR***	S40L	yes
	9	F	3.7	-7.15	I	***GHR***	S40L	yes
	10	F	11.5	-7.88	I	***GHR***	R43X	yes
	11	F	8.3	-8.10	I	***GHR***	R43X	yes
	12	F	7.9	-8.78	I	***GHR***	R43X	yes
	13	M	6.2	-6.13	I	***GHR***	R43X	yes
	14	M	7.2	-8.91	I	***GHR***	R43X	yes
	15	F	16.9	-6.89	IV	***GHR***	R43X	yes
	16	M	13.7	-9.36	I	***GHR***	R43X	yes
	17	M	2.4	-7.68	I	***GHR***	C48X	yes
	18	M	14.3	-8.36	I	***GHR***	C48X	yes
	19	F	0.7	< -4.00	I	***GHR***	Q65X	yes
	20	M	9.1	-4.06	I	***GHR***	V125A	yes
	21	M	5.1	-5.04	I	***GHR***	V125A	yes
	22	F	2.0	-6.72	I	***GHR***	R161C	yes
	23	F	6.4	-6.00	I	***GHR***	IVS6 ds+1 G to A	yes
	24	M	21.0	-5.00	V	***GHR***	IVS6 ds+792 A to G	yes
	25	M	6.0	-3.40	I	***GHR***	IVS6 ds+792 A to G	yes
	26	M	11.0	-4.60	II	***GHR***	IVS6 ds+792 A to G	yes
	27	F	7.0	-3.30	I	***GHR***	IVS6 ds+792 A to G	yes
	28	F	13.0	-3.50	IV	***GHR***	IVS6 ds+792 A to G	yes
	29	F	8.0	-5.97	I	***GHR***	IVS6 ds+792 A to G	yes
	30	F	7.0	-4.98	I	***GHR***	IVS6 ds+792 A to G	yes
	31	M	8.4	-8.74	I	***GHR***	Q216X	yes
	32	F	2.2	-4.46	I	***GHR***	G223G	yes
	33	M	5.8	-7.66	I	***GHR***	L229P	yes
	34	M	1.5	-6.00	I	***GHR***	IVS7 as-6 T to A	yes
	35	M	10.4	-7.13	I	***GHR***	IVS8 ds-1 G to C	yes
	36	F	12.4	-4.57	I	***GHR***	IVS8 ds-1 G to C	yes
	37	F	7.2	-7.11	I	***GHR***	IVS8 ds-1 G to C	yes
	38	F	12.0	-4.30	I	***GHR***	IVS9 ds+2 T to C	no
	39	F	4.0	-5.58	I	***STAT 5b***	G del at 1680	yes
	40	F	2.2	-5.81	I	***STAT 5b***	G del at 1680	yes
	41	M	13.4	-3.20	II	***IGFALS***	P73L	yes
	42	M	10.6	-2.82	I	***IGFALS***	L134Q and A ins at 546	no
	43	M	12.9	-2.45	I	***IGFALS***	D440N	yes
	44	M	11.9	-2.66	I	***IGFALS***	T ins at 1490	yes
Patients without a genetic diagnosis	45	M	1.8	-6.93	I	*GHR*	G223G	no
	46	M	0.5	-4.92	I	n.k.	n.a.	n.a.
	47	M	3.8	-7.82	I	n.k.	n.a.	n.a.
	48	F	9.7	-5.44	I	n.k.	n.a.	n.a.
	49	F	n.a.	< -4.00	I	n.k.	n.a.	n.a.
	50	F	n.a.	< -4.00	I	n.k.	n.a.	n.a.
	51	M	n.a.	< -4.00	I	n.k.	n.a.	n.a.
	52	M	n.a.	< -4.00	I	n.k.	n.a.	n.a.
	53	M	n.a.	< -4.00	I	n.k.	n.a.	n.a.

3.5.3 Identification and characterisation of novel *GHR* defects

Five of the 15 defects identified in the *GHR* of these GHI patients were novel. Their characterisation, as well as the clinical details of the patients in whom these defects were identified, are presented below.

3.5.3.1 Mutation C48X

This mutation was identified in 2 Argentinean brothers of 2 and 14 years with severe GHI, from a consanguineous marriage (patients 17 and 18, Table 3.2). They presented with short stature (-7.68 and -8.36 SDS for age and sex, respectively) and typical Laron facial features. They both had low IGF-I levels [undetectable (normal range per age and sex 20-158ng/ml) and 9ng/ml (n.r. 109-1471ng/ml), respectively], low IGFBP-3 levels [0.4mg/l (n.r. 1.2-3.7mg/l) and 0.6mg/l (n.r. 1.3-9.7 mg/ml), respectively] and undetectable ALS levels. GHBP levels were also undetectable. Sequencing of the *GHR* gene revealed the presence of a homozygous base change from C to A in exon 4 at position 197, in both patients (Figure 3.4).

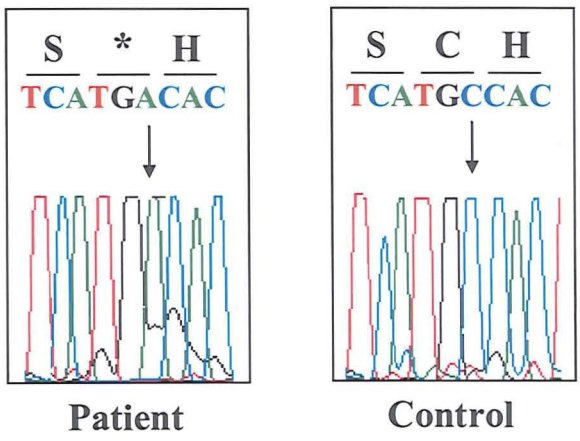

Figure 3.4 Chromatograms showing partial DNA and amino acid sequences from patients with the *GHR* C48X mutation and a normal control. The position of the C to A base change is indicated by the arrow. The stop codon is depicted with an asterisk.

This mutation leads to the creation of a premature stop codon at residue 48 (C48X). The resulting GHR protein is truncated prematurely and lacks most of the extracellular, transmembrane and intracellular domains.

3.5.3.2 Mutation Q216X

This mutation was identified in a Turkish 8-year-old patient with severe GHI from a consanguineous marriage (Patient 31 in Table 3.2). He presented with short stature (-8.74 SDS for age and sex) and typical Laron facial features. He had low IGF-I levels [5.1ng/ml (n.r. 77-374ng/ml)], low IGFBP-3 levels [0.3mg/l (n.r. 2.3-5.1ng/ml)] and undetectable ALS levels (n.r. 24.1-11.1mg/l). GHBP levels were undetectable. Sequencing of the *GHR* gene demonstrated a homozygous base change from C to T in exon 7 at position 699 (Figure 3.5).

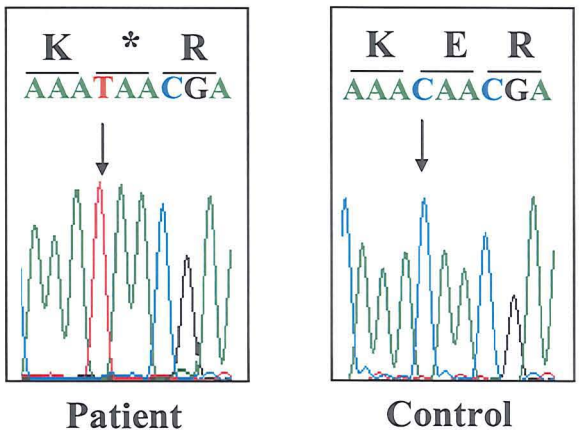

Figure 3.5 Chromatograms showing partial DNA and amino acid sequences for the patient with the *GHR* Q216X mutation and a normal control. The position of the C to T base change is indicated by the arrow. The stop codon is depicted with an asterisk.

This mutation, like the previous one, creates a premature stop codon at residue 216 (Q216X) leading to a prematurely truncated GHR protein, which lacks the last 48 residues of the extracellular domain and all of the transmembrane and intracellular domains.

3.5.3.3 Mutation L229P

This mutation was identified in 5.8-year-old Pakistani patient with severe GHI (patient 33, Table 3.2), who was the product of a consanguineous marriage. He presented with severe short stature (-7.66 SDS for age and sex) and typical Laron facial features. He had undetectable IGF-I levels (n.r. 37-257ng/ml), low IGFBP-3 levels [0.2mg/l (n.r.

1.8-3.9ng/ml)] and low ALS levels [0.3mg/l (n.r. 8.8-21.1mg/l)] GHBP levels were undetectable. Sequencing of the *GHR* gene revealed the presence of a homozygous base change from T to C in exon 7 at position 739 (Figure 3.6).

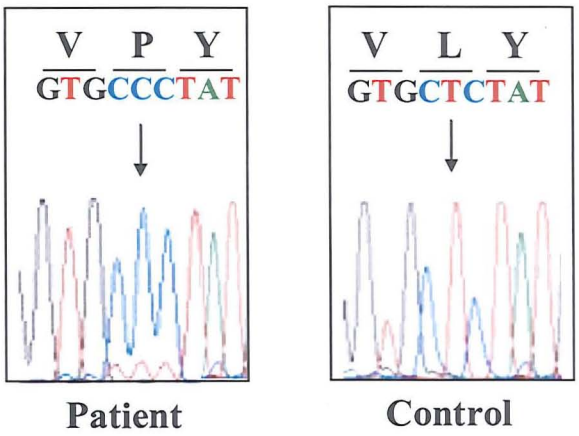

Figure 3.6 Chromatograms showing partial DNA and amino acid sequences for the patient with the GHR L229P mutation and a normal control. The position of the T to C base change is indicated by the arrow.

This base change results in a leucine to proline change at residue 229 (L229P). Leucine and proline have similar properties (they are neutral, non-polar amino acids), but different chemical structures. Leucine has a hydrophobic aliphatic side chain, which favours formation of α-helices, whereas proline has a cyclic structure that does not. Because of these chemical differences, a leucine to proline substitution is likely to induce a change in the GHR protein structure leading to a non-functional receptor.

3.5.3.4 Mutation IVS7 as-6 T to A

This mutation was identified in a 1.5-year-old patient with severe GHI from a consanguineous marriage (Patient 34 in Table 3.2). He presented with severe short stature (-6.00 SDS for age and sex) and typical Laron facial features. He had low IGF-I levels [4ng/ml (n.r. 8-141ng/ml)] and low IGFBP-3 levels [0.35mg/l (n.r. 1.1-3.8mg/ml)].

Sequencing of the *GHR* gene revealed the presence of homozygous T to A base change at the acceptor splice site of intron 7, position –6. In both parents, the same mutation was present in heterozygosity (Figure 3.7).

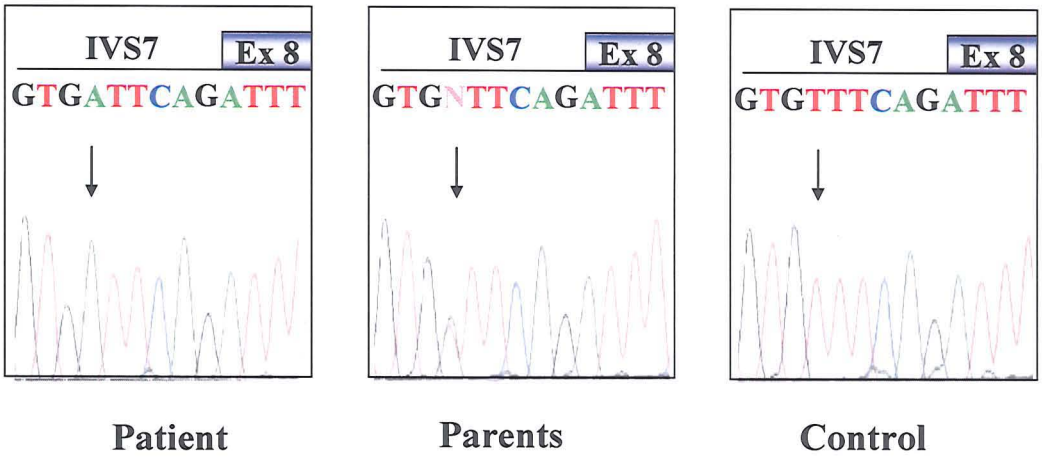

Figure 3.7 *GHR* polypyrimidine tract mutation IVS7 as-6 T to A. Chromatograms showing partial DNA sequences for the patient, his parents and the normal control are presented. The position of the mutation is indicated by the arrows.

This base change is localised in the polypyrimidine tract of intron 7 and is thought to alter the correct splicing of the GHR pre-mRNA. Its deleterious effect was studied and confirmed *in vitro* and results are presented in Chapter 4 of this Thesis.

3.5.3.5 Mutation IVS9 ds+2 T to C

This mutation was identified in heterozygosity in a 12-year-old Spanish patient from non-consanguineous marriage (patient 38, Table 3.2). She presented with short stature (-4.30 SDS for age and sex) and normal facial features. She had low IGF-I levels [43ng/ml (n.r. 126-1188ng/ml)], low IGFBP-3 levels [0.87mg/l (n.r. 2.0-9.3ng/ml)] and low ALS levels [7.4mg/l (n.r. 14-29mg/l)]. GHBP levels were extremely high [35634 pmol/l (normal adult range 534-5785pmol/l)].

Sequencing of the *GHR* revealed the presence of a T to C base change, on one allele, at the donor splice site of intron 9, position +2. No other mutations were detected in the *GHR* exons and their flanking introns. Further investigation revealed the presence of short stature in another two family members, namely the patient's mother and maternal grandfather. Sequencing of the *GHR* revealed the presence of the same single heterozygous mutation, identified in the patient, in both family members (Figure 3.8).

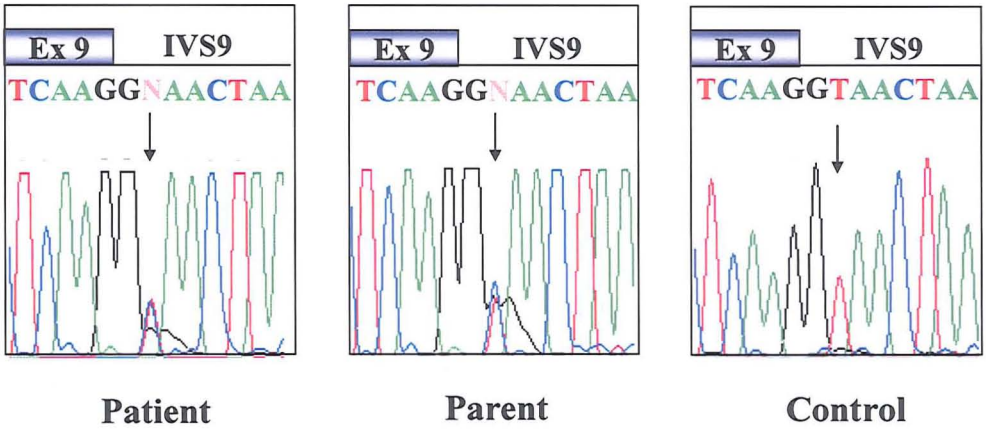

Figure 3.8 *GHR* mutation IVS9 ds+2 T to C. Chromatograms showing partial sequences from the patient, her mother and a normal control. The position of the mutation is indicated by the arrow.

This mutation abolishes the donor splice site of exon 9 and is likely to cause its skipping. RNA was extracted from peripheral leukocytes from the patient and a normal control and cDNA was synthesised. A first round of RT-PCR was performed using primers from exon 2 (primer 2FiGHRm, sequence reported in Appendix 3) to exon 10 (6RGHRm) and from exon 6 (6FGHRm) to exon 10 (10R3GHRm). These products were heminested using primers from exon 2 (2FfGHRm) to 6 (9RGHRm) and from exon 6 (6FGHRm) to 10 (6RGHRm) or from exon 8 (8FGHRm) to 10 (10R3GHRm), respectively. Results are shown in Figure 3.9.

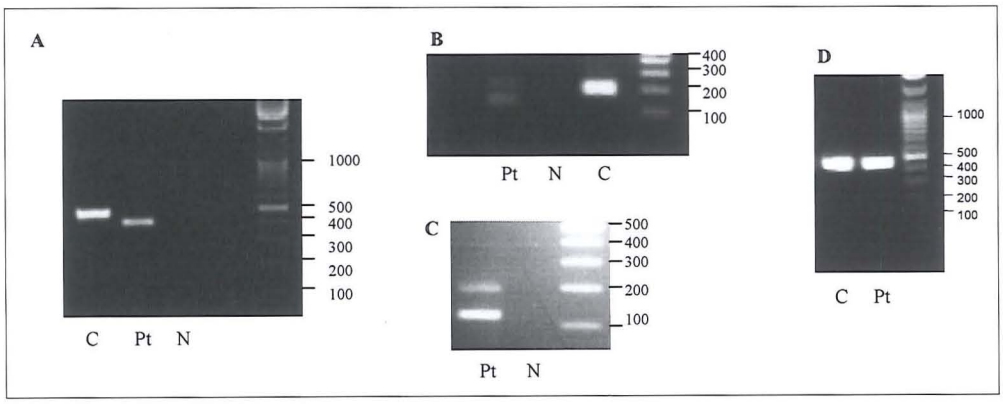

Figure 3.9 RT-PCR products from patient with the *GHR* IVS9 ds+2 T to C mutation. Panel A: RT-PCR products using primers from exon 6 to 10. The expected product size is 474 bp. Panel B: RT-PCR products using primers from exon 8 to 10. The expected product size is 187 bp. Panel C: a larger sample (20µl) of the RT-PCR product presented in panel B better demonstrates the presence of two products (187 bp and 117 bp). Panel D, RT-PCR products using primers from exon 2 to 6. Expected product size (452 bp). C, normal control; Pt, patient; N, negative control.

cDNA amplification using primers from exon 2 to 6 resulted in a product of the expected size from both patient and normal control. The heminested RT-PCR product using primers from exon 6 to 10 produced a band of the expected size (474 bp) from the normal control and a single smaller band (404 bp) from the patient, consistent with the skipping of exon 9 (70bp). Since no product from the patient's normal allele was detected, a different set of primers (from exon 8 to 10), which produce a shorter product, was used. cDNA amplification produced a band of the expected size (187 bp) alongside a smaller band of 117 bp. A single band of the expected size (187 bp) was obtained from the normal control. All RT-PCR products were gel extracted and sequenced, demonstrating the absence of exon 9 in the bands of 404 bp and 117 bp, with exon 8 splicing into exon 10 (Figure 3.10).

```
Patient   TTATTATCTT TGGAATATTT GGGCTAACAG TGATGCTATT TGTATTCTTA
Control   TTATTATCTT TGGAATATTT GGGCTAACAG TGATGCTATT TGTATTCTTA

Patient   TTTTCTAAAC AGCAAAG------ ---------- ---------- ----------
Control   TTTTCTAAAC AGCAAAGGAT TAAAATGCTG ATTCTGCCCC CAGTTCCAGT

Patient   ---------- ---------- ---------- ----------GAA GGAAAATTAG
Control   TCCAAAGATT AAAGGAATCG ATCCAGATCT CCTCAAGGAA GGAAAATTAG

Patient   AGGAGGTGAA CACAATCTTA GCCATTCATG ATAGCTATAA ACCCGAATTC
Control   AGGAGGTGAA CACAATCTTA GCCATTCATG ATAGCTATAA ACCCGAATTC
```

Figure 3.10 Partial cDNA sequences from the patient *GHR* IVS9 ds+2 T to C mutation and a control showing the skipping of exon 9.

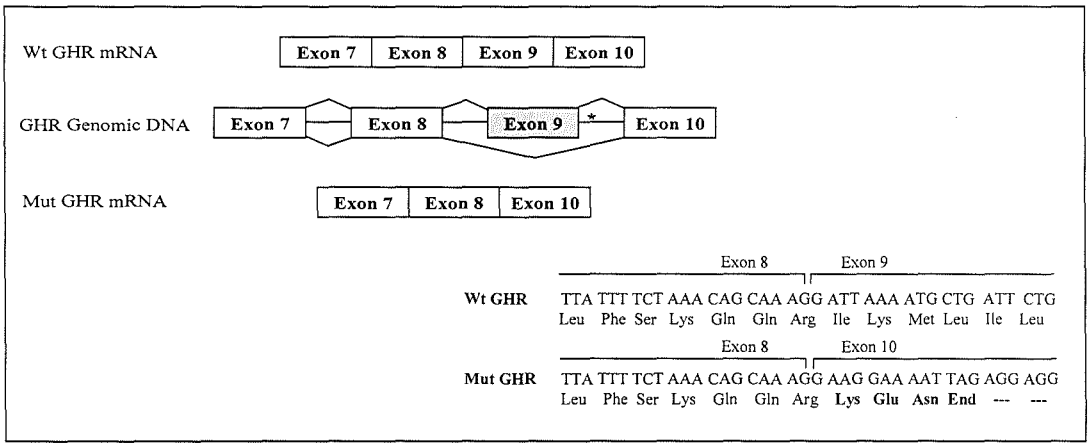

Figure 3.11 The *GHR* IVS9 ds+2 T to C mutation. On the left, normal and aberrant splicing is indicated. Mutation position is indicated by the asterisk. On the right, wild type (Wt GHR) and mutant (Mut GHR) GHR DNA sequences and translated products are shown. The splice junctions between exons are also indicated.

Skipping of exon 9 results in a frameshift, the appearance of three new amino acids and a premature stop codon (Figure 3.11). The resulting GHR protein is truncated prematurely and lacks 98% of the intracellular domain .

3.5.3.6 The Turkish cohort

Twenty one GHI patients in this study were from Turkey. One (patient 31, Table 3.2) was homozygous for the novel *GHR* Q216X mutation already described and one (patient 43, Table 3.2) for a novel *IGFALS* defect, presented later in this Chapter. In three patients with undetectable GHBP levels (patients 46-48, Table 3.2), no *GHR* mutation has yet been found.

The remaining 16 GHI patients were homozygous for one of the following deleterious mutations: R43X (7 patients), S40L (7 patients) or IVS2 ds+1 G to A (2 patients). All mutations have already been reported as causes of GHI (Amselem et al., 1991, Sobrier et al., 1997). Patients presented with severe short stature (ranging from –5.50 SDS to –9.30 SDS for age and sex) and typical Laron facial features. Biochemically, they all had high basal GH levels and low IGF-I, IGFBP-3 and ALS levels. GHBP levels were undetectable in all patients. Unfortunately, no data on the geographic location or the presence of a relationship among these patients, were available. In an attempt to identify a founder effect, microsatellite markers spanning 17Mb around the *GHR* locus, were used and the polymorphic site in *GHR* intron 9 was studied. Analysis of *GHR* intron 9 showed the presence of frame I in patients with mutations S40L and R43X (14 subjects) and of frame II in patients with the IVS2 mutation (2 subjects). Results for microsatellite marker analysis showed the same haplotype in 6 out of 7 patients with the R43X mutation, being identical 5.6Mb upstream of the *GHR*. The remaining patient shared 1Mb homology upstream the *GHR* locus with the other 6 patients. In the S40L group, all 7 patients were identical 12.5Mb downstream of the *GHR* locus. The same was true for the 2 patients with the IVS2 mutation, but for a different genotype (figure 3.12). These data suggest the presence of a common ancestor for patients with the same mutation.

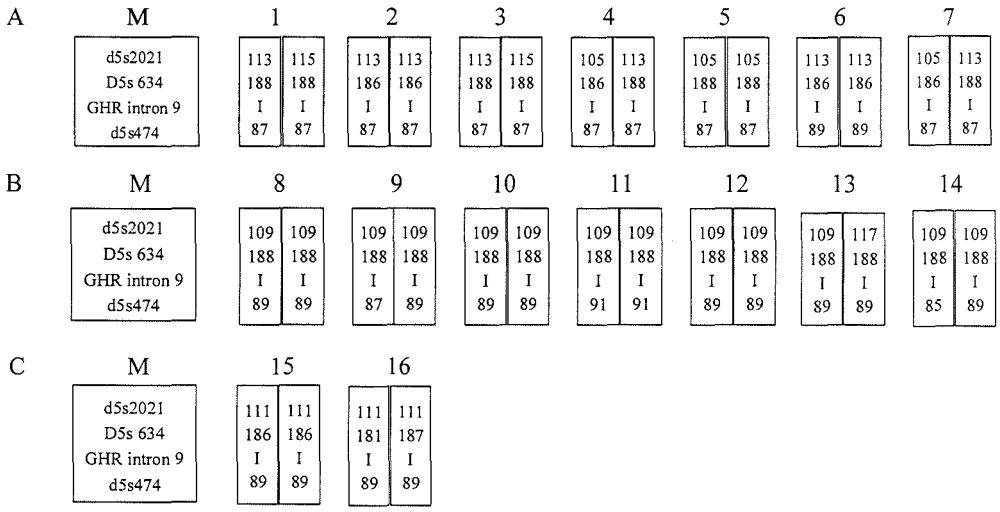

Figure 3.12 Genotype analysis of the Turkish cohort. The genotypes of patients with mutation S40L (panel A), R43X (panel B) and IVS2 ds+1 G to A (panel C) are indicated. M, marker. Numbers indicate the length(s) of the PCR amplification products from each microsatellite marker PCR.

3.5.4 Identification and characterisation of a novel *STAT5b* defect

Two sisters (patients 39 and 40 in Table 3.2) from a consanguineous family from Kuwait, were among the GHI patients with normal GHBP levels and no mutations in the *GHR* coding exons. Analysis of *GHR* common SNPs in these two patients and their parents revealed the presence of different haplotypes in the two siblings, thus excluding a defective *GHR* as the cause of GHI

Both sisters had facial features resembling those of classical Laron syndrome (Figure 3.13) and severe GHI (Table 3.3). Patient A was 3.9-year-old, her height was -5.58 SDS and she had juvenile idiopathic arthritis. Patient B was 2.19-year-old, her height was –5.81 SDS and she suffered from recurrent pulmonary infections. Both parents were of normal stature. The presence of a defective *STAT5b* was hypothesised. The DNA samples of the two children were analysed in collaboration with the Department of Paediatrics, Oregon Health and Sciences University, Portland, Oregon, US, revealing the presence of a novel homozygous Guanine deletion at the junction exon 13-intron 13 (1680delG) of *STAT5b*. This mutation is likely to cause a frameshift and a premature stop codon 16 amino acids downstream.

TABLE 3.3 CLINICAL CHARACTERISTICS OF THE TWO CHILDREN WITH *STAT5B* DEFECTS.

Patient	Sex	Pubertal stage	Age	Height SDS	IGF-I ng/ml	IGFBP-3 mg/L	ALS mg/L
A	F	I	3.99	-5.58	und n.r. 20-170	0.7 1.2-4.1	0.4 9.7-21.8
B	F	I	2.19	-5.81	und n.r. 20-158	0.8 1.2-3.7	0.8 8.0-19.5

und = undetectable levels. n.r., normal ranges for age and sex.

Figure 3.13 Front and side views of two sisters with *STAT5B* defect. Top: patient A, bottom patient B.

3.5.5 Identification and characterisation of novel *IGFALS* defects

Four GHI children had no mutations in the *GHR* coding exons and their GHBP levels were within the normal range. They belonged to four unrelated families of different ethnic origin. Their height SDS ranged from –2.45 to -3.20 SDS and all had normal facial features. Biochemically, they all had severe GHI, as demonstrated by the low levels of GH-dependent proteins.

Sequencing of the *IGFALS* identified 5 novel defects which are presented in Figure 3.14.

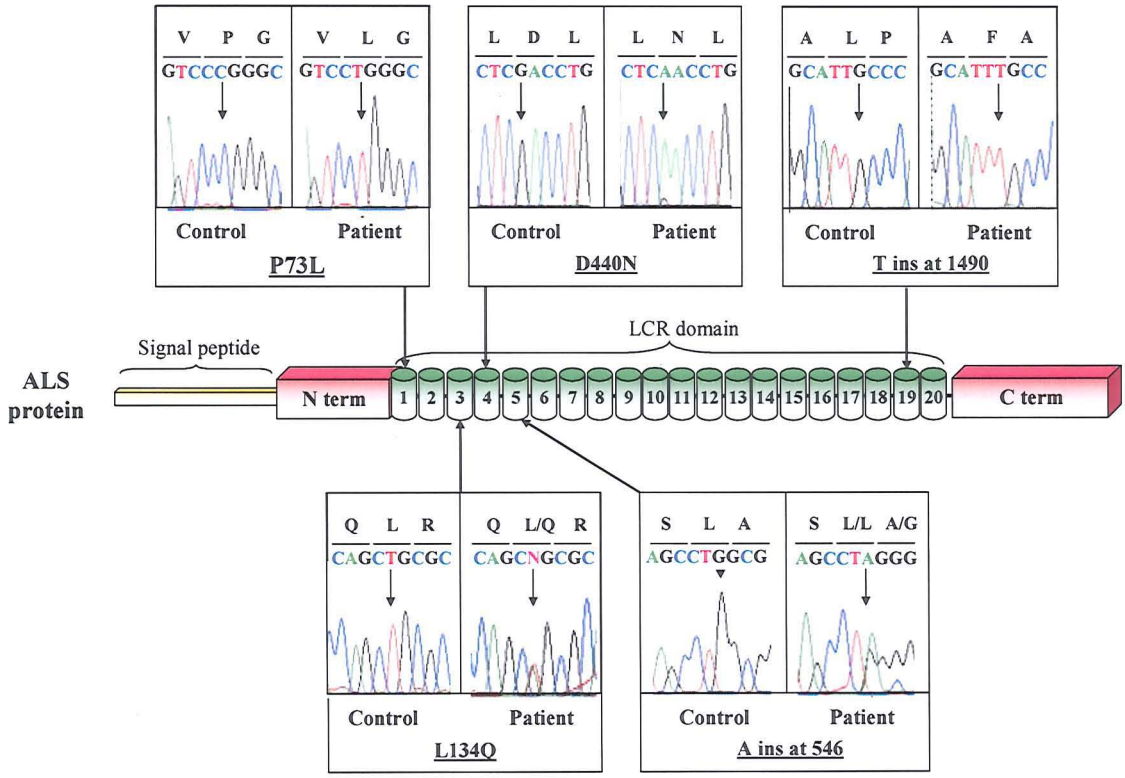

Figure 3.14 ALS protein structure and location of the novel *IGFALS* defects. Chromatograms showing partial DNA sequences from patients and normal control are also presented. The position of the base changes is indicated by the arrows. LCR, leucine-rich repeat domain.

3.5.5.1 Homozygous defect P73L

Patient A (patient 41, Table 3.2) was a 13.4-year-old boy. At the time of evaluation, his height was -3.20 SDS. His medical history and physical examination were otherwise unremarkable. His bone age was 12.5 years and he was pubertal stage II. His hormonal profile is presented in Table 3.4. His father and mother were consanguineous and had mild short stature (height SDS -1.10 and -2.20 SDS, respectively).

Sequencing analysis revealed the presence of a homozygous base change from C to T at position 218 resulting in a missense mutation with proline to leucine substitution (P73L) (Figure 3.14). Size exclusion chromatography did not detect the peaks corresponding to the ternary and binary complexes (Figure 3.15). The P73L mutation is localised in the leucine-rich repeat domain. Because of the different chemical properties of these two amino acids, the proline to leucine change is predicted to alter the secondary structure of the ALS protein.

3.5.5.2 Compound heterozygous defects L134Q and A insertion at 546

Patient B (patient 42, Table 3.2) was a 10.6 year-old boy. At the time of evaluation his height was -2.82 SDS, whereas the rest of his medical history and physical examination were unremarkable. He was pubertal stage I and had a bone age of 6.5 years. His hormonal profile is presented in Table 3.4. His mother and father were non-consanguineous and had mild short stature (-1.98 and -1.67 SDS, respectively).

Sequencing analysis revealed the presence of a heterozygous base change from T to A at position 401 causing a leucine to glutamine substitution (L134Q) and a heterozygous insertion of an adenine at position 546 (Figure 3.14). No peaks corresponding to the ternary and binary complexes were detected by means of size exclusion chromatography (Figure 3.15). The L134Q mutation is localised in the leucine-rich repeat domain and is likely to cause a change in the secondary structure of the ALS protein, whereas the A insertion at 546 causes a frameshift and the appearance of a premature stop codon.

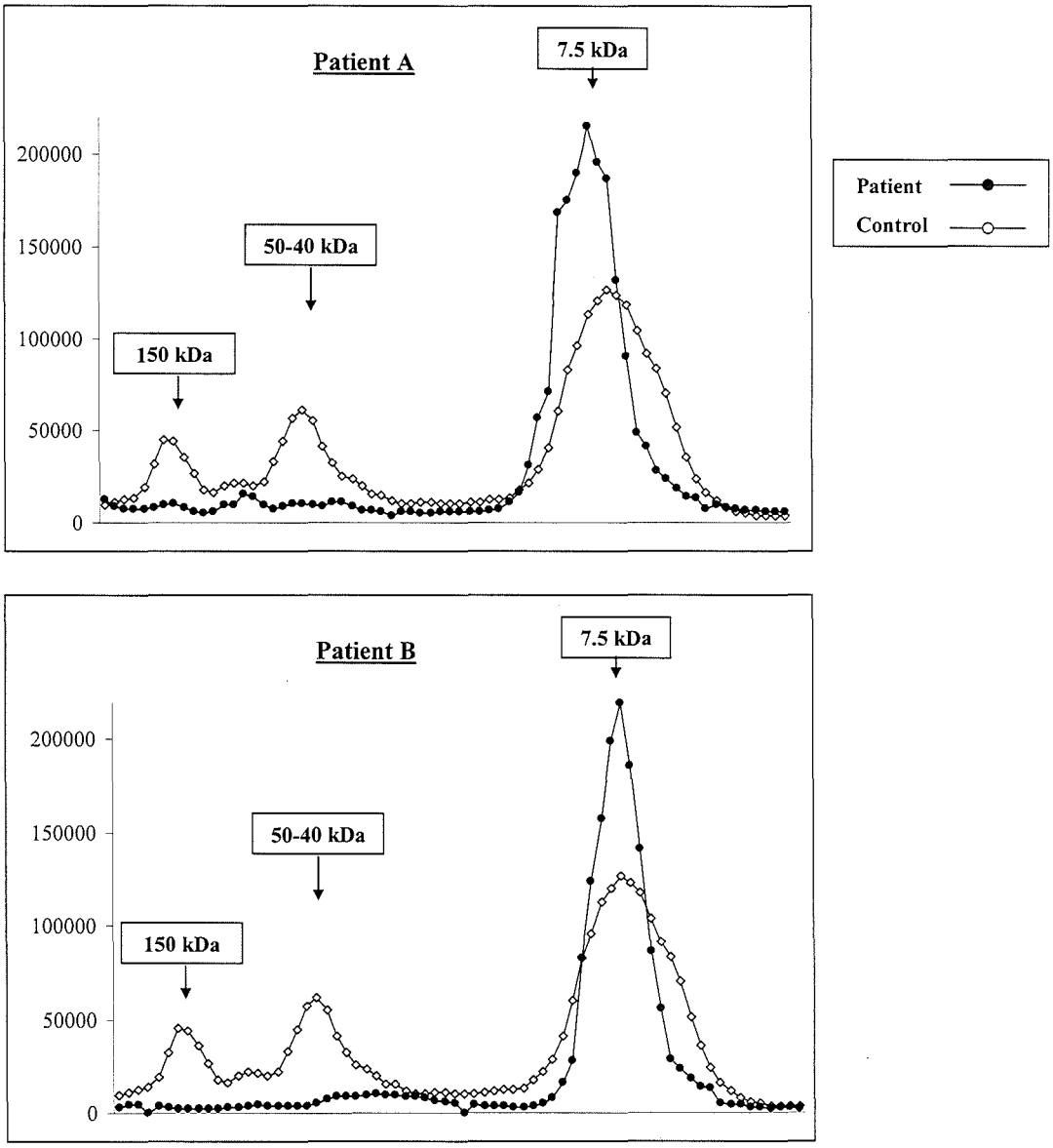

Figure 3.15 Results of size exclusion chromatography for two patients with *IGFALS* defects. Peaks corresponding to ternary complex IGF-I/IGFBP-3/ALS (150kDa), binary complex IGF-I/IGFBP-3 (50-40 kDa) and IGF-I (7.5 kDa) are indicated by the arrows.

3.5.5.3 Homozygous defect D440N

Patient C (Patient 43 in Table 3.2) was a 12.9 year-old boy of Turkish origin. At the time of evaluation his height was -2.45 SDS, whereas the rest of his medical history and physical examination were unremarkable. His bone age was 10.0 years and he was

pubertal stage I. His hormonal profile is presented in Table 3.4. His mother and father were consanguineous and had mild short stature (-2.80 and -2.00 SDS, respectively).

Sequencing analysis revealed the presence of a homozygous base change from G to A at position 1318 causing an Aspartic acid to Asparagine substitution (D440N) (Figure 3.14). This amino acid change lies within the leucine-rich repeat domain. Since the ALS structure has not yet been resolved, it is difficult to predict the consequence of this mutation at protein level. Nevertheless, the presence of an asparagine is predicted to create a novel N-glycosylation site in the ALS protein.

3.5.5.4 Homozygous T insertion at position 1490

Patient D (patient 44, Table 3.2) was a 11.9 year-old boy of Kurdish origin. At the time of evaluation his height was -2.66 SDS. His bone age was 9.6 years at 10.5 years of chronological age and he was pubertal stage I. His hormonal profile is presented in Table 3.4. His mother and father were consanguineous and had mild short stature (-3.4 and -2.3 SDS, respectively).

Sequencing analysis revealed the presence of a homozygous T insertion at position 1490 (Figure 3.14). This mutation is predicted to cause a frameshift and the appearance of a premature stop codon.

TABLE 3.4 CLINICAL CHARACTERISTICS OF THE 4 PATIENTS WITH *IGFALS* DEFECTS.

Patient	Sex	Pubertal stage	Age	Height SDS	GH levels (μU/ml) after provocation test	IGF-I level ng/ml (SDS)	IGFBP-3 level ng/ml (SDS)	ALS level mg/L
A	M	II	13.4	-3.2	185	40 (-3.06)	400 (-9.51)	und
B	M	I	10.6	-2.82	115	33 (-2.20)	200 (-9.59)	und
C	M	I	12.9	-2.45	159	28 (-3.32)	200 (-11.20)	und
D	M	I	11.9	-2.66	118	48 (-1.38)	900 (-5.31)	und

und, undetectable; SDS, standard deviation score.

3.5.6 Predictors of genomic defects in primary GHI

Data from the GHI population analysed in this study were pooled with data from another large genetically heterogeneous population reported in the European Pharmacia and Upjohn treatment study group published by Woods et al in 1997 (Woods et al., 1997)] and data from two studies on *GHR* dominant negative mutations: G to C at IVS8 as-1 and G to A at IVS9 ds+1 (Ayling et al., 1997, Iida et al., 1998). *GHR* defects were divided into missense, nonsense, splice mutations, mutations with a dominant negative effect and the pseudoexon 6Ψ mutation. Because of its peculiarity, the latter was considered separately from the other splice mutations. As all data belonged to patients with homozygous *GHR* defects, data from the compound heterozygote (V144D/R43X) patient reported by Woods et al. were excluded from the analysis.

Data on a total of 74 GHI subjects were analysed. GHI patients with dominant negative *GHR* mutations were significantly ($P<0.05$) taller than patients with GHI caused by *GHR* splice, nonsense and missense mutations. Moreover, patients with GHI caused by the pseudoexon 6Ψ mutation were significantly ($P<0.05$) taller than patients with GHI caused by nonsense and missense *GHR* mutations (Figure 3.16, on the left on panel A).

IGF-I levels were available for 45 patients. Patients with GHI caused by missense mutations had significantly ($P<0.05$) lower IGF-I SDS values compared to patients with GHI caused by pseudoexon 6Ψ, splice and dominant negative mutations. Moreover, patients with GHI caused by the pseudoexon 6Ψ mutation had significantly ($P<0.05$) higher IGF-I SDS values than patients with GHI caused by nonsense and missense *GHR* mutations (Figure 3.16, on the right in panel A).

Patients with GHI caused by *IGFALS* defects were compared to patients with GHI caused by *GHR* mutations. Patients with GHI due to ALS deficiency were significantly ($P<0.05$) taller than patients with GHI caused by splice, nonsense and missense mutations (Figure 3.16, on the left in panel B). Moreover, they had significantly ($P<0.05$) higher IGF-I SDS values compared to patients with GHI caused by *GHR* nonsense and missense mutations (Figure 3.16, on the right in panel B).

Panel A

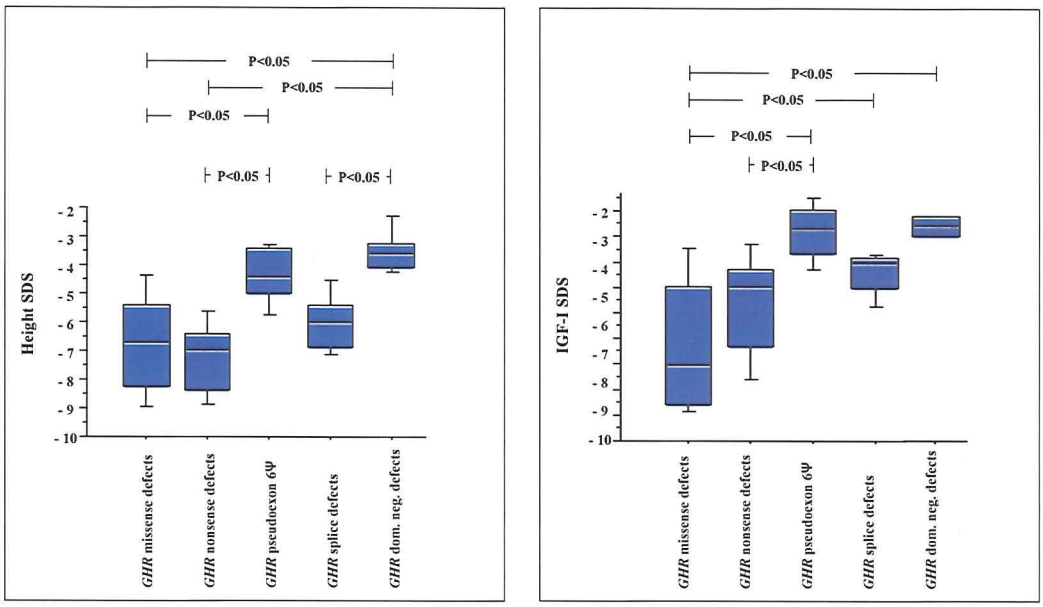

Panel B

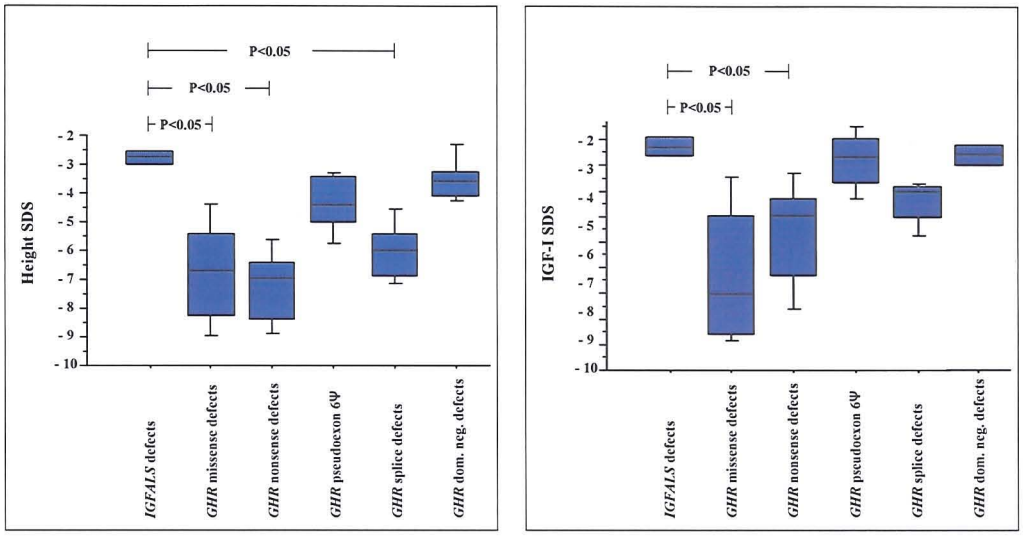

Mutation	cases n.	median
IGFALS defects	4	-2.74
GHR missense defects	19	-6.72
GHR nonsense defects	18	-6.96
GHR pseudoexon 6Ψ	11	-4.40
GHR splice defects	14	-6.00
GHR dom. neg. defects	8	-3.60

Mutation	cases n.	median
IGFALS defects	4	-2.63
GHR missense defects	11	-7.56
GHR nonsense defects	9	-7.96
GHR pseudoexon 6Ψ	11	-3.37
GHR splice defects	8	-6.07
GHR dom. neg. defects	2	-3.16

Figure 3.16 Predictors of genomic defects in primary GHI. Panel A: box plots for height and IGF-I SDS for patients with GHI caused by *GHR* mutations. Panel B box plots for height and IGF-I SDS for patients with GHI caused by *IGFALS* defects and *GHR* defects. Each boxplot depicts the median, the 25th and 75th percentiles. Whiskers depict minimum and maximum observed values. Median and standard deviation (St Dev) values for height (on the left) and IGF-I (on the right) for the 6 groups are also presented.

3.6 DISCUSSION

The population studied in this thesis represents one of the largest series of ethnically heterogeneous patients with GHI. Genetic characterisation identified several novel defects in the *GHR* and in other genes of the GH-IGFI axis, namely *STAT5b* and *IGFALS*. Analysis of the clinical data of the four patients with *IGFALS* defects, representing four of out of the 9 families known worldwide with ALS deficiency, allowed a better understanding of the novel emerging GHI phenotype associated with *IGFALS* defects. Moreover, the analysis of the genetic and clinical data of the entire GHI cohort, in combination with published data on additional GHI patients, allowed establishment of a relationship between GHI severity and the causative genetic defect, as well as between GHI severity and *GHR* type of mutation.

	GHR	***STAT5b***	***IGFALS***
n. of patients with genetic defects	38	2	4
total n. of mutations identified	15	1	5
n. of novel mutation identified	5	1	5

GHR defects and GHI

Growth failure in the presence of IGF-I deficiency and normal or high GH levels can be due either to the presence of a defective GH (Besson et al., 2005) or to the inability of cells to respond to GH (Kofoed et al., 2003, David et al., 2005). Failure to generate IGF-I in response to exogenous GH administration, points to the latter as the pathogenetic mechanism responsible for primary GHI. GH exerts its biological actions through binding to its receptor and any mutation leading to absence or a non-functional GHR, result in GHI. *GHR* mutations represent the most common cause of primary GHI and were present in 72% of GHI patients in this study. Five *GHR* defects were novel, including the first mutation in this gene to be identified in a polypyrimidine tract (see Chapter 4). A novel dominant negative mutation in the GHR intracellular region was also identified, possibly sharing the same pathogenetic mechanism to the other heterozygous mutations reported by Ayling and Iida (Ayling et al., 1997, Iida et al., 1998, Iida et al., 1999).

As expected, most of the *GHR* defects identified in this study were in the exons coding for the extracellular domain and resulted in the classical Laron phenotype, whereas defects in exons coding for the intracellular domain were rare and associated with non-classical GHI.

A wide phenotypic variability was found among subjects with different *GHR* defects, as demonstrated by the wide range of height SDS within patients with different mutations, as well as within patients with the same mutation. This finding supports the important role of environmental and individual genetic factors in determining height (Rosenbloom et al., 1994b). Nevertheless, when data from the cohort of patients analysed in this thesis were pooled with data from previously reported cases, a clear genotype–phenotype relationship was found between the severity of GHI type and the type of *GHR* defect. Patients with dominant negative mutations and the pseudoexon 6Ψ mutation had a significantly less severe phenotype compared to GHI subjects with nonsense, missense and splice mutations. The milder phenotype in subjects with dominant negative mutations could be explained by the three possible combinations of GHR dimerisation which can occur in these patients. A similar scenario can be hypothesised in subjects with the pseudoexon mutation 6Ψ. Although the pseudoexon defect causes GHI in homozygosity, the presence of the wild type GHR transcript has been documented in these patients (Metherell et al., 2001). For yet unknown reasons, a splice mutation may not always be 100% efficient in causing aberrant splicing and coexistence of normal and mutant transcripts may occur. Therefore, in patients with the pseudoexon mutation 6Ψ the wt/wt GHR dimer can be present alongside the non-functional wt/mt heterodimer and the non-functional mt/mt homodimer.

The presence of different ratios of mutant to wild type receptor can also explain the occurrence of different phenotypes within patients with the same splice mutation. Although all the dominant negative defects identified in the *GHR* have the same effect at the protein level – the same prematurely truncated protein – they generate different phenotypes. While the patient reported in this study and her affected family member, as well as the proband and mother reported by Ayling et al., had normal facial features (Ayling et al., 1997), the three GHI subjects reported by Iida et al. had classical Laron facial features (midfacial hypoplasia and prominent forehead) (Iida et al., 1998). Different phenotypes are known to occur when the genetic defect causes aberrant splicing

(Zhu et al., 1997, Lemahieu et al., 1999). This phenomenon has been described among the Ecuadorian GHI subjects with the E180 splice mutation (Rosenbloom and Guevara-Aguirre, 1998, Rosenbloom et al., 1999) but perhaps it has its maximum expression in GHI patients with the *GHR* pseudoexon 6Ψ mutations, as described in Chapter 5.

***STAT5b* and *IGFALS* defects and GHI**

At the time this study started, only one case of GHI due to a *STAT5b* defect (Kofoed et al., 2003) and one case of GHI due to a *IGFALS* defect (Domene et al., 2004) had been reported. The genetic analysis presented in this study allowed the identification of the second case of GHI due to a *STAT5b* defect. The analysis of genetic and clinical data from two GHI siblings with no mutations in the *GHR* and normal GHBP levels, led us to hypothesise a *STAT5b* defect, which was identified and reported in 2005 (Hwa et al., 2005), thanks to the collaboration with the group led by Dr Rosenfeld at the Oregon Health and Science University.

The description of the first case of short stature in a child with inactivation of the *IGFALS* (Domene et al., 2004) prompted us to consider the role of this protein in the genesis of GHI in four children with normal GHBP levels, mild growth failure and no defect in the *GHR* coding region. Five novel *IGFALS* defects in four unrelated patients were thus identified. Disappointingly, two of these patients were simultaneously studied elsewhere and their genetic analysis published independently from our results (Hwa et al., 2006, van Duyvenvoorde et al., 2008). Nevertheless, the four patients reported in this study represent the largest series of unrelated patients with *IGFALS* defects and analysis of their clinical data allowed observations on the novel emerging GHI phenotype associated with an inactive ALS protein.

All novel *IGFALS* mutations identified in this study resulted in undetectable ALS serum levels. Their deleterious effect was demonstrated either by western immunoblot analysis from other groups (Hwa et al., 2006, van Duyvenvoorde et al., 2008) or by size exclusion chromatography in this study. No ternary complex formation was, in fact, demonstrated from the serum samples of two ALS deficient patients. Moreover, in these patients, serum samples did not support the formation of the binary complex either. This is in discordance with what was previously shown for other *IGFALS* defects (Domene et al., 2004), but not surprising considering the practically null serum IGFBP-3 levels.

Circulating IGFBP-3 and IGF-I have a short half life when free or bound together in the relatively unstable binary complex IGF-I/ IGFBP-3. Binding to the ALS protein stabilises the complex increasing their half lives (Guler et al., 1989).

ALS deficiency due to inactivating *IGFALS* mutations resulted in a phenotype resembling growth hormone resistance. All patients in this study, as well as those reported in the literature (Domene et al., 2004, Domene et al., 2007, Heath et al., 2008) had normal or high GH levels, almost undetectable GH dependent proteins and no response to IGF-I generation test. Nevertheless, GHI patients with *IGFALS* defects had a milder phenotype, similar, in height SDS and IGF-I levels to that caused by *GHR* pseudoexon 6Ψ and dominant negative mutations and significantly less severe compared to that caused by *GHR* missense, nonsense or splice mutations. Interestingly, parents of ALS deficient patients, obligate single heterozygous carriers of the mutations, also had short stature, but to a lesser degree than their homozygous children. This suggests that single heterozygous *IGFALS* defects might be sufficient to affect final height.

An increased GH response to stimulation test was present in the four cases reported in this study, as well as in almost all reported cases. Patients with ALS deficiency have been shown to have a reduction in total as well as free circulating IGF-I (Hwa et al., 2006). It is widely accepted that free IGF-I is biologically active and its reduction, even minimal, may be sufficient to trigger an increased GH release from the pituitary and affect metabolism at tissue level. Moreover, the increased IGF-I clearance associated with ALS deficiency might explain the absence or mild response to rhGH observed in these patients (Domene et al., 2004).

Delayed puberty has been postulated to be part of the ALS deficiency phenotype (Domene et al., 2004, Domene et al., 2007). Three out of four patients were prepubertal at the time of this study. Nevertheless, a normal puberty was present in the one post-pubertal child in this series and was documented in another patient by a follow-up study (Hwa et al., 2006). This finding suggests that delayed puberty may be due to the individual genetic background rather than to *IGFALS* defects. It is possible, however, that ALS deficiency results in a profound alteration in IGF-I availability, with consequences at central and local level, which could influence normal pubertal development in individuals with a predisposing genetic background.

All subjects with *IGFALS* defects were male, and the same is true for the majority of reported cases. This observation is, at the moment, difficult to explain. However, it is possible that, for social reasons, the presence of short stature attracts more attention when the subject is a boy rather then a girl.

Limitation and future work

In 9 out of 53 patients, no mutations responsible for GHI have been identified yet. The presence of low or undetectable GHBP levels suggests that the defect lies within the *GHR*. Since no defects were found in its coding region, it is possible that a novel intronic or promoter *GHR* defect may be the cause of GHI in these patients. In six cases, analysis of cDNA extracted from leucocytes resulted in no GHR products. Since this could be due to the presence of a low amount of GHR mRNA in these cells, mRNA extraction from fibroblasts is part of future work.

The use of the Student's t-test (or non-parametric equivalent, such as Wilcoxon rank sum test) for the establishment of a genotype-phenotype relationship may be inappropriate in a population of partially related subjects, as it does not account for familial clustering. However, because of the severe phenotype, affected members of the same family are often referred together, making identification of a single index case arbitrary. Moreover, since consanguinity plays a fundamental role in the propagation of GHI, even if one index case per family could be identified, index cases with the same mutation, would likely be related, albeit belonging to different families. Furthermore, exclusion of affected family members would result in loss of information in an already small population. As GHI is a very rare disorder, application of multilevel analysis would be grossly inefficient.

CHAPTER 4

AN *IN VITRO* SPLICING ASSAY TO STUDY *GHR* SPLICE MUTATIONS

4.1 BACKGROUND

Approximately 20% of *GHR* defects resulting in GHI are splice mutations (David et al., 2005). Aberrant mRNA splicing is a common cause of genetic diseases with almost 1 in 2 disease-causing nucleotide changes disrupting a splicing element. Advances in splicing physiology have, in fact, led to reconsideration of nucleotide changes conventionally classified as harmless SNPs or missense/nonsense defects as potential mutations causing aberrant splicing, (Wang and Burge, 2008). The lack of a comprehensive understanding of the splicing regulatory elements, in combination with the complexity of the splicing process, makes it difficult to predict the consequences of a nucleotide change on mRNA splicing by using *in silico* prediction programs. These programs are fairly reliable when used to predict the effects of nucleotide changes occurring at the invariant donor and acceptor dinucleotide sequences, but become less efficient as nucleotide changes occur further away from the consensus splice site or in different splicing elements, such as the polypyrimidine tract (Thanaraj and Clark, 2001). In these cases, analysis of RNA extracted from patients' leucocytes or fibroblasts becomes mandatory for establishing the diagnosis. This, however, requires either blood sampling or a skin biopsy. Both techniques are invasive and may be difficult to perform in infants and children, particularly those with reduced body size, such as GHI patients. Analysis of RNA extracted from mammalian cells transfected with minigenes containing the mutation of interest has been used as an alternative to the analysis of patient mRNA (Cooper, 2005).

The *in vitro* splicing assay is a technique widely used to study the physiology of splicing and of its regulatory elements, but is not employed to study the consequences of naturally occurring mutations. It is based on the use of minigenes in a splicing reaction with nuclear extracts from cells, such as the HeLa (Anderson and Moore, 1997, Jurica and Moore, 2002). In 2001, the *in vitro* splicing assay was used to study the consequences of a *GHR* intronic defect (Metherell et al., 2001). Its results accurately predicted those by *in vivo* mRNA analysis. These findings were the the basis for this project.

4.2 ORIGINAL HYPOTHESIS AND AIMS

The aim of this project was to establish the diagnostic value of an *in vitro* splicing assay, based on a three-exon minigene system spliced in HeLa nuclear extracts, in assessing the consequences of genetic defects on mRNA splicing. In particular, the study aimed to 1) establish a rapid and reliable protocol for the creation of three-exon minigenes; 2) analyse *in silico* all *GHR* defects detected in the GHI study population, including nucleotide changes conventionally considered SNPs or missense and nonsense mutations; 3) study *in vitro* all nucleotide changes predicted *in silico* to cause aberrant splicing and those occurring in splice regulatory elements, but not predicted *in silico*; 4) compare the results obtained *in vitro* to those obtained *in silico* and *in vivo* from patient mRNA analysis.

4.3 MATERIALS AND METHODS

4.3.1 PCR and overlap-extension PCR

Wild type minigenes were created using PCR and overlap extension PCR techniques. The wild type *GHR* exon of interest was amplified from genomic DNA and L1 and L2 exons from Adml-par, a well-characterised splice reporter (sequence reported in Appendix 10.3.4), using a proof-reading polymerase. The three exons L1, GHRexon and L2, were joined together to form the wild type minigenes using the overlap extension PCR technique (Figure 4.1), as described in the Materials and Methods section 2.9.1.

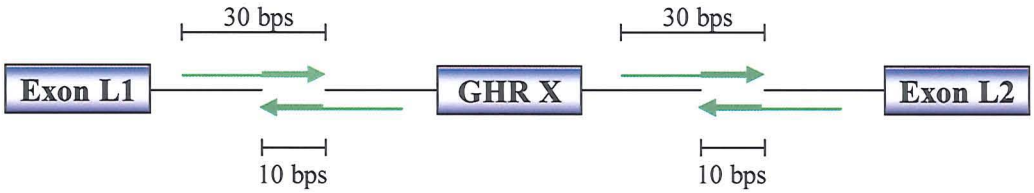

Figure 4.1 The three-exon minigene constructs. The *GHR* exon of interest (GHR X) and Adml-par exons L1 and L2 were amplified by PCR using specific forward and reverse primers (depicted in green) of approximately 30 bases (bps) designed to have a 10 bases overlap.

The splice reporter Adml-par (L1-L2) was amplified by conventional PCR using specific primers (for exon L1: primers T7-L1 and Admlpar-int51AS; for exon L2: primers Admlpar-int51S and L2A; primer sequences reported in Appendix 3:10.3.4) and used as positive control for the splicing reaction. The PCR products were run on a 1% agarose gel and those corresponding in size to the three-exon minigene, cut and purified by PCR gel extraction. The identity of the PCR product was confirmed by direct sequencing on the ABI 3700 Sequencer.

4.3.2 A-tailing and Cloning

Blunt-ended PCR reactions generated by *Phusion* polymerase (100U, Finnzymes) were A-tailed and cloned in the pGEM T-easy vector system (a T-vector cloning system). White colonies containing the insert were screened by PCR and direct sequencing.

4.3.3 Site-directed mutagenesis

The mutant minigenes were obtained from the corresponding wild types by site-directed mutagenesis as described in the Material and Methods section 2.7, using specific primers (sequences reported in Appendix 3: 10.3.5).

4.3.4 *In vitro* transcription and RNA purification

Wild type and mutant DNA minigenes and Adml-par were transcribed into mRNA in the presence of α^{32}P-GTP (10μCi). After 1 hour incubation at 37°C, reactions were mixed with RNA dye, heated at 98°C for 5 min and then run on a 4% polyacrylamide gel for 45 min at 980 Volts. Fluorescent markers were attached on the gel that was exposed overnight at -80°C and then subjected to autoradiography. The fluorescent-labelled gel image was used to excise the RNA bands from the gel. The RNA was extracted from the gel bands and stored at -20°C or used for the *in vitro* splicing assay.

4.3.5 *In vitro* splicing assay

5'-capped radiolabeled mRNA minigenes were incubated in 12.5μl splicing reaction mixture with 4μl of HeLa nuclear extracts (CilBiotech) at 30°C for 60 minutes. Controlled reactions were incubated on ice for the same time. At the end of the incubation, reactions were deproteinised and precipitated according to the protocol described in the Materials and Methods section 2.9.4, mixed with RNA loading dye, heated at 98°C for 5 min and run on a 8% denaturing polyacrylamide gel for 1 hour and 45 min at 980 Volt, before autoradiography.

All results were repeated at least three times. Magnesium concentration titration curves (final concentration ranging from 40 to 80mM) were also performed to optimise splicing conditions.

4.3.6 RNA extraction from denaturing polyacrylamide gels and RT-PCR

The bands of interest, corresponding in size to correctly spliced or aberrant products, were excised from the gel and retro-transcribed into DNA as described in Material and Methods (section 2.8.3). This was amplified by PCR using specific primers and analysed by direct sequencing on the ABI 3700 DNA Sequencer.

4.3.7 Splicing prediction programs

The Alex Dong Li's splice site finder (http://violin.genet.sickkids.on.ca/~ali/) was used to calculate the splice site score of wild type and mutant sequences.

4.3.8 RNA extraction from blood and RT-PCR

RNA was isolated from human blood using the PAXgene blood RNA Kit and the PAXgene Blood RNA Tubes (PreAnalytic) according to the manufacturer's recommendations. First-strand synthesis of cDNA was obtained by reverse transcription of RNA and amplified in a 12.5µl PCR reaction using specific primers (sequences reported in Appendix 10.3.2). To strength the specificity and sensitivity of the PCR technique GHR cDNA was then amplified using a heminested PCR technique. PCR products were electrophoresed on an agarose gel. In the presence of multiple bands for the same PCR product, these were cut from the gel, DNA purified from the gel and sequenced on the ABI 3700 Sequencer.

4.4 RESULTS

4.4.1 *GHR* nucleotide changes

All novel and previously identified defects and SNPs identified in the *GHR* during the course of the genetic study of the GHI population described in Chapter 3 of this Thesis, were analysed. Of these, nine were splice defects, seven were missense or nonsense defects and four SNPs (Table 4.1). The splice defects were located as follows: four nucleotide changes were within natural donor splice sites (G to A at IVS2 ds+1, G to A at IVS6 ds+1, G to C at IVS8 ds-1 and T to C at IVS9 ds+2), two base changes downstream to the natural donor splice site of exon 2 (A to C and A to G at IVS2 ds+4) and one upstream the acceptor splice site of intron 7, in the polypyrimidine tract (T to A at IVS7 as-6). Moreover, two nucleotide changes, one located deeply within intron 6 (A to G at pseudoexon 6Ψ ds-1) and one located deeply within exon 7 (C to T at exon 7 ds-62, also known as G223G) were also present. Both defects are known to create novel splice sites resulting in aberrant splicing.

4.4.2 *In silico* prediction scores

All sixteen novel and previously described *GHR* defects and the four SNPs were analysed *in silico* and results are presented in Table 4.1. The four base changes occurring within natural splice sites (G to A at IVS2 ds+1, G to A at IVS6 ds+1, G to C at IVS8 ds-1 and T to C at IVS9 ds+2) caused a reduction of the splice site prediction score, ranging from 12.15% to 30.80%, compared to the corresponding wild type. The two base changes occurring downstream of the donor splice site (A to C and A to G at IVS2 ds+4) and within the polypyrimidine tract (T to A at IVS7 as-6) caused a <10% reduction in the splice site score compared to the wild type (9.46%, 8.96% and 3.24%, respectively). The splice mutations known to create novel donor sites (A to G at 6Ψ ds-1 and C to T G223G within exon 7) resulted in an increase in the donor site prediction score of 13.33% and 40.48%, respectively.

Among the nonsense and missense defects, the C to T base change located within exon 4, conventionally known to produce the nonsense mutation R43X, resulted in a 51.34% increase in the score for a novel donor splice site located 87 bases upstream to the natural exon 4 donor site. The A to C base change conventionally known to result in

the R48X, however, resulted in a <5% score reduction for a potential acceptor splice site (cryptic splice site) within exon 4.

Two exonic base changes, SNPs rs6179 (G186G) and rs6176 (S491S), resulted in a 58% increase in the score for novel donor splice sites. The remaining 5 exonic base changes conventionally known to result in missense or nonsense mutations and the remaining two SNPs, did not produce scores suggestive of the creation of a novel splice site. The natural splice site scores for exon 4 and 7 were also calculated: exon 4 donor site 74.73, exon 4 acceptor site 92.00, exon 7 donor site 79.15, and exon 7 acceptor site 84.55.

TABLE 4.1 *IN SILICO* RESULTS.

Mutation type	exon/ intron	Mutation (mRNA position)	Wt score	Mt score	Variation (%)	Splice element
Missense/	exon 4	S40L (C to T at 173)	–	–	0.00	
Nonsense	exon 4	R43X (C to T at 181)	52.26	79.09	51.34	novel donor
	exon 4	C48X C to A at 198)	79.85	77.78	-2.59	cryptic acceptor
	exon 5	V125A (T to C at 428)	–	–	0.00	
	exon 6	R161C (C to T at 535)	–	–	0.00	
	exon 7	Q216X (C to T at 699)	–	–	0.00	
	exon 7	L229P (T to C at 740)	–	–	0.00	
Splice	intron 2	IVS2 ds+1 G to A	93.03	66.2	-28.84	donor
	intron 2	IVS2 ds+4 A to C	93.03	84.23	-9.46	donor
	intron 2	IVS2 ds+4 A to G	93.03	84.69	-8.96	donor
	intron 6	IVS6 ds+1 G to A	91.96	65.13	-29.18	donor
	6Ψ	6Ψ ds+1 A to G	79.36	89.94	13.33	novel donor
	intron 7	IVS7 ac-6 T to A	85.57	82.8	-3.24	acceptor
	exon 7	exon 7 ds-63 (C to T at 723)	66.3	93.14	40.48	novel donor
	intron 8	IVS8 ds-1 G to C	90.71	79.69	-12.15	donor
	intron 9	IVS9 ds+2 T to C	87	60.2	-30.80	donor
SNPs	exon 6	G186G (A to G at 601)	45.69	72.53	58.74	novel donor
	exon 10	S491S (C to T at 1516)	46.11	72.95	58.21	novel donor
	exon 10	I544L (A to C at 1673)	–	–	0.00	
	exon 10	P579T (A to C at 1778)	–	–	0.00	

Wt score, score for the wild type sequence; Mt score, score for the mutant sequence; 6Ψ, pseudoexon sequence; "-", no splice site identified.

4.4.3 Predicted consequences at mRNA and protein level according to the *in silico* prediction program

According to the *in silico* data, twelve nucleotide changes create or abolish splice sites, thus inducing aberrant splicing of the GHR mRNA. Seven nucleotide changes, IVS2 ds+1 G to A, IVS2 ds+4 A to G, IVS2 ds+4 A to C, IVS6 ds+1 G to A, IVS7 as-6 T to A, IVS8 ds-1 G to C and IVS9 ds+2 T to C, would result in exon skipping. The exon 4 mutation, conventionally known as R43X (T to C position 181 in the GHR mRNA) creates an alternative, preferred donor site (mutant score 79.09 vs wild type 74.73) and should result in the preferential use of the novel splice site with premature truncation of exon 4, a frameshift and a premature stop codon in the GHR mRNA. The exon 7 defect creates an alternative, preferred donor site within exon 7 (mutant score 93.14 vs wild type 79.15) and would result in the premature truncation of exon 7, the lack of 63 bases from the mature mRNA, no frameshift and a GHR protein lacking 21 amino acids. The nucleotide change in intron 6 (pseudoexon 6Ψ ds-1 A to G) increases the donor score for the pseudoexon and should result in the inclusion, in-frame, of the pseudoexon sequence in the mRNA and in a GHR protein with 36 additional amino acids.

4.4.4 *In vitro* splicing assay results

All those defects that were predicted to cause aberrant splicing were tested with the *in vitro* splicing assay. Five base changes [IVS2 ds+1 G to A, IVS6 ds+1 G to A, IVS9 ds+2 T to C and the two SNPs rs6179 (G186G) and rs6176 (S491S)] were not studied *in vitro* during the course of this project and are part of future work.

4.4.4.1 Defects in regulatory splicing elements: nucleotide changes IVS7 as-6 T to A and IVS8 ds-1 G to C

The wild type minigene L1-GHRexon8-L2 and the corresponding mutants were created to study the nucleotide changes IVS7 as-6 T to A, located in the polypyrimidine tract before exon 8 and the IVS8 ds-1 G to C, located at the donor splice site of exon 8. After 1 hour under standard splicing conditions, the wild type minigene produced a band of 277 bases corresponding to the three-exon-correctly-spliced product (L1-exon8-L2 mRNA) whose identity was confirmed by direct sequencing. Such a band was absent in both mutant minigenes. Both mutations resulted, instead, in the skipping of the mutation-

harbouring exons (GHR exon 8 in both cases) and in the appearance of a product 186 bases long, corresponding to exons L1 and L2 joined together, as confirmed by direct sequencing (Figure 4.2).

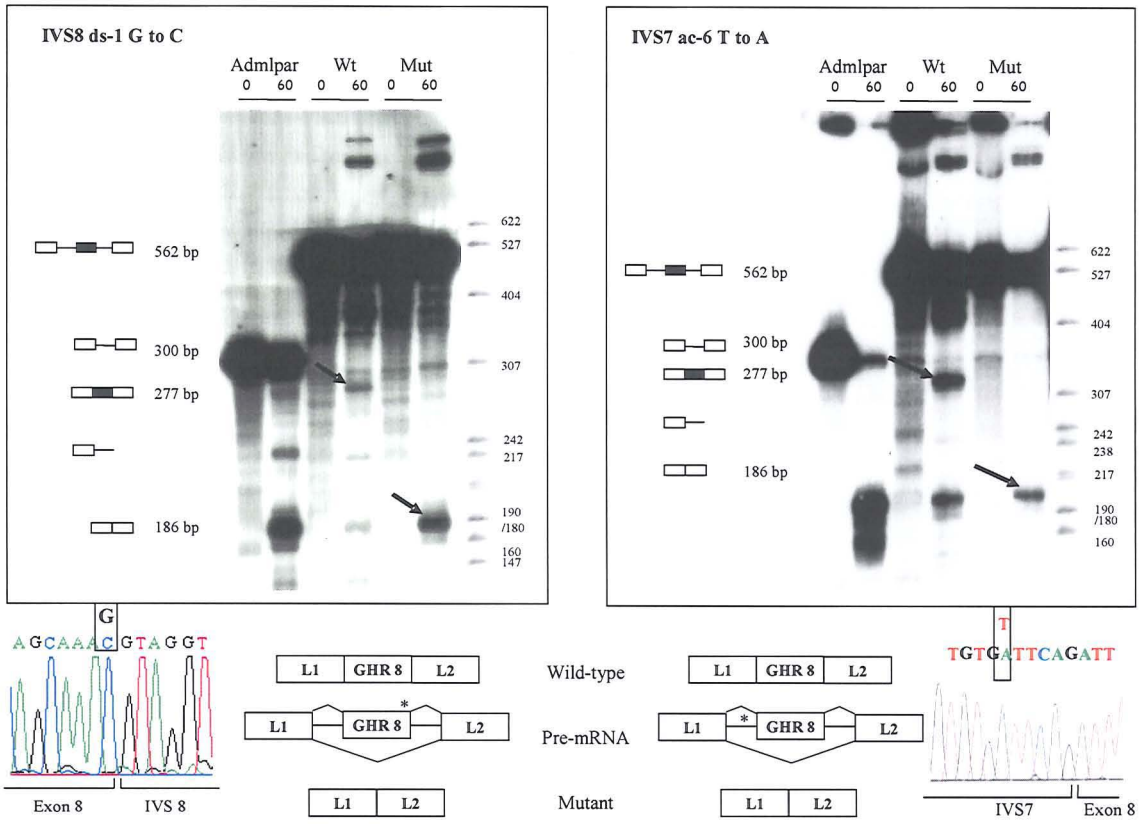

Figure 4.2 *GHR* mutations IVS8 ds-1 G to C and IVS7 ac-6 T to A. Top panels: in vitro splicing assay results. Bands corresponding to correct and aberrant spliced products are indicated by the arrows. Bands sizes are also indicated. Bottom panels: schematic representation of the splicing events for the wild type and mutant minigenes. Mutation location is indicated by an asterisk. Partial genomic sequences from patients DNA are also presented.

4.4.4.2 Defects downstream of the splice site: nucleotide changes IVS2 ds+4 A to G and IVS2 ds+4 A to C

The wild type minigene L1-GHRexon2-L2 and the corresponding mutants were created to study nucleotide changes IVS2 ds+4 A to G and IVS2 ds+4 A to C, both located downstream of the donor splice site of exon 2. After 1 hour under standard splicing conditions, the wild type minigene produced a band of 264 bases corresponding to the three-exon-correctly-spliced product (L1-exon2-L2 mRNA) whose identity was

confirmed by direct sequencing. Such a band was also detected in both mutant minigenes, indicating neither nucleotide change caused aberrant splicing (Figure 4.3).

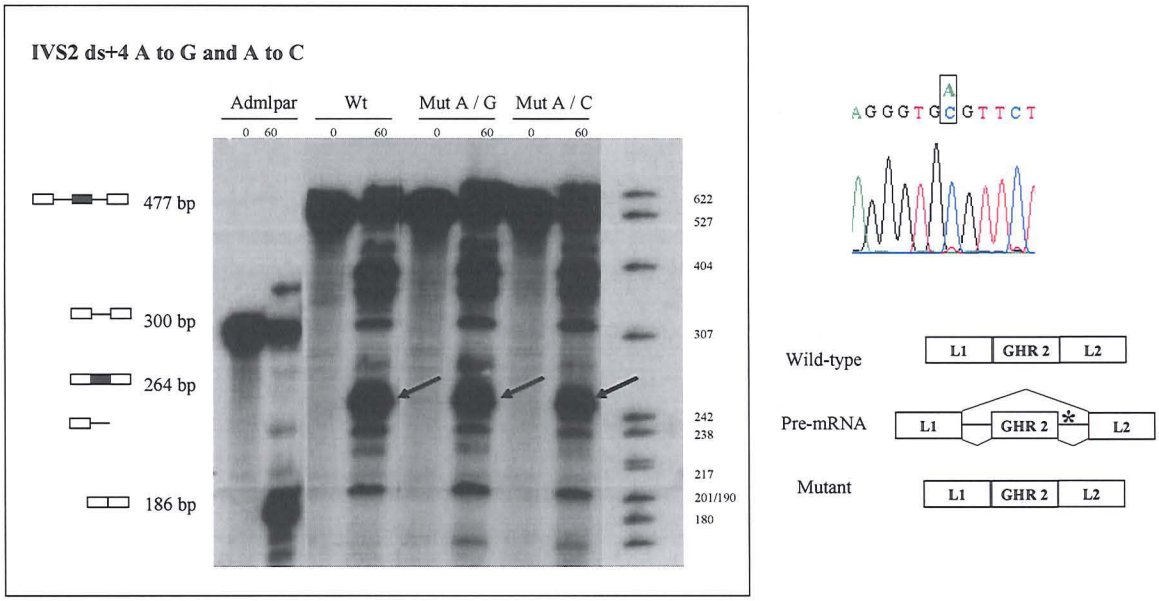

Figure 4.3 GHR IVS2 ds+4 A to G and A to C nucleotide changes. On the left: *in vitro* splicing assay results. Bands corresponding to correct and aberrant spliced products are indicated by the arrows. Bands sizes are also indicated. On the right: schematic representation of the splicing events for the wild type and mutant minigenes. Mutation location is indicated by the asterisk. Partial genomic sequence from patient DNA is also presented.

4.4.4.3 Exonic defects: nucleotide changes ex 7 ds-62 C to T and ex 4 (R43X) C to T

The wild type minigene L1-GHRexon7-L2 and the corresponding mutant were created to study the nucleotide change ex7 ds-62 C to T located deeply within exon 7 of the *GHR*, which was predicted to create a novel donor splice site 63 bases upstream the natural one (score for mutant =93.14 vs score for wild type = 79.15). After 1 hour under standard splicing conditions, the wild type minigene produced a band of 352 bases corresponding to the three-exon correctly spliced product (L1-exon7-L2 mRNA), the identity of which was confirmed by direct sequencing. A band of smaller size (289 bases) was, instead, produced by the splicing of the mutant minigene (Figure 4.4, left panel). Direct sequencing showed the presence of a product lacking the last 63 bases of exon 7. A band of similar size was produced by the wild type minigene. Direct sequencing of this

product showed it was an intermediate of the reaction, formed by exon L1, its intronic boundary and part of exon L2. *GHR* exon 7 was not present in this mRNA product.

The wild type minigene L1-GHRexon4-L2 and the corresponding mutant, were created to study the nucleotide change located deeply within exon 4 of the *GHR* conventionally known as R43X, predicted *in silico* to create a novel donor splice site preferred to the natural site (mutant score 79.09 versus wild type 74.73). After 1 hour under standard splicing conditions, both wild type and mutant minigenes produced a band of 316 bases, corresponding to the three-exon-correctly-spliced product (L1-exon4-L2 mRNA), the identity of which was confirmed by direct sequencing (Figure 4.4, right panel).

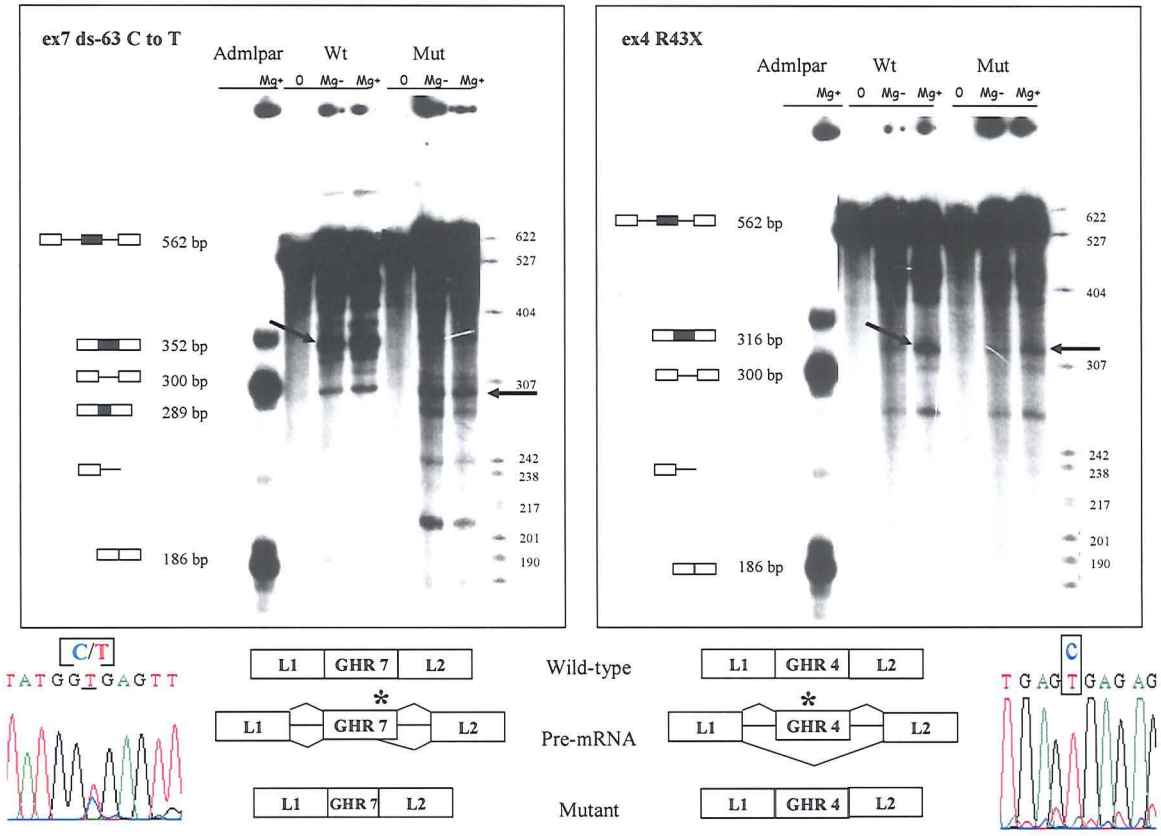

Figure 4.4 *GHR* mutations exon 7 ds-62 C to T and exon 4 R43X. Top panels: *in vitro* splicing assay results. Bands corresponding to correctly and aberrantly spliced products are indicated by arrows. Bands sizes are also indicated. Bottom panels: schematic representation of the splicing events for the wild type and mutant minigenes. Mutation position is indicated by the asterisk. Partial genomic sequences from patients DNA are also presented.

4.4.4.4 The pseudoexon defect: 6Ψ ds-1 A to G

The wild type minigene L1-GHR6Ψ-L2 and the corresponding mutant were created to study the nucleotide change 6Ψ ds-1 A to G, located deeply in intron 6 and predicted to create a novel donor splice site resulting in the insertion of the pseudoexon sequence in the mature GHR mRNA. After 1 hour under standard splicing conditions, the wild type minigene produced only a band of 186 bp corresponding to exons L1 and L2 joined together. The mutant minigene produced a band of 294 bases corresponding to the three-exon product L1-GHR6Ψ-L2 (Figure 4.5), as confirmed by direct sequencing.

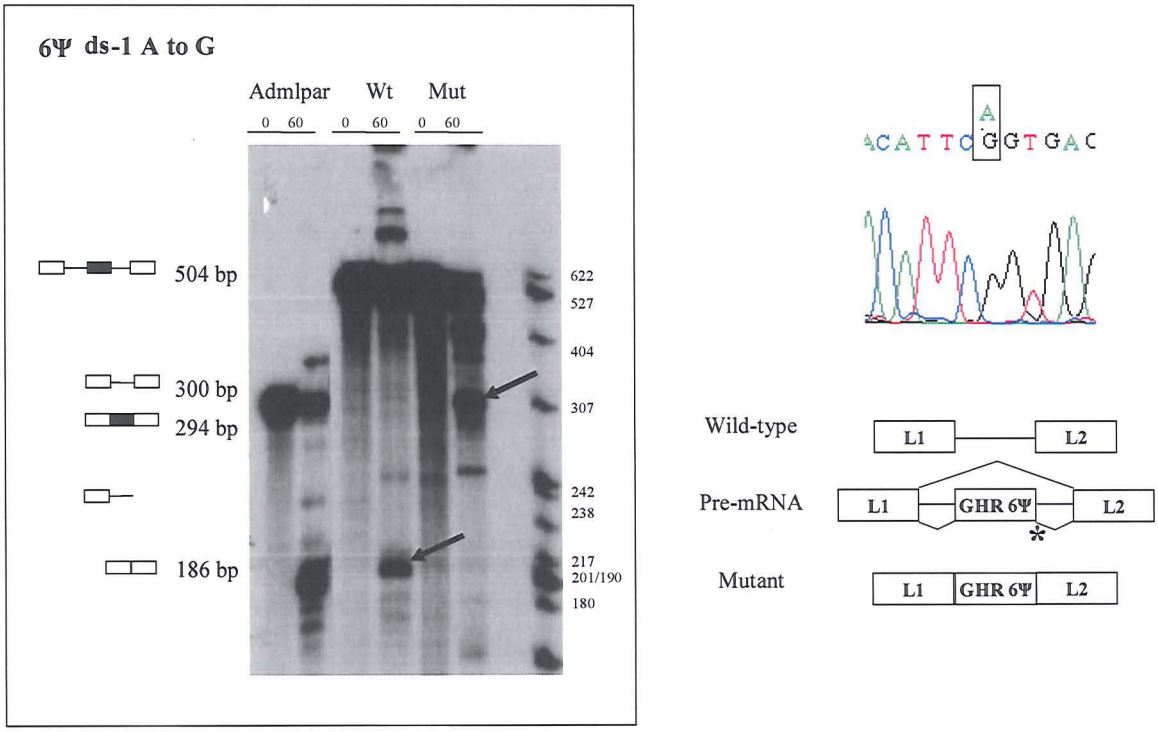

Figure 4.5 *GHR* pseudoexon mutation 6Ψ ds-1 A to G. Left panel: in vitro splicing assay results. The bands corresponding to correctly and aberrant spliced products are indicated by the arrows. Bands sizes are also indicated. Right panel: schematic representation of the splicing events for the wild type and mutant minigenes. Mutation position is indicated by the asterisk. Partial genomic sequences from patient DNA is also presented.

4.4.5 *In vivo* results and patients' data

mRNA extracted from patient leucocytes was available for the analysis of nucleotide changes IVS2 ds+4 A to C and IVS9 ds+2 C to T. *In vivo* results for mutations IVS8 ds-1 G to C, ex 7 ds-62 C to T and 6Ψ ds-1 A to G (pseudoexon mutation) were

available from previously published papers. Patient mRNA for analysis of mutations IVS2 ds+4 A to G, IVS7 as-6 T to A and R43X was not available. *In vivo* results showed skipping of the mutation-harbouring exons in the GHR mRNA of patients with nucleotide changes occurring at the invariant splice site sequences (IVS8 ds-1 G to C and IVS9 ds+2 C to T). mRNA analysis for mutations exon 7 ds-62 C to T and 6Ψ ds-1 A to G, revealed the absence of the last 63 bases of exon 7 and the activation and insertion of the pseudoexon sequence in the GHR mRNA, respectively. No product corresponding to the GHR mRNA was detected in patients with the IVS2 ds+4 A to C. The 6Ψ ds-1 A to G resulted in activation of the pseudoexon and inclusion of 108 additional nucleotides in the patient's GHR mRNA.

DNA analysis of GHI patients revealed that no additional nonsense or missense mutations were present in patients carrying the above nucleotide changes, except for the patient carrying the IVS2 ds+4 A to G base change, in whom a deleterious GHR homozygous defects (R161C) was found.

4.5 DISCUSSION

This study showed that the *in vitro* splicing assay can accurately identify nucleotide changes resulting in aberrant gene splicing. The assay was particularly helpful in cases of defects occurring outside the invariant nucleotides of the splice sites, for which the *in silico* prediction programs gave ambiguous results.

Base change	*In silico* results (score wild type vs mutant)	*In vitro* splicing results	*In vivo* results
IVS2 ds+4 A to G	93.03 vs 84.69	No effect on exon 2 splicing	SNP
IVS2 ds+4 A to C	93.03 vs 84.23	No effect on exon 2 splicing	n.a.
Exon 4 C to T R43X	52.26 vs 79.09	No effect on exon 4 splicing	R43X
Pseudoexon 6Ψ ds-1 A to G	79.36 vs 89.94	Pseudoexon insertion	Pseudoexon insertion
IVS7as-6 T to A	85.57 vs 82.80	Skipping of exon 8	n.a.
Exon 7 ds-62 C to T	66.30 vs 93.14	63 bases missing	63 bases missing
IVS8 ds-1 G to C	90.71 vs 79.69	Skipping of exon 8	Skipping of exon 8

n.a., not available

The *in vitro* splicing assay for defects within the invariant splice site sequence

Splice mutations are approximately 50% of DNA point mutations responsible for human genetic diseases. In the majority of cases, they affect the efficiency of mRNA splicing leading to mutant proteins, by abolishing a native splice site through a base change located within the invariant nucleotides of the donor or acceptor sites (Krawczak et al., 1992), and less frequently by altering other splicing elements, such as the polypyrimidine tract and the branch point (Li et al., 1998, Groussin et al., 2006). The aim of this study was to establish the diagnostic value of an *in vitro* assay, based on a three-exon minigene system spliced in HeLa nuclear extracts, to assess the consequences of genetic defects on mRNA splicing. All novel and previously identified nucleotide changes detected in the *GHR* of the GHI population were analysed *in silico* and those suspected of inducing aberrant splicing where studied *in vitro*, prioritising those occurring outside the splice sites. Splice sites are, in fact, characterised by invariant nucleotide sequences, with introns being flanked in 99% of cases by GT and AG dinucleotides at the 5' and 3' splice site, respectively (Berget, 1995, Burset et al., 2000)

and exons by the A/CAG sequence at the donor site and G at the acceptor site in over 60% of the cases (Burset et al., 2001). Therefore, any base change occurring at these positions can be easily and efficiently predicted to cause aberrant splicing. As expected, the use of the *in vitro* assay to test the base change disrupting the invariate nucleotides at the splice site (nucleotide change G to C at IVS8 ds-1) resulted in the skipping of the mutation-harbouring exon, thus confirming the *in silico* prediction and *in vivo* data (Woods et al., 1996).

The *in vitro* splicing assay for defects outside the invariant splice site sequence

The potential diagnostic application of the *in vitro* assay became evident in cases where the nucleotide change, either exonic or intronic, occurred outside the splice site consensus sequences. In this study, three defects were located either upstream of the acceptor (IVS7 as-6 T to A) or downstream of the donor splice site (IVS2 ds+4 A to C and IVS2 ds+4 A to G). The *in silico* analysis showed a modest score reduction (less than 10%) compared to wild type for all three nucleotide changes. In particular, the IVS7 as-6 T to A, located within the polypyrimidine tract, resulted in the smallest score reduction among the three, with only 3% reduction compared to the wild type, which would not have indicated this defect as the cause of GHI. The *in vitro* assay, however, showed clear skipping of the mutation-harbouring exon from the mRNA. Mutations in the polypyrimidine tract are rare and this is the first of its kind to be identified in the *GHR*. Although *in vivo* analysis to further confirm the occurrence of aberrant splicing is needed and is part of future work, it has to be noted that, due to nonsense mediated decay (NMD), no patient's GHR mRNA may be present.

The two nucleotide changes downstream of the donor splice site of exon 2 (IVS2 ds+4 A to C and IVS2 ds+4 A to G) resulted in a near-10% score reduction, suggesting the possible occurrence of aberrant splicing. Nevertheless, in both cases the *in vitro* assay showed correct inclusion of the GHR exon in the mRNA. No *in vivo* data are available for the IVS2 ds+4 A to C change, while the A to G change at the same position can be considered a rare SNP since it was found in a GHI patient homozygous for the deleterious R161C *GHR* defect (Amselem et al., 1993). Although no splicing regulatory element has yet been identified downstream of the donor splice site, the *in vitro* assay is important in patients in whom no other defects in the coding region are found and mRNA

analysis shows no product for the GHR mRNA, such as the patient carrying the IVS2 ds+4 A to C.

The discordant results between the *in silico* and *in vitro* data underline an important and yet well-known, limitation of the *in silico* prediction programs. There is, in fact, no rule to define the percent of change from the wild type which indicates the occurrence of aberrant splicing. Moreover, prediction programs become less efficient the further away the base change is located from the invariant splice site sequence. As a consequence, false negative or positive predictions can be easily made, as in the case of nucleotide changes IVS7 as-6 T to A and IVS2 ds+4 A to C or G.

The *in vitro* splicing assay for defects predicted to create novel splice sites

Five base changes resulted in a splice site score increase compare to the wild type. In four of these cases the increase was greater then 40%, suggesting the creation of novel splice sites. Among these cases was a base change conventionally classified as a nonsense mutation (C to T within exon 4, R43X). According to the *in silico* analysis, this base change creates a novel donor site stronger than the natural one (mutant donor site score 79.09 vs 74.73), which could result in its preferential use over the natural site. Nevertheless, the *in vitro* assay showed no difference in the splicing of the mutant minigene compared to the wild type. Unfortunately, no mRNA analysis was available. In cases like this, in which the nucleotide change is thought to create a nonsense mutation, mRNA analysis is generally not performed. Therefore, it is not possible to know whether the base change produces a mutant protein through a nonsense mutation or a splicing defect. In this particular case, the result at a protein level would have been the same - a prematurely truncated protein - but in other cases, a splice defect may result in a partially functional protein rather than a truncated non-functional one.

The C to T base change within exon 7 is an example of how the conventional classification of a defect could be misleading. This nucleotide change would normally be thought to result in the harmless synonymous SNP G223G whereas it has been proven at an mRNA level to be a splice defect, resulting in a mutant GHR protein (Baumbach et al., 1997). The *in vitro* assay proved to be accurate in demonstrating the occurrence of

aberrant splicing by showing the preferential use of the novel splice site over the natural one.

The nucleotide change A to G at 6Ψ ds-1 (pseudoexon mutation) located deeply in intron 6 was studied in this laboratory in 2001 (Metherell et al., 2001) and proved *in vivo* and with the *in vitro* assay to result in the activation of a pseudoexon and the insertion in-frame of a new amino acid sequence. The encouraging results obtained in 2001 with the *in vitro* splicing assay on the pseudoexon mutation, were the basis for this project, which aimed at establishing a quick and reliable protocol for the creation of minigenes and at testing different mutations, thus making the assay a valid alternative to patient mRNA analysis. The recreation of the pseudoexon minigene L1-GHR6Ψ-L2 confirmed previous findings but, more importantly, demonstrated the superiority of the *in vitro* assay over the *in silico* predictions.

Limitations

A limitation of this study is the small number of mutations studied and *in vivo* results available. Although, the three-exon minigene system spliced in nuclear extract is a widely used technique for studying regulatory splicing elements, it should not be forgotten that it is an *in vitro* system, and tissue specific differences may occur. Thus, the study of additional mutations, especially outside the invariant splice sites sequences in the *GHR* and other genes, and *in vivo* analysis is necessary for assessing further the accuracy of this system.

CHAPTER 5

THE *GHR* PSEUDOEXON 6Ψ: FROM DIAGNOSIS TO THERAPY

5.1 BACKGROUND

In 2001, Metherell et al. described a novel *GHR* intronic point mutation located between exons 6 and 7 (base change A to G). This was positioned at the donor splice site of a pseudoexon (6Ψ), which is normally not recognised by the splice machinery. Introns are rich in pseudoexons, which are not included in the mature mRNA for reasons which still remain unclear (Sun and Chasin, 2000). In the case of the *GHR* pseudoexon 6Ψ, Akker et al. demonstrated the presence of multiple sequences within the pseudoexon 6Ψ, which can bind the heterogeneous nuclear ribonucleoprotein particle E1 protein (hnRNP E1) and the U1 snRNP in the pre-spliceosomal complex and silence the pseudoexon 6Ψ. Moreover, the authors showed that a combination of the 5' splice site and the splicing silencing elements, is required for pseudoexon 6Ψ silencing (Akker et al., 2007).

In some cases, subtle changes in the pseudoexons are sufficient to lead to their activation and the *GHR* 6Ψ A to G defect is an example of such a case. This mutation leads to the recognition of the pseudoexon sequence and the inclusion of 108 additional nucleotides between exons 6 and 7 in the GHR mRNA. The result of this mutation is the production of an abnormal GHR protein with 36 additional amino acids in its extracellular domain (Metherell et al., 2001) (Figure 5.1).

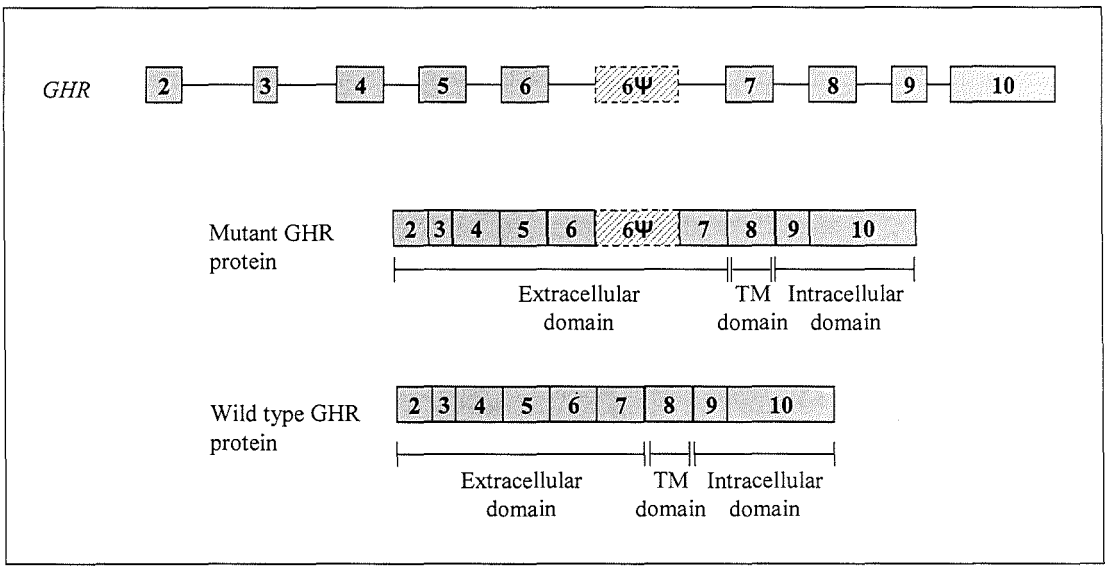

Figure 5.1 The *GHR* pseudoexon 6Ψ mutation. The A to G base change at the donor splice site of the pseudoexon leads to aberrant GHR splicing and the inclusion of 36 new amino acids in the GHR protein. TM, transmembrane domain.

Functional studies demonstrated that the mutant protein maintains its signaling properties, but has impaired cell surface trafficking (Maamra et al., 2006).

There is now a significant amount of literature demonstrating the relationship between splice defects and diseases. This has led to the development of new therapeutic tools, such as antisense oligonucleotides (ASOs), aimed at correcting aberrant splicing. ASOs are synthetic RNA molecules of approximately 10-20 nucleotides, designed to be complementary to a target sequence on the pre-mRNA. ASOs complementary to pre-mRNA splice sites, branch points or ESEs are effective in restoring aberrant splicing *in vitro* and in cell transfection systems and can restore exon inclusion or exclusion induced by splice mutations (Dominski and Kole, 1993, Sierakowska et al., 1996, Vacek et al., 2003, van Deutekom and van Ommen, 2003, Hua et al., 2007). The mechanism of action of ASOs is RNase H cleavage-independent. ASOs are thought to act by physically interfering with the apposition of spliceosome elements on the target pre-mRNA sequence (Kole and Sazani, 2001). The ASO approach has been used *in vitro* and *in vivo* to correct aberrant splicing defects leading to neuro-muscular diseases, with promising results and human trials are currently under way (Takeshima et al., 2006, van Deutekom et al., 2007).

Although mutations occurring in the GHR extracellular domain, such as the pseudoexon, are generally associated with typical GHI, also known as classical Laron syndrome, the four siblings in whom the pseudoexon defect was originally found, had non-classical GHI, with normal facial features and a mild degree of GHI (Bjarnason et al., 2002). The genetic study of GHI presented in Chapter 3 of this Thesis has now identified seven novel patients from 5 apparently unrelated families with the same pseudoexon 6Ψ defect.

5.2 HYPOTHESIS AND AIMS

The aim of this project was to define the relation between genotype and phenotype in patients with the pseudoexon 6Ψ mutation, by analysing auxological, biochemical, genetic and haplotype data from all known patients with severe short stature and GHI caused by the *GHR* 6Ψ ds-1 A to G defect. Moreover, this project aimed to correct the aberrant splicing caused by this mutation by use of RNA antisense oligonucleotides in an *in vitro* splicing assay and in a cell transfection system.

5.3 POPULATION

Eleven patients with the *GHR* 6Ψ ds-1 A to G (pseudoexon mutation) were studied. Four of these patients were the cohort reported in 2001. The remaining seven patients were part of the GHI study population presented in Chapter 3 of this thesis. Informed consent was obtained from all patients and their parents. Ethical approval was obtained by individual centres recruiting patients.

5.4 MATERIALS AND METHODS

5.4.1 Genotyping

Dinucleotide repeat markers spanning 17.10Mb around the *GHR* locus on chromosome 5 and SNPs present in the *GHR* intron 9 and presented in Chapter 3 of this Thesis (section 3.4.3), were used for the genotype analysis of GHI patients with the pseudoexon mutation IVS 6Ψ ds-1 A to G. Briefly, repeat markers were amplified from genomic DNA by PCR using specific primers (sequences reported in Appendix 3:10.3.8), denatured and electrophoresed. Results were analysed using Genescan and Genotyper software (Perkin Elmer Applied Biosystems, UK). For the analysis of the complex polymorphic *GHR* intronic region, intron 9 was amplified using specific primers (sequences reported in Appendix 3:10.3.1). PCR samples were visualised on a 1% agarose gel and analysed by direct sequencing on the ABI 3700 Sequencer. Haplotypes were indicated by Roman numerals according to the classification proposed by Amselem et al. (Amselem et al., 1989), and reported in Appendix 6.

5.4.2 PCR and sequencing

The wild type minigene L1-GHR6Ψ-L2 was created using PCR and overlap-extension PCR techniques as previously decsribed. The splice reporter Adml-par (L1-L2) was also amplified by conventional PCR and used as a positive control for the splicing reaction. The PCR products were run on a 1% agarose gel and those corresponding in size to the three-exon minigene, cut and purified by PCR gel extraction. The identity of the PCR product was confirmed by direct sequencing on the ABI 3700 Sequencer.

5.4.3 A-tailing and Cloning

Blunt-ended PCR reactions generated by the proof-reading polymerase were A-tailed and cloned in the pGEM T-easy vector system. White colonies containing the inserts were picked and cultured. Minipreparation of plasmid DNA was obtained using the Qiagen plasmid mini kit (Qiagen). The presence of the insert was assessed by direct sequencing.

5.4.4 Site-directed mutagenesis for the creation of mutant minigenes

The mutant GHR minigene was obtained by site-directed mutagenesis using specific primers (sequences reported in Appendix 3: 10.3.5) and the wild type minigene as a template.

5.4.5 *In vitro* transcription and RNA purification

Wild type and mutant DNA minigenes and Adml-par were transcribed into mRNA in the presence α^{32}P-GTP (10μCi). After 1 hour incubation at 37°C, reactions were mixed with RNA loading dye, heated at 98°C for 5 min and then run on a 4% polyacrylamide gel for 45 minutes at 980 Volts. Fluorescent markers were attached on the gel that was exposed overnight at -80°C and then subjected to autoradiography. The fluorescent-labelled gel image was used to excise the RNA bands from the gel. The RNA was extracted from the gel bands and stored at -20°C or used for the *in vitro* splicing assay.

5.4.6 Antisense oligonucleotides (ASOs)

Three 18-mer 2'O-methyl oligoribonucleosides complementary to the donor, acceptor and branch site of the *GHR* pseudoexon were designed and synthesised (Dharmacon). Their sequences are reported in Appendix 3:10.3.6. ASOs were tested at different concentrations (ranging from 0nM to 250nM) in the *in vitro* splicing assay and in a cell transfection system.

5.4.7 *In vitro* Splicing assay and ASOs

ASOs (final concentration ranging from 0nM to 250nM) were incubated at 30°C for 5 minutes with a 12.5μl splice reaction mixture prepared as described in Materials and Methods section 2.9.4, but without the addition of the RNA minigene. At the end of the incubation, 10fmol RNA was added and the reaction was incubated at 30°C for an additional hour. Control reactions were kept on ice for the same time.

To optimise ASOs efficiency the following modifications to the protocol were tested:

a) ASOs were first incubated at 30°C for 5 minutes with RNA and at the end of the incubation the complex was added to the splicing master mix and incubated for an additional hour, or

b) ASOs and RNA added together to the master mix and incubated at 30°C without any pre-incubation step.

At the end of the incubation, reactions were deproteinised, precipitated, mixed with RNA dye, heated at 98°C for 5 minutes and run on an 8% denaturing polyacrylamide gel for 1 hour and 45 minutes at 980 Volt, before autoradiography. The bands of interest, corresponding in size to correctly spliced or aberrant products, were excised from the gel and retro-transcribed into cDNA. This was amplified by PCR (RT-PCR) using specific primers for Adml-par exon L1 and exon L2 (sequences reported in Appendix 3:10.3.4) and products analysed by direct sequencing on the ABI 3700 DNA Sequencer.

5.4.8 Subcloning of minigenes in pcDNA 3.1

Wild type and mutant minigenes L1-GHR6Ψ-L2 were subcloned from the bacterial pGEM T-easy vector into the mammalian pcDNA 3.1 vector. The insert product was released from the parent vector and ligated into the destination vector according to the protocol described in Materials and Methods section 2.6.6. The ligation reaction was transformed into competent bacterial cells and the identity and correct orientation of the pcDNA3.1 L1-GHR6Ψ-L2 plasmid insert was assessed by direct sequencing on the ABI 3700 Sequencer.

5.4.9 Cell culture and transfection of ASOs

HEK293 cells (a gift from Dr P Chapple) were maintened in Dulbecco's minimum essential medium (DMEM, Sigma-Aldrich) with 10% fetal bovine serum (FBS, Sigma-Aldrich) at 37°C under 5% CO_2 and split when confluent. Before transfection, HEK 293 cells were seeded in 12-well plates. Cells were transiently transfected when approximately 50% confluent, with the mutant pcDNA3.1 L1-GHR6Ψ-L2 plasmid (50ng) and different concentrations of ASOs (final concentration ranging from to 0nM to 250nM) using Lipofectamine 2000 (Invitrogen) and the following protocol:

a) for each transfection 2.64µl of Lipofectamine 2000 was added to 107.36µl of Optimem (Invitrogen) in a 1.5ml tube and left to incubate at room temperature for 5 minutes;

b) the ASOs-plasmid-Lipofectamine 2000 complex was made as follows: according to the desired ASOs final concentration, xµl of one or more 100µM stock ASOs, were placed in 1.5ml autoclaved tube with 1µl of plasmid (50ng) and xµl of Optimem to a final volume of 100µl. In the negative control ASOs were omitted;

c) 100µl of the Lipofectamine2000/Optimem was added to the ASOs/plasmid/Lipofectamine 2000 reaction and the complex left at room temperature for 20 minutes;

d) the complex (200µl) and 1ml of cell media were added to each well of a 12-well plate to give a final volume of 1.2ml per well.

Cells were incubated for 48 hours at 37°C before harvesting.

5.4.10 RNA extraction and RT-PCR

Forty eight hours after transfection, cells were harvested, RNA extracted and reverse transcribed into cDNA. cDNA was amplified in the presence of 0.5µCurie of ^{32}P dCTP in a 12.5µl PCR reaction with *Taq* polymerase (Sigma) and specific primers for L1 and L2 (sequences reported in Appendix 3: 10.3.4). PCR products were electrophoresed on an 8% non-denaturating polyacrylamide gel (prepared as decribed in Materials and Methods section 2.5.4) prior to autoradiography and phosphoimaging.

5.4.11 Phospho imaging

Quantification of phospholabeled alternative splicing products was performed using the PhosphorImager and ImageQuant software (GE Healtcare) available at the Centre of Molecular Oncology at the William Harvey Research Institute. The percentage of alternative splicing was calculated as isoform/total of all isoforms.

5.4.12 Biochemical assessment

Serum IGF-I, IGFBP-3, ALS and GHBP were measured from venous blood samples, using an enzyme-linked immunosorbent assay (ELISA kit; Diagnostic System Laboratories, Inc. Webster, TX, USA) by Dr F. Miraki-Moud in the laboratories of Dr C. Camacho-Hubner at Barts and the London..

5.4.13 Statistical analysis

Results are presented as mean ± standard deviation from at least three separate experiments.

5.5 RESULTS

5.5.1 Clinical characteristics of patients with the IVS 6Ψ mutation

The 11 patients with the pseudoexon mutation had normal GHBP levels but differing degrees of GH insensitivity, as demonstrated by the wide range of growth failure and serum IGF, IGFBP-3 and ALS levels. Biochemical and auxological data for all 11 patients are shown in Table 5.1.

TABLE 5.1 AUXOLOGICAL AND BIOCHEMICAL DATA FOR THE 11 PATIENTS WITH THE *GHR* PSEUDOEXON MUTATION.

Family	Family member	Age (yrs) at assessment	Sex	Tanner Stage	Height (SDS)	GH (mU/l) Basal (Peak)	IGF-I (ng/ml) [NR]	Facial features
A	1	10	M	I	-4.4	16.7 (55.2)	23* [38-318]	normal
	2	14	M	I	-5.6	12.0 (203)	21* [39-537]	normal
	3	10	M	I	-3.9	52.4 (270)	20* [38-318]	normal
	4	14	M	II	-3.3	14.3 (86.7)	29* [39-537]	normal
	5	7	F	I	-5.0	(21.3)	32* [64-406]	normal
B	1	8	F	I	-6.0	(>100.0)	4* [64-406]	typical LS
C	1	21	M	V	-5.0	1.8	149 [49-550]	typical LS
D	1	6	M	I	-3.4	NA	36* [64-406]	typical LS
	2	11	M	II	-4.6	NA	132 [38-318]	typical LS
E	1	7	F	I	-3.3	18.0 (60.0)	53* [64-406]	normal
	2	13	F	IV	-3.5	25.0 (80.0)	113 [39-537]	normal

Patients A1-A4 were the four boys with non-classical GHI described in 2001. Patient A5's genetic diagnosis was established as part of the genetic analysis of the GHI population presented in this thesis. She was a member of the same highly consanguineous Pakistani family as patients A1-A4. Her height was -5.0 SDS and, similar to other

affected members of this family, she had normal facial features and a biochemically mild GHI phenotype.

Patient B1 was an 8-year-old female. Her grandparents were cousins of Pakistani origin. Her height was –6.0 SDS. She had a younger sibling with growth retardation and elevated GH levels (DNA not available for analysis). She had typical LS facial features, with a prominent forehead and mid-facial hypoplasia. Biochemically, she had severe GHI as demonstrated by the almost undetectable levels of GH-dependent proteins (IGF-I, IGFBP-3 and ALS).

Patient C1 was the 21-year-old son of two first-degree cousins of Palestinian-Arab origin. His height was –5.0 SDS. He had two other siblings with short stature (DNA not available for analysis). They all had typical LS facial features. Biochemically, he had a mild GHI phenotype. His IGF-I and IGFBP-3 values were normal.

Patients D1 and D2 were from a consanguineous Pakistani marriage. D1 was a 6-year-old male with a height SDS -3.4 and low IGF-I, IGFBP-3 and ALS levels. His brother, D2, age 11, height SDS -4.6, also had low ALS levels but normal IGF-I and IGFBP-3 levels reflecting his pubertal status. Both children had typical LS facial features.

Patients E1 and E2 were sisters from a consanguineous Pakistani family. They had similar height SDS scores of -3.3 and -3.5, respectively. Both displayed a normal facial phenotype, but E1 had subnormal IGF-I and IGFBP-3 levels, whereas her sister's values were normal for her age, again reflecting her pubertal status.

5.5.2 Genotype analysis of patients with the IVS 6Ψ mutation

Analysis of a 17.10Mb region on chromosome 5 surrounding the *GHR* locus, revealed the same genotype in affected members of three apparently unrelated families (A, B and C), suggesting a common ancestor. A recombination event downstream of the *GHR* locus, between markers D5S2087 and D5S474, had occurred in family B. Families D and E were not known to be related, but had the same haplotype being identical by descent upstream of the *GHR* and homozygous both at the *GHR* locus and downstream. The analysis of the single nucleotide polymorphisms in intron 9 of the *GHR* and of marker D5S2087 demonstrated the same genotype in all families (Figure 5.2) over a conserved region of at least 1.8Mb, suggestive of a common ancestor.

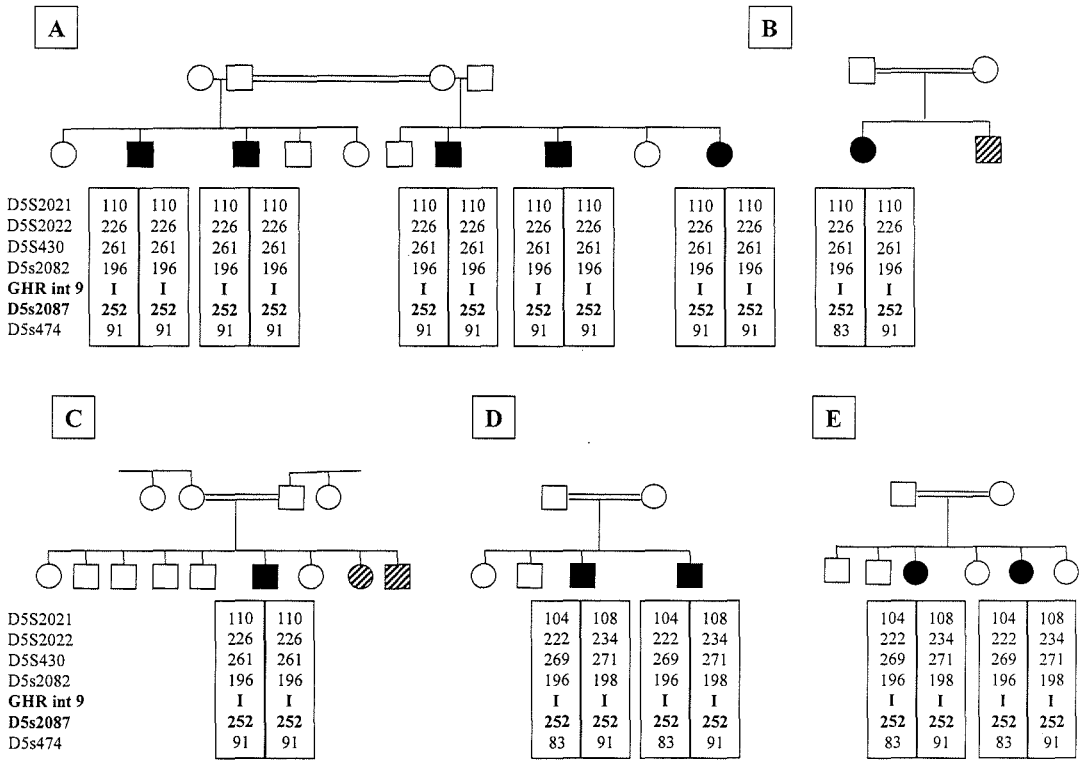

Figure 5.2 Family pedigrees and genotype analysis. Affected family members are shown in black, possibly affected in grey. In family A, the five cousins had identical genotypes. In family D, the brothers had identical genotypes and in family E the sisters had identical genotypes. The genotypes of the affected members of each family are indicated below the family trees in boxes. All families had an identical genotype at the *GHR* locus and marker D5S2087, as shown in bold.

5.5.3 Correction of aberrant splicing caused by the IVS 6Ψ mutation: effect of ASOs in the *in vitro* splicing assay

Three 2'O-methyl RNA ASOs were targeted to the donor (ASO 5') and acceptor (ASO 3') splice sites and branch point (ASO br) of the mutant pseudoexon sequence (Figure 5.3). Their ability to restore correct splicing was tested using the *in vitro* splicing assay and the L1-GHR6Ψ-L2 mutant minigene.

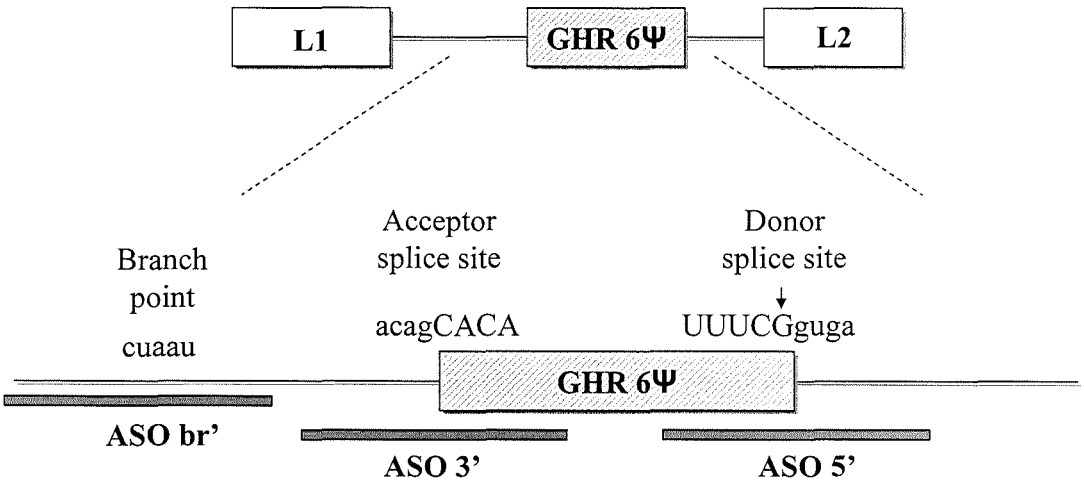

Figure 5.3 Diagram of the L1-GHR6Ψ-L2 mutant minigene and the ASO position within the minigene. The position of splice elements is also indicated. Mutation position is indicated by the arrow.

Each ASO was initially tested at a 250nM concentration. ASO 3' induced pseudoexon skipping from the mRNA, as demonstrated by the absence of the 294 bases band corresponding to the L1-GHR6Ψ-L2 mRNA and the appearance of the 186 bases band corresponding to exon L1 and L2 joined together (L1-L2 mRNA). ASO' 5' produced a modest pseudoexon skipping, whereas ASO br had practically no effect (Figure 5.4).

To assess whether targeting two splice elements is more effective than targeting a single element, two ASOs, each at a concentration of 125nM, were used in the same splice reaction. The combination ASO 3' – ASO 5' and ASO 3' – ASO br produced a modest pseudoexon exclusion from the mRNA, as demonstrated by the appearance of both mRNA spliced products L1-GHR6Ψ-L2 (294 bases) and L1-L2 mRNA (186 bases). Almost no pseudoexon skipping was seen for the combination ASO 5' – ASO br (Figure 5.4).

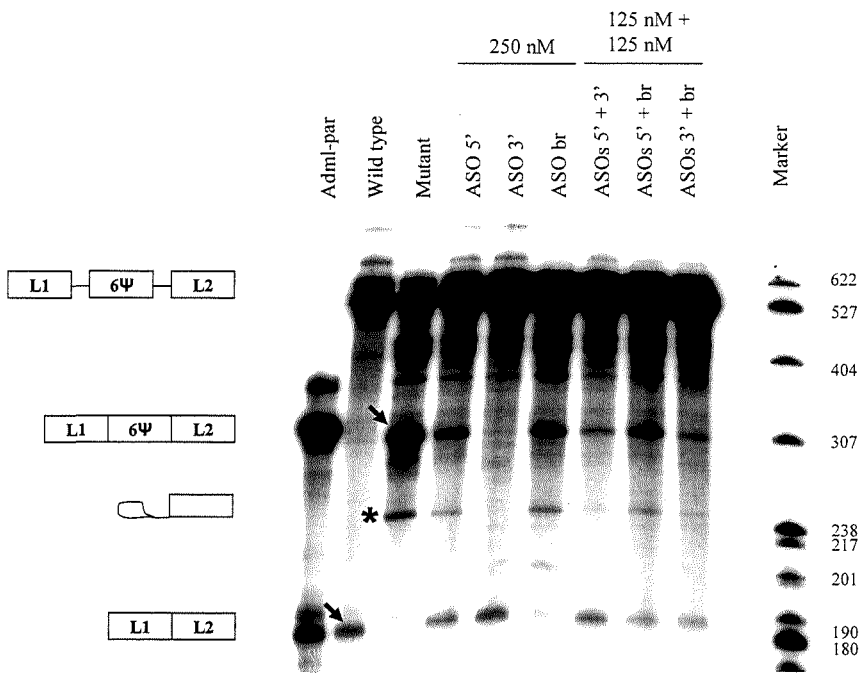

Figure 5.4 Effect of ASOs, alone or in combination, on the mutant L1-GHR6Ψ-L2 minigene splicing. The identity of each product is represented on the left. Splicing of Adml-par and the wild type and mutant minigenes L1-GHR6Ψ-L2, in the absence of ASOs, is also shown. One representative example of three separate experiments is presented. The position of the spliced products with (294 bases) and without the pseudoexon (186 bases) are indicated by arrows. The position of a lariat (intermediate of reaction) is indicated by the asterisk.

ASO 3' and 5', which had produced pseudoexon skipping, were further tested by titrating their concentrations from 250nM to 10nM. ASOs targeting the acceptor splice site (ASO 3') induced complete pseudoexon skipping from the mRNA at a concentration of 250nM, 125nM and 100nM. This effect was dose-dependent, with almost no effect at a concentration of 50nM and 10nM. ASOs targeting the donor splice site (ASO 5') produced a modest pseudoexon exclusion from the mRNA, with the maximum effect seen with concentrations of 250nM, 125nM and 100nM and almost no effect seen at 50nM and10 nM. (Figure 5.5).

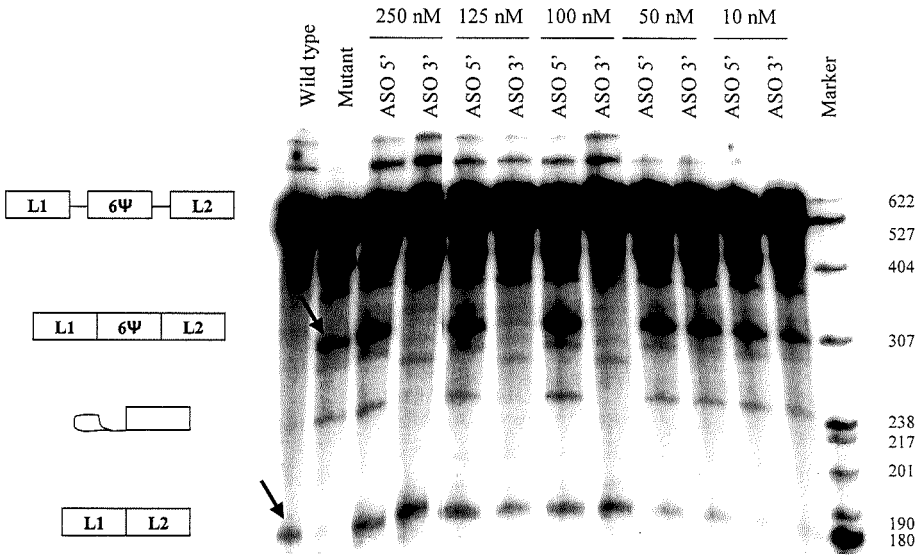

Figure 5.5 Dose-response analysis with ASOs 3' and 5'. The identity of each product is schematically represented on the left. Splicing of Adml-par and of the wild type and mutant minigenes L1-GHR6Ψ-L2, in the absence of ASOs, is also presented. One representative example of three separate experiments is presented. The position of the spliced products with (294 bases) and without the pseudoexon (186 bases) are indicated by arrows.

The ASO targeting the branch point (ASO br) did not cause exon skipping and reduced the efficacy of ASO 3' when used in combination. To test whether ASO br could act as an enhancer of pseudoexon inclusion, it was tested on the wild type L1-GHR6Ψ–L2 minigene at concentrations ranging between 250nM and 0nM. The addition of ASO br to the splice reaction had no effect on the wild type minigene splicing, as demonstrated by the absence of the 294 bases band corresponding to the L1-GHR6Ψ–L2 mRNA and the appearance of the 186 bases band corresponding to L1-L2 mRNA (Figure 5.6).

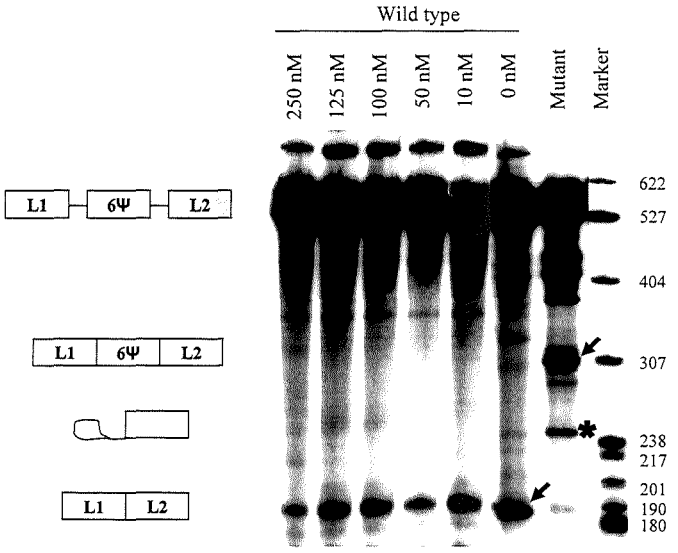

Figure 5.6 Effect of ASO targeting the branch point (ASO br) on the wild type L1-GHR6Ψ–L2 minigene. The different ASO br concentrations tested are indicated above. One representative example of three separate experiments is presented. Splice products with (286 bases) and without (186 bases) the pseudoexon 6Ψ are indicated by arrows. The position of an intermediate of reaction (lariat) is indicated by the asterisk. The identity of each product is schematically represented on the left.

5.5.4 Correction of aberrant splicing caused by the IVS 6Ψ mutation: effect of ASOs in HEK293 cells

The three ASOs targeting the donor (ASO 5') and acceptor (ASO 3') splice sites and the branch point (ASO br) were transfected with the pcDNA3.1 L1-GHR6Ψ–L2 mutant plasmid in HEK 293 cells. Two ASO concentrations (250nM and 125nM), which *in vitro* were effective in inducing pseudoexon skipping, were tested. Mock-transfected cells (no ASO) showed no skipping of the pseudoexon. ASO 3' induced a 91.8±11.6% and 100±0% pseudoexon exclusion at a concentration of 250nM and 125nM, respectively. The ASO directed against the donor splice site produced a modest pseudoexon skipping 31.8±10.3% and 46.2±19.0% at a concentration of 250nM and 125nM, respectively. ASO br tested at a concentration of 250nM resulted in no pseudoexon skipping. Two ASOs, at 125nM concentration each, were then tested in the same splice reaction. The combination ASO5'-ASO3' resulted in a 49.1±37.3% pseudoexon exclusion, whereas the combination ASO5'-ASO Br and ASO3'-ASO Br resulted in 21.7±7.5% and 13.4±2.3% pseudoexon exclusion, respectively (Figure 5.7).

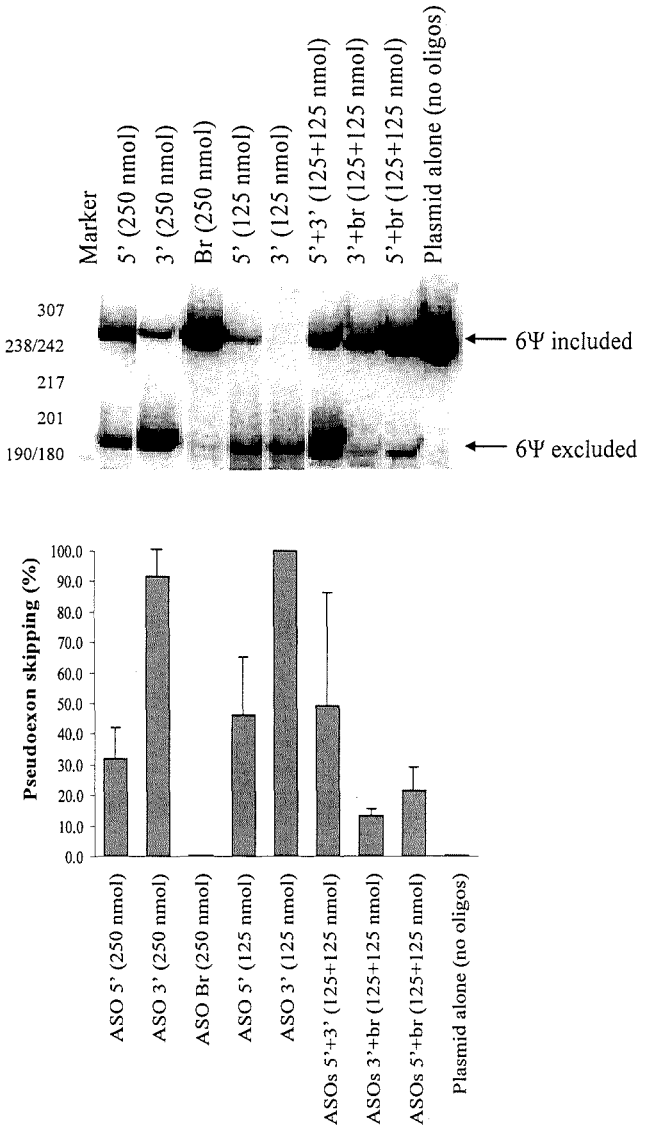

Figure 5.7 Effect of ASOs in HEK293 cells. A) HEK293 cells were transfected with plamid pcDNA3.1 L1-GHR6Ψ-L2 carrying the pseudoexon mutation ds-1 A to G and with one or more ASOs. One representative example of three separate experiments is presented. The position of the bands corresponding to the mRNA product with (294 bases) or without (186 bases) the pseudoexon is indicated. B) Quantitative data are presented as mean±standard deviation.

5.6 DISCUSSION

The *GHR* pseudoexon mutation 6Ψ A to G responsible for GHI has the unique characteristic of being associated with a wide range of phenotypes. Antisense oligonucleotides are effective in correcting aberrant gene splicing caused by this mutation, both *in vitro* and in a cell transfection system and represent a promising therapeutic tool for these patients.

Phenotypic variability associated with the *GHR* pseudoexon defect

The genetic study of GHI, the results of which are presented in Chapter 3 of this Thesis, demonstrated that the pseudoexon mutation was responsible for causing GHI in seven novel cases. Clinical data for these patients were pooled together with those of the initial 4 cases described in 2001, with the aim to identify the genotype-phenotype relationship of this mutation. Analysis of morphological features, as well as biochemical and auxological data, revealed the presence of a wide range of phenotypes associated with this mutation. Phenotypic variability in GHI patients with the same mutation has been described (Rosenbloom et al., 1990, Rosenfeld et al., 1994, Woods et al., 1997), but was particularly striking in patients with the pseudoexon mutation. The 5 members of family A had normal facial features and a mild degree of GHI, with low but detectable IGF-I levels and heights ranging from –3.3 to –5.6 SDS. The remaining six patients have phenotypes varying between mild GHI with no typical Laron features (patient E1 and 2), to very severe GHI coupled with typical LS facial features (patient B1), which is more severe than that originally reported (Metherell et al., 2001)..

The variability in clinical phenotypes observed in patients carrying the pseudoexon mutation may be due to the presence of transcript heterogeneity. The presence of a splice mutation may result in competitive use of the normal and mutant splice sites and the production of different transcripts. Analysis of cDNA from patients carrying splice mutations has demonstrated that multiple abnormal splicing events can occur alongside the production of varying amounts of the normal splice product (Zhu et al., 1997, Lemahieu et al., 1999). It is, therefore, possible that mildly affected subjects in the pseudoexon cohort have a GHR transcript ratio in favour of the normal protein, while severely affected patients have a ratio in favour of the mutant GHR.

Alternative explanations for the clinical heterogeneity over and above that observed with typical missense and nonsense mutations of the GHR can be envisaged. The inclusion of the pseudoexon leads to impaired trafficking of the GHR (Maamra et al., 2006). Genetic variability in components of GHR processing and trafficking might, conceivably, have a greater influence on the mutant GHR than they do on the wild type. The same may be true for components of the receptor degradation pathways.

Use of ASOs for correction of the aberrant splicing caused by the 6Ψ *GHR* defect

The presence of a wide range of phenotypes associated with the pseudoexon mutation leads one to speculate that there could be an even milder phenotype associated with it. The possibility arises that the pseudoexon mutation could be responsible for a small number of idiopathic short stature patients. The potential clinical involvement of this defect beyond GHI led to the search for a therapeutic tool to restore correct *GHR* splicing. The RNA antisense approach (ASOs) is currently used to correct aberrant splicing causing neurodegenerative diseases and haematopoietic disorders, with promising results *in vitro* as well as in animal models (Dominski and Kole, 1993, Sierakowska et al., 1996, Vacek et al., 2003, van Deutekom and van Ommen, 2003, Hua et al., 2007). The present study is the first to adopt this technique to correct an endocrine disorder. The A to G base change at the 5' splice-site responsible for GHI in patients with the pseudoexon mutation, does not create a new donor splice-site, but increases the base-pair match of the existing donor site with the U1 snRNA. The simultaneous activation of a cryptic acceptor splice site leads to the recognition by the spliceosome of the pseudoexon sequence and its inclusion in the mature mRNA (Metherell et al., 2001, Akker et al., 2007).

This study tested the use of ASOs for blocking the aberrant splice site or other major splicing elements within the *GHR* pseudoexon, affecting the ability of the splicing machinery to recognise the pseudoexon sequence and, thus, restoring correct gene splicing. An ASO directed against the mutant donor splice site of the pseudoexon was tested alongside ASOs targeted against two additional major splicing regulatory elements: the acceptor splice site and the branch point. The efficiency and optimal conditions of the three ASOs were first tested using the *in vitro* splicing assay and then in

HEK293 cells transfected with the mutant plasmid. This cell transfection system was used because of the non-availability of cells from patients with the pseudoexon mutation.

As expected, the effect of the ASOs was dose-dependent, with an optimal effect seen at concentrations between 100-250nM. Surprisingly, the most effective ASO in restoring correct splicing, both *in vitro* and in the cell system, was the one against the acceptor splice site whereas the ASO against the donor splice site, where the pseudoexon mutation occurs, only showed a modest effect. Since very little is known about the precise mechanism of action of the ASOs, it is difficult to explain this finding. The presence of a different accessibility of the acceptor versus the donor splice sites in the two cell lines used in this study (HeLa cells for the *in vitro* splicing assay and HEK293 cells for cell transfection studies) may justify the superior efficacy of the ASO targeting the 3' splice site compared to the ASO targeting the 5' splice site and testing of ASOs on additional cell lines would be advisable.

Although some studies have suggested that targeting more than one splice element can be more effective than targeting a single one, this study demonstrated that simultaneous use of two ASOs is less effective and partially abolished the effect of individual ASOs, both *in vitro* and the cell system. This was particularly evident in the case of the ASO targeting the branch point (ASO br) which, used together with other ASOs, significantly blunted their effect. The mechanism responsible for this phenomenon remains unknown, but a promoting effect of the ASO br on *GHR* pseudexon inclusion appears unlikely. In fact, when tested *in vitro* on the wild type *GHR* minigene, the ASO br did not result in inclusion of the pseudoexon in the spliced mRNA.

Limitations

A limitation of this study is the lack of data on the effect of ASOs on the cells of GHI patients expressing the mutant *GHR*. Although the results of this study suggest a sequence-specific effect of the 3' ASO, the possibility cannot be excluded that this ASO can also block additional splice sites similar to the *GHR* 6Ψ pseudoexon, located in other pre-mRNAs. Assessment of the specific skipping of the *GHR* pseudoexon induced by the 3' ASO in the cells of GHI patients is potential future work, as is the use of a scrambled 3' ASO, which may provide further information on the ASO specific sequence effect.

Conclusion

In conclusion, the *GHR* pseudoexon mutation is associated with a wide range of GHI phenotypes and should, therefore, be considered in all GHI patients in whom no mutation in the coding region of the *GHR* is found, regardless of the severity of their disease. Use of RNA antisense nucleotides for restoring aberrant splicing caused by the *GHR* pseudoexon mutation appears promising and results from this study could form the basis for gene therapy in patients with GHI caused by this defect.

CHAPTER 6

GHR ALTERNATIVE EXONS AND PSEUDOEXONS

6.1 BACKGROUND

The pre-mRNA of a gene can be spliced in different ways (Johnson et al., 2003). This process, called alternative splicing, is abundantly used in higher eukaryotes and is believed to play a fundamental role in producing multiple transcripts from the same pre-mRNA, which differ in structure and function according to the type of tissue or developmental stage (Modrek et al., 2001, Stetefeld and Ruegg, 2005, Blencowe, 2006) (Figure 6.1). The reason why some exons are always included in the mature mRNA (constitutive exon), whereas others are only expressed in certain tissues or developmental stages (alternative exon) remains unknown. Possible explanations for this phenomenon include the presence (or absence) of tissue- or developmental-specific splicing factors in the gene-surrounding environment and the inefficient recognition of the alternative exon by the splicing machinery (Stamm et al., 1994, Stamm et al., 2000).

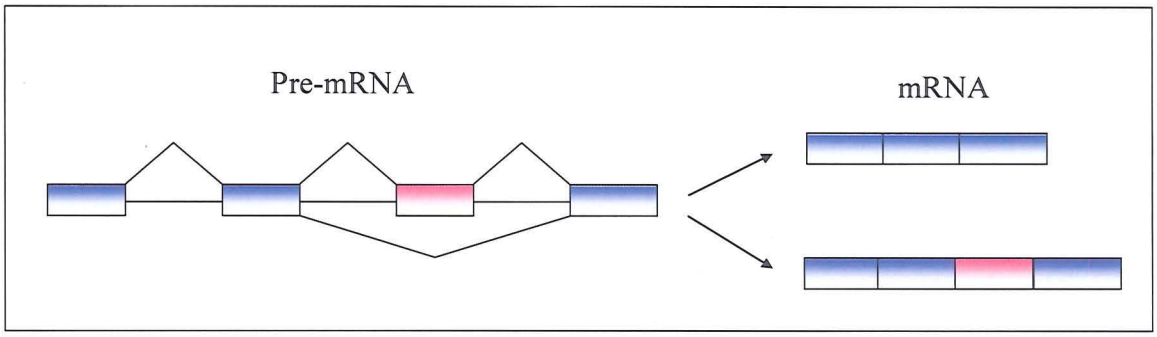

Figure 6.1 Schematic representation of alternative splicing. Coding exons are presented in blue and the alternative exon in pink.

The activation of an alternative exon can either maintain the open reading frame resulting in a novel translation product, or cause the appearance of a premature stop codon and potential degradation of the alternative protein variant. The latter often causes gene silencing and is a well recognised regulatory process of gene expression. Determination of gender in the *Drosophila*, which results from alternative gene splicing in embryonic life, is an example of this process. Inclusion of an alternative exon in the sex-lethal protein pre-mRNA, in fact, results in the appearance of a premature stop codon leading to a truncated non-functional protein, which is responsible for male development (Gebauer et al., 1998). In addition to its regulatory role in physiological processes, alternative splicing is also thought to be involved in the pathogenesis of various diseases.

In particular, an association between neoplasia and expression of alternative splice variants of proteins involved in cell adhesion and migration has been proposed (Gunthert et al., 1991).

DNA and RNA analysis has shown that, in addition to constitutive and alternative exons, introns are rich in sequences matching the consensus donor and acceptor splice sites. Such potential exons, are known as pseudoexons. Pseudoexons greatly outnumber real exons. Although their splice sites often match the consensus sequence better than real exons splice sites, they are not recognised by the spliceosome. It is thought that the presence or absence of additional splice elements, such as silencers and enhancers, as well as the exon surrounding environment, greatly influence the recognition of pseudoexons. However, subtle DNA changes in the pseudoexon sequences are at times sufficient to activate them. These events are generally associated with a disease (Akker et al., 2007) and such an example is the intronic mutation identified in 2001 by our group in the *GHR* of four children with non-classical GHI (Metherell et al., 2001).

To date, no functional transcripts deriving from the expression of alternative exons located in the intronic regions between coding exons of the *GHR* have been described. The d3-GHR, a GHR protein that lacks 22 amino acids, in fact, derives from a gene variant, which lacks the genomic sequence coding for exon 3 (Pantel et al., 2000). The only example of alternative splicing occurring in the *GHR* is the GHR variant arising from the utilisation of a splice site different to the natural splice site in exon 9. This variant (GHR 1-279) encodes for a prematurely truncated receptor that lacks most of its intracellular domain. It is expressed in several tissues (Ballesteros et al., 2000) and exerts a dominant negative effect on the wild type GHR (Ross et al., 1997). While the physiological role of this transcript remains unclear, its discovery unveiled its therapeutic potential in the treatment of GH/IGF-I disorders (Wilkinson et al., 2007).

The identification of alternative exons and pseudoexons relies on the study of mRNA from normal tissues and from patient samples, respectively. With this approach, however, transcripts present at a very low concentration or inducing mRNA nonsense mediated decay (NMD) may not be recognised unless specific probes targeting the novel exons are used. The currently available *in silico* exon prediction programs are able to predict constitutive coding exons in uncharacterised genes. Programs, such as FEX have an internal exon prediction accuracy of 77%, with a specificity of 79% (Solovyev et al.,

1994b, Solovyev et al., 1994a). Nevertheless, these programs rely on the recognition of exons, which would not interrupt the open reading frame (ORF) of a gene and, thus, automatically exclude exons that would cause a frameshift. Such exons may exist and prematurely truncated transcripts may have a regulatory role.

The identification of alternative exons and regions rich in potential exons in the *GHR* may shed new light on the physiology of the GH/IGF-I axis and help the diagnostic screening of GHI patients with no mutations in the *GHR* coding region.

6.2 HYPOTHESIS AND AIMS

The aim of the study was to: a) create an algorithm for identifying potential alternative exons and pseudoexons in the *GHR;* b) compare these results to those obtained using an available *in silico* exon prediction program and ESTs; c) test the presence of potential novel exons in human cDNA; d) investigate the presence of newly identified exons in cDNA samples of GHI patients with no mutations in the *GHR* coding region.

6.3 COMPUTATIONAL APPROACH

6.3.1 Criteria used for the construction of the algorithm

The *GHR* sequence was obtained from www.ensembl.org. An arbitrary 1339 bases before the initial GHR Methionine and 48 bases after the last *GHR* coding triplet were used to select the 154,935 nucleotide sequence, which was analysed for the presence of alternative exons and pseudoexons. The Alex Dong Li's splice site finder (http://violin.genet.sickkids.on.ca/~ali/) was used to identify all potential donor and acceptor splice sites as well as branch points. This *in silico* program, which uses matrices described by Shapiro and Senapathy (Shapiro and Senapathy, 1987), was chosen over other available programs because it allows automatic matching of acceptor sites and branch points.

The matrix for the algorithm was created with the help of Dr Dimopoulos, epidemiologist at Imperial College, using R version 2.6.2 (R Development Core Team, 2008, R Foundation for Statistical Computing, Vienna, Austria). This is a freely available software language and environment for statistical computing and graphics (www.r-project.org). R provides a wide variety of statistical (linear and nonlinear modelling, classical statistical tests, time-series analysis, classification, clustering) and graphical techniques, and is highly extensible. The R language is a well-developed, simple and effective programming language which includes conditionals, loops, user-defined recursive functions and input and output facilities.

Bioconductor and its package *seqinr* were used for importing genomic data and translating triplets into amino acids or stop codons. Bioconductor is an open source and open development software project aimed at providing tools for the analysis and comprehension of genomic data (www.bioconductor.org). Bioconductor is based primarily on the R programming language. The majority of Bioconductor components are distributed as R packages, which are add-on modules for R.

The following criteria were used to identify potential *GHR* alternative exons and pseudoexons:

a. the presence of a score ≥ 65 for donor and acceptor splice sites. This threshold was arbitrary and corresponded to the lowest score among donors and acceptors sites of constitutive *GHR* exons (*GHR* donor splice site =65.3);

b. the presence of at least one branch point sequence in the 60 bases upstream to the acceptor splice site, characterised by the consensus sequence CU(A/G)A(C/U) (Wu et al., 1999, Smith and Valcarcel, 2000);

c. an exon length between 50 and 200 bases. This range corresponds to the average length of an exon in humans (Lander et al., 2001);

d. the presence of a polypyrimidine tract, defined by a nucleotide ratio C+T/A+G ≥0.5 in the 20 bases upstream of the acceptor splice site. This arbitrary cut-off corresponded to the lowest ratio identified upstream of constitutive exons in the *GHR* and met the requirement of a sequence significantly enriched in pyrimidines between the branch point and the acceptor splice site, especially next to the latter (Coolidge et al., 1997).

The potential novel exonic sequences resulting from this first analysis were purged, discarding those a) sharing multiple donor or acceptor splice sites by choosing the best scoring consensus sequences, and b) having an acceptor score <80 as well as a branch point score <90. These criteria reflected what occurs naturally in the *GHR* as well as in other genes (Sironi et al., 2004).

The remaining potential exons were further purged using the following more stringent criteria: 1) a cut-off value ≥ 74 for the acceptor splice site; 2) a cut-off value ≥71 for the branch point. These new thresholds corresponded to the lowest scores for *GHR* constitutive exons (lowest acceptor score =74.7, lowest branch point score= 71.6).

Each of the remaining potential exons was inserted in the GHR mRNA according to its position relative to the constitutive exons and the resulting sequence was translated into an amino acid sequence. Stop codons were identified by the presence of TGA, TAG or TAA triplets. This criterion allowed subclassification of potential exons into those

potentially maintaining the ORF and those creating a premature stop codon in the novel GHR transcript.

6.3.2 Bioinformatic tools

The *in silico* exon prediction program FEX (http://linux1.softberry.com/berry.phtml?topic=fex&group=help&subgroup=gfind) was used to identify novel potential exons in the *GHR* and its results were compared to those obtained with the novel algorithm created in this study. FEX was preferred over other *in silico* programs because it is free on the web, simple to use and widely adopted for the identification of coding exons. The reported accuracy of FEX in recognising exons, determined on a set of 210 genes (with 761 internal exons), is 70%, with a specificity of 63%. The internal exon prediction accuracy is 77%, with a specificity of 79%. The recognition quality computed at the level of individual nucleotides is 87% for exons sequences (Solovyev et al., 1994b, Solovyev et al., 1994a).

Expressed sequence tags (ESTs) were retrieved from Ensembl (www.enseml.org) and NCBI (www.ncbi.nlm.nih.gov) databases.

6.4 MATERIALS AND METHODS

6.4.1 Primer design

Forward and reverse primer pairs (sequences reported in Appendix 3, 10.3.7) 20-26 bases long with a GC content of approximately 40% were designed to anneal within the potential novel exons.

6.4.2 PCR and sequencing

The presence of the identified alternative exons was tested in liver cDNA, since this is the tissue in which GHR is expressed the most. The standard PCR technique was used to amplify liver cDNA (courtesy of Prof. M. Korbonits), in a 12.5μl reaction with specific primer pairs (sequences reported in Appendix 3: 10.3.2 and 10.3.7) and *Taq* polymerase (Sigma). To improve the specificity and sensitivity of the PCR technique, potential exons were amplified using a hemi-nested PCR technique. Briefly, 1µl from the first PCR reaction was used in a second 12.5µl PCR reaction and amplified with a second set of primers, one of which corresponded to the primer used in the first PCR reaction, and the second primer annealed within the first round PCR product. To identify the junction between a constitutive exon and the putative new exon, a forward primer was designed to bind within the *GHR* constitutive exon and the reverse primer within the novel exon. To identify the junction between the putative new exon and a constitutive exon, the forward primer was designed to bind within the novel exon and the reverse primers within the constitutive exons (Figure 6.2). PCR products were electrophoresed on an agarose gel. In the presence of multiple bands for the same PCR product, these were cut from the gel, purified and sequenced on the ABI 3700 Sequencer.

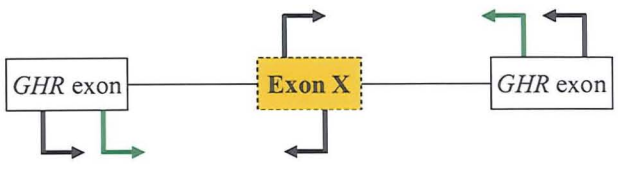

Figure 6.2 Schematic diagram showing the design of primers for the identification of novel *GHR* exons. Primers used in hemi-nested PCRs are presented in green. Constitutive exons are presented as white boxes and the novel exon as an orange box.

6.5 RESULTS

6.5.1 Identification of *GHR* pseudoexon/alternative exons

Analysis of the 154,935 nucleotide-long sequence of the GHR gene identified 3561 acceptor splice sites with a score ≥ 65 and a branch sequence in the upstream region and 1639 donor splice sites with a score ≥ 65. 5710 sequences with an acceptor, a donor splice site, a branch site and a length between 50 and 200 nucleotide were identified. After purging for the presence of a polypyrimidine tract, 3093 potential exons were obtained. After excluding potential exons not fulfilling the criteria of having an acceptor score <80 as well as a branch point score <90, 2018 potential exons were obtained which included all constitutive *GHR* exons.

To narrow down the number of potential exons, the 2018 exons were purged using more stringent criteria. After applying a cut-off score ≥ 74 for the acceptor splice site and ≥ 71 for the branch point, 1441 potential exons and the 9 constitutive *GHR* exons were left.

Almost all novel potential exons identified shared multiple donor or acceptor splice sites. After selecting the best-scoring consensus sequences, 687 potential exons remained, including the 9 constitutive *GHR* exons. Their predicted length corresponded to that reported in public databases, with the exception of exon 10, whose predicted length was 189 bases instead of 972 bases. After purging for those before the beginning of exon 2 and after the beginning of exon 10, 460 exons remained.

After excluding the 9 natural *GHR* exons, the remaining 451 potential exons where inserted in the *GHR* mRNA according to their genomic position. The majority of potential exons were located in IVS2 (197 exons), IVS3 (171 exons) and IVS 6 (38).

310 potential exons were predicted to cause a frameshift and the appearance of a premature stop codon. 141 potential exons were predicted not to cause the appearance of a premature stop codon. Of these, 22 were also predicted not to cause a frameshift and among them was the pseudoexon 6Ψ in IVS 6 (Table 6.1).

TABLE 6.1 POTENTIAL *GHR* EXONS AND PREDICTED CONSEQUENCES AT MRNA LEVEL.

	Potential exons creating a stop codon		Potential exons not creating a stop codon	
	not causing frameshift	causing frameshift	not causing frameshift	causing frameshift
IVS 2	0	138	7	52
IVS 3	0	114	13	44
IVS 4	0	11	0	7
IVS 5	0	7	1	4
IVS 6	0	27	1 (6Ψ)	10
IVS 7	0	4	0	0
IVS 8	0	8	0	2
IVS 9	0	1	0	0
Total	0	310	22	119

Intronic location and number of potential exons per intron (IVS) are indicated.

6.5.2 ESTs results

Four ESTs were annoted on Ensembl for the GHR gene: ENSESTT00000021994, ENSESTT00000021996, ENSESTT00000021988, ENSESTT00000021992.

The ENSESTT00000021994 partly corresponded to the GHR intracellular domain (part of exon 8, exon 9 and part of exon 10). The ENSESTT00000021996 corresponded to the 3' UTR region.

ENSESTT00000021988 and ENSESTT00000021992 were annotated as novel transcripts and their composition is depicted in Figure 6.3

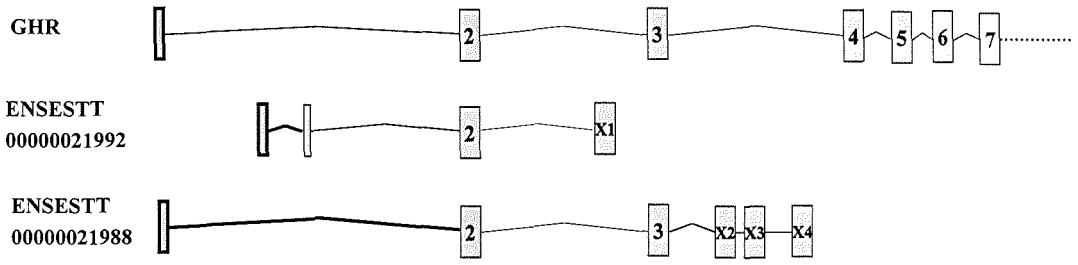

Figure 6.3 Schematic representation of two ESTs reported for the GHR.

ENSESTT00000021992 is composed of four exons (Figure 6.3). The first two exons constitute a 5'UTR and are followed by *GHR* exon 2 and by a novel exon, arbitrarily called X1 for the purpose of this Thesis. This exon is located in IVS2, 53,707 bases downstream of the *GHR* exon 2 donor site and is 163 bases long. The predicted transcript for this EST is 608 bases long and translates into a 45 amino acid sequence. The ATG starting codon of this transcript is predicted to correspond to the wild type GHR starting codon in exon 2, whereas the stop codon is located within exon X1.

ENSESTT00000021988 is composed of 6 exons (Figure 6.3). The first exon is in the 5'UTR and contains the ATG codon for the initial methionine. This exon is followed by the *GHR* exons 2 and 3 and by three novel exons located in intron 3, which, for the purpose of this Thesis, will be arbitrarily called exons X2, X3 and X4. The length of these novel exons is 32, 145 and 161 bases, respectively. The predicted transcript for this EST is 566 bases long and translates into a 69 amino acid sequence. The location of the ATG starting codon for this transcript is predicted 10 bases upstream of the start of *GHR* exon 2 whereas its stop codon is predicted within exon X3.

6.5.3 Results from FEX *IN SILICO* exon prediction program

The same 154,535 nucleotide-long *GHR* sequence was analysed for coding and alternative exons using the FEX *in silico* exon prediction program. A total of 161 potential exons were identified. Of these, 159 were located after the triplet coding for the start of the GHR protein. Seven of 9 natural *GHR* exons and the pseudoexon 6Ψ were included in these. *GHR* exons 8 and 9 were not recognised. FEX correctly identified the position and length of 5 (exons 3, 5, 6, 7, 10) out of the 7 identified constitutive *GHR* exons and those of the pseudoexon 6Ψ. The beginning of exon 4, corresponding to its acceptor site was correctly identified, but the predicted exon length was shorter than that reported in public databases (87 versus 130 nucleotides). The beginning and end of exon 2 were not correctly identified. Moreover, its predicted lenght was longer than that reported in public databases (122nt versus 81nt). Of the four potential exons (X1-X4) present in the *GHR* ESTs, only one corresponding to exon X2 was identified, even though predicted to be a first exon of 31 bases. Neither exon X1, X3, X4 were predicted by FEX.

6.5.4 Identification of alternative GHR variants

Three out 4 exons (exons X1-X3) described in the two ESTs were identified by the new algorithm. Their predicted length was: exon X1= 64 bases, exon X2= 139 bases, exon X3= 145 bases. After insertion in the GHR mRNA, all three were predicted to create a frameshift and a premature stop codon. The presence of exon X4 was not predicted.

Primers were designed to amplify the four exons X1-X4 based on the ESTs and the algorithm predictions. Amplification of liver cDNA with a heminested PCR technique, using two sense primers in the GHR exon 2 (2FiGHRm and 2FfGHRm) and an antisense primer in exon X1 (exon X1R), produced three products (Figure 6.4), which were cut from the gel, purified and sequenced. The smaller product of approximately 110 bases revealed the presence of a sequence corresponding to 58 bases within exon X1. The other two fainter products did not sequence and their identity remains unknown. Amplification of liver cDNA using a sense primer in exon X1 (exon X1F) and two antisense primers in the *GHR* exon 6 (6RGHRm) and 5 (5RGHRm), resulted in a product of approximately 800 bases (Figure 6.4). This was cut from the gel, purified and sequenced, revealing a novel 613 base-long sequence, which spliced into the *GHR* exon 3 (Figure 6.5). This novel exon – exon Xa – is likely to continue into exon X1, and thus be more than 900 bases long. Since the chromatogram did not show its remaining upstream 200 nucleotides, exons X1 and Xa will be considered as two separate exons.

Amplification of GHR liver cDNA using primers annealing to sequences within exon X2 did not result in PCR products.

Amplification of GHR liver cDNA with a heminested PCR technique, using primers annealing to sequences within exon X3 resulted in two products of approximately 150 bases [sense primers in exon 2 (2FiGHRm and 2FfGHRm) and antisense primer in exon X3 (exon X3R)] and 400 bases [sense primer in exon X3 (exon X3F) and antisense primers in exon 6 (6RGHRm) and 5 (5RGHRm)] (Figure 6.4). These products revealed the presence of a sequence corresponding to exon X3, located between *GHR* exons 3 and 4 (Figure 6.6). This novel exon is predicted to produce a frameshift and the appearance of a premature stop codon 96 residues after the first methionine when inserted in the wild

type GHR mRNA and after 57 residues when inserted in the d3-GHR mRNA (Figure 6.7).

Amplification of GHR liver cDNA using primers annealing to sequences within exon X4 did not result in any PCR product.

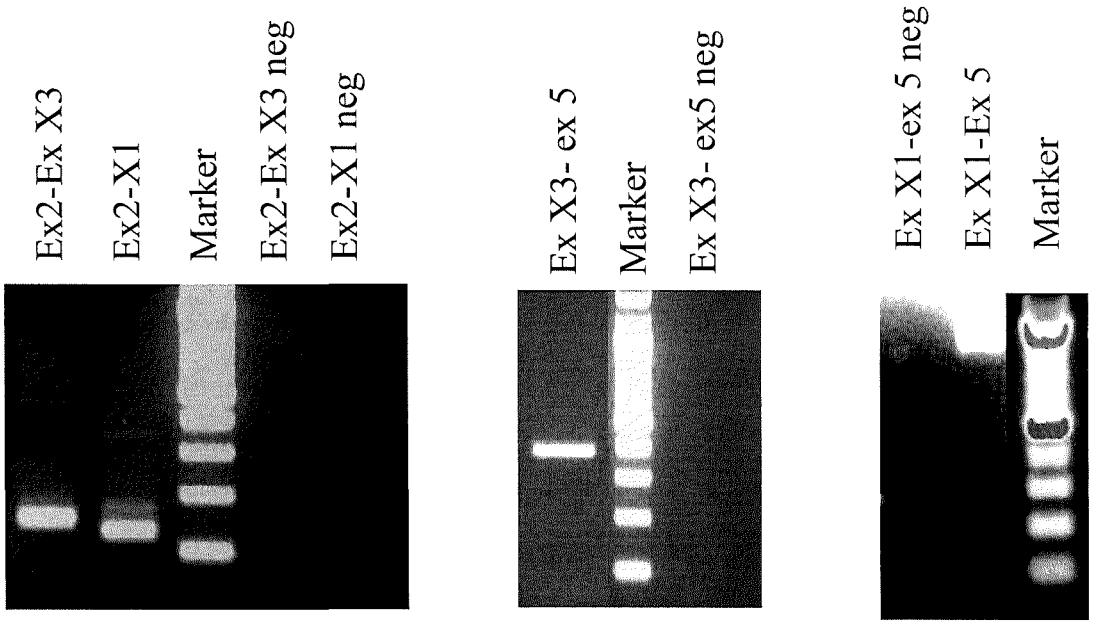

Figure 6.4 RT-PCR products from liver cDNA using primers against *GHR* exons X1 and X3.

The presence of the newly identified altermative exons X1, Xa and X3 was investigated in GHI patients with no defects in the *GHR* coding region. cDNA from leukocytes was amplified using the above primers, but revealed the presence of multiple non-specific products.

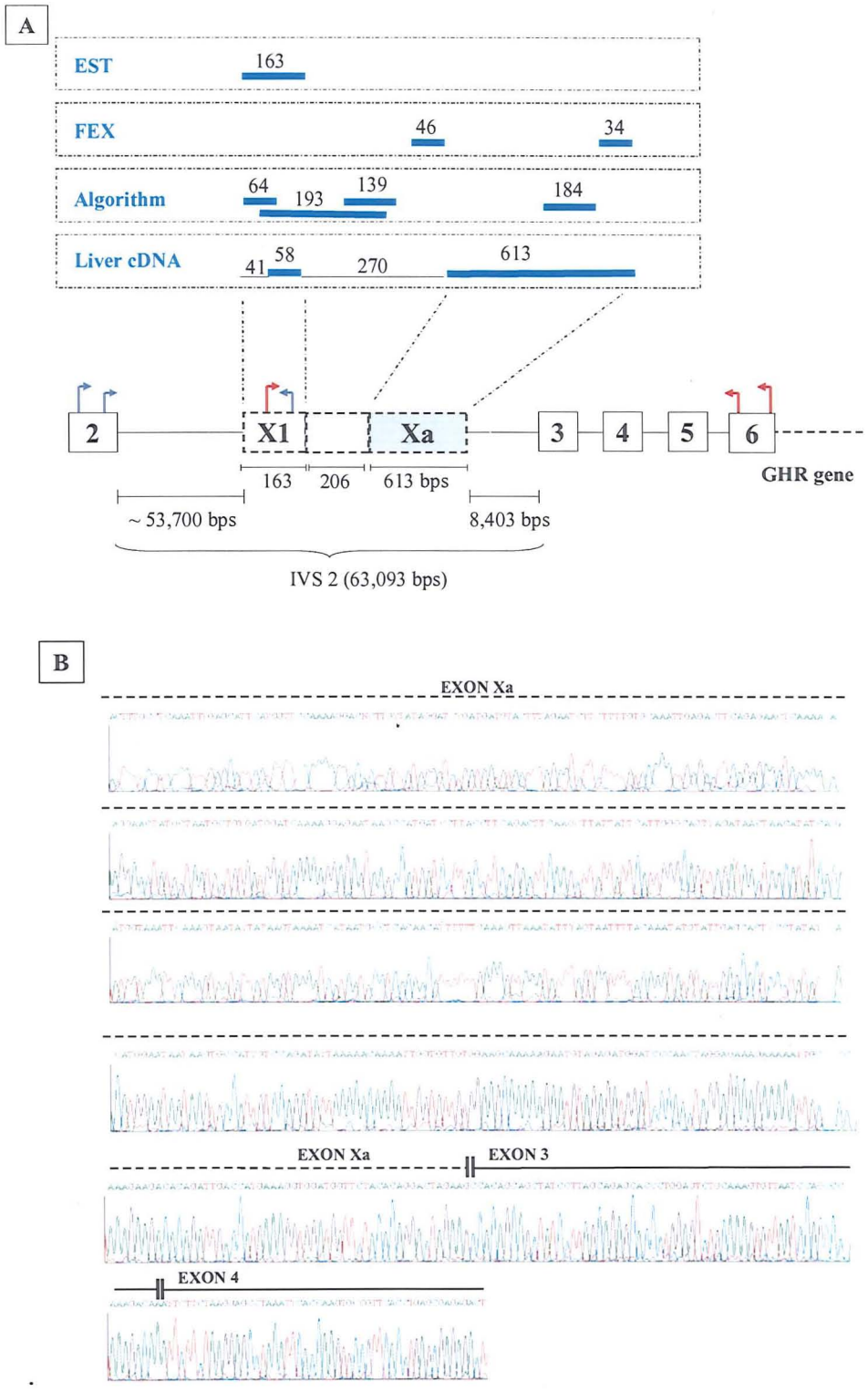

Figure 6.5 Novel GHR transcript with an alternative exon in intron 2. Panel A: schematic representation of the *GHR* genomic sequence containing exons X1 and Xa. Primer location is also depicted. Exons for this region, identified by ESTs and cDNA analysis and predicted by FEX and the novel algorithm, are also presented overhead as blue rectangles and their length in bases is indicated. Panel B: exon Xa sequence resulting from liver cDNA amplification. The junctions between the alternative exon Xa and the *GHR* coding exons 3 and 4 are also indicated.

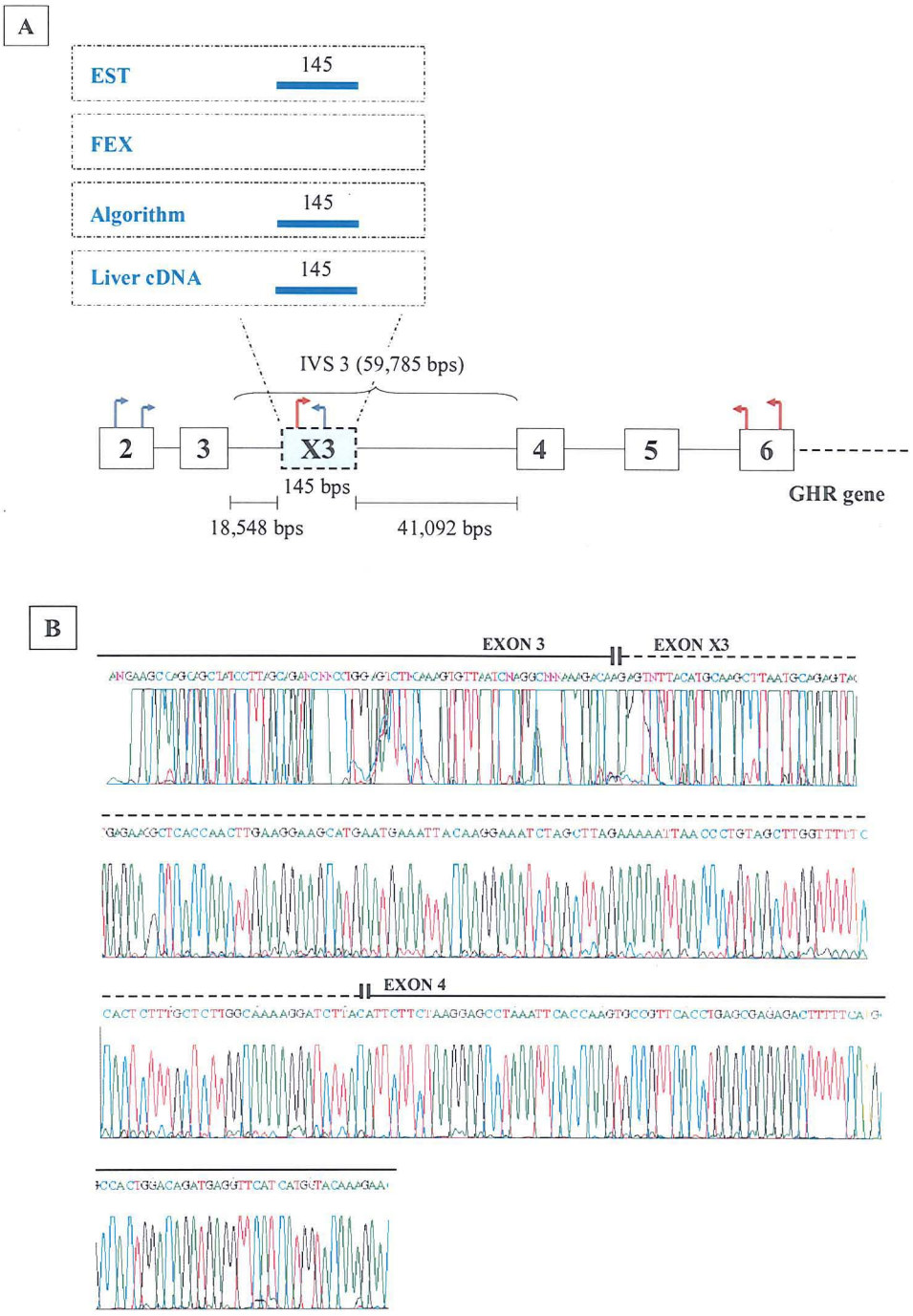

Figure 6.6 Novel GHR transcript with alternative exon X3 in intron 3. Panel A: schematic representation of the *GHR* genomic sequence containing exon X3. Primer location is also indicated. Exons for this region, identified by ESTs and cDNA analysis and predicted by FEX and the novel algorithm are also presented overhead as blue rectangles and their length in bases is indicated. Panel B: partial sequence resulting from liver cDNA amplification. The junctions between the alternative exon X3 and the *GHR* coding exons 3 and 4 are also indicated.

GHR wt MDLWQLLLTL ALAGSSDAFS GSEATAAILS RAPWSLQSVN PGLKTNSSKE
GHR X3 MDLWQLLLTL ALAGSSDAFS GSEATAAILS RAPWSLQSVN PGLKTRVLHA

GHR wt PKFTKCRSPE RETFSCHWTD EVHHGTKNLG PIQLFYTR
GHR X3 SLMQSREAHQ LEGSMNEITR KSSLEKLTL*

GHR d3 wt MDLWQLLLTL ALAGSSDAFS GSEDSSKEPK FTKCRSPERE
GHR d3 X3 MDLWQLLLTL ALAGSSDAFS GSEGVLHASL MQSREAHQLE

GHR d3 wt TFSCHWTDEV HHGTKNLGPI QLFYTR
GHR d3 X3 GSMNEITRKS SLEKLTL*

Figure 6.7 Amino acid sequences for the novel GHR transcript. Top: the amino acid sequence of the wild type GHR (GHR wt) is compared to the predicted amino acid sequence of the novel GHR transcript with alternative exon X3 (GHR X3). Bottom: amino acid sequence of the two transcripts in the absence of exon 3 (GHR d3 wt, and GHR d3 X3). Frameshift and the appearance of a novel amino acid sequence are indicated in blue.

6.5.5 Comparison between FEX and the novel algorithm

For the purpose of this Chapter, exons present in public databases or identified by cDNA analysis will be considered as true exons, as opposed to false exons not present in public databases or not identified by cDNA analysis.

The novel algorithm correctly identified 9 out of 9 constitutive exons, the pseudoexon 6Ψ and 3 out of 3 alternative exons (exon X1, Xa and X3), thus resulting in the prediction of 13 out of 13 true exons. In particular, it predicted the presence of an exon of 184 bases for the region containing exon Xa and the presence of two exons of 64 and 193 bases for the region containing exon X1. An exon of 139 bases was predicted in the region between exon X1 and Xa (Figure 6.5). Moreover, the algorithm correctly predicted the position of the acceptor splice site of the 9 constitutive exons, the pseudoexon 6Ψ and the alternative exon X3 and correctly predicted the donor splice site of 8 out of 9 constitutive exons, the pseudoexon 6Ψ and the alternative exon X3. The predicted donor splice site of exon 10 (last exon of the *GHR*) was 189 bases distal to the acceptor site compared to 972 bases annotated on public databases. The algorithm also

predicted the presence of 445 false exons, of which 21 would not cause a frameshift or the appearance of a premature stop codon if inserted in the mRNA.

The *in silico* exon prediction program FEX identified 7 out of 9 constitutive exons, the pseudoexon 6Ψ and exon Xa but did not predict exons X1 and X3, thus resulting in the prediction of 8 out 13 positive exons. Moreover, it correctly predicted the position of the acceptor splice site of 5 constitutive exons and the pseudoexon 6Ψ, and correctly predicted the donor splice site of 6 constitutive exons, the pseudoexon 6Ψ and exon Xa. The algorithm also predicted the presence of 151 false exons, all of which would maintain the ORF, when inserted in the mRNA.

6.6 DISCUSSION

In this study, a novel exon prediction algorithm was specifically designed to search for alternative exons in the *GHR*. Its results, combined with the analysis of ESTs annotated in public databases, identified the first two alternative transcripts for the *GHR*, both of which arose from the use of novel alternative exons located in intronic sequences between constitutively expressed *GHR* coding exons.

Alternative splicing is abundantly used in higher eukaryotes and is thought to play a fundamental role in determining their functional diversity and complexity (Modrek et al., 2001, Stetefeld and Ruegg, 2005, Blencowe, 2006). In 40-60% of human genes, the inclusion or exclusion of alternative exons within constitutive exons gives rise to structurally and functionally different transcripts from the same pre-mRNA, in different tissues and developmental stages (Johnson et al., 2003). To date no *GHR* variants arising from the use of alternative exons, are known, with the exception of alternative first exons in the 5' untranslated region (Pekhletsky et al., 1992, Edens and Talamantes, 1998).

The identification of alternative exons relies on the alignment of genomic sequences to ESTs available from public databases and to cDNA deriving from different tissues and developmental stages (Gelfand et al., 1999, Kan et al., 2001, Modrek et al., 2001). *In silico* programs, such as the exon prediction program FEX, are important tools for the identification of coding exons from uncharacterised genes, but are of little help when looking for alternative exons or genomic areas containing pseudoexons. The identification of the latter is, generally, an incidental finding during analysis of patient mRNA.

Comparison between the novel algorithm and the *in silico* prediction program.

The algorithm presented in this study was constructed specifically for the systematic search of *GHR* alternative exons or pseudoexons located in intronic regions between constitutive exons. Like all exon prediction programs, the algorithm was based on the fundamentals of gene splicing, but the identification of promoters, translation initiating and terminating sites and poly(A)-signals was not included as its purpose was to search for internal exons. Compared to a largely used *in silico* exon prediction program (FEX), the algorithm was better in recognising constitutive and alternative exons. In fact,

not only did it predict all constitutive *GHR* exons, but also predicted the pseudoexon 6Ψ and the three novel alternative exons identified by cDNA analysis in this study. Moreover, compared to FEX, it had a superior splice site recognition accuracy. This may be explained by the use of criteria, which take into consideration the characteristics of alternative exons. Identification of a potential exon did not, in fact, require the strict adherence of its splice elements to a consensus sequence, thus differentiating this algorithm from other available *in silico* prediction programs. Alternative exons are characterised by a reduced number of regulatory elements and by splice elements that deviate from the consensus sequences more than the splice sites of constitutive exons (Stamm et al., 1994, Stamm et al., 2000). The cut off value (score > 65) used in this study to identify splice sites, reflected a mere 65% adherence to the consensus sequences and was chosen based on the characteristics of the *GHR* exon splice sites. Thus, although the algorithm is potentially applicable to any gene, the cut-off values used were specific for the *GHR*.

Another important difference between the algorithm developed in this study and other i*n silico* exon prediction programs, was the omission of the requirement to maintain the ORF after insertion of the predicted exons in the mRNA. *In silico* programs are designed to identify constitutive coding exons and require potential regions to meet the fundamental criteria of protein coding, such as maintenance of the ORF. Nevertheless, the presence of alternative exons which, when included in the mRNA give rise to premature protein truncation have been described and alternative splicing leading to non-functional proteins is a well recognised regulatory process (Gebauer et al., 1998).

Similarly to FEX, the algorithm identified numerous additional potential exons, confirming that introns are rich in sequences that resemble potential exons. To further improve the sensitivity of the algorithm, the presence of exonic hexamers corresponding to enhancers and silencers could have been taken into account. These splice elements are very important in determining exon expression and/or silencing, but their prediction is extremely difficult. Hexamers corresponding to exonic silencers are not well characterised and the hexameric sequences of exonic enhancers highly diverge from consensus sequences (Watakabe et al., 1993, Liu et al., 1998, Blencowe, 2000, Cartegni et al., 2002). Despite these difficulties, introduction of these criteria in the algorithm is part of future work.

Identification of novel GHR transcripts

Analysis of *GHR* intronic regions revealed that introns 2, 3 and 6 were the richest in sequences resembling potential exons. The GHR 6Ψ pseudoexon described in 2001 is, in fact, located in intron 6 and was among the predicted exons. Comparison of the results obtained from the novel algorithm and the GHR ESTs was performed for selecting intronic regions to be screened for the presence of alternative exons. This led to the identification of novel *GHR* transcripts arising from the expression of alternative exons. One of these exons was located in intron 3 and its sequence and length were correctly predicted by the algorithm, but not recognised by FEX. This alternative exon was present in one EST, but was predicted to be joined at its 5' splice site to additional alternative exons and not to splice into the *GHR* coding exons. The results of this study demonstrated, instead, that this novel alternative exon is inserted between the *GHR* coding exons 3 and 4. It does not have a polyadenylation signal (AAUAAA sequence) and is predicted to result in a frameshift and the appearance of a premature stop codon. The translation product of this novel *GHR* transcript lacks the amino acid sequence corresponding to the GH binding domain. Nevertheless, it remains to be clarified whether it has a regulatory effect on the wild type GHR.

Screening of liver cDNA identified a second intronic region located in intron 2, which is recognised by the splice machinery. Although two novel exons (X1 and Xa) have been predicted to arise from this region, it is more likely that they are part of a single alternative exon, approximately 900 nucleotides long, which splices into exon 3 of the *GHR*. The beginning of this alternative exon was correctly identified by the algorithm, although its length was predicted to be 68 nucleotides long. This is not surprising, since one of the criteria for exon identification was a maximum length of 200 nucleotides.

These two novel transcripts may simply represent biological noise and, in this respect, analysis of *GHR* from other species may be of help. Conservation of an element among species is, in fact, highly suggestive of its functional significance. The possibility arises that these novel alternative transcripts may have a regulatory effect in specific tissues or developmental stages. Moreover, the presence of a SNP or a genetic defect within splice elements of these novel exons may increase the expression of the latter, resulting in the overexpression of the novel GHR variants over the wild type GHR, or

simply in silencing of the wild type *GHR* leading to GHI. The presence of these two novel alternative transcripts was investigated in GHI patients with no mutations in the *GHR* coding exons, but amplification of cDNA from leukocytes failed to produce specific products. This may be a consequence of the absence of GHR mRNA in these patients or may simply reflect the low amount of these transcripts in tissues other than liver. Nevertheless, the presence of activating mutations in these alternative exons cannot be excluded, since screening at genomic level was not performed in these patients.

Conclusion

The novel algorithm created in this study was superior to a largely used *in silico* exon prediction program in identifying *GHR* constitutive and alternative exons. The results obtained with this novel algorithm, in conjunction with EST analysis, allowed the identification of the first two *GHR* alternative transcripts known to date. The discovery of these novel coding regions prompts the screening of these DNA sequences in GHI patients with no mutations in the *GHR* constitutive coding exons. Moreover, increasing the expression of these regions with a target gene therapy may represent a potential novel approach to modulating GH sensitivity.

CHAPTER 7

HETEROZYGOUS DEFECTS OF THE ACID-LABILE SUBUNIT GENE IN IDIOPATHIC SHORT STATURE

7.1 BACKGROUND

Short stature is one of the most common cause of referral to paediatric endocrinologists. When no specific aetiology can be identified, a diagnosis of idiopathic short stature (ISS) is made. Into this category fall patients with heights 2 standard deviation scores (SDS) below the mean and normal birth size, in whom no endocrine or systemic diseases are found and no known genetic causes of short stature or other factors compromising growth are present (Wit et al., 2008a, Wit et al., 2008b). The biochemical profile and response to GH treatment of ISS patients is heterogeneous (Wit and Rekers-Mombarg, 2002, Leschek et al., 2004, Hintz, 2005) and could be influenced by the presence of multiple, as yet unidentified, pathological mechanisms contributing to short stature. Numerous genes in the GH-IGF-I axis are known to be involved in linear growth in childhood (Walenkamp and Wit, 2006, Weedon et al., 2008) and molecular investigations have recently identified several functional mutations in genes coding for key proteins in patients previously labelled as having ISS (Ayling et al., 1997, Metherell et al., 2001) Single heterozygous defects in the *GHR* have been proposed as possible causes of ISS (Goddard et al., 1995), but data are inconclusive as cosegregation of short stature and the heterozygous state is poor (Rosenbloom et al., 1994a). Defects in the Short stature HOmeoboX (SHOX) gene have also been reported to be associated with isolated or familial ISS in up to 4% of cases (Rappold et al., 2002).

The clinical role of the acid-labile subunit (ALS), an 84-86 kDa protein, which circulates in the serum and binds to IGF-I and IGFBP-3 to form the circulating ternary complex (Baxter, 1994), has come under scrutiny since the recent discovery of a homozygous inactivating mutation in the ALS gene (*IGFALS)* in a patient with mild growth retardation (Domene et al., 2004). The observation that heterozygous parents of patients with homozygous *IGFALS* defects (Hwa et al., 2006, Domene et al., 2007, Duyvenvoorde et al., 2008, Heath et al., 2008) are of short stature, was the basis for this project.

7.2 ORIGINAL HYPOTHESIS AND AIMS

The aim of this study was to investigate the role of heterozygous *IGFALS* defects in the pathogenesis of mild short stature by direct sequencing of the *IGFALS* in a cohort of prepubertal ISS patients. Moreover, the study aimed to analyse the auxological and biochemical profile of ISS patients with single heterozygous *IGFALS* defect, and compare these data to those obtained from ISS children without *IGFALS* defects. The impact of single heterozygous *IGFALS* defects on ternary complex formation was also assessed by means of size exclusion chromatography and the presence of the same defect in first degree family members of ISS children with heterozygous *IGFALS* defects was investigated.

7.3 STUDY POPULATION

Patients of Caucasian origin followed at the Paediatric Endocrine Unit at the Royal London Hospital, London, UK were included in the study. Inclusion criteria were: prepubertal status, height SDS $\leq$ -1.88 at $\geq$ 3 years of age, birth weight and/or birth length SDS > -2.0 and exclusion of GH deficiency by peak GH level after glucagon provocation test $\geq$10mU/l. Exclusion criteria were: chromosomal or genetic abnormalities, disproportionate short stature, chronic illnesses or endocrine disease. Parents and siblings of the ISS population were also enrolled in the study. Unrelated controls of normal stature and similar ethnic origin to the study population were also included and their *IGFALS* sequenced to derive the allele frequency of the newly identified mutations. All patients and parents gave written informed consent and the study was approved by the North East London Research Ethics Committee.

Height and weight were measured using standard anthropometric techniques (Cameron, 2002) and were converted into SDS. Birth weight SDS was calculated according to the LMS method (Cole, 1990, Freeman et al., 1995). Body mass index (BMI) was calculated as follows: Weight (Kilograms)/Height (meters) squared. BMI SDS was calculated according to the UK 1990 standards (Cole et al., 1995). Pubertal status was assessed according to the criteria of Tanner (Marshall and Tanner, 1969, Marshall and Tanner, 1970). Boys were considered prepubertal if genitalia were stage 1 and testicular volume was < 4ml (Zachmann et al., 1974). Girls were prepubertal if breast development was stage 1 (Marshall and Tanner, 1969). DNA was available from 52 of these ISS patients for *IGFALS* analysis and from 50 normal controls.

7.4 MATERIALS AND METHODS

7.4.1 DNA extraction from blood samples and PCR

Genomic DNA was extracted from peripheral blood leucocytes. *IGFALS* exons 1 and 2 and their intronic boundaries were amplified by PCR using specific primers (primer sequences reported in Appendix 3: 10.3.3). Cycling conditions were 95°C for 2 min (1 cycle); 95°C for 30 sec, 63°C for 30 sec and 72°C for 30 sec (35 cycles); and 72°C for 5 min. PCR products were visualised on 1% agarose gel and sequenced using the ABI 3700 automated DNA sequencer. SNPs data were obtained from the Ensembl database (www.ensembl.org).

7.4.2 Size exclusion chromatography

Samples were fractioned on a HiPrep 16/60 Sephacryl S-200HR column as described in Materials and Methods 2.9.3. Briefly, serum samples (100µl) were incubated overnight at 22°C with $3.5x10^6$ counts per minute of ^{125}I-labeled IGF-I and then cross-linked with 5mM disuccinimidyl suberate. After 30 min, the cross-linking reaction was stopped by adding 1M Tris HCl. Five hundred ml were loaded into the column and 1ml fractions were collected and counted. Incorporation of ^{125}I-labeled IGF-I in the ternary complex was calculated as: (sum of iodine count per minute in the ternary complex / total iodine count per minute) x100.

7.4.3 Biochemical assessment

The biochemical assessment of all patients and the family members of those carrying the *IGFALS* mutations, was performed by assessing serum IGF-I, IGFBP-3 and ALS concentrations from venous blood samples. GH-dependent proteins levels were measured by Dr J Jones at the Diagnostic Systems Laboratories (DSL), GKT, School of Medicine King's Denmark Hill Campus, London, UK, using an enzyme-linked immunosorbent assay (ELISA kit; Diagnostic System Laboratories, Inc. Webster, TX, USA) as described in Chapter 3, section 3.4.5, of this Thesis. Normative values were obtained from DSL.

7.4.4 Statistical Analysis

Statistical analyses were performed using R version 2.6.2 (R Development Core Team, 2008, R Foundation for Statistical Computing, Vienna, Austria). Numerical variables were expressed as median (range) and categorical variables as number (percent). Comparison between continuous variables was performed using Wilcoxon's rank sum test. Comparison between categorical variables was performed using Fisher's exact test. A two-sided p-value <0.05 was considered indicative of statistical significance.

7.5 RESULTS

7.5.1 Auxological and biochemical characteristics of ISS subjects

Fifty two prepubertal unrelated patients (14 female, 38 male) of Caucasian origin were included in the study. Median age was 7.9 yrs (range 3.0 to 14.5 yrs) and birth weight SDS was -0.54 (-1.92 to 0.80). Median height SDS was -2.48 (-3.60 to -1.91), weight SDS -2.43 (-4.24 to 0.43) and BMI SDS -0.69 (–3.24 to 1.33). Median IGF-I SDS was -0.42 (-3.50 to 2.74), IGFBP-3 SDS was -0.40 (-2.30 to 0.90) and ALS SDS was -0.67 (-5.64 to 7.88).

7.5.2 Genetic analysis

Direct sequencing of the *IGFALS* identified 4 single heterozygous base changes. These were: C to T at position 65 (P22L), C to T at 860 (P287L), C to G at 1357 (L453V) and C to T at 1577 (P526L) (Figure 7.1).

These four variants were not detected in 50 normal controls. The C to T base change at position 860 (P287L) has never been reported in the Caucasian population, but was found among the 38 Latino participants in the Multiethnic Cohort (MEC), with a reported T allele frequency of 0.014 (average Het.+/- std err 0.006 +/- 0.052) (refSNP ID: rs35706152, www.ensembl.org). Since no validation status or anthropometric data for this variant are available, the P287L was considered a potentially deleterious mutation. A fifth novel base change G to A at position 1478 (R493H) was also detected in 1 of 52 ISS patients. This variant was also present in 1 of 50 normal stature controls and was, therefore, considered a single nucleotide polymorphism.

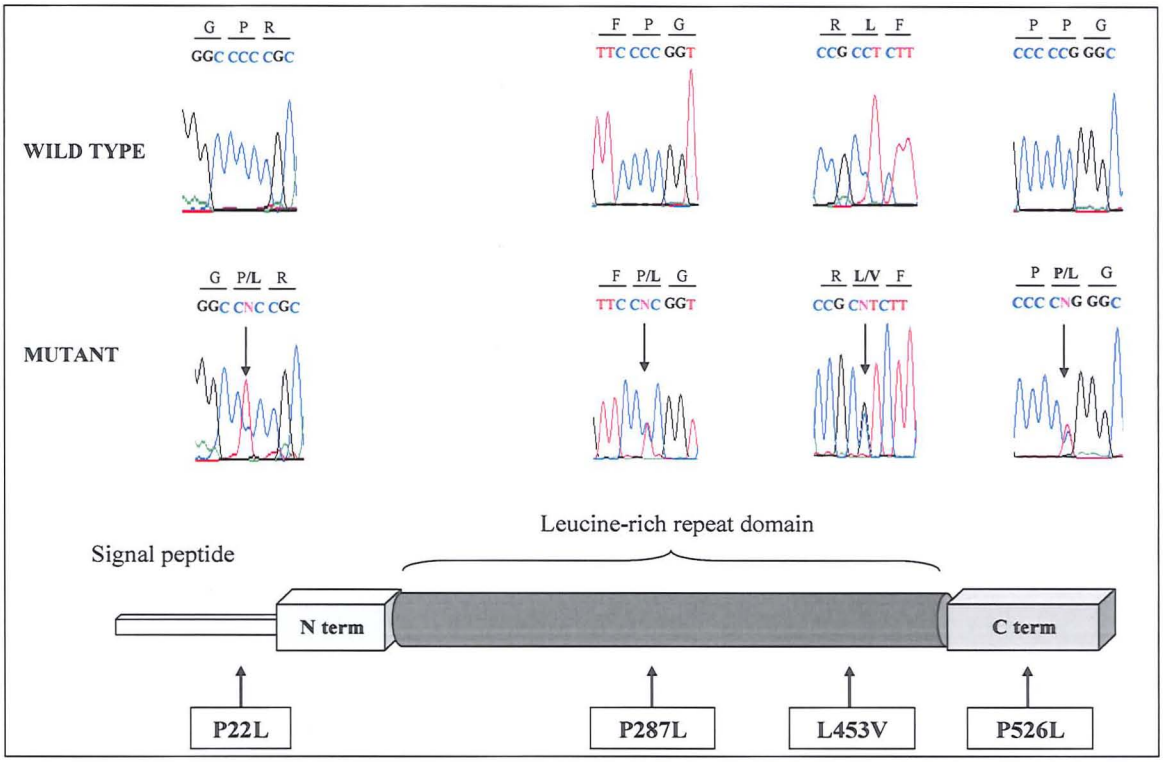

Figure 7.1 Schematic representation of the IGFALS gene. Partial chromatograms of sequence analysis show the 4 single heterozygous mutations. Partial DNA and predicted amino acid sequence are also indicated. Arrows indicate point mutation locations.

7.5.3 Auxological and biochemical data of the 5 ISS children with *IGFALS* defects

IGFALS mutations were present in 5/52 ISS children (9.6%). The heights of the 5 ISS index cases with *IGFALS* defects were significantly lower (p=0.033) than those of subjects without *IGFALS* defects [median -3.24 SDS (range -3.39 to -2.33) versus -2.44 SDS (range -3.60 to -1.91)]. Weight SDS values in ISS patients with *IGFALS* defects were significantly lower (p=0.031) compared to those of subjects without *IGFALS* defects [-3.73 SDS (range -4.24 to -2.64) versus -2.24 SDS (range -3.85 to -0.43)]. BMI SDS values were also significantly lower (p=0.025) in the ISS subjects with *IGFALS* defects [-2.14 SDS (range -3.24 to -1.18) versus -0.57 SDS (range -2.87 to 1.33)]. There was no significant difference (p=0.60) in birth weight between subjects with and without *IGFALS* defects [-0.55 SDS (range -1.59 to 0.12) versus -0.53 SDS (range -1.92 to 0.65), Figure 7.2].

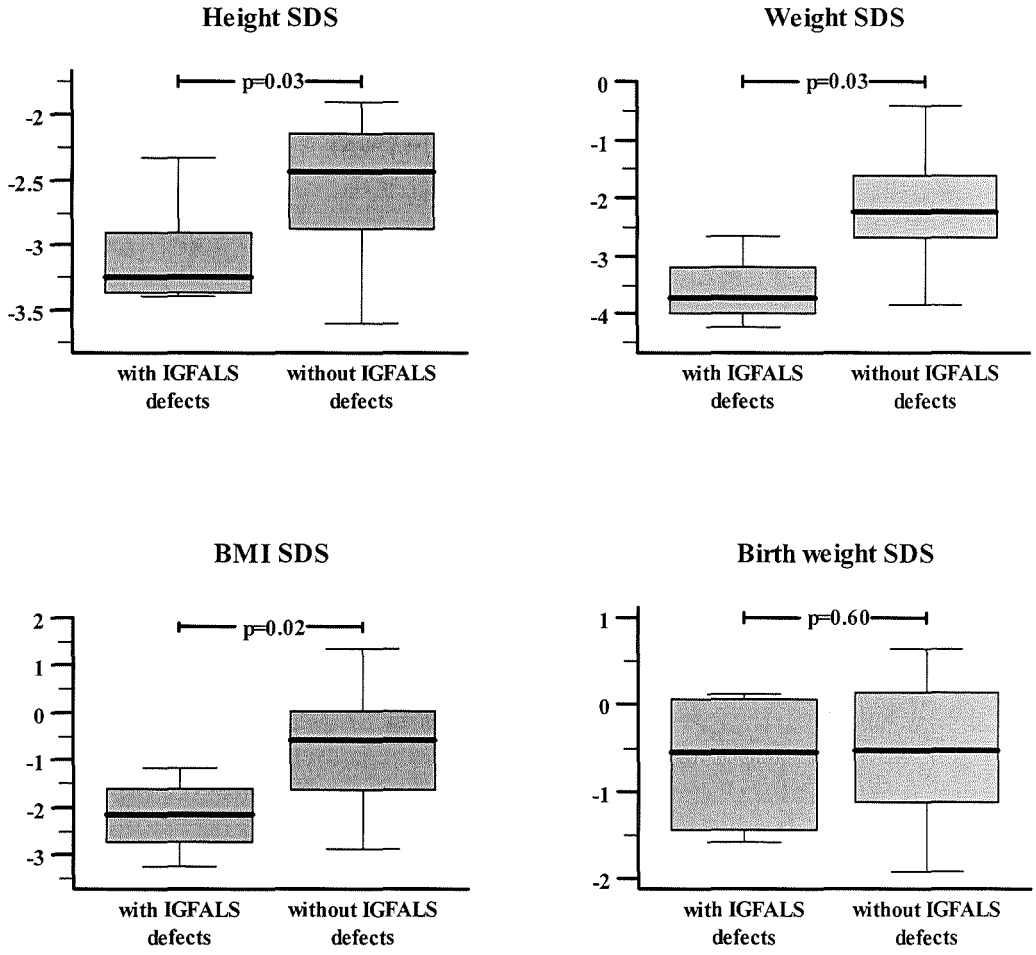

Figure 7.2 Boxplots for height SDS, weight SDS, BMI SDS and birth weight SDS for prepubertal ISS patients with and without *IGFALS* defects. Each boxplot depicts the median, the 25th and 75th percentiles. Whiskers depict minimum and maximum observed values.

No significant differences were found between subjects with and without *IGFALS* variants in the following serum peptide SDS values [ISS with *IGFALS* defects versus ISS without *IGFALS* defects, median (range)]: IGF-I [-0.79 SDS (-2.35 to 0.54) versus -0.34 (-3.50 to 2.74), p=0.15], IGFBP-3 [-0.30 SDS (-1.03 to 1.30) versus -0.40 SDS (-2.30 to 0.90), p= 0.47] and ALS [-1.84 SDS (-2.54 to 1.92) versus -0.61 SDS (-5.64 to 7.88), p= 0.47].

7.5.4 Auxological and biochemical data of the family members of ISS children with *IGFALS* defects

DNA samples from all 6 siblings and 7 of 10 parents of the index cases with *IGFALS* defects were available and were sequenced for *IGFALS* mutations (family trees for the patients with *IGFALS* defects are shown in Figure 7.3).

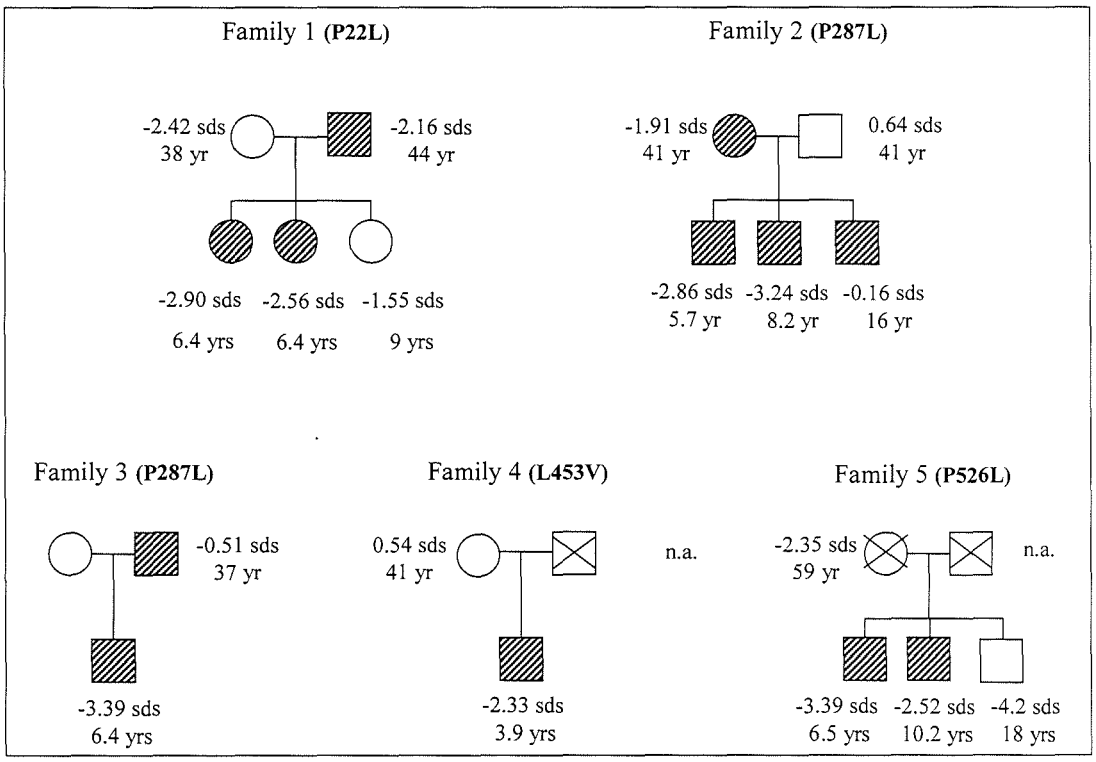

Figure 7.3 Family trees for the 5 ISS index patients with single heterozygous mutations (P22L, P287L, L453V and P526L) in the *IGFALS*. Height SDS and age are indicated. Affected family members are indicated in grey. Family members for whom DNA was not available are indicated with a cross. SDS, standard deviation score; n.a., not available; P, Proline; L, Leucine; V, Valine.

Four of the six siblings, in Families 1, 2 and 5, were also carriers of the heterozygous defect. Three of these siblings were prepubertal (families 1, 2 and 5), showed similar growth retardation to the index cases and met the criteria of ISS. One sibling was pubertal (age 16 years, Family 2) and his height was -0.16 SDS. In Family 5, one sibling with no *IGFALS* defect had a height SDS of -4.2 at age 18 years. His birth weight SDS was -3.27 and he had a diagnosis of small for gestational age with no catch

up. The biochemical and auxological data of patients and family members are shown in Table 7.1.

In three of the seven available parents, in Families 1, 2 and 3, the same single heterozygous *IGFALS* defect seen in the index case was found. All carriers had short stature, but less so than affected prepubertal subjects within the same families. Their height, weight and BMI SDS, as well as biochemical data are shown in Table 7.1. For Family 4, only one parent (mother) was available to study. Her height was normal (+0.50 SDS) and no *IGFALS* defect was found. No DNA sample and auxological data were available for the patient's father. For Family 5, neither parent was available to study.

TABLE 7.1 HEIGHT SDS AND BIOCHEMICAL DATA IN INDEX CASES AND AFFECTED FAMILY MEMBERS WITH SINGLE HETEROZYGOUS *IGFALS* DEFECTS.

Family	Mutation	Patient	Gender	Age (yrs)	Height (SDS)	IGF-I (SDS)	IGBP3 (SDS)	ALS (SDS)
1	P22L	Index	F	6.4	-2.90	-0.71	-0.61	-2.45
		Sibling	F	6.4	-2.56	1.97	1.15	-2.54
		Parent	M	41	-2.16	1.39	1.05	-0.96
2	P287L	Index	M	8.2	-3.24	-2.46	-2.15	-1.09
		Sibling	M	5.7	-2.86	-0.06	-0.47	-0.84
		Sibling	M	16.4	-0.16	1.15	-0.21	1.96
		Parent	F	41	-1.91	-0.18	-0.87	0.42
3	P287L	Index	M	6.4	-3.39	-0.79	1.30	-1.84
		Parent	M	38	-0.51	n.a.	n.a.	-1.26
4	L453V	Index	M	3.9	-2.22	-2.40	-1.32	-2.37
5	P526L	Index	M	6.5	-3.39	0.80	0.82	1.92
		Sibling	M	10.2	-2.52	1.58	1.18	5.07

DNA was not available for one parent in Family 4 and both parents in Family 5. No *IGFALS* defect was detected in the parent from Family 4. n.a., not available.

7.5.5 Size exclusion chromatography

Serum samples from patients carrying the four variants (P22L, P287L, L453V and P526L) were run on size exclusion chromatography. A reduction in the peak corresponding to the ternary complex was observed for serum samples from patients with defects P22L, P287L and L453V, whereas a modest increase was observed for the serum sample of a patient with the P526L variant. The amount of ^{125}I IGF-I incorporation in the ternary complex was calculated and compared to that obtained from a normal serum sample. This showed a reduction for mutations P22L, P287L and L453V, ranging from -21.65% (mutation P287L) to -63.91% (mutation L453V). Mutation P526L resulted in a 27.20% increased incorporation of IGF-I in the ternary complex compared to normal (Figure 7.4).

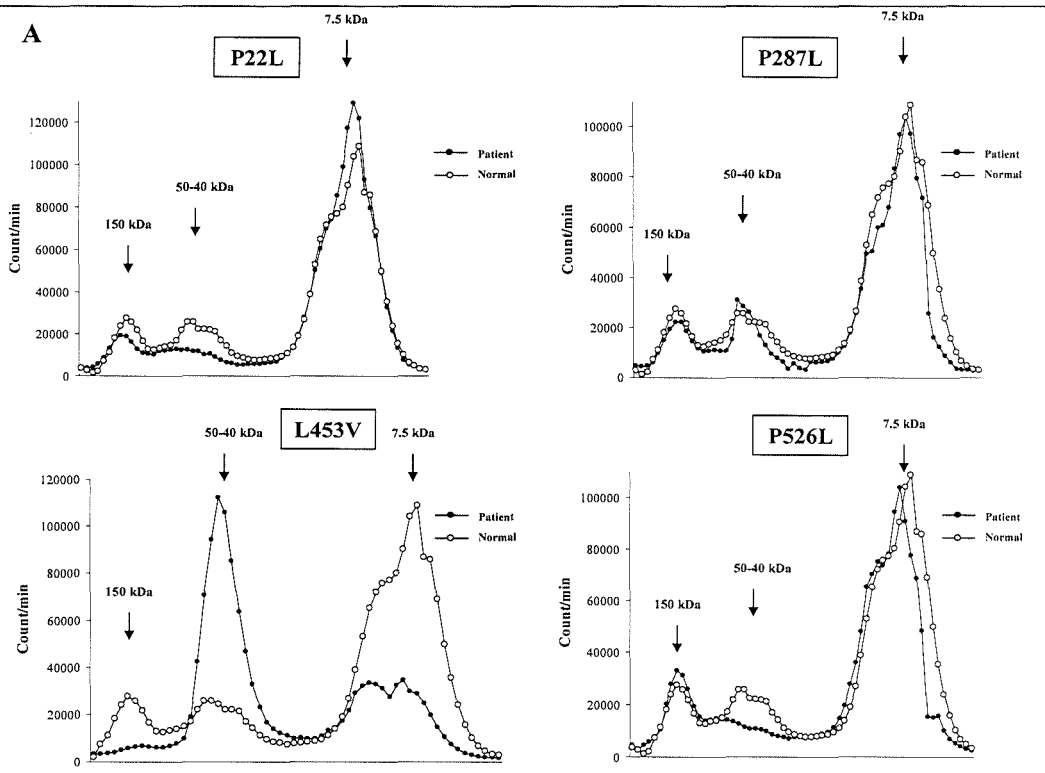

B

Mutation	^{125}I IGF-I incorporation in ternary complex	^{125}I IGF-I incorporation in ternary complex compared to wild type	serum ALS SDS
P22L	6.88%	-28.03 %	-2.45
P287L	7.49%	-21.65 %	-1.84
L453V	3.45%	-63.91 %	-2.37
P526L	12.16%	27.20 %	1.92
wild type	9.56 % ± 0.20	100 %	

Figure 7.4 Panel A: results of size exclusion chromatography. The position of the ternary complex (predicted molecular weight 150kDa), binary complex (predicted molecular weight 40-50kDa) and unbound IGF-I (predicted molecular weight 7.5kDa) are indicated. Panel B: incorporation of ^{125}I IGF-I in the ternary complex and corresponding serum ALS SDS values. ^{125}I IGF-I incorporation in the wild type ternary complex is expressed as mean±standard deviation (n=3).

7.6 DISCUSSION

In this study, 9.6% of patients with ISS had a single heterozygous *IGFALS* defect. The study of relatives of index cases showed that the same defects were present in other family members who were also short. These defects were not found in any of the 50 normal controls or in any SNP database.

The identification of ISS aetiology is of great importance, since it can guide therapy in children with short stature. Linear growth is under the influence of many genetic, hormonal and metabolic factors and the GH-IGF-I axis plays a fundamental role. Hence its components are obvious candidates for genetic causes of growth failure (Walenkamp and Wit, 2006).

Identification of acid-labile subunit defects in idiopathic short stature patients

Most of the circulating IGF-I is bound to IGFBP-3 in a relatively unstable binary complex, which stabilises by binding to the ALS protein to form a ternary complex (Baxter, 1994, Boisclair et al., 2001). The half-lives of the free IGF-I and of the binary complex IGF-I/ IGFBP-3 in the circulation are of minutes. However, when bound in a ternary complex, the half-life of circulating IGF-I is increased to 12-15 hours (Guler et al., 1989). ALS is, thus, believed to be an important regulator of IGF-I bioavailability in the serum, increasing its half-life and regulating its clearance (Binoux and Hossenlopp, 1988). The importance of ALS in influencing linear growth has recently been unveiled with the demonstration of absence of serum ALS and severe deficiencies of IGF-I and IGFBP-3 in patients with homozygous *IGFALS* mutations who have mild growth failure (Domene et al., 2004, Hwa et al., 2006, Domene et al., 2007, Duyvenvoorde et al., 2008, Heath et al., 2008).

We wished to test the hypothesis that heterozygous *IGFALS* defects contributes towards the phenotype of patients with ISS. We analysed 52 unrelated ISS children and found single heterozygous *IGFALS* defects in 5. Moreover, the study of family members showed that relatives with heterozygous *IGFALS* defects were also short. Surprisingly, all defects found in this study were missense mutations involving a proline or leucine. Three out of four defects were, in fact, proline to leucine amino acid changes. Because of the chemical differences between these two amino acids, this defect is likely to induce a

change in the ALS secondary structure, possibly leading to a non-functional protein. Leucine has a hydrophobic aliphatic side chain that favours the formation of α-helices, whereas proline has a cyclic structure that does not. Moreover, proline induces a bend in the amino acids chain.

The C to G base change at position 1438 (L453V) caused the most profound change in the ability of patient serum to form a ternary complex. It is of note that, the result of this mutation might be a splicing defect rather than an amino acid change as the C to G nucleotide change creates a strong enhancer for the SRp 55 protein in *IGFALS* exon 2 (score 3.3 versus 5.3; ESEfinder3.0), which may result in aberrant gene splicing and the creation of a profoundly altered ALS protein.

Size exclusion chromatography showed that ternary complex formation was affected by all four mutations and results were in accordance with the impact of these mutations on the levels of ALS measured in the serum. Three mutations (P22L, P287L and L453V) resulted in a decrease in the formation of the ternary complex, as shown by the decreased IGF-I incorporation. The P287L and L453V mutations are localised in two of the predicted leucine-rich repeats and may affect ALS secondary structure. Mutation P22L is localised in the predicted ALS signal peptide. According to SignalP 3.0 prediction program (Bendtsen et al., 2004), this mutation is likely to affect the cleavage site and may thus hinder the processing and secretion of the ALS protein. The P526L mutation is localised in the C-terminal domain of the ALS protein. Its presence resulted in a modest increased peak corresponding to the ternary complex suggesting that it may increase the affinity of ALS for the binary complex and perhaps retard the release of IGF-I at the site of action.

Reduced IGF-I, IGFBP-3 and ALS levels were present in most heterozygous *IGFALS* patients, although no significant differences were found between ISS children with and without *IGFALS* defects. This is not surprising, since the latter cohort is a heterogeneous population with still unidentified genetic abnormalities. Reduction in GH dependent protein levels was also reported in the heterozygous parents of patients with ALS deficiency (Hwa et al., 2006, Domene et al., 2007, Duyvenvoorde et al., 2008, Heath et al., 2008), as well as in an *IGFALS* heterozygous animal model. Ueki et al (Ueki et al., 2000) demonstrated that mice with only one *IGFALS* allele have a 50% reduction in liver ALS mRNA and a 17% and 40% reduction of IGF-I and IGFBP-3 serum levels,

respectively. The ALS protein in the serum is in molar excess relative to IGFs and this is thought to be important in maintaining and promoting the affinity of ALS for the binary complex IGF/IGFBP (Holman and Baxter, 1996). A change in the ratio ALS/binary complex may be occurring in the heterozygous *IGFALS* patients, explaining, at least in part, the phenotype.

Prepubertal patients with *IGFALS* defects were significantly slimmer compared to ISS prepubertal children with no *IGFALS* defects. Malnutrition, eating disorders or major illnesses were excluded in all cases. A different availability of IGF-I resulting from single heterozygous *IGFALS* defects may have an effect on the metabolism of these patients. Postpubertal patients, however, did not exhibit low BMI values.

Homozygous versus single heterozygous ALS defects: effects on stature

In this study, the range of height SDS in patients with single heterozygous *IGFALS* defects was similar to that reported in patients with homozygous *IGFALS* defects (Domene et al., 2004, Hwa et al., 2006, Domene et al., 2007) suggesting that, despite the profound difference in the biochemical phenotype, the effect on growth is similar. The liver and local production of IGF-I in patients with *IGFALS* defects appears to be normal and seems to be able to support linear growth, despite an alteration in the circulating IGF-I levels. Unfortunately, measurement of free IGF-I is a difficult and sophisticated technique and free IGF-I levels are not routinely monitored.

Identification of *IGFALS* defects within family members of affected ISS children

Analysis of family members of the affected patients showed that heterozygous *IGFALS* defects were related to short stature. However, this relationship varied with pubertal status. Prepubertal heterozygous *IGFALS* patients were significantly shorter than ISS patients without *IGFALS* defects, despite the fact that there was no significant difference in IGF-I, IGFBP-3 and ALS levels. Postpubertal heterozygous *IGFALS* patients had higher height SDS values compared to prepubertal *IGFALS* patients in the corresponding families. It is possible that the near-normalisation in height SDS in the pubertal sibling from Family 2 reflects a pubertal growth spurt. Unfortunately, no prepubertal or follow-up data were available for this patient. A near-normal adult height

has been reported in homozygote and compound heterozygote *IGFALS* patients and in their heterozygote parents (Hwa et al., 2006, Domene et al., 2007, Duyvenvoorde et al., 2008, Heath et al., 2008), The broad range of adult height SDS in individuals with heterozygous and homozygous *IGFALS* defects may indicate that this genetic defect is not sufficient to determine the final height and is only one of many contributors to a complex genetic and environmental scenario.

Limitation

A limitation of this study is the relatively small number of ISS patients included. The analysis of a larger population is required to confirm the frequency and contribution of single heterozygous *IGFALS* defects to short stature. Further prospective studies are also needed to clarify whether the discrepancy in height observed between prepubertal and postpubertal patients is a real phenomenon or simply reflects the fact that *IGFALS* defects only affect final height in the presence of a genetic defect or polymorphism in one or more genes. Moreover, *in vitro* characterisation of the detected mutations was not performed as this requires the establishment of a cell expression system for ALS mutant proteins and the analysis of their interaction with IGF-I/ IGFBP-3. However, the amino acid changes induced by these mutations are likely to affect the ALS secondary structure and have a deleterious effect on protein function.

Conclusion

In conclusion, a single heterozygous defect in the *IGFALS* was found in 9.6% of ISS children and in their relatives with short stature. Prepubertal children with *IGFALS* defects were significantly shorter than ISS children without *IGFALS* defects, but did not have significantly lower GH-dependent protein levels. The study of a larger population is required to accurately define the prevalence of this genetic finding in the ISS population.

CHAPTER 8

FINAL DISCUSSION

8.1 SUMMARY OF FINDINGS

Short stature is a common reason for referral to paediatric endocrinologists. It can be due to several causes, among which resistance to the action of GH due to genetic defects, namely growth hormone insensitivity. Nevertheless, it has been estimated that in approximately 80% of referred children no aetiology can be identified and they are classified as ISS (Wit et al., 2008b). Significant effort is made to understand the causes of short stature. Identification of novel genes, as well as characterisation of novel defects in known genes responsible for growth failure, can shed new light of the physiology of longitudinal growth and guide therapy in children with short stature.

The overall aim of this thesis was to identify and characterise the molecular mechanism of GHI and ISS. The GH-IGF-I axis plays a fundamental role in promoting longitudinal growth and all its elements are strong candidates when searching for molecular defects causing growth failure. A large, ethnically heterogeneous, population of patients with primary GHI was genetically characterised. All subjects had severe GH resistance as demonstrated by the high GH levels and low or undetectable GH dependent proteins levels, not increasing after administration of exogenous GH. Nevertheless, despite a similar biochemical profile, different degrees of growth failure were present.

The initial genetic screening of these patients started with the analysis of the *GHR*. GH exerts its biological actions through the binding to its receptor and any mutation leading to the absence or to a non-functional GHR, results in GHI. *GHR* mutations represent the most common cause of primary GHI and were present in the majority of patients in this study. During the course of the project several novel defects in the *GHR* were identified. Among these was a novel single heterozygous mutation hypothesised to exert a dominant negative effect similarly to the two single heterozygous *GHR* defects identified by Ayling et al. and Iida et al. (Ayling et al., 1997, Iida et al., 1998). Although all three mutations occur in the genomic region coding for the GHR intracellular domain and share the same pathogenetic mechanism, they produce different phenotypes. The child studied during the course of this project and her two affected family members, presented with non-classical GHI, characterised by mild short stature and normal facial features. This finding is in agreement with the cases reported by Ayling et al., but dissimilar to the cases described by Iida et al. The three patients described by Iida et al.

had, in fact, classical Laron facial features: prominent forehead and saddle nose. Different phenotypes in patients with the same mutation are known to occur when the defect causes aberrant gene splicing. This phenomenon was documented in the Equadorian GHI population carrying the E180 splice mutation (Rosenbloom et al., 1999) and has is maximum expression in patients with the *GHR* pseudoexon 6Ψ mutation, as described in Chapter 5 of this Thesis.

The *GHR* pseudoexon 6Ψ was identified in our laboratories in 2001. DNA is rich in intronic sequences resembling coding exons, which are not normally included in the mature mRNA and are known as pseudoexons. The *GHR* pseudoexon 6Ψ defect is an example of how a subtle DNA change can lead to the recognition of these intronic sequences by the splicing machinery and lead to their inclusion in the mRNA. When the pseudoexon 6Ψ mutation was identified, it was believed to represent a rare GHI-causing defect. The four children, in whom it was reported, had normal facial features and mild GHI. The genetic characterisation of a large heterogeneous GHI cohort performed during the course of this study identified several new cases of GHI due to the pseudoexon 6Ψ defect. Although genotype analysis suggests a common ancestor for these patients, the pseudoexon defect still appears to be a more common cause of GHI than initially thought and should be looked for in GHI patients with no *GHR* mutations.

Analysis of the 11 patients with the pseudoexon mutation identified so far, showed a wide range of phenotypes arising from this defect. Patients presented with normal or classical Laron facial features and GHI severity ranged from mild to severe with a wide range of biochemical profiles. This variability in phenotypes is likely to arise from the presence of low amounts of wild type GHR. Because of the complexity of mRNA splicing, a defect may not always be completely efficient in causing aberrant splicing. In patients with the pseudoexon 6Ψ mutation, low quantities of the wild type GHR transcript were demonstrated to occur alongside the mutant GHR. Individual factors may play a role in determining the efficiency of aberrant splicing and therefore the presence of a different ratio of mutant to wild type transcript in patients with the same genetic defect.

The presence of the wild type GHR, even at low levels, may also account for the significant milder phenotype observed in patients with GHI due to single heterozygous defects with a dominant negative effect, albeit in these patients, the functional wild type

GHR dimer can be present alongside the non-functional mutant homozygous dimer and the non-functional mutant heterozygous dimer.

Among the novel *GHR* defects identified during this study was a homozygous mutation in the polypyrimidine tract. Defects in this splice element are extremely rare and this is the first of its kind to be identified in the *GHR*. The majority of splice mutations identified so far in the *GHR* and in other genes, disrupt the invariant dinucleotide sequences at their splice sites and their effect on mRNA splicing are easily predicted. Nevertheless, in recent years an increasing number of mutations outside the splice sites has been identified. These defects are intronic or exonic and can disrupt splice elements such as enhancers, silencers, branch points or polypyrimidine tracts. The lack of a comprehensive understanding of these splice regulatory elements in combination with their scarce adherence to consensus sequences, makes it extremely difficult to predict the consequences at a mRNA level of a base change occurring in these elements. For this reason, analysis of RNA extracted from patient leucocytes or fibroblasts is mandatory for establishing the diagnosis. Obtaining tissue samples can, however, be difficult especially from infants and children, particularly those with reduced body size, as are those with GHI.

One of the aims of this thesis was to establish the diagnostic value of an *in vitro* splicing assay as an alternative technique for assessing the consequences of genetic defects on mRNA splicing. The assay was based on a three-exon minigene system spliced in HeLa nuclear extracts and was employed to assess the effect of *GHR* mutations identified in the GHI population. The *in vitro* splicing assay is widely used to study the physiology of splicing and of its regulatory elements, but had not been employed to study the consequences of naturally occurring mutations. If validated, this could represent a quicker and straightforward alternative to RNA analysis from patient samples or from transfected cells. Although the splicing assay was used in 2001 to study the consequences of the *GHR* pseudoexon 6Ψ defect (Metherell et al., 2001), data on its accuracy in predicting the effect of other splice mutations were not available. Moreover, a reliable protocol for the creation of three-exon minigenes was lacking. Considerable effort was, therefore, made to establish the latter during the course of this project. Having achieved this, several mutant and the corresponding wild type minigenes were produced, allowing the study of *GHR* mutations. As a collateral project to this Thesis, I also used the *in vitro*

splicing assay to assess seven different defects identified in a gene responsible for familial glucocorticoid deficiency, namely the melanocortin receptor accessory protein (MRAP) gene. Because of its non-pertinence to the main theme of this Thesis, the results of the *in vitro* splicing assay on MRAP mutations, published in 2005 in Nature Genetics (Metherell et al., 2005), are not included.

The results of the *in vitro* splicing assay on *GHR* defects, presented in Chapter 4, support the validity of this assay in identifying nucleotide changes resulting in aberrant gene splicing. The comparison between *in silico* and *in vitro* results demonstrated that the splicing assay was particularly helpful in case of defects occurring outside the invariant nucleotides of the splice sites, for which the *in silico* prediction programs gave ambiguous results. Since only a small number of mutations were studied and very few *in vivo* data were available, more data are required to further validate this system, as discussed in the "Future Prospects" section.

The discovery of the *GHR* pseudoexon 6Ψ mutation was the basis for another part of this project. The obvious interest of our group in this mutation and the finding that it is not such a rare cause of GHI, as initially thought, led to the search for a therapeutic tool aimed at correcting aberrant *GHR* splicing caused by this defect. The RNA antisense approach is a promising tool in gene therapy. It has been tested for correcting aberrant splicing which causes neurodegenerative diseases and haematopoietic disorders, with promising results both *in vitro* and in animal models. The results presented in Chapter 5 of this Thesis are the first to demonstrate the efficiency of this tool in correcting an endocrine disorder. Three ASOs directed against the three major splicing elements – the donor and acceptor splice sites and the branch point – were designed and tested using the *in vitro* splicing assay and a cell transfection system. Near-complete restoration of correct *GHR* splicing was seen with the ASO targeting the acceptor splice site. Although this result requires confirmation with *in vivo* studies on patient cells and the specific activity of this ASO needs further testing, ASOs appear to be a valid option for gene therapy in GHI patients with the pseudoexon 6Ψ defect. Interestingly, the most effective ASO was the one targeting the acceptor splice site, whereas the ASO targeting the donor splice site where the pseudoexon defect is localised, only had a modest effect. This could be explained by cell specific differences in accessibility of the donor versus the acceptor splice site. Additional studies to confirm these findings are required.

Genetic characterisation of a large GHI population in this Thesis, allowed the identification of novel defects in the *GHR*, but also in other genes, such as *STAT5b* and *IGFALS*. The second ever reported case of GHI due to a *STAT5b* mutation was identified during the course of this project, in collaboration with Dr Rosenfeld's group at the Department of Paediatrics, Oregon, US and reported in 2005 (Hwa et al., 2005). Direct sequencing of the *GHR* and analysis of *GHR* SNPs in the two patients and their parents allowed exclusion of the involvement of the *GHR* and the search for other candidate genes. The involvement of the *STAT5b* was investigated based on the co-existance, in these children, of GHI and immunological disorders, as previously described by Kofoed et al. (Kofoed et al., 2003).

At the time this project started, very little was known on the relationship between ALS deficiency due to *IGFALS* defects and GHI. The description of the first case of ALS deficiency (Domene et al., 2004) prompted consideration of the role of *IGFALS* as a cause of GHI in children with no evidence of *GHR* defects. Three children, homozygous for novel defects and one child, compound heterozygous for two novel *IGFALS* defects, were identified during the course of this project. These patients belonged to four of the nine families known worldwide with *IGFALS* defects. Although two of these patients were simultaneously studied elsewhere and the genetic data published by other authors (Hwa et al., 2006, van Duyvenvoorde et al., 2008), the four children reported in this project represent the largest series of unrelated subjects with *IGFALS* defects studied in one single centre. When data from GHI patients with *IGFALS* defects were compared to those of GHI patients with nonsense or missense *GHR* defects, no significant difference in IGF-I levels between the two groups was found, despite the significant difference in height SDS. This confirms the milder degree of growth failure observed in GHI due to ALS deficiency, which is similar to that observed in GHI due to *GHR* dominant negative mutations and to the *GHR* pseudoexon mutation.

No pubertal delay was present in at least two out of the four patients described in this Thesis, which is in disagreement with other ALS deficient patients (Domene et al., 2004, Domene et al., 2007) and suggests that a delayed puberty may be due to the individual genetic background rather than to *IGFALS* defects.

Data analysis from ALS deficient patients and their affected family members led to the interesting observation that parents of ALS deficient patients, obligate single

heterozygous carriers of *IGFALS* mutations, also had short stature, albeit to a lesser degree than their homozygote children. This observation suggested that single heterozygous *IGFALS* defects may be sufficient to affect final height. Data available on the single *IGFALS* null allele mouse model confirmed this observation (Ueki et al., 2000). This led us to speculate that single heterozygous *IGFALS* defects may be implicated in the pathogenesis of ISS. To test this hypothesis the *IGFALS* was studied in a large cohort of ethnically homogenous prepubertal ISS children. In 9.6% of ISS patients, a single heterozygous *IGFALS* defect was identified. ISS children with heterozygous *IGFALS* defects were significantly shorter than ISS patients without *IGFALS* defects, despite no significant difference in IGF-I, IGFBP-3 and ALS levels. Although all mutations are predicted to cause a major change in the ALS secondary structure, serum samples from ISS children with *IGFALS* defects tested by means of size exclusion chromatography showed a modest alteration in ternary complex formation compared to a normal control. The ALS protein is in molar excess relative to IGF-I and II in the serum and this is thought to be important in maintaining and promoting the affinity of ALS for the binary complex IGF/IGFBP (Holman and Baxter, 1996). The occurrence of single heterozygous defects may induce a change in the ratio ALS to binary complex and a change in the affinity and availability of IGF-I at tissue level explaining, at least in part, the phenotype.

IGFALS defects were also found in short stature family members of affected index cases. Interestingly, postpubertal subjects with single heterozygous *IGFALS* defects had higher height SDS values compared to prepubertal affected patients in the corresponding families. Although this so far remains an observation it has to be noted that the height discrepancy between pre and post pubertal status can also be observed in patients with homozygous *IGFALS* defects and ALS deficiency.

8.2 FUTURE PROSPECTS

8.2.1 The *GHR* polypyrimidine tract mutation

The base change localised in the polypyrimidine tract of *GHR* exon 8 resulted in clear exon skipping when assessed by the *in vitro* splicing assay. Nevertheless, the three-

exon minigene system spliced in nuclear extract is an *in vitro* system, and tissue-specific differences may occur. Study of patient mRNA is particularly advisable in the case of the polypyrimidine tract mutation. Obtaining patient leukocytes or fibroblasts was sought during the course of this project, but was not possible. As an alternative, confirmation of the effect of this mutation may be obtained by transfecting cells, such as HEK293 or CHO, with a mutant minigene. Moreover, it may be of interest to demonstrate that the T to C base change affects the binding of spliceosome elements such as U2AF or hnRNP to the polypyrimidine tract, thus inhibiting the first steps of GHR mRNA splicing (Figure 8.1).

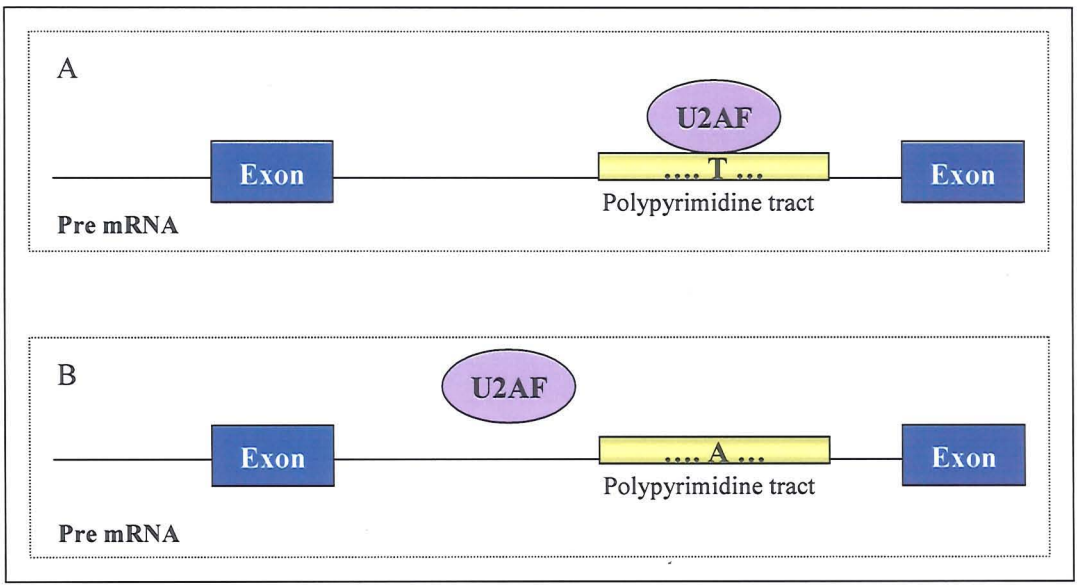

Figure 8.1 Effect of the polypyrimidine tract mutation on GHR splicing. Apposition of the U2AF splice element takes place in the wild type GHR mRNA (Panel A), but is prevented in the mutant GHR mRNA (Panel B).

8.2.2 Identification of novel *GHR* defects

In several GHI patients, no mutations in the *GHR* coding region could be identified. The presence of undetectable or very low serum GHBP levels in these patients suggests the presence of a defective *GHR*. Study of the *GHR* promoter region and patient RNA could lead to the identification of a promoter defect or a intronic mutation activating a novel pseudoexon.

8.2.3 Validation of the *in vitro* splicing assay

This thesis provides evidence of the validity of the *in vitro* splicing assay for demonstrating the occurrence of aberrant mRNA splicing caused by mutations localised at the splice sites or in other regulatory elements. Nevertheless, few data on the *in vivo* effect of the *GHR* mutations studied were available and are required in order to validate the results obtained with the *in vitro* assay. This can be achieved by analysing patients' RNA or RNA extracted by cells transfected with minigenes. Moreover, the study of additional mutations, especially outside the invariant splice site sequences in the *GHR* and in other genes, and the corresponding *in vivo* analysis, is advisable to further assess the accuracy of this system.

8.2.4 Modulation of GH sensitivity by increasing the expression of *GHR* alternative transcripts

At least two novel alternative *GHR* exons were identified during the course of this project. If inserted in the mature mRNA, both exons would cause a frameshift and the appearance of a stop codon a few amino acids after the signal peptide. The novel alternative *GHR* transcripts arising from these exons are predicted to be prematurely truncated and lack GH binding domains. Although a possible functional role for these transcripts cannot be excluded, they are likely to represent biological noise and be susceptible to nonsense mediated decay. It could, therefore, be hypothesised that increasing the expression of these exons could lead to silencing of the *GHR* and modulation of GH sensitivity at specific tissues. This could potentially be achieved by targeting exonic silencers in these exons with specific ASOs, or by designing a bifunctional ASO. The latter consists of an RNA sequence complementary to the target pre-mRNA to which a non-complementary tail, mimicking an exonic enhancer motif or a small peptide resembling the SR protein RS domain enhancer, is attached.

8.2.5 The role of *IGFALS* defects in ISS

ALS traps IGF-I and II in the circulation limiting their transendothelial passage and can thus be considered one of the principal regulators of IGFs bioavailability. Very little is, however, known on ALS physiology and its role outside the circulation. Although the relation between growth failure and ALS deficiency arising from homozygous *IGFALS*

defects has been demonstrated, the relation between growth failure and single heterozygous *IGFALS* mutations suggested in this study requires further confirmation. Screening of a larger population of ISS patients is required, but, more importantly, assessment of the frequency of *IGFALS* defects in the normal population is mandatory.

The defects identified in this study are likely to cause a profound alteration in the ALS secondary structure, according to *in silico* prediction programs and based on the nature of the base changes. Nevertheless, size exclusion chromatography only detected a modest change in ternary complex formation. Expression of the wild type and mutant ALS proteins in a cell system, such as HEK293 or CHO cells, as well as reconstitution and *in vitro* study of ternary complex formation, is advisable.

8.3 CONCLUDING REMARKS

This thesis focused on identifying and characterising the molecular defects underlying GHI and ISS. The genetic analysis of a large genetically heterogeneous population identified several novel defects in three genes in the GH/IGF-I axis: *GHR*, *STAT5b* and *IGFALS*. Moreover, the study of the clinical and genetic data of this large cohort combined with published data from another large heterogenous GHI cohort and from two studies on *GHR* mutations with a dominant negative effect identified a genotype/phenotype relationship between *GHR* defects and GHI severity.

The genetic characterisation of a large GHI population revealed that the *GHR* pseudoexon 6Ψ defect is more frequent than initially thought. The results of this Thesis suggest that the ASOs approach is a potentially effective gene therapy for restoration of correct mRNA splicing in these patients.

Identification and analysis of patients with ALS deficiency caused by *IGFALS* defects and the observation of short stature in their heterozygote parents, led to hypothesise the involvement of *IGFALS* in the pathogenesis of ISS. Data gathered in this thesis supported this hypothesis.

In several GHI patients, no genetic diagnosis was obtained during the course of this project. Undetectable GHBP serum levels suggested the presence of a defective *GHR*. An

algorithm for the identification of intronic DNA sequences in the *GHR*, which could represent alternative exons or pseudoexons, was created. Several potential regions were identified, two of which were expressed in liver cDNA. This finding could be the basis for future studies aiming at modulating GH response in specific tissues.

CHAPTER 9

REFERENCES

ABELIOVICH, D., LAVON, I. P., LERER, I., COHEN, T., SPRINGER, C., AVITAL, A. & CUTTING, G. R. (1992) Screening for five mutations detects 97% of cystic fibrosis (CF) chromosomes and predicts a carrier frequency of 1:29 in the Jewish Ashkenazi population. *Am J Hum Genet,* 51, 951-6.

AKKER, S. A., MISRA, S., ASLAM, S., MORGAN, E. L., SMITH, P. J., KHOO, B. & CHEW, S. L. (2007) Pre-spliceosomal binding of U1 small nuclear ribonucleoprotein (RNP) and heterogenous nuclear RNP E1 is associated with suppression of a growth hormone receptor pseudoexon. *Mol Endocrinol,* 21, 2529-40.

ALLEN, L. H. (1994) Nutritional influences on linear growth: a general review. *Eur J Clin Nutr,* 48 Suppl 1, S75-89.

ALTER, J., LOU, F., RABINOWITZ, A., YIN, H., ROSENFELD, J., WILTON, S. D., PARTRIDGE, T. A. & LU, Q. L. (2006) Systemic delivery of morpholino oligonucleotide restores dystrophin expression bodywide and improves dystrophic pathology. *Nat Med,* 12, 175-7.

AMBROSIO, R., FIMIANI, G., MONFREGOLA, J., SANZARI, E., DE FELICE, N., SALERNO, M. C., PIGNATA, C., D'URSO, M. & URSINI, M. V. (2002) The structure of human STAT5A and B genes reveals two regions of nearly identical sequence and an alternative tissue specific STAT5B promoter. *Gene,* 285, 311-8.

AMIT, T., YOUDIM, M. B. & HOCHBERG, Z. (2000) Clinical review 112: Does serum growth hormone (GH) binding protein reflect human GH receptor function? *J Clin Endocrinol Metab,* 85, 927-32.

AMSELEM, S., DUQUESNOY, P., ATTREE, O., NOVELLI, G., BOUSNINA, S., POSTEL-VINAY, M. C. & GOOSSENS, M. (1989) Laron dwarfism and mutations of the growth hormone-receptor gene. *N Engl J Med,* 321, 989-95.

AMSELEM, S., DUQUESNOY, P., DURIEZ, B., DASTOT, F., SOBRIER, M. L., VALLEIX, S. & GOOSSENS, M. (1993) Spectrum of growth hormone receptor mutations and associated haplotypes in Laron syndrome. *Hum Mol Genet,* 2, 355-9.

AMSELEM, S., SOBRIER, M. L., DUQUESNOY, P., RAPPAPORT, R., POSTEL-VINAY, M. C., GOURMELEN, M., DALLAPICCOLA, B. & GOOSSENS, M. (1991) Recurrent nonsense mutations in the growth hormone receptor from patients with Laron dwarfism. *J Clin Invest,* 87, 1098-102.

ANDERSON, K. & MOORE, M. J. (1997) Bimolecular exon ligation by the human spliceosome. *Science,* 276, 1712-6.

ARGETSINGER, L. S., CAMPBELL, G. S., YANG, X., WITTHUHN, B. A., SILVENNOINEN, O., IHLE, J. N. & CARTER-SU, C. (1993) Identification of JAK2 as a growth hormone receptor-associated tyrosine kinase. *Cell,* 74, 237-44.

AYLING, R. M., ROSS, R., TOWNER, P., VON LAUE, S., FINIDORI, J., MOUTOUSSAMY, S., BUCHANAN, C. R., CLAYTON, P. E. & NORMAN, M. R. (1997) A dominant-negative mutation of the growth hormone receptor causes familial short stature. *Nat Genet,* 16, 13-4.

BACHRACH, L. K., MARCUS, R., OTT, S. M., ROSENBLOOM, A. L., VASCONEZ, O., MARTINEZ, V., MARTINEZ, A. L., ROSENFELD, R. G. & GUEVARA-AGUIRRE, J. (1998) Bone mineral, histomorphometry, and body composition in adults with growth hormone receptor deficiency. *J Bone Miner Res,* 13, 415-21.

BALLESTEROS, M., LEUNG, K. C., ROSS, R. J., IISMAA, T. P. & HO, K. K. (2000) Distribution and abundance of messenger ribonucleic acid for growth hormone receptor isoforms in human tissues. *J Clin Endocrinol Metab,* 85, 2865-71.

BAUMANN, G. (1991) Growth hormone heterogeneity: genes, isohormones, variants, and binding proteins. *Endocr Rev,* 12, 424-49.

BAUMANN, G., AMBURN, K. D. & BUCHANAN, T. A. (1987) The effect of circulating growth hormone-binding protein on metabolic clearance, distribution, and degradation of human growth hormone. *J Clin Endocrinol Metab,* 64, 657-60.

BAUMBACH, L., SCHIAVI, A., BARTLETT, R., PERERA, E., DAY, J., BROWN, M. R., STEIN, S., EIDSON, M., PARKS, J. S. & CLEVELAND, W. (1997) Clinical, biochemical, and molecular investigations of a genetic isolate of growth hormone insensitivity (Laron's syndrome). *J Clin Endocrinol Metab,* 82, 444-51.

BAXTER, R. C. (1990) Circulating levels and molecular distribution of the acid-labile (alpha) subunit of the high molecular weight insulin-like growth factor-binding protein complex. *J Clin Endocrinol Metab,* 70, 1347-53.

BAXTER, R. C. (1994) Insulin-like growth factor binding proteins in the human circulation: a review. *Horm Res,* 42, 140-4.

BENDTSEN, J. D., NIELSEN, H., VON HEIJNE, G. & BRUNAK, S. (2004) Improved prediction of signal peptides: SignalP 3.0. *J Mol Biol,* 340, 783-95.

BERG, M. A., PEOPLES, R., PEREZ-JURADO, L., GUEVARA-AGUIRRE, J., ROSENBLOOM, A. L., LARON, Z., MILNER, R. D. & FRANCKE, U. (1994) Receptor mutations and haplotypes in growth hormone receptor deficiency: a global survey and identification of the Ecuadorean E180splice mutation in an oriental Jewish patient. *Acta Paediatr Suppl,* 399, 112-4.

BERGET, S. M. (1995) Exon recognition in vertebrate splicing. *J Biol Chem,* 270, 2411-4.

BESSON, A., SALEMI, S., DELADOEY, J., VUISSOZ, J. M., EBLE, A., BIDLINGMAIER, M., BURGI, S., HONEGGER, U., FLUCK, C. & MULLIS, P. E. (2005) Short stature caused by a biologically inactive mutant growth hormone (GH-C53S). *J Clin Endocrinol Metab,* 90, 2493-9.

BINDER, G., BAUR, F., SCHWEIZER, R. & RANKE, M. B. (2006) The d3-growth hormone (GH) receptor polymorphism is associated with increased responsiveness to GH in Turner syndrome and short small-for-gestational-age children. *J Clin Endocrinol Metab,* 91, 659-64.

BINOUX, M. & HOSSENLOPP, P. (1988) Insulin-like growth factor (IGF) and IGF-binding proteins: comparison of human serum and lymph. *J Clin Endocrinol Metab,* 67, 509-14.

BJARNASON, R., BANERJEE, K., ROSE, S. J., ROSBERG, S., METHERELL, L., CLARK, A. J., ALBERTSSON-WIKLAND, K. & SAVAGE, M. O. (2002) Spontaneous growth hormone secretory characteristics in children with partial growth hormone insensitivity. *Clin Endocrinol (Oxf),* 57, 357-61.

BLACK, D. L. (2003) Mechanisms of alternative pre-messenger RNA splicing. *Annu Rev Biochem,* 72, 291-336.

BLENCOWE, B. J. (2000) Exonic splicing enhancers: mechanism of action, diversity and role in human genetic diseases. *Trends Biochem Sci,* 25, 106-10.

BLENCOWE, B. J. (2006) Alternative splicing: new insights from global analyses. *Cell,* 126, 37-47.

BLUM, W. F., MACHINIS, K., SHAVRIKOVA, E. P., KELLER, A., STOBBE, H., PFAEFFLE, R. W. & AMSELEM, S. (2006) The growth response to growth hormone (GH) treatment in children with isolated GH deficiency is independent of the presence of the exon 3-minus isoform of the GH receptor. *J Clin Endocrinol Metab,* 91, 4171-4.

BOISCLAIR, Y. R., RHOADS, R. P., UEKI, I., WANG, J. & OOI, G. T. (2001) The acid-labile subunit (ALS) of the 150 kDa IGF-binding protein complex: an important but forgotten component of the circulating IGF system. *J Endocrinol,* 170, 63-70.

BOISCLAIR, Y. R., SETO, D., HSIEH, S., HURST, K. R. & OOI, G. T. (1996) Organization and chromosomal localization of the gene encoding the mouse acid labile subunit of the insulin-like growth factor binding complex. *Proc Natl Acad Sci U S A,* 93, 10028-33.

BOUCHERON, C., DUMON, S., SANTOS, S. C., MORIGGL, R., HENNIGHAUSEN, L., GISSELBRECHT, S. & GOUILLEUX, F. (1998) A single amino acid in the DNA binding regions of STAT5A and STAT5B confers distinct DNA binding specificities. *J Biol Chem,* 273, 33936-41.

BROWN, R. J., ADAMS, J. J., PELEKANOS, R. A., WAN, Y., MCKINSTRY, W. J., PALETHORPE, K., SEEBER, R. M., MONKS, T. A., EIDNE, K. A., PARKER, M. W. & WATERS, M. J. (2005) Model for growth hormone receptor activation based on subunit rotation within a receptor dimer. *Nat Struct Mol Biol,* 12, 814-21.

BRYANT, J., BAXTER, L., CAVE, C. B. & MILNE, R. (2007) Recombinant growth hormone for idiopathic short stature in children and adolescents. *Cochrane Database Syst Rev,* CD004440.

BURATTI, E., BARALLE, M., DE CONTI, L., BARALLE, D., ROMANO, M., AYALA, Y. M. & BARALLE, F. E. (2004) hnRNP H binding at the 5' splice site correlates with the pathological effect of two intronic mutations in the NF-1 and TSHbeta genes. *Nucleic Acids Res,* 32, 4224-36.

BURGE, C., TUSCHL, T. & SHARP, P. (1999) Splicing of precursors to mRNAs by the spliceosomes. *The RNA world.* 2nd ed ed. Cold Spring Harbor, New York, Cold Spring Harbor Laboratory Press.

BURREN, C. P., WOODS, K. A., ROSE, S. J., TAUBER, M., PRICE, D. A., HEINRICH, U., GILLI, G., RAZZAGHY-AZAR, M., AL-ASHWAL, A., CROCK, P. A., ROCHICCIOLI, P., YORDAM, N., RANKE, M. B., CHATELAIN, P. G., PREECE, M. A., ROSENFELD, R. G. & SAVAGE, M. O. (2001) Clinical and endocrine characteristics in atypical and classical growth hormone insensitivity syndrome. *Horm Res,* 55, 125-30.

BURSET, M., SELEDTSOV, I. A. & SOLOVYEV, V. V. (2000) Analysis of canonical and non-canonical splice sites in mammalian genomes. *Nucleic Acids Res,* 28, 4364-75.

BURSET, M., SELEDTSOV, I. A. & SOLOVYEV, V. V. (2001) SpliceDB: database of canonical and non-canonical mammalian splice sites. *Nucleic Acids Res,* 29, 255-9.

CAMERON, N. (2002) British growth charts for height and weight with recommendations concerning their use in auxological assessment. *Ann Hum Biol,* 29, 1-10.

CARLSSON, L. M. (1996) Partial growth hormone insensitivity in childhood. *Baillieres Clin Endocrinol Metab,* 10, 389-400.

CARRASCOSA, A., ESTEBAN, C., ESPADERO, R., FERNANDEZ-CANCIO, M., ANDALUZ, P., CLEMENTE, M., AUDI, L., WOLLMANN, H., FRYKLUND, L. & PARODI, L. (2006) The d3/fl-growth hormone (GH) receptor polymorphism does not influence the effect of GH treatment (66 microg/kg per day) or the spontaneous growth in short non-GH-deficient small-for-gestational-

age children: results from a two-year controlled prospective study in 170 Spanish patients. *J Clin Endocrinol Metab,* 91, 3281-6.

CARTEGNI, L., CHEW, S. L. & KRAINER, A. R. (2002) Listening to silence and understanding nonsense: exonic mutations that affect splicing. *Nat Rev Genet,* 3, 285-98.

CARTEGNI, L. & KRAINER, A. R. (2002) Disruption of an SF2/ASF-dependent exonic splicing enhancer in SMN2 causes spinal muscular atrophy in the absence of SMN1. *Nat Genet,* 30, 377-84.

CARTEGNI, L. & KRAINER, A. R. (2003) Correction of disease-associated exon skipping by synthetic exon-specific activators. *Nat Struct Biol,* 10, 120-5.

CARTEGNI, L., WANG, J., ZHU, Z., ZHANG, M. Q. & KRAINER, A. R. (2003) ESEfinder: A web resource to identify exonic splicing enhancers. *Nucleic Acids Res,* 31, 3568-71.

CARTER-SU, C., SCHWARTZ, J. & SMIT, L. S. (1996) Molecular mechanism of growth hormone action. *Annu Rev Physiol,* 58, 187-207.

CHIN, E., ZHOU, J., DAI, J., BAXTER, R. C. & BONDY, C. A. (1994) Cellular localization and regulation of gene expression for components of the insulin-like growth factor ternary binding protein complex. *Endocrinology,* 134, 2498-504.

CLACKSON, T. & WELLS, J. A. (1995) A hot spot of binding energy in a hormone-receptor interface. *Science,* 267, 383-6.

COLAPIETRO, P., GERVASINI, C., NATACCI, F., ROSSI, L., RIVA, P. & LARIZZA, L. (2003) NF1 exon 7 skipping and sequence alterations in exonic splice enhancers (ESEs) in a neurofibromatosis 1 patient. *Hum Genet,* 113, 551-4.

COLE, T. J. (1990) The LMS method for constructing normalized growth standards. *Eur J Clin Nutr,* 44, 45-60.

COLE, T. J., FREEMAN, J. V. & PREECE, M. A. (1995) Body mass index reference curves for the UK, 1990. *Arch Dis Child,* 73, 25-9.

CONTE, F., SALLES, J. P., RAYNAL, P., FERNANDEZ, L., MOLINAS, C., TAUBER, M. & BIETH, E. (2002) Identification of a region critical for proteolysis of the human growth hormone receptor. *Biochem Biophys Res Commun,* 290, 851-7.

COOLIDGE, C. J., SEELY, R. J. & PATTON, J. G. (1997) Functional analysis of the polypyrimidine tract in pre-mRNA splicing. *Nucleic Acids Res,* 25, 888-96.

COOPER, T. A. (2005) Use of minigene systems to dissect alternative splicing elements. *Methods,* 37, 331-40.

CROOKE, S. (2001) *Antisense Drug Technology. Principles, Strategies, and Applications,* New York, CRC.

CUNNINGHAM, B. C., ULTSCH, M., DE VOS, A. M., MULKERRIN, M. G., CLAUSER, K. R. & WELLS, J. A. (1991) Dimerization of the extracellular domain of the human growth hormone receptor by a single hormone molecule. *Science,* 254, 821-5.

CUNNINGHAM, B. C. & WELLS, J. A. (1993) Comparison of a structural and a functional epitope. *J Mol Biol,* 234, 554-63.

CWYFAN HUGHES, S., MASON, H. D., FRANKS, S. & HOLLY, J. M. (1997) Modulation of the insulin-like growth factor-binding proteins by follicle size in the human ovary. *J Endocrinol,* 154, 35-43.

DAI, J. & BAXTER, R. C. (1992) Molecular cloning of the acid-labile subunit of the rat insulin-like growth factor binding protein complex. *Biochem Biophys Res Commun,* 188, 304-9.

DAI, J. & BAXTER, R. C. (1994) Regulation in vivo of the acid-labile subunit of the rat serum insulin-like growth factor-binding protein complex. *Endocrinology,* 135, 2335-41.

DARNELL, J. E., JR., KERR, I. M. & STARK, G. R. (1994) Jak-STAT pathways and transcriptional activation in response to IFNs and other extracellular signaling proteins. *Science,* 264, 1415-21.

DAVEY, H. W., XIE, T., MCLACHLAN, M. J., WILKINS, R. J., WAXMAN, D. J. & GRATTAN, D. R. (2001) STAT5b is required for GH-induced liver IGF-I gene expression. *Endocrinology,* 142, 3836-41.

DAVID, A., METHERELL, L. A., CLARK, A. J., CAMACHO-HUBNER, C. & SAVAGE, M. O. (2005) Diagnostic and therapeutic advances in growth hormone insensitivity. *Endocrinol Metab Clin North Am,* 34, 581-95, viii.

DE KLEIN, A., RIEGMAN, P. H., BIJLSMA, E. K., HELDOORN, A., MUIJTJENS, M., DEN BAKKER, M. A., AVEZAAT, C. J. & ZWARTHOFF, E. C. (1998) A G-->A transition creates a branch point sequence and activation of a cryptic exon, resulting in the hereditary disorder neurofibromatosis 2. *Hum Mol Genet,* 7, 393-8.

DE VOS, A. M., ULTSCH, M. & KOSSIAKOFF, A. A. (1992) Human growth hormone and extracellular domain of its receptor: crystal structure of the complex. *Science,* 255, 306-12.

DELHANTY, P. & BAXTER, R. C. (1996) The cloning and expression of the baboon acid-labile subunit of the insulin-like growth factor binding protein complex. *Biochem Biophys Res Commun,* 227, 897-902.

DEMAMBRO, V. E., CLEMMONS, D. R., HORTON, L. G., BOUXSEIN, M. L., WOOD, T. L., BEAMER, W. G., CANALIS, E. & ROSEN, C. J. (2008) Gender-specific changes in bone turnover and skeletal architecture in igfbp-2-null mice. *Endocrinology,* 149, 2051-61.

DOMENE, H. M., BENGOLEA, S. V., MARTINEZ, A. S., ROPELATO, M. G., PENNISI, P., SCAGLIA, P., HEINRICH, J. J. & JASPER, H. G. (2004) Deficiency of the circulating insulin-like growth factor system associated with inactivation of the acid-labile subunit gene. *N Engl J Med,* 350, 570-7.

DOMENE, H. M., SCAGLIA, P. A., LTEIF, A., MAHMUD, F. H., KIRMANI, S., FRYSTYK, J., BEDECARRAS, P., GUTIERREZ, M. & JASPER, H. G. (2007) Phenotypic effects of null and haploinsufficiency of acid-labile subunit in a family with two novel IGFALS gene mutations. *J Clin Endocrinol Metab,* 92, 4444-50.

DOMINSKI, Z. & KOLE, R. (1993) Restoration of correct splicing in thalassemic pre-mRNA by antisense oligonucleotides. *Proc Natl Acad Sci U S A,* 90, 8673-7.

DOS SANTOS, C., ESSIOUX, L., TEINTURIER, C., TAUBER, M., GOFFIN, V. & BOUGNERES, P. (2004) A common polymorphism of the growth hormone receptor is associated with increased responsiveness to growth hormone. *Nat Genet,* 36, 720-4.

DUYVENVOORDE, H., KEMPERS, M., TWICKER, M., DOORN, J., GERVER, W., NOORDAM, K., LOSEKOOT, M., KARPERIEN, M., WIT, J. M. & HERMUS, A. (2008) Homozygous and heterozygous expression of a novel mutation of the Acid-Labile Subunit. *Eur J Endocrinol.*

EDENS, A. & TALAMANTES, F. (1998) Alternative processing of growth hormone receptor transcripts. *Endocr Rev,* 19, 559-82.

ESHET, R., LARON, Z., PERTZELAN, A., ARNON, R. & DINTZMAN, M. (1984) Defect of human growth hormone receptors in the liver of two patients with Laron-type dwarfism. *Isr J Med Sci,* 20, 8-11.

FAIRBROTHER, W. G. & CHASIN, L. A. (2000) Human genomic sequences that inhibit splicing. *Mol Cell Biol,* 20, 6816-25.

FANG, P., KOFOED, E. M., LITTLE, B. M., WANG, X., ROSS, R. J., FRANK, S. J., HWA, V. & ROSENFELD, R. G. (2006) A mutant signal transducer and activator of transcription 5b, associated with growth hormone insensitivity and insulin-like growth factor-I deficiency, cannot function as a signal transducer or transcription factor. *J Clin Endocrinol Metab,* 91, 1526-34.

FIRTH, S. M., GANESHPRASAD, U. & BAXTER, R. C. (1998) Structural determinants of ligand and cell surface binding of insulin-like growth factor-binding protein-3. *J Biol Chem,* 273, 2631-8.

FLORINI, J. R., EWTON, D. Z. & COOLICAN, S. A. (1996) Growth hormone and the insulin-like growth factor system in myogenesis. *Endocr Rev,* 17, 481-517.

FREEMAN, J. V., COLE, T. J., CHINN, S., JONES, P. R., WHITE, E. M. & PREECE, M. A. (1995) Cross sectional stature and weight reference curves for the UK, 1990. *Arch Dis Child,* 73, 17-24.

FU, X. D. (1995) The superfamily of arginine/serine-rich splicing factors. *Rna,* 1, 663-80.

FUH, G., CUNNINGHAM, B. C., FUKUNAGA, R., NAGATA, S., GOEDDEL, D. V. & WELLS, J. A. (1992) Rational design of potent antagonists to the human growth hormone receptor. *Science,* 256, 1677-80.

FUKATA, J., DIAMOND, D. J. & MARTIN, J. B. (1985) Effects of rat growth hormone (rGH)-releasing factor and somatostatin on the release and synthesis of rGH in dispersed pituitary cells. *Endocrinology,* 117, 457-67.

GASTIER, J. M., BERG, M. A., VESTERHUS, P., REITER, E. O. & FRANCKE, U. (2000) Diverse deletions in the growth hormone receptor gene cause growth hormone insensitivity syndrome. *Hum Mutat,* 16, 323-33.

GEBAUER, F., MERENDINO, L., HENTZE, M. W. & VALCARCEL, J. (1998) The Drosophila splicing regulator sex-lethal directly inhibits translation of male-specific-lethal 2 mRNA. *Rna,* 4, 142-50.

GELFAND, M. S., DUBCHAK, I., DRALYUK, I. & ZORN, M. (1999) ASDB: database of alternatively spliced genes. *Nucleic Acids Res,* 27, 301-2.

GENT, J., VAN KERKHOF, P., ROZA, M., BU, G. & STROUS, G. J. (2002) Ligand-independent growth hormone receptor dimerization occurs in the endoplasmic reticulum and is required for ubiquitin system-dependent endocytosis. *Proc Natl Acad Sci U S A,* 99, 9858-63.

GLUCKMAN, P. D., GUNN, A. J., WRAY, A., CUTFIELD, W. S., CHATELAIN, P. G., GUILBAUD, O., AMBLER, G. R., WILTON, P. & ALBERTSSON-WIKLAND, K. (1992) Congenital idiopathic growth hormone deficiency associated with prenatal and early postnatal growth failure. The International Board of the Kabi Pharmacia International Growth Study. *J Pediatr,* 121, 920-3.

GODDARD, A. D., COVELLO, R., LUOH, S. M., CLACKSON, T., ATTIE, K. M., GESUNDHEIT, N., RUNDLE, A. C., WELLS, J. A. & CARLSSON, L. M. (1995) Mutations of the growth hormone receptor in children with idiopathic short stature. The Growth Hormone Insensitivity Study Group. *N Engl J Med,* 333, 1093-8.

GODOWSKI, P. J., LEUNG, D. W., MEACHAM, L. R., GALGANI, J. P., HELLMISS, R., KERET, R., ROTWEIN, P. S., PARKS, J. S., LARON, Z. & WOOD, W. I. (1989) Characterization of the human growth hormone receptor gene and

demonstration of a partial gene deletion in two patients with Laron-type dwarfism. *Proc Natl Acad Sci U S A,* 86, 8083-7.

GOODYER, C. G., ZOGOPOULOS, G., SCHWARTZBAUER, G., ZHENG, H., HENDY, G. N. & MENON, R. K. (2001) Organization and evolution of the human growth hormone receptor gene 5'-flanking region. *Endocrinology,* 142, 1923-34.

GOVERS, R., TEN BROEKE, T., VAN KERKHOF, P., SCHWARTZ, A. L. & STROUS, G. J. (1999) Identification of a novel ubiquitin conjugation motif, required for ligand-induced internalization of the growth hormone receptor. *Embo J,* 18, 28-36.

GRAVELEY, B. R. (2000) Sorting out the complexity of SR protein functions. *Rna,* 6, 1197-211.

GRAVHOLT, C. H. (2005) Clinical practice in Turner syndrome. *Nat Clin Pract Endocrinol Metab,* 1, 41-52.

GRONOWSKI, A. M., ZHONG, Z., WEN, Z., THOMAS, M. J., DARNELL, J. E., JR. & ROTWEIN, P. (1995) In vivo growth hormone treatment rapidly stimulates the tyrosine phosphorylation and activation of Stat3. *Mol Endocrinol,* 9, 171-7.

GROUSSIN, L., HORVATH, A., JULLIAN, E., BOIKOS, S., RENE-CORAIL, F., LEFEBVRE, H., CEPHISE-VELAYOUDOM, F. L., VANTYGHEM, M. C., CHANSON, P., CONTE-DEVOLX, B., LUCAS, M., GENTIL, A., MALCHOFF, C. D., TISSIER, F., CARNEY, J. A., BERTAGNA, X., STRATAKIS, C. A. & BERTHERAT, J. (2006) A PRKAR1A mutation associated with primary pigmented nodular adrenocortical disease in 12 kindreds. *J Clin Endocrinol Metab,* 91, 1943-9.

GUDBJARTSSON, D. F., WALTERS, G. B., THORLEIFSSON, G., STEFANSSON, H., HALLDORSSON, B. V., ZUSMANOVICH, P., SULEM, P., THORLACIUS, S., GYLFASON, A., STEINBERG, S., HELGADOTTIR, A., INGASON, A., STEINTHORSDOTTIR, V., OLAFSDOTTIR, E. J., OLAFSDOTTIR, G. H., JONSSON, T., BORCH-JOHNSEN, K., HANSEN, T., ANDERSEN, G., JORGENSEN, T., PEDERSEN, O., ABEN, K. K., WITJES, J. A., SWINKELS, D. W., DEN HEIJER, M., FRANKE, B., VERBEEK, A. L., BECKER, D. M., YANEK, L. R., BECKER, L. C., TRYGGVADOTTIR, L., RAFNAR, T., GULCHER, J., KIEMENEY, L. A., KONG, A., THORSTEINSDOTTIR, U. & STEFANSSON, K. (2008) Many sequence variants affecting diversity of adult human height. *Nat Genet,* 40, 609-15.

GULER, H. P., ZAPF, J., SCHMID, C. & FROESCH, E. R. (1989) Insulin-like growth factors I and II in healthy man. Estimations of half-lives and production rates. *Acta Endocrinol (Copenh),* 121, 753-8.

GUNTHERT, U., HOFMANN, M., RUDY, W., REBER, S., ZOLLER, M., HAUSSMANN, I., MATZKU, S., WENZEL, A., PONTA, H. & HERRLICH, P. (1991) A new variant of glycoprotein CD44 confers metastatic potential to rat carcinoma cells. *Cell,* 65, 13-24.

HANAMURA, A., CACERES, J. F., MAYEDA, A., FRANZA, B. R., JR. & KRAINER, A. R. (1998) Regulated tissue-specific expression of antagonistic pre-mRNA splicing factors. *Rna,* 4, 430-44.

HANSEN, J. A., LINDBERG, K., HILTON, D. J., NIELSEN, J. H. & BILLESTRUP, N. (1999) Mechanism of inhibition of growth hormone receptor signaling by suppressor of cytokine signaling proteins. *Mol Endocrinol,* 13, 1832-43.

HARTMAN, M. L., VELDHUIS, J. D., VANCE, M. L., FARIA, A. C., FURLANETTO, R. W. & THORNER, M. O. (1990) Somatotropin pulse frequency and basal

concentrations are increased in acromegaly and are reduced by successful therapy. *J Clin Endocrinol Metab,* 70, 1375-84.

HEATH, K. E., ARGENTE, J., BARRIOS, V., POZO, J., DIAZ-GONZALEZ, F., MARTOS-MORENO, G. A., CAIMARI, M., GRACIA, R. & CAMPOS-BARROS, A. (2008) Primary acid-labile subunit deficiency due to recessive IGFALS mutations results in postnatal growth deficit associated with low circulating insulin growth factor (IGF)-I, IGF binding protein-3 levels, and hyperinsulinemia. *J Clin Endocrinol Metab,* 93, 1616-24.

HENNIGHAUSEN, L. & ROBINSON, G. W. (2008) Interpretation of cytokine signaling through the transcription factors STAT5A and STAT5B. *Genes Dev,* 22, 711-21.

HINTZ, R. L. (2005) Growth hormone treatment of idiopathic short stature: clinical studies. *Growth Horm IGF Res,* 15 Suppl A, S6-8.

HO, K. K. (2007) Consensus guidelines for the diagnosis and treatment of adults with GH deficiency II: a statement of the GH Research Society in association with the European Society for Pediatric Endocrinology, Lawson Wilkins Society, European Society of Endocrinology, Japan Endocrine Society, and Endocrine Society of Australia. *Eur J Endocrinol,* 157, 695-700.

HO, K. Y., EVANS, W. S., BLIZZARD, R. M., VELDHUIS, J. D., MERRIAM, G. R., SAMOJLIK, E., FURLANETTO, R., ROGOL, A. D., KAISER, D. L. & THORNER, M. O. (1987) Effects of sex and age on the 24-hour profile of growth hormone secretion in man: importance of endogenous estradiol concentrations. *J Clin Endocrinol Metab,* 64, 51-8.

HO, S. N., HUNT, H. D., HORTON, R. M., PULLEN, J. K. & PEASE, L. R. (1989) Site-directed mutagenesis by overlap extension using the polymerase chain reaction. *Gene,* 77, 51-9.

HOLMAN, S. R. & BAXTER, R. C. (1996) Insulin-like growth factor binding protein-3: factors affecting binary and ternary complex formation. *Growth Regul,* 6, 42-7.

HUA, Y., VICKERS, T. A., BAKER, B. F., BENNETT, C. F. & KRAINER, A. R. (2007) Enhancement of SMN2 exon 7 inclusion by antisense oligonucleotides targeting the exon. *PLoS Biol,* 5, e73.

HUBER, C., ROSILIO, M., MUNNICH, A. & CORMIER-DAIRE, V. (2006) High incidence of SHOX anomalies in individuals with short stature. *J Med Genet,* 43, 735-9.

HUGHES, P. C., RIBEIRO, J. & HUGHES, I. A. (1986) Body proportions in Turner's syndrome. *Arch Dis Child,* 61, 506-7.

HWA, V., HAEUSLER, G., PRATT, K. L., LITTLE, B. M., FRISCH, H., KOLLER, D. & ROSENFELD, R. G. (2006) Total absence of functional acid labile subunit, resulting in severe insulin-like growth factor deficiency and moderate growth failure. *J Clin Endocrinol Metab,* 91, 1826-31.

HWA, V., LITTLE, B., ADIYAMAN, P., KOFOED, E. M., PRATT, K. L., OCAL, G., BERBEROGLU, M. & ROSENFELD, R. G. (2005) Severe growth hormone insensitivity resulting from total absence of signal transducer and activator of transcription 5b. *J Clin Endocrinol Metab,* 90, 4260-6.

IIDA, K., TAKAHASHI, Y., KAJI, H., NOSE, O., OKIMURA, Y., ABE, H. & CHIHARA, K. (1998) Growth hormone (GH) insensitivity syndrome with high serum GH-binding protein levels caused by a heterozygous splice site mutation of the GH receptor gene producing a lack of intracellular domain. *J Clin Endocrinol Metab,* 83, 531-7.

IIDA, K., TAKAHASHI, Y., KAJI, H., TAKAHASHI, M. O., OKIMURA, Y., NOSE, O., ABE, H. & CHIHARA, K. (1999) Functional characterization of truncated

growth hormone (GH) receptor-(1-277) causing partial GH insensitivity syndrome with high GH-binding protein. *J Clin Endocrinol Metab,* 84, 1011-6.

IMADA, K., BLOOM, E. T., NAKAJIMA, H., HORVATH-ARCIDIACONO, J. A., UDY, G. B., DAVEY, H. W. & LEONARD, W. J. (1998) Stat5b is essential for natural killer cell-mediated proliferation and cytolytic activity. *J Exp Med,* 188, 2067-74.

IRANMANESH, A., GRISSO, B. & VELDHUIS, J. D. (1994) Low basal and persistent pulsatile growth hormone secretion are revealed in normal and hyposomatotropic men studied with a new ultrasensitive chemiluminescence assay. *J Clin Endocrinol Metab,* 78, 526-35.

ISAKSSON, O. G., JANSSON, J. O. & GAUSE, I. A. (1982) Growth hormone stimulates longitudinal bone growth directly. *Science,* 216, 1237-9.

ISAKSSON, O. G., LINDAHL, A., NILSSON, A. & ISGAARD, J. (1987) Mechanism of the stimulatory effect of growth hormone on longitudinal bone growth. *Endocr Rev,* 8, 426-38.

ISGAARD, J., MOLLER, C., ISAKSSON, O. G., NILSSON, A., MATHEWS, L. S. & NORSTEDT, G. (1988) Regulation of insulin-like growth factor messenger ribonucleic acid in rat growth plate by growth hormone. *Endocrinology,* 122, 1515-20.

JANOSI, J. B., FIRTH, S. M., BOND, J. J., BAXTER, R. C. & DELHANTY, P. J. (1999) N-Linked glycosylation and sialylation of the acid-labile subunit. Role in complex formation with insulin-like growth factor (IGF)-binding protein-3 and the IGFs. *J Biol Chem,* 274, 5292-8.

JOHANSSON, A. G., BURMAN, P., WESTERMARK, K. & LJUNGHALL, S. (1992) The bone mineral density in acquired growth hormone deficiency correlates with circulating levels of insulin-like growth factor I. *J Intern Med,* 232, 447-52.

JOHNSON, J. M., CASTLE, J., GARRETT-ENGELE, P., KAN, Z., LOERCH, P. M., ARMOUR, C. D., SANTOS, R., SCHADT, E. E., STOUGHTON, R. & SHOEMAKER, D. D. (2003) Genome-wide survey of human alternative pre-mRNA splicing with exon junction microarrays. *Science,* 302, 2141-4.

JORGE, A. A., MARCHISOTTI, F. G., MONTENEGRO, L. R., CARVALHO, L. R., MENDONCA, B. B. & ARNHOLD, I. J. (2006) Growth hormone (GH) pharmacogenetics: influence of GH receptor exon 3 retention or deletion on first-year growth response and final height in patients with severe GH deficiency. *J Clin Endocrinol Metab,* 91, 1076-80.

JURICA, M. S. & MOORE, M. J. (2002) Capturing splicing complexes to study structure and mechanism. *Methods,* 28, 336-45.

KAJI, H., NOSE, O., TAJIRI, H., TAKAHASHI, Y., IIDA, K., TAKAHASHI, T., OKIMURA, Y., ABE, H. & CHIHARA, K. (1997) Novel compound heterozygous mutations of growth hormone (GH) receptor gene in a patient with GH insensitivity syndrome. *J Clin Endocrinol Metab,* 82, 3705-9.

KALNINA, Z., ZAYAKIN, P., SILINA, K. & LINE, A. (2005) Alterations of pre-mRNA splicing in cancer. *Genes Chromosomes Cancer,* 42, 342-57.

KAN, Z., ROUCHKA, E. C., GISH, W. R. & STATES, D. J. (2001) Gene structure prediction and alternative splicing analysis using genomically aligned ESTs. *Genome Res,* 11, 889-900.

KHOO, B., ROCA, X., CHEW, S. L. & KRAINER, A. R. (2007) Antisense oligonucleotide-induced alternative splicing of the APOB mRNA generates a novel isoform of APOB. *BMC Mol Biol,* 8, 3.

KHOSRAVI, M. J., DIAMANDI, A., MISTRY, J., KRISHNA, R. G. & KHARE, A. (1997) Acid-labile subunit of human insulin-like growth factor-binding protein complex: measurement, molecular, and clinical evaluation. *J Clin Endocrinol Metab,* 82, 3944-51.

KIM, S. O., JIANG, J., YI, W., FENG, G. S. & FRANK, S. J. (1998) Involvement of the Src homology 2-containing tyrosine phosphatase SHP-2 in growth hormone signaling. *J Biol Chem,* 273, 2344-54.

KOFOED, E. M., HWA, V., LITTLE, B., WOODS, K. A., BUCKWAY, C. K., TSUBAKI, J., PRATT, K. L., BEZRODNIK, L., JASPER, H., TEPPER, A., HEINRICH, J. J. & ROSENFELD, R. G. (2003) Growth hormone insensitivity associated with a STAT5b mutation. *N Engl J Med,* 349, 1139-47.

KOLE, R. & SAZANI, P. (2001) Antisense effects in the cell nucleus: modification of splicing. *Curr Opin Mol Ther,* 3, 229-34.

KOSTYO, J. L., HOTCHKISS, J. & KNOBIL, E. (1959) Stimulation of amino acid transport in isolated diaphragm by growth hormone added in vitro. *Science,* 130, 1653-4.

KRATZSCH, J., SELISKO, T. & BIRKENMEIER, G. (1995) Identification of transformed alpha 2-macroglobulin as a growth hormone-binding protein in human blood. *J Clin Endocrinol Metab,* 80, 585-90.

KRAWCZAK, M., REISS, J. & COOPER, D. N. (1992) The mutational spectrum of single base-pair substitutions in mRNA splice junctions of human genes: causes and consequences. *Hum Genet,* 90, 41-54.

KRECIC, A. M. & SWANSON, M. S. (1999) hnRNP complexes: composition, structure, and function. *Curr Opin Cell Biol,* 11, 363-71.

LABARTA, J. I., GARGOSKY, S. E., SIMPSON, D. M., LEE, P. D., ARGENTE, J., GUEVARA-AGUIRRE, J. & ROSENFELD, R. G. (1997) Immunoblot studies of the acid-labile subunit (ALS) in biological fluids, normal human serum and in children with GH deficiency and GH receptor deficiency before and after long-term therapy with GH or IGF-I respectively. *Clin Endocrinol (Oxf),* 47, 657-66.

LANDER, E. S., LINTON, L. M., BIRREN, B., NUSBAUM, C., ZODY, M. C., BALDWIN, J., DEVON, K., DEWAR, K., DOYLE, M., FITZHUGH, W., FUNKE, R., GAGE, D., HARRIS, K., HEAFORD, A., HOWLAND, J., KANN, L., LEHOCZKY, J., LEVINE, R., MCEWAN, P., MCKERNAN, K., MELDRIM, J., MESIROV, J. P., MIRANDA, C., MORRIS, W., NAYLOR, J., RAYMOND, C., ROSETTI, M., SANTOS, R., SHERIDAN, A., SOUGNEZ, C., STANGE-THOMANN, N., STOJANOVIC, N., SUBRAMANIAN, A., WYMAN, D., ROGERS, J., SULSTON, J., AINSCOUGH, R., BECK, S., BENTLEY, D., BURTON, J., CLEE, C., CARTER, N., COULSON, A., DEADMAN, R., DELOUKAS, P., DUNHAM, A., DUNHAM, I., DURBIN, R., FRENCH, L., GRAFHAM, D., GREGORY, S., HUBBARD, T., HUMPHRAY, S., HUNT, A., JONES, M., LLOYD, C., MCMURRAY, A., MATTHEWS, L., MERCER, S., MILNE, S., MULLIKIN, J. C., MUNGALL, A., PLUMB, R., ROSS, M., SHOWNKEEN, R., SIMS, S., WATERSTON, R. H., WILSON, R. K., HILLIER, L. W., MCPHERSON, J. D., MARRA, M. A., MARDIS, E. R., FULTON, L. A., CHINWALLA, A. T., PEPIN, K. H., GISH, W. R., CHISSOE, S. L., WENDL, M. C., DELEHAUNTY, K. D., MINER, T. L., DELEHAUNTY, A., KRAMER, J. B., COOK, L. L., FULTON, R. S., JOHNSON, D. L., MINX, P. J., CLIFTON, S. W., HAWKINS, T., BRANSCOMB, E., PREDKI, P., RICHARDSON, P., WENNING, S., SLEZAK, T., DOGGETT, N., CHENG, J. F., OLSEN, A.,

LUCAS, S., ELKIN, C., UBERBACHER, E., FRAZIER, M., et al. (2001) Initial sequencing and analysis of the human genome. *Nature,* 409, 860-921.

LANDSMAN, T. & WAXMAN, D. J. (2005) Role of the cytokine-induced SH2 domain-containing protein CIS in growth hormone receptor internalization. *J Biol Chem,* 280, 37471-80.

LANNING, N. J. & CARTER-SU, C. (2006) Recent advances in growth hormone signaling. *Rev Endocr Metab Disord,* 7, 225-35.

LARON, Z. (1999) Natural history of the classical form of primary growth hormone (GH) resistance (Laron syndrome). *J Pediatr Endocrinol Metab,* 12 Suppl 1, 231-49.

LARON, Z. (2004) Laron syndrome (primary growth hormone resistance or insensitivity): the personal experience 1958-2003. *J Clin Endocrinol Metab,* 89, 1031-44.

LARON, Z., AVITZUR, Y. & KLINGER, B. (1995) Carbohydrate metabolism in primary growth hormone resistance (Laron syndrome) before and during insulin-like growth factor-I treatment. *Metabolism,* 44, 113-8.

LARON, Z., BLUM, W., CHATELAIN, P., RANKE, M., ROSENFELD, R., SAVAGE, M. & UNDERWOOD, L. (1993) Classification of growth hormone insensitivity syndrome. *J Pediatr,* 122, 241.

LARON, Z. & KLINGER, B. (1994) Laron syndrome: clinical features, molecular pathology and treatment. *Horm Res,* 42, 198-202.

LARON, Z., PERTZELAN, A. & MANNHEIMER, S. (1966) Genetic pituitary dwarfism with high serum concentation of growth hormone--a new inborn error of metabolism? *Isr J Med Sci,* 2, 152-5.

LARON, Z., SAREL, R. & PERTZELAN, A. (1980) Puberty in Laron type dwarfism. *Eur J Pediatr,* 134, 79-83.

LEMAHIEU, V., GASTIER, J. M. & FRANCKE, U. (1999) Novel mutations in the Wiskott-Aldrich syndrome protein gene and their effects on transcriptional, translational, and clinical phenotypes. *Hum Mutat,* 14, 54-66.

LEONG, S. R., BAXTER, R. C., CAMERATO, T., DAI, J. & WOOD, W. I. (1992) Structure and functional expression of the acid-labile subunit of the insulin-like growth factor-binding protein complex. *Mol Endocrinol,* 6, 870-6.

LESCHEK, E. W., ROSE, S. R., YANOVSKI, J. A., TROENDLE, J. F., QUIGLEY, C. A., CHIPMAN, J. J., CROWE, B. J., ROSS, J. L., CASSORLA, F. G., BLUM, W. F., CUTLER, G. B., JR. & BARON, J. (2004) Effect of growth hormone treatment on adult height in peripubertal children with idiopathic short stature: a randomized, double-blind, placebo-controlled trial. *J Clin Endocrinol Metab,* 89, 3140-8.

LETTRE, G., JACKSON, A. U., GIEGER, C., SCHUMACHER, F. R., BERNDT, S. I., SANNA, S., EYHERAMENDY, S., VOIGHT, B. F., BUTLER, J. L., GUIDUCCI, C., ILLIG, T., HACKETT, R., HEID, I. M., JACOBS, K. B., LYSSENKO, V., UDA, M., BOEHNKE, M., CHANOCK, S. J., GROOP, L. C., HU, F. B., ISOMAA, B., KRAFT, P., PELTONEN, L., SALOMAA, V., SCHLESSINGER, D., HUNTER, D. J., HAYES, R. B., ABECASIS, G. R., WICHMANN, H. E., MOHLKE, K. L. & HIRSCHHORN, J. N. (2008) Identification of ten loci associated with height highlights new biological pathways in human growth. *Nat Genet,* 40, 584-91.

LEUNG, D. W., SPENCER, S. A., CACHIANES, G., HAMMONDS, R. G., COLLINS, C., HENZEL, W. J., BARNARD, R., WATERS, M. J. & WOOD, W. I. (1987)

Growth hormone receptor and serum binding protein: purification, cloning and expression. *Nature,* 330, 537-43.

LI, M., KUIVENHOVEN, J. A., AYYOBI, A. F. & PRITCHARD, P. H. (1998) T-->G or T-->A mutation introduced in the branchpoint consensus sequence of intron 4 of lecithin:cholesterol acyltransferase (LCAT) gene: intron retention causing LCAT deficiency. *Biochim Biophys Acta,* 1391, 256-64.

LIN, C. H. & PATTON, J. G. (1995) Regulation of alternative 3' splice site selection by constitutive splicing factors. *Rna,* 1, 234-45.

LIN, J. X., MIETZ, J., MODI, W. S., JOHN, S. & LEONARD, W. J. (1996) Cloning of human Stat5B. Reconstitution of interleukin-2-induced Stat5A and Stat5B DNA binding activity in COS-7 cells. *J Biol Chem,* 271, 10738-44.

LIU, H. X., CARTEGNI, L., ZHANG, M. Q. & KRAINER, A. R. (2001) A mechanism for exon skipping caused by nonsense or missense mutations in BRCA1 and other genes. *Nat Genet,* 27, 55-8.

LIU, H. X., ZHANG, M. & KRAINER, A. R. (1998) Identification of functional exonic splicing enhancer motifs recognized by individual SR proteins. *Genes Dev,* 12, 1998-2012.

LIU, J., BOYD, C. K., KOBAYASHI, Y., CHASE, C. C., JR., HAMMOND, A. C., OLSON, T. A., ELSASSER, T. H. & LUCY, M. C. (1999) A novel phenotype for Lardon dwarfism in miniature Bos indicus cattle suggests that the expression of growth hormone receptor 1A in liver is required for normal growth. *Domest Anim Endocrinol,* 17, 421-37.

LOPEZ-BIGAS, N., AUDIT, B., OUZOUNIS, C., PARRA, G. & GUIGO, R. (2005) Are splicing mutations the most frequent cause of hereditary disease? *FEBS Lett,* 579, 1900-3.

LOU, H., HELFMAN, D. M., GAGEL, R. F. & BERGET, S. M. (1999) Polypyrimidine tract-binding protein positively regulates inclusion of an alternative 3'-terminal exon. *Mol Cell Biol,* 19, 78-85.

LU, Q. L., RABINOWITZ, A., CHEN, Y. C., YOKOTA, T., YIN, H., ALTER, J., JADOON, A., BOU-GHARIOS, G. & PARTRIDGE, T. (2005) Systemic delivery of antisense oligoribonucleotide restores dystrophin expression in body-wide skeletal muscles. *Proc Natl Acad Sci U S A,* 102, 198-203.

MAAMRA, M., MILWARD, A., ESFAHANI, H. Z., ABBOTT, L. P., METHERELL, L. A., SAVAGE, M. O., CLARK, A. J. & ROSS, R. J. (2006) A 36 residues insertion in the dimerization domain of the growth hormone receptor results in defective trafficking rather than impaired signaling. *J Endocrinol,* 188, 251-61.

MANNOR, D. A., WINER, L. M., SHAW, M. A. & BAUMANN, G. (1991) Plasma growth hormone (GH)-binding proteins: effect on GH binding to receptors and GH action. *J Clin Endocrinol Metab,* 73, 30-4.

MANOHARAN, M. (1999) 2'-carbohydrate modifications in antisense oligonucleotide therapy: importance of conformation, configuration and conjugation. *Biochim Biophys Acta,* 1489, 117-30.

MARSHALL, W. A. & TANNER, J. M. (1969) Variations in pattern of pubertal changes in girls. *Arch Dis Child,* 44, 291-303.

MARSHALL, W. A. & TANNER, J. M. (1970) Variations in the pattern of pubertal changes in boys. *Arch Dis Child,* 45, 13-23.

MARTINEZ-CONTRERAS, R., FISETTE, J. F., NASIM, F. U., MADDEN, R., CORDEAU, M. & CHABOT, B. (2006) Intronic binding sites for hnRNP A/B and hnRNP F/H proteins stimulate pre-mRNA splicing. *PLoS Biol,* 4, e21.

MAURAS, N., BLIZZARD, R. M., LINK, K., JOHNSON, M. L., ROGOL, A. D. & VELDHUIS, J. D. (1987) Augmentation of growth hormone secretion during puberty: evidence for a pulse amplitude-modulated phenomenon. *J Clin Endocrinol Metab,* 64, 596-601.

METHERELL, L. A., AKKER, S. A., MUNROE, P. B., ROSE, S. J., CAULFIELD, M., SAVAGE, M. O., CHEW, S. L. & CLARK, A. J. (2001) Pseudoexon activation as a novel mechanism for disease resulting in atypical growth-hormone insensitivity. *Am J Hum Genet,* 69, 641-6.

METHERELL, L. A., CHAPPLE, J. P., COORAY, S., DAVID, A., BECKER, C., RUSCHENDORF, F., NAVILLE, D., BEGEOT, M., KHOO, B., NURNBERG, P., HUEBNER, A., CHEETHAM, M. E. & CLARK, A. J. (2005) Mutations in MRAP, encoding a new interacting partner of the ACTH receptor, cause familial glucocorticoid deficiency type 2. *Nat Genet,* 37, 166-70.

MEYER, D. J., CAMPBELL, G. S., COCHRAN, B. H., ARGETSINGER, L. S., LARNER, A. C., FINBLOOM, D. S., CARTER-SU, C. & SCHWARTZ, J. (1994) Growth hormone induces a DNA binding factor related to the interferon-stimulated 91-kDa transcription factor. *J Biol Chem,* 269, 4701-4.

MILLAR, D. S., LEWIS, M. D., HORAN, M., NEWSWAY, V., EASTER, T. E., GREGORY, J. W., FRYKLUND, L., NORIN, M., CROWNE, E. C., DAVIES, S. J., EDWARDS, P., KIRK, J., WALDRON, K., SMITH, P. J., PHILLIPS, J. A., 3RD, SCANLON, M. F., KRAWCZAK, M., COOPER, D. N. & PROCTER, A. M. (2003) Novel mutations of the growth hormone 1 (GH1) gene disclosed by modulation of the clinical selection criteria for individuals with short stature. *Hum Mutat,* 21, 424-40.

MILWARD, A., METHERELL, L., MAAMRA, M., BARAHONA, M. J., WILKINSON, I. R., CAMACHO-HUBNER, C., SAVAGE, M. O., BIDLINGMAIER, C. M., CLARK, A. J., ROSS, R. J. & WEBB, S. M. (2004) Growth hormone (GH) insensitivity syndrome due to a GH receptor truncated after Box1, resulting in isolated failure of STAT 5 signal transduction. *J Clin Endocrinol Metab,* 89, 1259-66.

MITCHELL, T. J. & JOHN, S. (2005) Signal transducer and activator of transcription (STAT) signalling and T-cell lymphomas. *Immunology,* 114, 301-12.

MODREK, B., RESCH, A., GRASSO, C. & LEE, C. (2001) Genome-wide detection of alternative splicing in expressed sequences of human genes. *Nucleic Acids Res,* 29, 2850-9.

MOULTON, H. M., FLETCHER, S., NEUMAN, B. W., MCCLOREY, G., STEIN, D. A., ABES, S., WILTON, S. D., BUCHMEIER, M. J., LEBLEU, B. & IVERSEN, P. L. (2007) Cell-penetrating peptide-morpholino conjugates alter pre-mRNA splicing of DMD (Duchenne muscular dystrophy) and inhibit murine coronavirus replication in vivo. *Biochem Soc Trans,* 35, 826-8.

NILSEN, T. (1998) RNA-RNA interactions in nuclear pre-mRNA splicing. *RNA structure and function.* Cold Spring Harbor, New York Cold Spring Harbor Laboratory Press.

O'SHEA, J. J. (1997) Jaks, STATs, cytokine signal transduction, and immunoregulation: are we there yet? *Immunity,* 7, 1-11.

OHLSSON, C., BENGTSSON, B. A., ISAKSSON, O. G., ANDREASSEN, T. T. & SLOOTWEG, M. C. (1998) Growth hormone and bone. *Endocr Rev,* 19, 55-79.

OOI, G. T., COHEN, F. J., TSENG, L. Y., RECHLER, M. M. & BOISCLAIR, Y. R. (1997) Growth hormone stimulates transcription of the gene encoding the acid-

labile subunit (ALS) of the circulating insulin-like growth factor-binding protein complex and ALS promoter activity in rat liver. *Mol Endocrinol,* 11, 997-1007.

OOI, G. T., HURST, K. R., POY, M. N., RECHLER, M. M. & BOISCLAIR, Y. R. (1998) Binding of STAT5a and STAT5b to a single element resembling a gamma-interferon-activated sequence mediates the growth hormone induction of the mouse acid-labile subunit promoter in liver cells. *Mol Endocrinol,* 12, 675-87.

PAGANI, F. & BARALLE, F. E. (2004) Genomic variants in exons and introns: identifying the splicing spoilers. *Nat Rev Genet,* 5, 389-96.

PAGANI, F., BURATTI, E., STUANI, C., BENDIX, R., DORK, T. & BARALLE, F. E. (2002) A new type of mutation causes a splicing defect in ATM. *Nat Genet,* 30, 426-9.

PAN, Q., SALTZMAN, A. L., KIM, Y. K., MISQUITTA, C., SHAI, O., MAQUAT, L. E., FREY, B. J. & BLENCOWE, B. J. (2006) Quantitative microarray profiling provides evidence against widespread coupling of alternative splicing with nonsense-mediated mRNA decay to control gene expression. *Genes Dev,* 20, 153-8.

PANTEL, J., MACHINIS, K., SOBRIER, M. L., DUQUESNOY, P., GOOSSENS, M. & AMSELEM, S. (2000) Species-specific alternative splice mimicry at the growth hormone receptor locus revealed by the lineage of retroelements during primate evolution. *J Biol Chem,* 275, 18664-9.

PEKHLETSKY, R. I., CHERNOV, B. K. & RUBTSOV, P. M. (1992) Variants of the 5'-untranslated sequence of human growth hormone receptor mRNA. *Mol Cell Endocrinol,* 90, 103-9.

PEQUIGNOT, M. O., DEY, R., ZEVIANI, M., TIRANTI, V., GODINOT, C., POYAU, A., SUE, C., DI MAURO, S., ABITBOL, M. & MARSAC, C. (2001) Mutations in the SURF1 gene associated with Leigh syndrome and cytochrome C oxidase deficiency. *Hum Mutat,* 17, 374-81.

PILOTTA, A., MELLA, P., FILISETTI, M., FELAPPI, B., PRANDI, E., PARRINELLO, G., NOTARANGELO, L. D. & BUZI, F. (2006) Common polymorphisms of the growth hormone (GH) receptor do not correlate with the growth response to exogenous recombinant human GH in GH-deficient children. *J Clin Endocrinol Metab,* 91, 1178-80.

POWELL, G. F., BRASEL, J. A. & BLIZZARD, R. M. (1967) Emotional deprivation and growth retardation simulating idiopathic hypopituitarism. I. Clinical evaluation of the syndrome. *N Engl J Med,* 276, 1271-8.

PREECE, M. A., LAW, C. M. & DAVIES, P. S. (1986) The growth of children with chronic paediatric disease. *Clin Endocrinol Metab,* 15, 453-77.

RAM, P. A. & WAXMAN, D. J. (1999) SOCS/CIS protein inhibition of growth hormone-stimulated STAT5 signaling by multiple mechanisms. *J Biol Chem,* 274, 35553-61.

RANKE, M. B. (1996) Towards a consensus on the definition of idiopathic short stature. *Horm Res,* 45 Suppl 2, 64-6.

RAPPOLD, G., BLUM, W. F., SHAVRIKOVA, E. P., CROWE, B. J., ROETH, R., QUIGLEY, C. A., ROSS, J. L. & NIESLER, B. (2007) Genotypes and phenotypes in children with short stature: clinical indicators of SHOX haploinsufficiency. *J Med Genet,* 44, 306-13.

RAPPOLD, G. A., FUKAMI, M., NIESLER, B., SCHILLER, S., ZUMKELLER, W., BETTENDORF, M., HEINRICH, U., VLACHOPAPADOUPOULOU, E., REINEHR, T., ONIGATA, K. & OGATA, T. (2002) Deletions of the homeobox

gene SHOX (short stature homeobox) are an important cause of growth failure in children with short stature. *J Clin Endocrinol Metab,* 87, 1402-6.

RHOADS, R. P., GREENWOOD, P. L., BELL, A. W. & BOISCLAIR, Y. R. (2000) Organization and regulation of the gene encoding the sheep acid-labile subunit of the 150-kilodalton insulin-like growth factor-binding protein complex. *Endocrinology,* 141, 1425-33.

RICHMAN, C., BAYLINK, D. J., LANG, K., DONY, C. & MOHAN, S. (1999) Recombinant human insulin-like growth factor-binding protein-5 stimulates bone formation parameters in vitro and in vivo. *Endocrinology,* 140, 4699-705.

ROSEN, T., HANSSON, T., GRANHED, H., SZUCS, J. & BENGTSSON, B. A. (1993) Reduced bone mineral content in adult patients with growth hormone deficiency. *Acta Endocrinol (Copenh),* 129, 201-6.

ROSEN, T., JOHANNSSON, G., JOHANSSON, J. O. & BENGTSSON, B. A. (1995) Consequences of growth hormone deficiency in adults and the benefits and risks of recombinant human growth hormone treatment. A review paper. *Horm Res,* 43, 93-9.

ROSENBLOOM, A. L. & GUEVARA-AGUIRRE, J. (1998) Lessons from the genetics of laron syndrome. *Trends Endocrinol Metab,* 9, 276-83.

ROSENBLOOM, A. L., GUEVARA-AGUIRRE, J., ROSENFELD, R. G. & FIELDER, P. J. (1994a) Is there heterozygote expression of growth hormone receptor deficiency? *Acta Paediatr Suppl,* 399, 125-7.

ROSENBLOOM, A. L., GUEVARA-AGUIRRE, J., ROSENFELD, R. G. & FRANCKE, U. (1999) Growth hormone receptor deficiency in Ecuador. *J Clin Endocrinol Metab,* 84, 4436-43.

ROSENBLOOM, A. L., GUEVARA-AGUIRRE, J., ROSENFELD, R. G. & POLLOCK, B. H. (1994b) Growth in growth hormone insensitivity. *Trends Endocrinol Metab,* 5, 296-303.

ROSENBLOOM, A. L., GUEVARA AGUIRRE, J., ROSENFELD, R. G. & FIELDER, P. J. (1990) The little women of Loja--growth hormone-receptor deficiency in an inbred population of southern Ecuador. *N Engl J Med,* 323, 1367-74.

ROSENFELD, R. G., KOFOED, E., LITTLE, B., WOODS, K., BUCKWAY, C., PRATT, K. & HWA, V. (2004) Growth hormone insensitivity resulting from post-GH receptor defects. *Growth Horm IGF Res,* 14 Suppl A, S35-8.

ROSENFELD, R. G., ROSENBLOOM, A. L. & GUEVARA-AGUIRRE, J. (1994) Growth hormone (GH) insensitivity due to primary GH receptor deficiency. *Endocr Rev,* 15, 369-90.

ROSS, J. A., NAGY, Z. S., CHENG, H., STEPKOWSKI, S. M. & KIRKEN, R. A. (2007) Regulation of T cell homeostasis by JAKs and STATs. *Arch Immunol Ther Exp (Warsz),* 55, 231-45.

ROSS, R. J., ESPOSITO, N., SHEN, X. Y., VON LAUE, S., CHEW, S. L., DOBSON, P. R., POSTEL-VINAY, M. C. & FINIDORI, J. (1997) A short isoform of the human growth hormone receptor functions as a dominant negative inhibitor of the full-length receptor and generates large amounts of binding protein. *Mol Endocrinol,* 11, 265-73.

SAMBROOK, J., FRITSCH, E. & MANIATIS, T. (1989) *Molecular cloning: a laboratory manual.* , Cold Spring Harbor.

SANFORD, J. R. & BRUZIK, J. P. (1999) Developmental regulation of SR protein phosphorylation and activity. *Genes Dev,* 13, 1513-8.

SAVAGE, M. O., ATTIE, K. M., DAVID, A., METHERELL, L. A., CLARK, A. J. & CAMACHO-HUBNER, C. (2006) Endocrine assessment, molecular

characterization and treatment of growth hormone insensitivity disorders. *Nat Clin Pract Endocrinol Metab,* 2, 395-407.

SAVAGE, M. O., BLUM, W. F., RANKE, M. B., POSTEL-VINAY, M. C., COTTERILL, A. M., HALL, K., CHATELAIN, P. G., PREECE, M. A. & ROSENFELD, R. G. (1993) Clinical features and endocrine status in patients with growth hormone insensitivity (Laron syndrome). *J Clin Endocrinol Metab,* 77, 1465-71.

SCHAEFER, G. B., ROSENBLOOM, A. L., GUEVARA-AGUIRRE, J., CAMPBELL, E. A., ULLRICH, F., PATIL, K. & FRIAS, J. L. (1994) Facial morphometry of Ecuadorian patients with growth hormone receptor deficiency/Laron syndrome. *J Med Genet,* 31, 635-9.

SCHALCH, D. S. (1967) The influence of physical stress and exercise on growth hormone and insulin secretion in man. *J Lab Clin Med,* 69, 256-69.

SCHARF, A. & LARON, Z. (1972) Skull changes in pituitary dwarfism and the syndrome of familial dwarfism with high plasma immunoreactive growth hormone--a Roentgenologic study. *Horm Metab Res,* 4, 93-7.

SCHILLER, S., SPRANGER, S., SCHECHINGER, B., FUKAMI, M., MERKER, S., DROP, S. L., TROGER, J., KNOBLAUCH, H., KUNZE, J., SEIDEL, J. & RAPPOLD, G. A. (2000) Phenotypic variation and genetic heterogeneity in Leri-Weill syndrome. *Eur J Hum Genet,* 8, 54-62.

SCHINDLER, C. & DARNELL, J. E., JR. (1995) Transcriptional responses to polypeptide ligands: the JAK-STAT pathway. *Annu Rev Biochem,* 64, 621-51.

SHAPIRO, M. B. & SENAPATHY, P. (1987) RNA splice junctions of different classes of eukaryotes: sequence statistics and functional implications in gene expression. *Nucleic Acids Res,* 15, 7155-74.

SHIMON, I. & MELMED, S. (1997) Structure and function of somatostatin receptors in growth hormone control. *J Endocrinol,* 155 Suppl 1, S3-6; discussion S7-8.

SHIN, C., FENG, Y. & MANLEY, J. L. (2004) Dephosphorylated SRp38 acts as a splicing repressor in response to heat shock. *Nature,* 427, 553-8.

SIERAKOWSKA, H., SAMBADE, M. J., AGRAWAL, S. & KOLE, R. (1996) Repair of thalassemic human beta-globin mRNA in mammalian cells by antisense oligonucleotides. *Proc Natl Acad Sci U S A,* 93, 12840-4.

SILHA, J. V., MISHRA, S., ROSEN, C. J., BEAMER, W. G., TURNER, R. T., POWELL, D. R. & MURPHY, L. J. (2003) Perturbations in bone formation and resorption in insulin-like growth factor binding protein-3 transgenic mice. *J Bone Miner Res,* 18, 1834-41.

SINGH, R., VALCARCEL, J. & GREEN, M. R. (1995) Distinct binding specificities and functions of higher eukaryotic polypyrimidine tract-binding proteins. *Science,* 268, 1173-6.

SIRONI, M., MENOZZI, G., RIVA, L., CAGLIANI, R., COMI, G. P., BRESOLIN, N., GIORDA, R. & POZZOLI, U. (2004) Silencer elements as possible inhibitors of pseudoexon splicing. *Nucleic Acids Res,* 32, 1783-91.

SKORDIS, L. A., DUNCKLEY, M. G., YUE, B., EPERON, I. C. & MUNTONI, F. (2003) Bifunctional antisense oligonucleotides provide a trans-acting splicing enhancer that stimulates SMN2 gene expression in patient fibroblasts. *Proc Natl Acad Sci U S A,* 100, 4114-9.

SMITH, C. W. & VALCARCEL, J. (2000) Alternative pre-mRNA splicing: the logic of combinatorial control. *Trends Biochem Sci,* 25, 381-8.

SMITH, P. J., ZHANG, C., WANG, J., CHEW, S. L., ZHANG, M. Q. & KRAINER, A. R. (2006) An increased specificity score matrix for the prediction of SF2/ASF-specific exonic splicing enhancers. *Hum Mol Genet,* 15, 2490-508.

SOBRIER, M. L., DASTOT, F., DUQUESNOY, P., KANDEMIR, N., YORDAM, N., GOOSSENS, M. & AMSELEM, S. (1997) Nine novel growth hormone receptor gene mutations in patients with Laron syndrome. *J Clin Endocrinol Metab,* 82, 435-7.

SOLOVYEV, V. V., SALAMOV, A. A. & LAWRENCE, C. B. (1994a) Predicting internal exons by oligonucleotide composition and discriminant analysis of spliceable open reading frames. *Nucleic Acids Res,* 22, 5156-63.

SOLOVYEV, V. V., SALAMOV, A. A. & LAWRENCE, C. B. (1994b) The prediction of human exons by oligonucleotide composition and discriminant analysis of spliceable open reading frames. *Proc Int Conf Intell Syst Mol Biol,* 2, 354-62.

SPELLMAN, R. & SMITH, C. W. (2006) Novel modes of splicing repression by PTB. *Trends Biochem Sci,* 31, 73-6.

SPRANGER, J. (1992) International classification of osteochondrodysplasias. The International Working Group on Constitutional Diseases of Bone. *Eur J Pediatr,* 151, 407-15.

STAMM, S., ZHANG, M. Q., MARR, T. G. & HELFMAN, D. M. (1994) A sequence compilation and comparison of exons that are alternatively spliced in neurons. *Nucleic Acids Res,* 22, 1515-26.

STAMM, S., ZHU, J., NAKAI, K., STOILOV, P., STOSS, O. & ZHANG, M. Q. (2000) An alternative-exon database and its statistical analysis. *DNA Cell Biol,* 19, 739-56.

STEIN, D., FOSTER, E., HUANG, S. B., WELLER, D. & SUMMERTON, J. (1997) A specificity comparison of four antisense types: morpholino, 2'-O-methyl RNA, DNA, and phosphorothioate DNA. *Antisense Nucleic Acid Drug Dev,* 7, 151-7.

STETEFELD, J. & RUEGG, M. A. (2005) Structural and functional diversity generated by alternative mRNA splicing. *Trends Biochem Sci,* 30, 515-21.

SUN, H. & CHASIN, L. A. (2000) Multiple splicing defects in an intronic false exon. *Mol Cell Biol,* 20, 6414-25.

SUWANICHKUL, A., BOISCLAIR, Y. R., OLNEY, R. C., DURHAM, S. K. & POWELL, D. R. (2000) Conservation of a growth hormone-responsive promoter element in the human and mouse acid-labile subunit genes. *Endocrinology,* 141, 833-8.

TAKAHASHI, Y. & CHIHARA, K. (1998) Clinical significance and molecular mechanisms of bioinactive growth hormone (review). *Int J Mol Med,* 2, 287-91.

TAKESHIMA, Y., YAGI, M., WADA, H., ISHIBASHI, K., NISHIYAMA, A., KAKUMOTO, M., SAKAEDA, T., SAURA, R., OKUMURA, K. & MATSUO, M. (2006) Intravenous infusion of an antisense oligonucleotide results in exon skipping in muscle dystrophin mRNA of Duchenne muscular dystrophy. *Pediatr Res,* 59, 690-4.

TANNENBAUM, G. S. & LING, N. (1984) The interrelationship of growth hormone (GH)-releasing factor and somatostatin in generation of the ultradian rhythm of GH secretion. *Endocrinology,* 115, 1952-7.

TANNER, J., WHITEHOUSE, R., CAMERON, N., MARSHALL, W., HEALY, M. & H, G. (1983) *Assessment of Skeletal Maturity and Prediction of Adult Height (Tw2 Method)* London, Academic Press.

TEGLUND, S., MCKAY, C., SCHUETZ, E., VAN DEURSEN, J. M., STRAVOPODIS, D., WANG, D., BROWN, M., BODNER, S., GROSVELD, G. & IHLE, J. N.

(1998) Stat5a and Stat5b proteins have essential and nonessential, or redundant, roles in cytokine responses. *Cell,* 93, 841-50.

THANARAJ, T. A. & CLARK, F. (2001) Human GC-AG alternative intron isoforms with weak donor sites show enhanced consensus at acceptor exon positions. *Nucleic Acids Res,* 29, 2581-93.

TREISMAN, R., ORKIN, S. H. & MANIATIS, T. (1983) Specific transcription and RNA splicing defects in five cloned beta-thalassaemia genes. *Nature,* 302, 591-6.

TWIGG, S. M., KIEFER, M. C., ZAPF, J. & BAXTER, R. C. (1998) Insulin-like growth factor-binding protein 5 complexes with the acid-labile subunit. Role of the carboxyl-terminal domain. *J Biol Chem,* 273, 28791-8.

UDY, G. B., TOWERS, R. P., SNELL, R. G., WILKINS, R. J., PARK, S. H., RAM, P. A., WAXMAN, D. J. & DAVEY, H. W. (1997) Requirement of STAT5b for sexual dimorphism of body growth rates and liver gene expression. *Proc Natl Acad Sci U S A,* 94, 7239-44.

UEKI, I., OOI, G. T., TREMBLAY, M. L., HURST, K. R., BACH, L. A. & BOISCLAIR, Y. R. (2000) Inactivation of the acid labile subunit gene in mice results in mild retardation of postnatal growth despite profound disruptions in the circulating insulin-like growth factor system. *Proc Natl Acad Sci U S A,* 97, 6868-73.

UMPLEBY, A. M. & RUSSELL-JONES, D. L. (1996) The hormonal control of protein metabolism. *Baillieres Clin Endocrinol Metab,* 10, 551-70.

VACEK, M., SAZANI, P. & KOLE, R. (2003) Antisense-mediated redirection of mRNA splicing. *Cell Mol Life Sci,* 60, 825-33.

VALCARCEL, J. & GREEN, M. R. (1996) The SR protein family: pleiotropic functions in pre-mRNA splicing. *Trends Biochem Sci,* 21, 296-301.

VAN CAUTER, E., LATTA, F., NEDELTCHEVA, A., SPIEGEL, K., LEPROULT, R., VANDENBRIL, C., WEISS, R., MOCKEL, J., LEGROS, J. J. & COPINSCHI, G. (2004) Reciprocal interactions between the GH axis and sleep. *Growth Horm IGF Res,* 14 Suppl A, S10-7.

VAN CAUTER, E., PLAT, L. & COPINSCHI, G. (1998) Interrelations between sleep and the somatotropic axis. *Sleep,* 21, 553-66.

VAN DER EERDEN, B. C., KARPERIEN, M. & WIT, J. M. (2003) Systemic and local regulation of the growth plate. *Endocr Rev,* 24, 782-801.

VAN DEUTEKOM, J. C., JANSON, A. A., GINJAAR, I. B., FRANKHUIZEN, W. S., AARTSMA-RUS, A., BREMMER-BOUT, M., DEN DUNNEN, J. T., KOOP, K., VAN DER KOOI, A. J., GOEMANS, N. M., DE KIMPE, S. J., EKHART, P. F., VENNEKER, E. H., PLATENBURG, G. J., VERSCHUUREN, J. J. & VAN OMMEN, G. J. (2007) Local dystrophin restoration with antisense oligonucleotide PRO051. *N Engl J Med,* 357, 2677-86.

VAN DEUTEKOM, J. C. & VAN OMMEN, G. J. (2003) Advances in Duchenne muscular dystrophy gene therapy. *Nat Rev Genet,* 4, 774-83.

VAN DUYVENVOORDE, H. A., KEMPERS, M. J., TWICKLER, T. B., VAN DOORN, J., GERVER, W. J., NOORDAM, C., LOSEKOOT, M., KARPERIEN, M., WIT, J. M. & HERMUS, A. R. (2008) Homozygous and heterozygous expression of a novel mutation of the acid-labile subunit. *Eur J Endocrinol,* 159, 113-20.

VAN KERKHOF, P., GOVERS, R., ALVES DOS SANTOS, C. M. & STROUS, G. J. (2000) Endocytosis and degradation of the growth hormone receptor are proteasome-dependent. *J Biol Chem,* 275, 1575-80.

VELDHUIS, J. D., IRANMANESH, A., HO, K. K., WATERS, M. J., JOHNSON, M. L. & LIZARRALDE, G. (1991) Dual defects in pulsatile growth hormone secretion and clearance subserve the hyposomatotropism of obesity in man. *J Clin Endocrinol Metab,* 72, 51-9.

VENABLES, J. P. (2006) Unbalanced alternative splicing and its significance in cancer. *Bioessays,* 28, 378-86.

VIDARSDOTTIR, S., WALENKAMP, M. J., PEREIRA, A. M., KARPERIEN, M., VAN DOORN, J., VAN DUYVENVOORDE, H. A., WHITE, S., BREUNING, M. H., ROELFSEMA, F., KRUITHOF, M. F., VAN DISSEL, J., JANSSEN, R., WIT, J. M. & ROMIJN, J. A. (2006) Clinical and biochemical characteristics of a male patient with a novel homozygous STAT5b mutation. *J Clin Endocrinol Metab,* 91, 3482-5.

WALENKAMP, M. J., VIDARSDOTTIR, S., PEREIRA, A. M., KARPERIEN, M., VAN DOORN, J., VAN DUYVENVOORDE, H. A., BREUNING, M. H., ROELFSEMA, F., KRUITHOF, M. F., VAN DISSEL, J., JANSSEN, R., WIT, J. M. & ROMIJN, J. A. (2007) Growth hormone secretion and immunological function of a male patient with a homozygous STAT5b mutation. *Eur J Endocrinol,* 156, 155-65.

WALENKAMP, M. J. & WIT, J. M. (2006) Genetic disorders in the growth hormone - insulin-like growth factor-I axis. *Horm Res,* 66, 221-30.

WANG, Z. & BURGE, C. B. (2008) Splicing regulation: from a parts list of regulatory elements to an integrated splicing code. *Rna,* 14, 802-13.

WATAKABE, A., TANAKA, K. & SHIMURA, Y. (1993) The role of exon sequences in splice site selection. *Genes Dev,* 7, 407-18.

WEEDON, M. N., LANGO, H., LINDGREN, C. M., WALLACE, C., EVANS, D. M., MANGINO, M., FREATHY, R. M., PERRY, J. R., STEVENS, S., HALL, A. S., SAMANI, N. J., SHIELDS, B., PROKOPENKO, I., FARRALL, M., DOMINICZAK, A., JOHNSON, T., BERGMANN, S., BECKMANN, J. S., VOLLENWEIDER, P., WATERWORTH, D. M., MOOSER, V., PALMER, C. N., MORRIS, A. D., OUWEHAND, W. H., ZHAO, J. H., LI, S., LOOS, R. J., BARROSO, I., DELOUKAS, P., SANDHU, M. S., WHEELER, E., SORANZO, N., INOUYE, M., WAREHAM, N. J., CAULFIELD, M., MUNROE, P. B., HATTERSLEY, A. T., MCCARTHY, M. I. & FRAYLING, T. M. (2008) Genome-wide association analysis identifies 20 loci that influence adult height. *Nat Genet,* 40, 575-83.

WEEDON, M. N., LETTRE, G., FREATHY, R. M., LINDGREN, C. M., VOIGHT, B. F., PERRY, J. R., ELLIOTT, K. S., HACKETT, R., GUIDUCCI, C., SHIELDS, B., ZEGGINI, E., LANGO, H., LYSSENKO, V., TIMPSON, N. J., BURTT, N. P., RAYNER, N. W., SAXENA, R., ARDLIE, K., TOBIAS, J. H., NESS, A. R., RING, S. M., PALMER, C. N., MORRIS, A. D., PELTONEN, L., SALOMAA, V., DAVEY SMITH, G., GROOP, L. C., HATTERSLEY, A. T., MCCARTHY, M. I., HIRSCHHORN, J. N. & FRAYLING, T. M. (2007) A common variant of HMGA2 is associated with adult and childhood height in the general population. *Nat Genet,* 39, 1245-50.

WELTE, T., LEITENBERG, D., DITTEL, B. N., AL-RAMADI, B. K., XIE, B., CHIN, Y. E., JANEWAY, C. A., JR., BOTHWELL, A. L., BOTTOMLY, K. & FU, X. Y. (1999) STAT5 interaction with the T cell receptor complex and stimulation of T cell proliferation. *Science,* 283, 222-5.

WIERINGA, B., MEYER, F., REISER, J. & WEISSMANN, C. (1983) Unusual splice sites revealed by mutagenic inactivation of an authentic splice site of the rabbit beta-globin gene. *Nature,* 301, 38-43.

WILKINSON, I. R., FERRANDIS, E., ARTYMIUK, P. J., TEILLOT, M., SOULARD, C., TOUVAY, C., PRADHANANGA, S. L., JUSTICE, S., WU, Z., LEUNG, K. C., STRASBURGER, C. J., SAYERS, J. R. & ROSS, R. J. (2007) A ligand-receptor fusion of growth hormone forms a dimer and is a potent long-acting agonist. *Nat Med,* 13, 1108-13.

WIT, J. M., CLAYTON, P. E., ROGOL, A. D., SAVAGE, M. O., SAENGER, P. H. & COHEN, P. (2008a) Idiopathic short stature: definition, epidemiology, and diagnostic evaluation. *Growth Horm IGF Res,* 18, 89-110.

WIT, J. M., REITER, E. O., ROSS, J. L., SAENGER, P. H., SAVAGE, M. O., ROGOL, A. D. & COHEN, P. (2008b) Idiopathic short stature: management and growth hormone treatment. *Growth Horm IGF Res,* 18, 111-35.

WIT, J. M. & REKERS-MOMBARG, L. T. (2002) Final height gain by GH therapy in children with idiopathic short stature is dose dependent. *J Clin Endocrinol Metab,* 87, 604-11.

WOELFLE, J., CHIA, D. J. & ROTWEIN, P. (2003) Mechanisms of growth hormone (GH) action. Identification of conserved Stat5 binding sites that mediate GH-induced insulin-like growth factor-I gene activation. *J Biol Chem,* 278, 51261-6.

WOLLMANN, H. A., KIRCHNER, T., ENDERS, H., PREECE, M. A. & RANKE, M. B. (1995) Growth and symptoms in Silver-Russell syndrome: review on the basis of 386 patients. *Eur J Pediatr,* 154, 958-68.

WOODS, K. A., DASTOT, F., PREECE, M. A., CLARK, A. J., POSTEL-VINAY, M. C., CHATELAIN, P. G., RANKE, M. B., ROSENFELD, R. G., AMSELEM, S. & SAVAGE, M. O. (1997) Phenotype: genotype relationships in growth hormone insensitivity syndrome. *J Clin Endocrinol Metab,* 82, 3529-35.

WOODS, K. A., FRASER, N. C., POSTEL-VINAY, M. C., SAVAGE, M. O. & CLARK, A. J. (1996) A homozygous splice site mutation affecting the intracellular domain of the growth hormone (GH) receptor resulting in Laron syndrome with elevated GH-binding protein. *J Clin Endocrinol Metab,* 81, 1686-90.

WOODS, K. A. & SAVAGE, M. O. (1996) Laron syndrome: typical and atypical forms. *Baillieres Clin Endocrinol Metab,* 10, 371-87.

WU, J. Y. & MANIATIS, T. (1993) Specific interactions between proteins implicated in splice site selection and regulated alternative splicing. *Cell,* 75, 1061-70.

WU, S., ROMFO, C. M., NILSEN, T. W. & GREEN, M. R. (1999) Functional recognition of the 3' splice site AG by the splicing factor U2AF35. *Nature,* 402, 832-5.

XIAO, S. H. & MANLEY, J. L. (1997) Phosphorylation of the ASF/SF2 RS domain affects both protein-protein and protein-RNA interactions and is necessary for splicing. *Genes Dev,* 11, 334-44.

XIAO, S. H. & MANLEY, J. L. (1998) Phosphorylation-dephosphorylation differentially affects activities of splicing factor ASF/SF2. *Embo J,* 17, 6359-67.

ZACHMANN, M., PRADER, A., KIND, H. P., HAFLIGER, H. & BUDLIGER, H. (1974) Testicular volume during adolescence. Cross-sectional and longitudinal studies. *Helv Paediatr Acta,* 29, 61-72.

ZAHLER, A. M., NEUGEBAUER, K. M., LANE, W. S. & ROTH, M. B. (1993) Distinct functions of SR proteins in alternative pre-mRNA splicing. *Science,* 260, 219-22.

ZHANG, L., VINCENT, G. M., BARALLE, M., BARALLE, F. E., ANSON, B. D., BENSON, D. W., WHITING, B., TIMOTHY, K. W., CARLQUIST, J., JANUARY, C. T., KEATING, M. T. & SPLAWSKI, I. (2004) An intronic mutation causes long QT syndrome. *J Am Coll Cardiol,* 44, 1283-91.

ZHANG, X. H. & CHASIN, L. A. (2004) Computational definition of sequence motifs governing constitutive exon splicing. *Genes Dev,* 18, 1241-50.

ZHANG, X. H., LESLIE, C. S. & CHASIN, L. A. (2005) Dichotomous splicing signals in exon flanks. *Genome Res,* 15, 768-79.

ZHANG, Y., JIANG, J., BLACK, R. A., BAUMANN, G. & FRANK, S. J. (2000) Tumor necrosis factor-alpha converting enzyme (TACE) is a growth hormone binding protein (GHBP) sheddase: the metalloprotease TACE/ADAM-17 is critical for (PMA-induced) GH receptor proteolysis and GHBP generation. *Endocrinology,* 141, 4342-8.

ZHANG, Z. & KRAINER, A. R. (2004) Involvement of SR proteins in mRNA surveillance. *Mol Cell,* 16, 597-607.

ZHU, Q., WATANABE, C., LIU, T., HOLLENBAUGH, D., BLAESE, R. M., KANNER, S. B., ARUFFO, A. & OCHS, H. D. (1997) Wiskott-Aldrich syndrome/X-linked thrombocytopenia: WASP gene mutations, protein expression, and phenotype. *Blood,* 90, 2680-9.

ZOGOPOULOS, G., ALBRECHT, S., PIETSCH, T., ALPERT, L., VON SCHWEINITZ, D., LEFEBVRE, Y. & GOODYER, C. G. (1996) Fetal- and tumor-specific regulation of growth hormone receptor messenger RNA expression in human liver. *Cancer Res,* 56, 2949-53.

CHAPTER 10

APPENDICES

10.1 APPENDIX 1: LABORATORY EQUIPMENT

Equipment	Manufacturer
Pipettes	
Pipettes P2, P20, P100, P200, P1000	Gilson, Inc, USA
Balances	
Can 28 automatic electrovalence	WT Avery Ltd, Midlands, UK
Mettler PM 300	Gallenkamp, London, UK
Centrifuges	
Sorvall OTD-55B Ultracentrifuge	Du Pont (UK) Ltd. Stevenage, Herts, UK
Sorvall RT 6000B	Du Pont (UK) Ltd. Stevenage, Herts, UK
Beckman J-6B	Beckman Instruments, CA, USA
Falcon 6/300	Sanyo Gallenkamp PLC, Leicester, UK
Microcentaur microcentrifuge	MSC, UK
Water tank	
Grant JB1 and SE 10	Chemlab Instruments, Hornchurch, Essex, UK
Electrophoresis Tanks	
Electrophoresis Tank	BRL, Pisley, UK
Power supply units	
LKB Bromma 2197	LKB Instruments Ltd, Croyden, Sussex, UK
Gibco BRL 400L	Life Technologies Ltd, Paisley, UK
Spectrophotometer	
ND-1000 UV/Vis	NanoDrop Technologies, USA
pH meter	
EDT GP 353	Pentacourt Ltd, Haltead, Essex, UK
Thermocyclers	
GeneAmp PCR system 9700	PE Applied Biosystem, Cheshire, UK
GeneAmp PCR system 2400	PE Applied Biosystem, Cheshire, UK
Hybaid Omnigene thermal cycler	Hybaid Life Science Int., UK
Ultraviolet transilluminator	
UVP 20	Genetic Research Instruments, Herts, UK
DNA sequencer	
ABI Prism 377 DNA sequencer	Perkin Elmer Corporation, Foster City, Ca, USA

Iodine counter	
NE 1600	Nuclear enterprises, UK
Fraction collector	
2070 Ultrorac	LKB Bromma, USA
Pump tubes	
PVC flowmeasured Orange/green	Pulse Instrumentation LTD, USA
Phosphor Screen	
Phosphor Screen	Amersham Biosciences, GE Healthcare, USA
Gel dryer	
Gel dryer Model 583	Biorad, Hemel Hempstead, Hertfordshire, UK
Liquid nitrogen storage	
Cryostat	Jencons, Bedfordshire, UK
Cryolab	Statebourne Cryogenics, Tyne and Wear, UK
Laminar flow cabinet	
Envair MSC 11	Envair Ltd, Rossendale, Lanc, UK
Temperature controlled incubators	
LEEC MK 11	Luckams, Sussex, UK
Orbital incubator Innova 4300	New Brunswick Scientific, UK
CO2 incubators	
LEEC CO2 incubators	LEEC Ltd, Nottingham, UK
Water purification system	
MilliQ	Waters Millipore, Harrow, UK
Camera	
Kodak ID and ID image analysis software	Kodak Ltd, Hemel Hempstead, Herts, UK

10.2 APPENDIX 2: SOLUTIONS, BUFFERS AND MEDIA

10.2.1 ASOs dilution

ASOs were dispatched dried and were diluted with TE to obtain a 100mM stock using the following protocol:

a) 5 volumes of TE were added per x nmol of ASO (e.g. add 421.25µl of TE to 84.25nmol of ASO);

b) ASOs absorbance at 260nm was assessed using a spectrophotometer;

c) ASOs concentration in µM was calcultated as follows:

ASOs µM = (absorbance at 260nm/extension coefficient) x1.000.000

d) xµl of TE were added to dilute the ASOs to obtain a 100mM concentration.

10.2.2 DEPC treated H_2O (0.1%)

Dissolve 1ml of Diethyl Pyrocarbonate (DEPC) in 1L of dH_2O, stir overnight and autoclave.

10.2.3 Soc medium

Prepare the following solutions:

- 250mM KCl solution: dissolve 1.86g of 2.5mM KCl in 100ml of deionized water;
- 1M solution of $MgCl_2$: dissolve 20.33g of 10mM $MgCl_2$ in 100ml deionized water, and autoclave.
- 2M solution of glucose: weigh out 36g of 20mM glucose and dissolve in a final volume of 100ml deionized water. Filter sterile this solution.

For 1 litre of Soc medium: dissolve 20g of 2% Tryptone, 5g 0.5% Yeast extract, 0.5g NaCl (0.05%) in 950ml of water. Add 10ml of the stock KCl and then adjust pH to 7.0 with 5M NaOH. Bring the volume to 980ml with deionised water and autoclave. Let the solution cool to 55°C and then add 10ml of the filter-sterilised 2M glucose and 10ml of 1M $MgCl_2$. Store at room temperature.

10.2.4 RNA dye mixture (Formamide/EDTA/XC/BPB gel-loading buffer)

Dissolve 10ml of Formamide 10ml, 10mg of Xylene cyanol FF 10mg and 10mg of Bromophenol blue in 0.5 EDTA (pH 8.0) 200µl.

10.2.5 10% SDS

Dissolve 10g of SDS in 80ml of dH_2O and heat to 68°C to dissolve. Adjust to a final volume of 100ml with dH_2O.

10.2.6 LB Agar

Dissolve 8g of Agar and 9g of LB Broth in 400ml of dH_2O and autoclave.

10.2.7 LB broth

Dissolve 10g of LB broth in 400ml of dH_2O and autoclave.

10.2.8 3M Sodium Acetate

Dissolve 40.8g of sodium acetate in 80ml of dH_2O. Adjust to pH 7.6 with glacial acetic acid, make up to a final volume of 100ml and autoclave.

10.2.9 Buffer A

Dissolve 0.05M NaH_2PO_4 and 0.15M NaCl in 1L of dH_2O and adjust to pH 7.2. Filter and degas the solution.

10.2.10 TAE

Dissolve 40mM Tris, 20mM acetic acid and 1mM EDTA and adjust to pH 8.5.

10.2.11 TBE

Dissolve 45mM tris, 45mM borate and 1mM EDTA and adjust to pH 8.

10.3 APPENDIX 3: OLIGONUCLEOTIDE SEQUENCES

10.3.1 Sequences of oligonucleotides used for *GHR* amplification:

Ex 2 F	5' TAC AAC CTG CTG TTT GAG TTC 3'
Ex 2 R	5' ACT GAC TAC TGC ATT CCT CC 3'
Ex 3 F	5' GTT GGT TTG GGA AGC TGA GG 3'
Ex 3 R	5' GGA TAG TAG CTT AAT TAC AC 3'
Ex 4 F	5' TCA CAT ATG ACT CAC CTG 3'
Ex 4 R	5' AGG TAC ATC CAT GGA GAG 3'
Ex 5 F	5' ACT TAA GCT ACA ACA TGA 3'
Ex 5 R	5' GCT TCC CCA TTT ATT TAG TC 3'
Ex 6 F	5' TTG GTC TTC TGA GAA GAA TGC C 3'
Ex 6 R	5' ATA GAA AGA AAA GTC AAA GTG TAA G 3'
Ex 7 F	5' GAA TAC CTG TAG TGT TCA TTG C 3'
Ex 7 R	5' GCT CAA GGT CTC TCA TCC TG 3'
Ex 8 F	5' AAA CTG TGC TTC AAC TAT TCG 3'
Ex 8 R	5' GGA GAT AAA AGT GTA CTA GG 3'
Ex 9 F	5' GCT ATA ATT GAG AAT ATG TAG C 3'
Ex 9 R	5' CAT ATG ACA GGA GTC TTC AGG TG 3'
Ex 10 F1	5' GAG TTT CTT TTC ATA GAT CTT C 3'
Ex 10 R2	5' GCT GGT GTA ATG TCG CTC A 3'
Ex 10 F2	5' TGA AGG AGC TGA GTC AAC TC 3'
Ex 10 R1	5' CTT TGC TAT TAA ATA CGT AGC 3'
Int 6F	5' TTG TGA TCC AGT CAA CAG TGA CT 3'
Int 6R	5' TCT TGT TTG ACT TAG CAT CCA AT 3'

10.3.2 Sequences of oligonucleotides used for GHR mRNA RT-PCR

2FiGHRm	5' ATG GAT CTC TGG CAG CTG CTG TTG 3'
2FfGHRm	5' GGA TCA AGT GAT GCT TTT TCT GGA AGT G 3'
5FGHRm	5' ACC CAT ACA GCT GTT CTA TAC CAG AAG G 3'
5RGHRm	3' GGC ATT CTT TCC ATT CTT GAG TCC ATT C 5'
6RGHRm	3' ATT CAA CCC AAG AGT CAT CAC TGT GG 5'
7FGHRm	5' CGA AAC TCT GGA AAT TAT GGC GAG TTC AGT GAG GT 3'
8FGHRm	5' GGG CTA ACA GTG ATG CTA 3'

9RGHRm	3' CCA CGC AAT GCA GAT ATT CAG AAA GG 5'
10r3GHRm	3' ACC AAC TGA ACA AAA TCA TGC CTT AG 5'
GAPDHF	5' TCC CAT CAC CAT CTT CCA 3'
GAPDHR	3' AGC AAC AGG GTG GTG GAC 5'

10.3.3 Sequences of oligonucleotides used for *IGFALS* amplification

1fALS	GGCACGAGGGGGTTAACAGA
1rALS	AAATGCGGCTGCTGGGGTT
2fALS	GCTTCCGGCTGTGCTGGTAT
2rALS	CAGAAACTCTACCTGGACCG
3fALS	GCAGCCTCTGGGACCTCAA
3rALS	ACCTTCACCGGCCTCTCG
4fALS	CTCTGGGAACTGTCTCCGGAA
4rALS	GAAGGCATGGCGGCCC

10.3.4 Sequences of oligonucleotides used for minigenes construction:

T7-L1	5' TAA TAC GAC TCA CTA TAG GGA GAC CGG CAG ATC AGC TT 3'
Admlpar-int51 AS	5' TTATTAACCCTCACTAAAG 3'
Admlpar-int51 S	5' GCA GTA GTC AAG GGT TTC C 3'
L2A	5' ATC CAA GAG TAC TGG AAA GAC CG 3'
Exon2spl F	5' CTC ACT AAA GAT AAT GGT CTG CTT TTA ATT GCT 3'
Exon2spl R	5' ATT TCC ACC CTC AGT GTT GCA GTA GTC A 3'
Exon4 spl F	5' CTC ACT AAA GGA TCA CAT ATG ACT CAC CTG ATT 3'
Exon4 spl R	5' TGA CTA CTG CCC ATG GAG AGG AAA ATC AGA A 3'
Exon8 spl F	5' CTC ACT AAA GGC ATT GAG TTG TTG ACT CTT TGG 3'
Exon8 spl R	5' TTC TTT GGT ATT TTG TAC GCA GTA GTC A3'
Ps spl F	5' TTA GCA GTA GTG AAG GGT TTC CTT GAA GCT TTC GT 3'
Ps spl R	5' ACG AAA GCT TCA AGG AAA CCC TTG ACT ACT GCT AA 3'

10.3.5 Sequences of oligonucleotides used for site-directed mutagenesis:

Exon2sdm 1F	5' CTG GAA GTG AGG GTG GGT TCT GCT TTT CCA TTT CC 3'
Exon2sdm 1R	5' GGA AAT GGA AAA GCA GAA CCC ACC CTC ACT TCC AG 3'
Exon2sdm 2F	5' GGA AAT GGA AAA GCA GAA CGC ACC CTC ACT TCC AG 3'
Exon2sdm 2R	5' CTG GAA GTG AGG GTG CGT TCT GCT TTT CCA TTT CC 3'
Exon4sdm S	5' AGT GCC GTT CAC CTG AGT GAG AGA CTT TTT CAT GC 3'

Exon4sdm AS	5' GCA TGA AAA AGT CTC TCA CTC AGG TGA ACG GCA CT 3'
Exon8sdm S	5' CTG GAA ATT ATG GTG AGT TCA GTG AGG 3'
Exon8sdm AS	5' CCT CAC TGA ACT CAC CAT AAT TTC CAG 3'
Exon8sdm S	5' ATT TTA TAT GTT TTC AAC GAT TAA AAT GCT GAT TC 3'
Exon8sdm AS	5' GAA TCA GCA TTT TAA TCG TTG AAA ACA TAT AAA AT 3'
Ps sdm F	5' TGA GAC ACC AGG ACA TTC GGT GAG CCA CTG AAA AAG 3'
Ps sdm R	5' CTT TTT CAG TGG CTC ACC GAA TGT CCT GGT GTC TCA 3'

10.3.6 Sequences of antisense oligonucleotides (ASOs)

ASO branch	Mu.mU.mA.mG.mA.mA.mU.mU.mA.mG.mU.mU.mA.mU.mA.mU.mU.mG
ASO 3' splice	mU.mG.mU.mG.mG.mC.mU.mG.mU.mG.mG.mU.mU.mA.mG.mA.mC.mA
ASO 5' splice	mU.mU.mC.mA.mG.mU.mG.mG.mC.mU.mC.mA.mC.mC.mG.mA.mA.mU

10.3.7 Sequences of oligonucleotides used for identification of alternative *GHR* exons:

EXON X1F	5' CCTACTTCCAAGAGAACGAAAT 3'
EXON X1R	3' GCTCCTGCCACTCTGTGTCT 5'
EXON X2F	5' GGTCCATGCTCACATATCAA 3'
EXON X2R	3' CTTGATATGTGAGCATGGACCCC 5'
EXON X3F	5' GCCTAATGCAGAGTAGAGAAGC 3'
EXON X3R	3' CCTTCAAGTTGGTGAGCTTCTC 5'
EXON X4F	5' GCAAGTTGCACAGCTGGGATTC 3'
EXON X4R	3' CCCAGCTGTGCAACTTGCTAGT 5'

10.3.8 Sequences of oligonucleotides used for genotyping:

D5s2021 F	5' TTC TAC GGA TTC CAA TCA C 3'
D5s2021 R	3' CAA AAG CAA CTT AAC CAC G 5'
D5s2022 F	5' CTT CAT TGC ACT CCA GC 3'
D5s2022 R	3' GGC CAA TAA GTT TAT ATC GG 3'
D5s 430 F	5' TCT GCC CAG CAA TTC CAT AG 3'
D5s430 R	3' GGC AAG CAA TTT TCA CAG TTT T 5'
D5s 2082 F	5' ACC CCT AAG CCC TAG CA 3'
D5s 2082 R	3' CCC TAC CCT GTG AAA CCT 5'
D5s2087 F	5' TAG CAC CTA GCC AGT GCC TAG C 3'

D5s2087 R	3' CCA AAA GTC ATT TAG GAG CAG GTC 5'
D5s474 F	5' CTGAGGTAGCCTACACCT 3'
D5s474 R	3' AGAACGAATAGGACAAATGC 5'

10.4 APPENDIX 6: *GHR* FRAMEWORKS

GHR frameworks in 35 healthy controls. Location of polymorphic sites in intron 9. From Amselem S. et al. (Amselem et al., 1989).

Frame	IVS nt112	IVS nt124	IVS nt168	IVS nt199	IVS nt212	IVS nt213	Chr. studied (n=70)
I	A	G	C	T	T	T	37
II	A	G	C	C	-	-	14
III	G	G	C	T	-	-	12
IV	A	G	C	T	-	-	5
V	A	A	C	T	-	-	1
VI	A	G	T	T	T	T	1

10.5 APPENDIX 7: ADML-PAR GENOMIC SEQUENCE

GGGAGACCGGCAGATCAGCTTGGCCGCGTCCATCTGGTCATCTAGGATCTGATATCA
TCGATGAATTCGAGCTCGGTACCCCGTTCGTCCTCACTCTCTTCCGCATCGCTGTCTG
CGAGGGCCAGCTGTTGGGgtgagtactccctctcaaaagcgggcatgacttctgccctcgagttattaaccctcactaaagc
agtagtcaagggtttccttgaagctttcgtgctgaccctgtccctttttttccacAGCTGCAGGTCGACGTTGAGGACAA
ACTCTTCGCGGTCTTTCCAGTACTCTTGGAT

Exon L1 and L2 sequences are indicated in capital letters.

10.6 APPENDIX 8: ALGORITHM FOR THE IDENTIFICATION OF NOVEL *GHR* EXONS

```
dat <- read.table("E:/AAA RESEARCH/alessia/R code ale/splice.csv",
header=TRUE, sep=",", na.strings="", dec=".", strip.white=TRUE)
datacc=data.frame(dat[dat$accdon=="a",])
datdon=dat[dat$accdon=="d",]
pseud=c()
yy=0
for(ii in 1: length(rownames(datacc))){
      ack=datacc$base[ii]+14
      lenk=(datdon$base+1)-ack+1
      lenk1=lenk[lenk<202]
      lenk1=lenk1[lenk1>51]
      lenk2=lenk1
            if(length(lenk2)>0){
            for(tt in 1:length(lenk2)){
                  yy=yy+1
                  pseud$acc[yy]=datacc$base[ii]+14
                  pseud$length[yy]=lenk2[tt]
                  pseud$don[yy]=pseud$acc[yy]+pseud$length[yy]-1
                  pseud$accorigin[yy]=datacc$base[ii]
                  pseud$donorig[yy]=pseud$acc[yy]+pseud$length[yy]-
2
                  pseud$scoreacc[yy]=datacc$probabil[ii]
                  pseud$scorebr[yy]=datacc$scorebr[ii]
      pseud$scoredon[yy]=datdon$probabil[datdon$base==pseud$donorig
[yy]]
                  }}
      print(c(ii,lenk2))
      }
pseud=as.data.frame(pseud)

intron <- read.table("E:/AAA RESEARCH/alessia/R code ale/full
GHRgene.txt", header=FALSE, sep=",", na.strings="NA", dec=".",
strip.white=TRUE)
intron2=as.character(intron[1,1])
intron3=strsplit(intron2,"")[[1]]
intron4=c()
intron4$intr=as.character(intron3)
intron4=as.data.frame(intron4)
intron4[1:10,1]
pseud3=pseud
yy=0
for(uy in 1:length(pseud3$acc)){
      numbasi=20
      if(pseud3$acc[uy]<=numbasi) next
      ales=intron4[(pseud3$acc[uy]-numbasi):(pseud3$acc[uy]-1),]
      cbases=grep("c", ales)
      tbases=grep("t", ales)
      pseud3$accb[uy]=pseud3$acc[uy]
      pseud3$c[uy]=length(cbases)
      pseud3$t[uy]=length(tbases)
      totalct=length(cbases)+length(tbases)
      totalag=numbasi-totalct
      pseud3$ratio[uy]=round(totalct/numbasi, 3)
      pseud3$ct[uy]=length(cbases)+length(tbases)
            }
pseud4=pseud3[pseud3$ratio>0.5,]

      pseud6=pseud4
```

```
pseud6$include=ifelse(pseud6$scoreacc<80,ifelse(pseud6$scorebr>90,
"y", "n"),"y")
pseud7=pseud6[pseud6$include=="y",]

pseud8=pseud7
pseud8$include=ifelse(pseud8$scoreacc>=74,ifelse(pseud8$scorebr>=71
, "y", "n"),"n")
pseud9=pseud8[pseud8$include=="y",]

rownames(pseud9)=seq(1:nrow(pseud9))
pseud9$bestk=NA
for(uu in 1:nrow(pseud9)) {
      if(is.na(pseud9$bestk[uu])==FALSE) next
      acck=pseud9$acc[uu]
      whk=as.numeric(rownames(pseud9)[pseud9$acc==acck])
      mk=max(pseud9$scoredon[whk])
      whmax=whk[match(mk , pseud9$scoredon[whk])]
      pseud9$bestk[whk]="no"
      pseud9$bestk[whmax]="yes"
      }
pseud10=pseud9[pseud9$bestk=="yes",]

pseud10$prdop=ifelse(pseud10$acc<1329, "elim",
ifelse(pseud10$acc>153916, "elim", "keep"))
pseud11=pseud10[pseud10$prdop=="keep",]

mrn <- read.table("E:/AAA RESEARCH/alessia/R code ale/mRNA
GHR.txt", header=FALSE, sep="", na.strings="NA", dec=".",
strip.white=TRUE)
mrn2=as.character(mrn[1,1])
mrn3=strsplit(mrn2,"")[[1]]
mrn4=c()
mrn4$intr=as.character(mrn3)
mrn4=as.data.frame(mrn4)

coffpos=c(1,33,114,180,310,483,662,828,919,989)
coff=c(1340,1409,     64502,64567,   124353,124482,   130380,
130552,   135287, 135465,   146670, 146835,
      148892, 148982,   153515, 153584,   153916)
cofend=c(1409, 64567, 124482, 130552, 135465, 146835, 148982,
153584, 154862)
costart=c(1340, 64502, 124353, 130380, 135287, 146670, 148892,
153515, 153916)
      ex1=costart[1]:cofend[1]
      ex2=costart[2]:cofend[2]
      ex3=costart[3]:cofend[3]
      ex4=costart[4]:cofend[4]
      ex5=costart[5]:cofend[5]
      ex6=costart[6]:cofend[6]
      ex7=costart[7]:cofend[7]
      ex8=costart[8]:cofend[8]
      ex9=costart[9]:cofend[9]
      mrnanorm=intron4[c(ex1,ex2,ex3,ex4,ex5,ex6,ex7,ex8,ex9),1]
      exs=c()
      exs[[1]]=ex1
      exs[[2]]=ex2
      exs[[3]]=ex3
            exs[[4]]=ex4
```

```
      exs[[5]]=ex5
      exs[[6]]=ex6
      exs[[7]]=ex7
      exs[[8]]=ex8
      exs[[9]]=ex9
exs1=exs
library(seqinr)
pseud12=pseud11
pseud12$stop=NA
for(rt in 1:length(pseud12$acc)){
      exs=exs1
      difk=pseud12$acc[rt]-cofend
      difk1=difk[difk>0]
      if(length(difk1)==0) next
      difk1=min(difk1)
      endnum=match(difk1, difk)
      if((pseud12$acc[rt]-costart[endnum+1])>0)  {
      pseud12$stop[rt]="nk"
                  next
                  }
      if((pseud12$don[rt]-costart[endnum+1])>0)  {
            pseud12$stop[rt]="nk"
                  next
                  }
      if(length(difk1)==0)    {
      pseud12$stop[rt]="nk"
                  next
                  }
      exs[[endnum]]=c(exs[[endnum]],
pseud12$acc[rt]:pseud12$don[rt])
      mrnanew=as.character(intron4[c(exs[[1]],exs[[2]],exs[[3]],exs
[[4]],exs[[5]],exs[[6]],exs[[7]],exs[[8]],exs[[9]]),1])
      aak=getTrans(mrnanew)
      stopk=grep("[*]", aak)
      if(length(stopk)>0){
            pseud12$stop[rt]="y"
                  }}
      pseud12$stop[is.na(pseud12$stop)==TRUE]="no stop"
      summary(as.factor(pseud12$stop))
      pseud13=pseud12[pseud12$stop=="no stop",]
      pseud13=as.data.frame(pseud13)
      nrow(pseud13)

pseud13$bestkacc=NA
for(uu in 1:nrow(pseud13)){
      if(is.na(pseud13$bestkacc[uu])==FALSE) next
      donk=pseud9$don[uu]
      whk=as.numeric(rownames(pseud13)[pseud9$don==donk])
      mk=max(pseud13$scoreacc[whk])
      whmax=whk[match(mk , pseud13$scoreacc[whk])]
      pseud13$bestkacc[whk]="no"
      pseud13$bestkacc[whmax]="yes"
      }
pseud14=pseud13[pseud13$bestk=="yes",]
pseud14$mult3=ifelse((pseud14$length/3)!=round(pseud14$length, 0),
"not mu3", "mu3")
      pseud15=pseud14[pseud14$mult3=="mu3",]
```